Republic of Iraq

Ministry of Higher Education

and Scientific Research

University of Babylon/College of Science

Chemistry Department

Preparation of monolithic Columns and used it in flow injection Analysis and microfluidic systems for determination of Copper and Nickel

A thesis

Submitted to the Council of College of Science

University of Babylon in Partial Fulfillment of the

Requirements for the Degree of Doctor of

Philosophy in Chemistry

By

Salam Mohammed Nasser Shalhoom Al-Kafaji

B.Sc. College of Science- University of Babylon 2012

M.Sc. College of Science- University of Babylon 2015

Supervised by

Prof. Dr. Ahmed Ali Abdul- Sahib Al-karimi

Prof. Dr. Dakhil Nassir Taha Al-Zurgany

2022 A.D **1444 A.H**

جمهورية العراق

وزارة التعليم العالي والبحث العلمي

جامعة بابل /كلية العلوم

قسم الكيمياء

تحضير اعمدة المونوليث و استخدامها في انظمة الحقن الجرياني والمايكروفلوديك لتقدير عنصري النحاس والنيكل

أطروحة مقدمة

إلى مجلس كلية العلوم / جامعة بابل

كجزء من متطلبات نيل درجة فلسفة الدكتوراه في العلوم/ الكيمياء

تقدم بها

سلام محمد ناصر شلهوم الخفاجي

بكالوريوس علوم كيمياء – جامعة بابل 2012

ماجـــستير علوم كـيمياء – جامعة بابل 2015

بأشراف

أ.د. احمد علي عبد الصاحب الكريمي

أ.د. داخل ناصر طه الزركاني

1444 هـ

2022 م

(وَيَسْئَلُونَكَ عَنِ الرُّوحِ قُلِ
الرُّوحُ مِنْ أَمْرِ رَبِّي وَمَا
أُوتِيتُم مِّن الْعِلْمِ إِلاَّ قَلِيلاً۝)

سورة الإسراء: الآية 85

Dedication

Firs and formost I want to thank who helping me to finsh this work properly, and the moments are not good without his remembrance ……Mighty Allah.

To the one who conveyed the message and fulfilled the trust.. and advised the nation.. to the prophet of mercy and the light of the worlds…… may God's prayers and peace be upon him and his family ……The chosen one, Mohammad.

To those who are the cause of existence.. and with them every servant turns to the idol ……...The pure Ahlulbayt.

To the one who taught me to give without waiting, and I carry his name with pride, I ask God to extend his life..... my dear father.

To my late angel. To the meaning of love and the meaning of tenderness, and dedication. To whom her prayer was the secret of my success ……..... my dear mother (may God have mercy on her).

To the one who supported me in my way, stayed up nights with me and humiliated the difficulties of me..... my patient wife.

To my renewed hope in life, my future support and my beloved children....……. Ahmed and Kawthar.

To the warm hearts that still support me .....my brothers and sisters .

SALAM

ACKNOWLEDGEMENT

Thanks and appreciation very much to mighty Allah, and his massenger Mohammad (May Allah bless and grant him), and his family, companions, and those who follow his approach to the Day of Judgment.

I want to express my special appreciation and thanks to my supervisors, professor Dr. Dakhil Nasser Taha and professor Dr. AHMED Ali ALKARIMI, for their tremendous mentoring, encouraging and supervision during my research and allowing me to grow as a researcher scientist.

I want to thank and express my profound gratitude and deep regards to the University of Babylon, College of Science, and all chemistry department staff.

Special thanks to my family; words can not express how grateful I am to my father, brothers, and sisters for every thing you did for me.

Many thanks to my wife for her patient in everything. I cannot thank you enough for encouraging, moral support and assistance.

To my dear son (AHMED) and my beloved daughter (Kawthar), I would like to express my thanks for every moment you were patient with me.

To all post gradute students and all the people who helped me during my study I woul to say many thanks

I will keep on trusting You for my future .

Salam Mohammed Al-Khafaji

Committee Certification

We, the examiner committee, certify that we have read the thesis entitled "**Preparation of monolithic Columns and used it in flow injection Analysis and microfluidic systems for determination of Copper and Nikel**" and examined the student (*Salam Mohammed Nasser Shalhoom Al-Khafaji*) in its contents at 10 / 11 / 2022, and that in our opinion it is accepted as a thesis for the degree of **Doctorate** of Philosophy in chemistry with (**Excellent**) estimation.

Signature:
Name: **Dr. Hassan Thamir Abdulsahib**
Title: Professor
Address: Basrah University
College of Sciences, Chemistry
Date: / / 2022
(**Chairman**)

Signature:
Name: **Dr. Khdeeja Jabbar Ali**
Title: Professor
Address: Kufa University
College of education for girls, Chemistry
Date: / / 2022
(**Member**)

Signature:
Name: **Dr. Faiq Fathallah Karam**
Title: Professor
Address: Qadisiyah University
College of Sciences, Chemistry
Date: / / 2022
(**Member**)

Signature:
Name: **Dr. Ahmed Saadoon Abbas**
Title: Assistant Professor
Address: Babylon University
College of Sciences, Chemistry
Date: / / 2022
(**Member**)

Signature:
Name: **Dr. Fouad Fadhil AL-Qaim**
Title: Assistant Professor
Address: Babylon University
College of Sciences for Women, Chemistry
Date: / / 2022
(**Member**)

Signature:
Name: **Dr. Ahmed Ali Abdul-Sahib**
Title: Professor
Address: Babylon University
College of Sciences, Chemistry
Date: / / 2022
(**Member and Supervisor**)

Signature:
Name: **Dr. Dakhil Nassir Taha**
Title: Professor
Address: AL-Amal University College
Pharmacy Department
Date: / / 2022
(**Member and Supervisor**)

Approved by the College Committee on Graduate Studies

Signature:
Name: **Mohammed Mansour Kadhum Al kafaji**
Title: Professor
Address: Dean of College of Science – University of Babylon.
Date: / / 2022

الخلاصة

تم تحضير اعمدة فصل كرموتوغرافية تتكون من ثلاث مونمرات وهي glycidy1) methacrylate (GMA) , Acrylic acid (A. acid) and acryl amid بشكل عمود فصل ايوني موجب قوي داخل عمود زجاجي من ماده البوروسلكيت (بطول 60 ملم وبقطر داخلي 1,5ملم وقطر خارجي 3 ملم) باستخدام مصدرللاشعة الفوق بنفسجية أي بلمرة ضوئية.

تم تحضير خليط البلمرة باستخدام المونمرات غليسيديل ميثاكريلات (GMA) (glycidyle metharcrylate) وأكريل أميد (A.Am) (acryl amide) و Acrylic acid, ورابط متشابك (EDMA) (ethylene dimethacrylate) وبادئ 2,2-dimethoxy-2-phenyl (acetophenone)(DMPA) .

وتم اذابة الخليط باستخدام مذيب بروجيني يحتوي على 1-haxanol و ethanol وهو مذيب جيد للمونمرات والماده الرابطه والبادئ وغير جيد لذابة البوليمر وكان الزمن المستغرق لتكون البوليمر 4 دقيقة داخل كابينة التشعيع.

تم تشخيص البوليمر المتكون باستخدام عدت تقنيات وهي طيف الاشعة الحمراء (FTIR),الرنين النووي المغناطيسي لبروتون الهيدروجين (^{1}HNMR), وتحليل (BET) ,والمجهر الالكتروني الماسح (FESEM) .

لاثبات تكون البوليمر وايضا لدراسة بعض خصائص البوليمر مثل حجم المسام والمساحة السطحية كذلك تم دراسة بعض خصائص البوليمر مثل وقت التشعيع ,المسافة بين مصدر التشعيع وعمود البوليمر ,نفاذية عمود البوليمر ,المسامية ,السعة الكلية للعمود ,الانتفاخية .

تم فتح حلقة الايبوكسي في ميثاكريلات الجليسيديل لتشكيل مجموعات كبريتيت كعمود تبادل كاتيون عن طريق ضخ محلول كبريتات داخل عمود الفصل لغرض تحويل حلقة الايبوكسي الى مبادل ايوني موجب قوي.

تم تحضير كاشف جديد متخصص لعنصر النيكل (II) imidazole-azoligand((E) 2((4methoxyphenol)diazenyl)-4,5-diphenyl-1-Himidazole

تم تصميم أنظمة جديده (HPLC-FIA و microfluidic) مربوطه بشكل مباشر مع HPLC-Pump لتحديد مقياس الطيف الضوئي للنحاس (I) والنيكل (II) وباستخدام كاشف متخصص النيوكبرون و (كاشف MPDADPI الجديد) عند λmax = 453 و 518 نانومتر على التوالي.

تم تطبيق الطريقة المباشرة بالاعتماد على الظروف المثلى لتحديد Cu (I) و Ni (II) بواسطة الكاشفين. تم إنشاء الرسوم البيانية للمعايرة لكل نظام جديد ضمن مدى خطية (0.05-17) و (0.005-2.9) ملغم .مل$^{-1}$. كانت قيم الخطية (0.9980) R2، 0.9951. كان حد قيم الكشف 0.039 و 0.001 ملغم . مل$^{-1}$. كان حد قيم القياس الكمي 0.129 و 1 ملغم .مل$^{-1}$.

الطريقة الغير مباشره استخدمت لتحديد هذه الأيونات من خلال تقنيتين ، الأولى هي مقياس الامتصاص الذري لتحديد النحاس والنيكل ، بينما الثانية هي طريقة القياس الطيفي باستخدام كاشف النيوكبرون الانتقائي لتحديد النحاس. تم تطبيق قانون لامبرت بير منحنى المعايرة ضمن مدى خطية (1-35) ، LOD 0.269 و LOQ 0.807 ملغم مل$^{-1}$.على التوالي.

تم تطبيق طريقة HPLC-FIA المقترحة بنجاح لتحديد Cu (I) و Ni (II) في العينات القياسية ، وعينات المياه بيئة من محطه المعيميرة في محافظه بابل –مدينة الحله .وتم حساب عمر العمود وكان 50 يومًا.

Summary

(Ter – monomers) glycidy1 methacrylate (GMA) , Acrylic acid (A. acid) and acryl amid were used to make monolithic column which was manufactured as strong cation exchange column. A borosilicate tube (60 mm in length) with 1.5 mm, and 3.0 mm (i.d and o.d respectively) was used for in-situ copolymerization using U.V light source.

The polymerization mixture was prepared by mixing (Ter – monomers) (GMA,A.acid,A.amid) with crosslinker (ethylene dimethacrylate) (EDMA) and initiator (2,2-dimethoxy-2-phenyl acetophenone) (DMPA) was dissolved in porogenic solvent consisting of ethanol and 1-hexanol. The time taken to form the polymer inside the borosilicate column in the irradiation cabin was 4 minutes.

Various techniques were used such as FTIR, ^{1}HNMR, BET, and SEM, to prove the formation of the polymer and also study the properties of the polymer such as pore size and surface area.

The epoxy ring was opened in glycidyl methacrylate to form sulfite groups as a cation exchange column by pumping a sulfate solution into the separation column for the purpose of converting the epoxy ring into a strong positive ion exchanger.

Synthesis of imidazole-azolifand(E)2((4methoxyphenol) diazenyl)-4,5-diphenyl -1-Himidazole.

New HPLC-FIA and microfluidic systems using as online designed for the spectrophotometric determination of Copper(I) and Nickel (II) by using neocuprion and (new reagent MPDADPI)Orange reagents at λmax= 453 and 518 nm respectively.

Online method applied by depending on the optimum conditions were conducted for the determination of Cu (II) and Ni (II)by the two reagents. The calibration graphs were constructed for each new system with linear ranges (0.05-17) and (0.005-2.9) $mg.mL^{-1}$. The linearity (R^2) values were 0.9980, 0.9995. The limit of detection values were 0.039 and 0.001 $mg.mL^{-1}$. The limit of quantification values were 0.129 and 1 $mg.mL^{-1}$.

Off-line method applied to determine these ions by two techniques were used, The first one is atomic absorption spectrophotometer to determine copper,and nickel, while the second one is spectrophotometric method using selective neocuproine reagent to determine copper. Beers' Lambert law was applied to constrict the calibration curve with linear ranges (1-35) (0.5-32) , LOD 0.269 ,LOQ 0.807 , LOD 0.3 and LOQ 0.9 $mg.L^{-1}$ respectively.

Investigateing of monolithic column by irradiation time, the distance between the irradiation source and the monolith column, permeability of the monolith, chelating capacity for monolithic column, porosity and swelling measurement.

The proposed HPLC-FIA method was successfully applied for the determination of Cu(II) & Ni(II)in standard samples, and water samples.

The age of the column was calculated and it was 50 days.

Declaration

we certify that this thesis **" Preparation of monolithic Columns and used it in flow injection Analysis and microfluidic systems for determination of Copper and Nickel."** has been prepared under our supervision at Chemistry Department – College of Science/ University of Babylon, as a partial requirement for the degree of philosophy doctor in analytical chemistry.

Signature:

Supervisor: Prof. Dr. Ahmed Ali Alkarimi

Date: / /2022

Signature:

Supervisor: Prof. Dr. Dakhil Nassir Taha

Date: / /2022

Forwarding for debate

In view of the available recommendations, I forward this thesis for debate by the examining committee.

Signature:

Name: Prof. Dr. Abbas Jasim Atiyah

Title: Head of Chemistry Department - College of Science/ University of Babylon

Date: / /2022

List of Abbreviations

Abbreviation	Meaning
LSC	Liquid-solid chromatography
AES	Atomic Emission Spectrometry
GSC	Gas-Solid chromatography
GLC	Gas-Liquid chromatography
LLC	Liquid-Liquid chromatography
HPLC	High-pressure liquid chromatography
IEC	Ion exchange chromatography
HIC	Hydrophobic interaction chromatography
IMAC	Immobilized metal affinity chromatography
FIA- HPLC	Flow injection technique and High-performance liquid chromatography
CEC	capillary electrochromatography
µ-HPLC	micro-high performance liquid chromatography
GC	gas chromatography
HSM	hybrid silica-based monolith
LC	liquid chromatography
UHPLC	ultra high performance liquid chromatography
GMA	Glycidyl methacrylate
PGMA	Polyglycidyl methacrylate
PEEK	polyetheretherketone
BET	Brunauer-Emmett-Teller
SEM	Scanning electron microscope
BJH	Barrett-Joyner-Halenda
TMSO	3- (trimethoxysilyl) propylmethacrylate
EDMA	Ethylene dimethacrylate
DAP	2, 2-Dimethoxy-2-phenylacetophenone
ACA	Acrylic acid
AAM	Acrylamide
DMPA	2,2-dimethoxy-2-phenylacetophenone
AIBN	2,2- azoisobutyronitrile
DMF	Dimethylformamide
DMSO	Dimethyl sulfoxide
BSEs	Backscattered electrons
SEs	Secondary electrons
IUPAC	International Union of Pure and Applied Chemistry
LCL	Lower control limits
UCL	Upper control limits
CL	Control Limits
PSI	pounds per square inch
FT-I.R	Fourier-transform infrared spectroscopy
^{1}H- NMR	Proton nuclear magnetic resonance
SD	Standard deviation
RSD	Relative standard deviation
Con.	Concentration

LOD	**Limit of Detection**
LOQ	**Limit of Quantitation**
CFA	**Continuous Flow Analysis**
CFIA	**Continuous Flow Injection Analysis**
SE	**Standard error**
MPDADPI	**imidazole-azo ligand ((E)-2-((4 methoxyphenol)diazenyl)-4,5-diphenyl-1-Himidazole.**
UV-Vis	**Ultraviolet-visible**
CHN	**Carbon Hydrogen Nitrogen**
FAAS	**Flame Atomic Absorption Spectrometry**
FI	**Flow Injection**
FIA	**Flow Injection Analysis**
D.Q.S	**Data Acquisition System**
LC	**Liquid Chromatography**
LOV	**Lab-on-Valve**
rFIA	**Reversed Flow Injection Analysis**
SCFA	**Segmented Continuous Flow Analysis**
SFIA	**Stop Flow Injection Analysis**
SI	**Sequential Injection**
SIA	**Sequential Injection Analysis**
µTAS	**Micro Total Analysis System**

List of Contents

List of Figures

List of Tables

1. Introduction

(1.1) Chromatography

Tswett is commonly regarded as the inventor of chromatography.[1] Chromatography's a crucial biophysical method for separating, identifying, and purifying mixture components for qualitative and quantitative analysis [2].

The mobile phase is an essential component of all chromatographic systems, as it is responsible for the transfer of the movement of the analytes throughout the column and the use of a stationary phase, either coated onto the column or the beads of resin [3]. Analytes are separated as a function of their exposure duration within the column of separation through weak interactions between the stationary phase and analytes depending on their chemical structure.[4].

As opposed to other forms of isolation, "chromatography" allows for a wider variety of materials, tools, and procedures to be utilized [5].

"size exclusion, Ion exchange, partition, surface adsorption" are the 4 isolation strategies that take molecule properties and interaction type into account. "Column, paper chromatography, thin layer" all use variations on the stationary bed principle [2]. Column chromatography is often used to purify proteins[6].

The chromatographic method relies on these 3 factors for its foundation.

1- Every stationary phase consists of a solid component, or a layer of liquid which is adsorbed on the solid support's surface.

2- The mobile phase is always made up of a liquid or gaseous constituent, and never any solids.

3- Molecular partitioning [4-7].

As illustrated in scheme Classification of chromatography methods according to various applied techniques. Fig (1.1) [5,8].

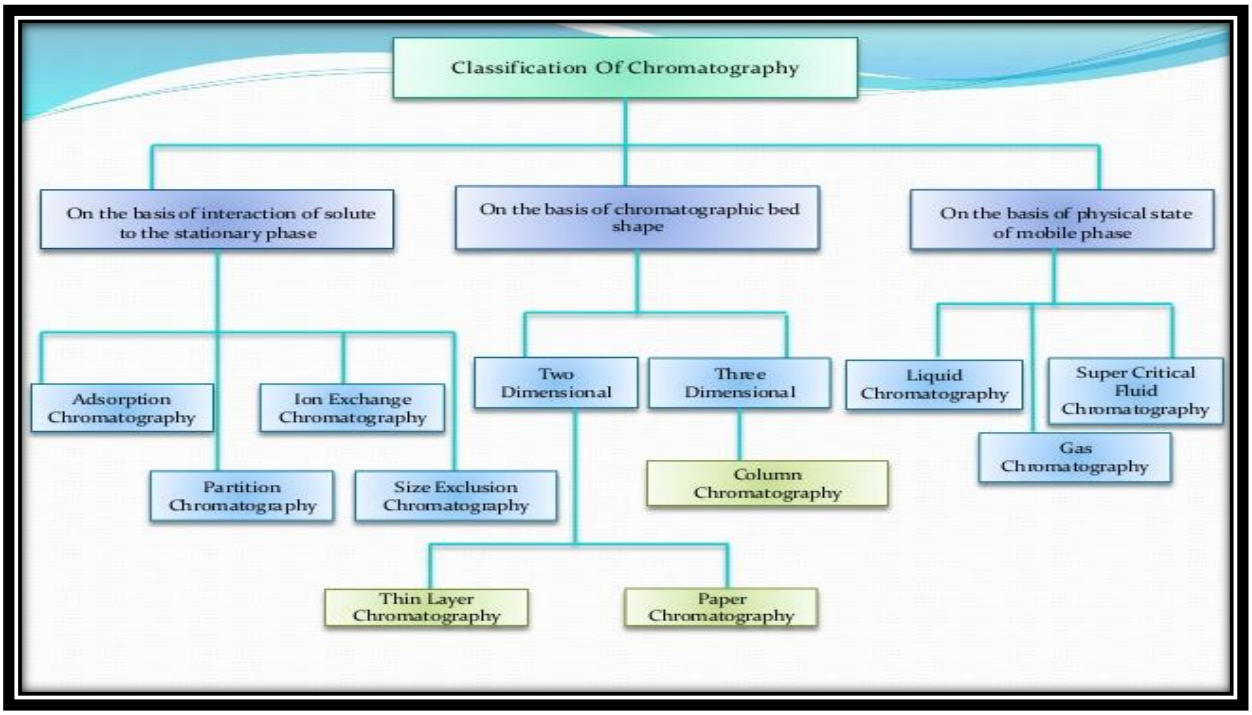

Fig.1.1 A classification system for chromatography that takes into account the numerous methods that can be used within the area.

(1.2) Physique-based classification [8]:-

In the 1st approach, the mobile phase and stationary phase are considered in their physical states. They may be broken down into four distinct classes:

I. ***gas-solid***
II. ***Gas-liquid***
III. ***liquid-liquid***
IV. ***liquid-solid***

(1.3) Distinctions made according to the degree of interaction between the mobile and stationary phases [8,9]:-

I. ***Gas-Liquid chromatography{GLC}***
II. ***Liquid-Liquid chromatography {LLC}***
III. ***Liquid-solid chromatography {LSC}***
IV. ***Gas-Solid chromatography {GSC}***

(1.4) Chromatography types according to their underlying physical or chemical framework [9]:-

1. Chromatography of Columns
2. **Chromatography of Ion-exchange**
3. Chromatography of Gel-permeation (molecular sieve)
4. Chromatography of Affinity
5. Chromatography of Paper
6. Chromatography of Thin-layer
7. Chromatography of Gas
8. Chromatography of Dye-ligand
9. Chromatography of Hydrophobic interaction
10. Chromatography of Pseudo affinity
11. Chromatography High-pressure liquid

1.4.1 - Column chromatography [10,11]

Biomolecules can be cleaned up using this method. The sample being detached is implemented to the column (the stationary phase) initially, followed by the wash buffer (aka. The mobile phase) (as shown in figure (1.2).Their movement is guaranteed by the internal material of the column resting upon the fiberglass base. Over time and space, the samples are stored in a well at the device's base. .

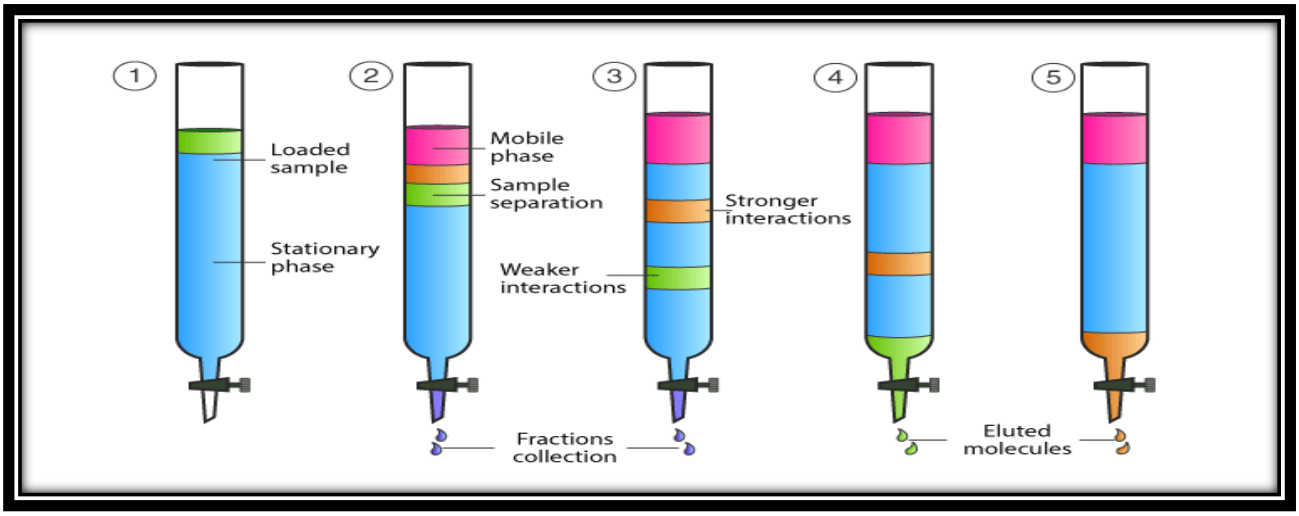

Figure (1.2).Column chromatography.

(1.4.2)- Ion- exchange chromatography [5,6]

Electrostatic interactions between charged protein groups and solid support material are used in IEC. Altering the buffer solution's [acidity, ionic strength or ion salt concentration] is used to remove proteins from the column. Negatively-

charged proteins're adsorbed by anion-exchange matrices, which are positively charged ion-exchange matrices. Cation-exchange matrices, on the other hand, are made up of negatively charged groups and adsorb positively charged proteins. (Fig.1.3)

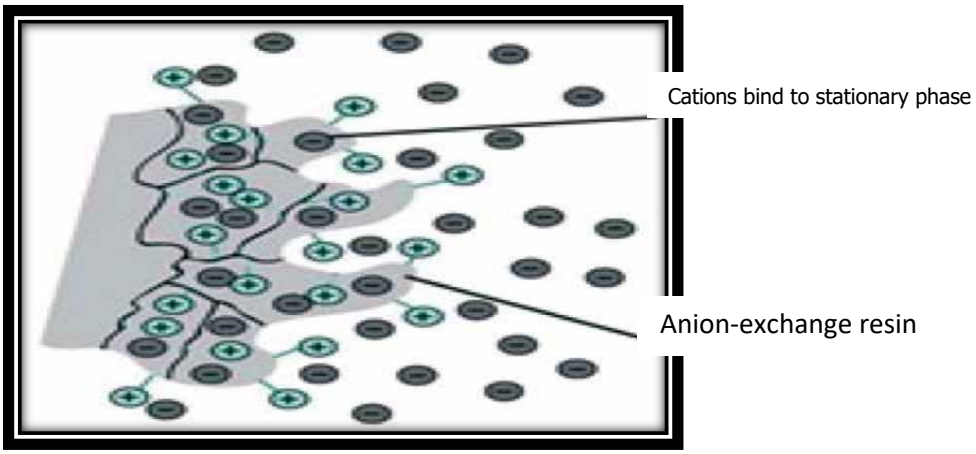

Figure (1.3) Ion- exchange chromatography.

Inorganic ion chromatography 'stationary phase' is an ionic functional group covalently bonded to a polymer resin that is cross-linked, most often divinylbenzene polystyrene that's cross-linked.[12,15,14).]

These static charges have counterions which are free to move and be dislodged via ions with stronger attractive forces.

There are four distinct types of ion-exchange resins:

i. **strong acid cation exchangers**
ii. **weak acid cation exchangers**
iii. **strong base anion exchangers**
iv. **weak base anion exchangers.**

The scheme enumerates a number of widely used ion-exchange resins [(12,13)].

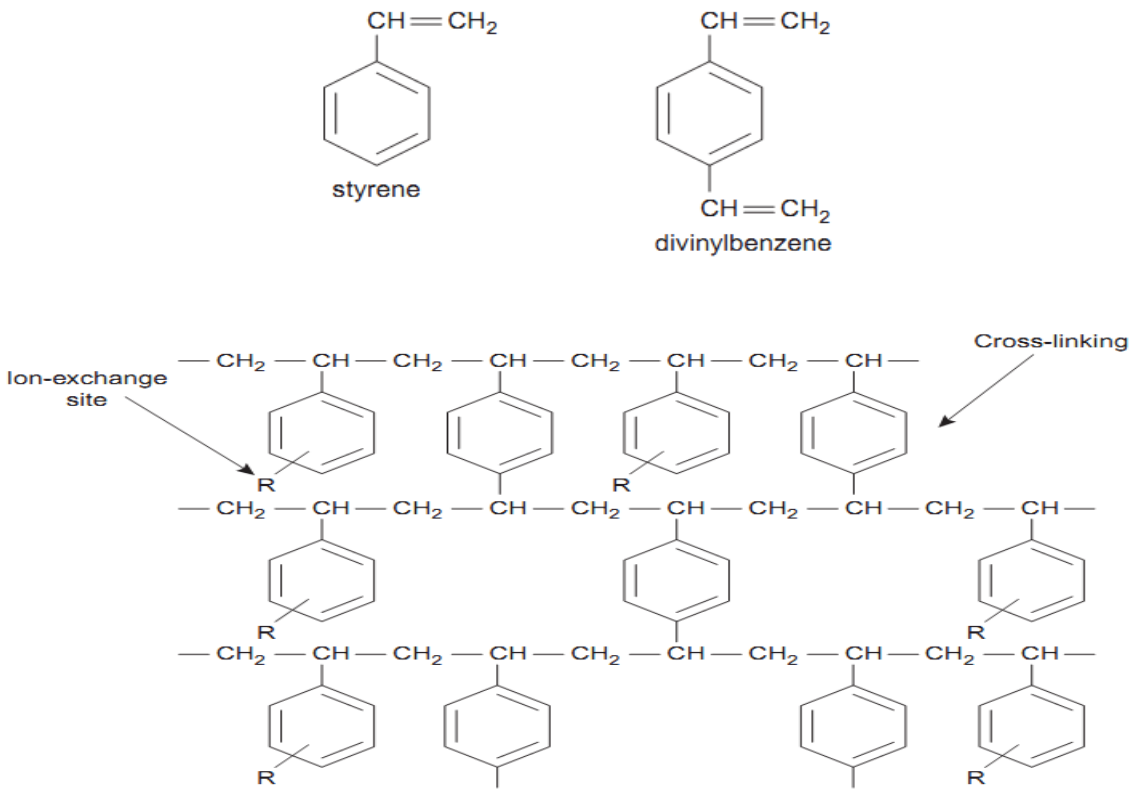

Figure (1.4) This lists many widely used ion-exchange resins.

The functional group of sulfonic acid of strong acid cation exchangers stays in the anionic state, allowing it to continue exchanging ions even in very acidic environments. Yet, at pH values below four, the weak acid cation exchanger's fumctional groups are totally protonated, rendering them unable to operate as an exchanger.

Despite being designed to function in highly basic environments, the exchangers of strong base anions maintain their positive charge. The pH must be somewhat basic for weak base anion exchangers to keep their protonation state. A poor base anion exchanger's positive charge and, by extension, its exchange capability, are depleted in more basic environments[8]. Table (1.1) shows types of function group ion- exchange.

Table (1.1) Types of function group ion- exchange.

Type	Functional Group	Examples
strong acid cation exchanger	sulfonic acid	$-SO_3^-$ $-CH_2CH_2SO_3^-$
weak acid cation exchanger	carboxylic acid	$-COO^-$ $-CH_2COO^-$
strong base anion exchanger	quaternary amine	$-CH_2N(CH_3)_3^+$ $-CH_2CH_2N(CH_2CH_3)_3^+$
weak base anion exchanger	amine	$-NH_3^+$ $-CH_2CH_2NH(CH_2CH_3)_2^+$

A monovalent cation, denoted by M+, undergoes an ion exchange process at a strong acid exchange site, which is denoted by:

$$-SO_3^-\text{–}H^+(s) + M^+(aq) \rightleftharpoons -SO_3^-\text{–}M^+(s) + H^+(aq)$$

For this particular ion-exchange process, the equilibrium constant, which is sometimes referred to as "the selectivity coefficient", is:

$$K = \frac{\{-SO_3^-\text{–}M^+\}[H^+]}{\{-SO_3^-\text{–}H^+\}[M^+]}$$

under which the square brackets {} denote a surface concentration.

$$D = \frac{\text{amount of } M^+ \text{ in stationary phase}}{\text{amount of } M^+ \text{ in mobile phase}} = \frac{\{-SO_3^-\text{–}M^+\}}{[M^+]} = K\frac{\{-SO_3^-\text{–}H^+\}}{[H^+]}$$

The value of D depends on how much H^+ is present in the mobile phase, and hence on its pH. [16,17].

Porous polymer beads which are micron-sized or the resin coated on porous silica particles are used to integrate ion-exchange resins within HPLC columns. The degree of cross-linking and the strength of the exchange site in the resin both have a role in its selectivity. The latter plays a pivotal role since it determines the resin's permeability and, by extension, the ease with which exchange sites may be accessed. As D decreases, the following is a rough order of selectivity for a typical strong acid cation exchange resin:

$$Al^{3+} > Ba^{2+} > Pb^{2+} > Ca^{2+} > Ni^{2+} > Cd^{2+} > Cu^{2+} > Co^{2+} > Zn^{2+} > Mg^{2+} > Ag^{+} > K^{+} > NH_4^{+} > Na^{+} > H^{+} > Li^{+}$$

It' has been shown that higher-charged ions have a stronger attraction than their lower-charged counterparts. Among a set of charged ions, the ones with the smallest hydrated radius or the highest polarizability form the strongest bonds. The typical order of cation and anion exchangers in a strong base is:

$$SO_4^{2-} > I^{-} > HSO_4^{-} > NO_3^{-} > Br^{-} > NO_2^{-} > Cl^{-} > HCO_3^{-} > CH_3COO^{-} > OH^{-} > F^{-}$$

Furthermore, ions possesing a bigger charge and a smaller hydrated radius bond more firmly in comparison to ions with a lesser charge and a larger radius that is hydrated. Retention period of a solute in 'IEC' is based on its acidity and ionic composition within the mobile phase, which is typically an aqueous buffer. Changes in the mobile phase's ionic strength or acidity can be made over a period of time, allowing for gradient elutions. [18,19].

The field of biochemistry[21] and the field of water analysis[20]have both benefited greatly from the use of ion-exchange chromatography . Proteins[22], amino acids[21], sugars, drugs, nucleotides, consumer goods, and clinical samples are just some of the many substances that have been analyzed using ion-exchange chromatography. [23,24].

(1.4.3)-Gel- permeation (molecular sieve) chromatography

This technique relies on molecular size differences between macromolecules to guide the selection of separating conditions, with dextran-containing components playing a central role. This method is commonly used to lessen the saltiness of protein solutions and calculate their molecular weights. The inert, pore-sized molecules that make up the stationary phase of a gel-permeation column are very useful. At a steady pace, the column is constantly flushed with the solution, which contains molecules of varying sizes [6,25].

Gel particle pores are too small to let through molecules that are too large and are instead trapped in the narrow space between them. Molecules of a greater size are able to flow swiftly throughout the column's interior because they can fit through the gaps between the porous particles. Diffusion into holes occurs for molecules that are smaller than the pores, and a proportionately longer exits path which is shown for smaller molecules when they leave the column[26–28] as shown Fig (1.5).

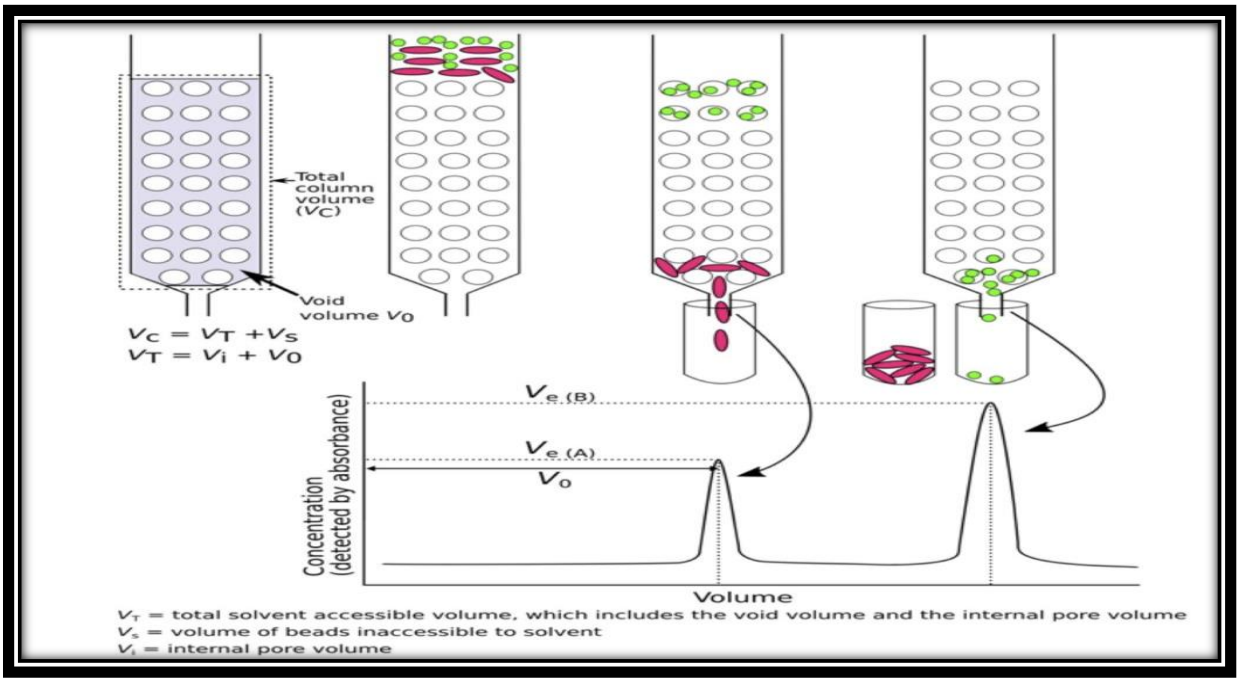

Figure (1.5) Technique gel- permeation chromatography

(1.4.4)-Affinity chromatography [29,30] .

Hormones , enzymes , antibodies , target proteins and nucleic acids may all be separated using this chromatography method. The column's filling material is bound by a ligand that forms a compound with a target protein (polyacrylamide, dextran, cellulose, etc.). The ligand-binding protein is kept in the column due to its attachment to the support that is solid, whereas free proteins pass through. The acidity of the column is adjusted or a salt solution is added, which causes the bound protein to dissociate and flow out of the column. (Fig.1.6).

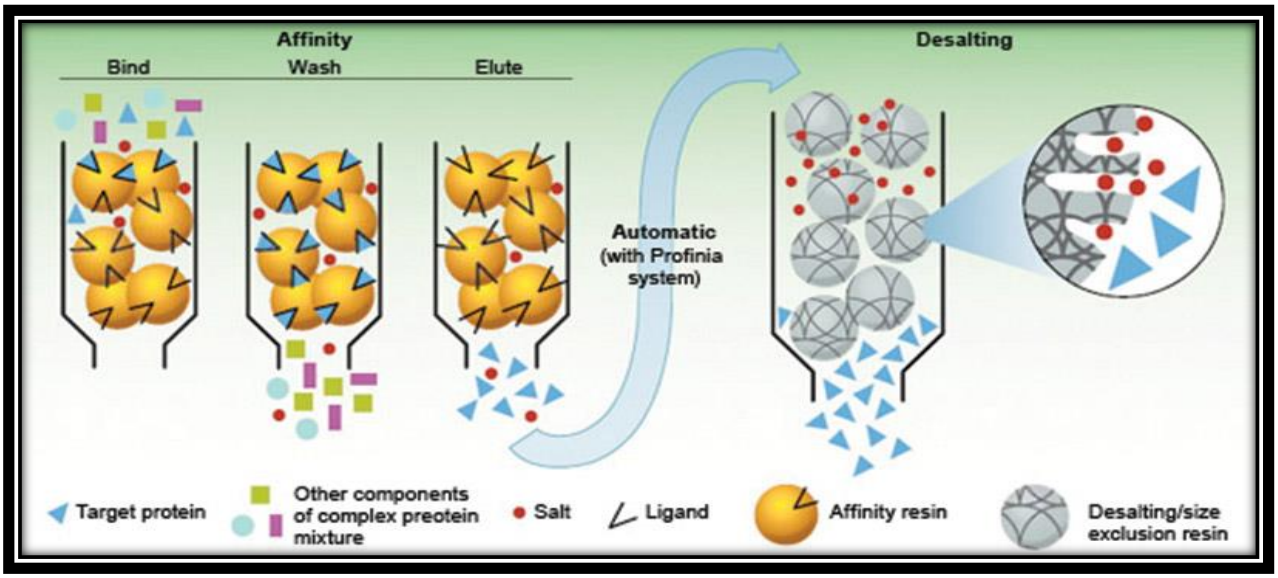

Fig. (1.6) Affinity chromatography.

(1.4.5)-Paper chromatography [31-33]

A blanket of highly saturated cellulose is used as a support material in paper chromatography. Throughout this technique, water drops settled in the pores of thick filter paper, serving as the stationary 'liquid phase'. The mobile phase is the fluid used during the development stage. In chromatography parlance, paper chromatography is known as a "liquid-liquid" technique Fig .(1.7).

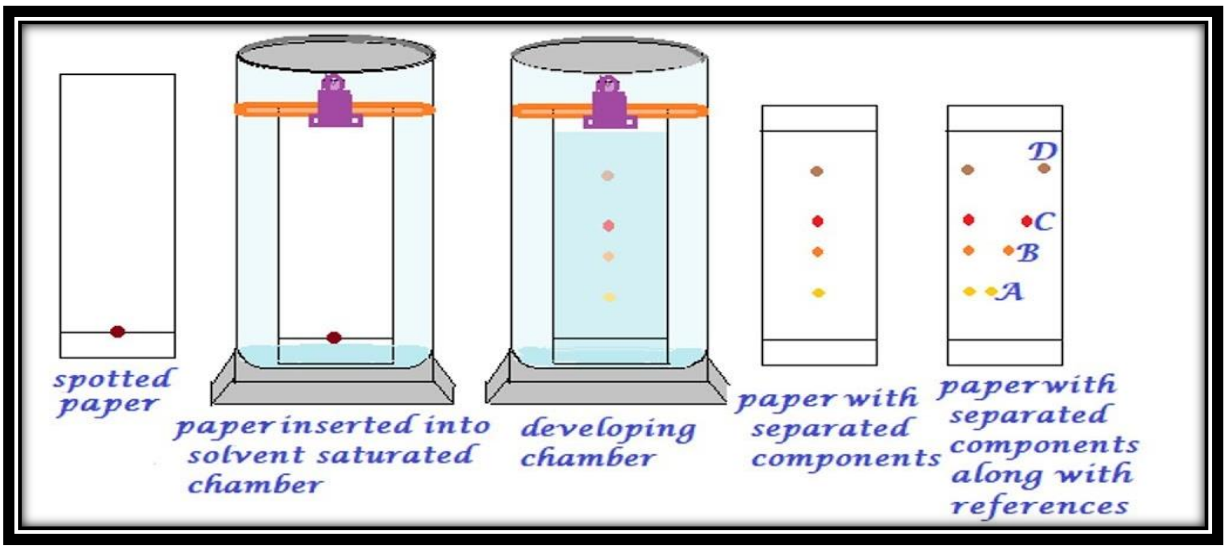

Figure (1.7) paper chromatography

(1.4.6)-Thin-layer chromatography [34]

As a kind of "solid-liquid adsorption" chromatography, thin-layer chromatography is a useful tool. The adsorbent coating on the glass plates represents the stationary phase under this technique. All solid materials are employed as adsorbents. These three materials (alumina&silica gel&cellulose) can all be used in column chromatography [35]. The mobile phase is seen to rise through the stationary phase in this process. Because of the action of the capillary, the solvent moves upward along the wet thin plate. A pipette is used to dump a mixture on the bottom portions of the plate, and the method then propels the liquid upward at varying flow rates. That's how you get your analytes all neatly separated. This velocity of ascent is influenced by the polarity of both the substance and solvent.Fig.(1.8) [36].

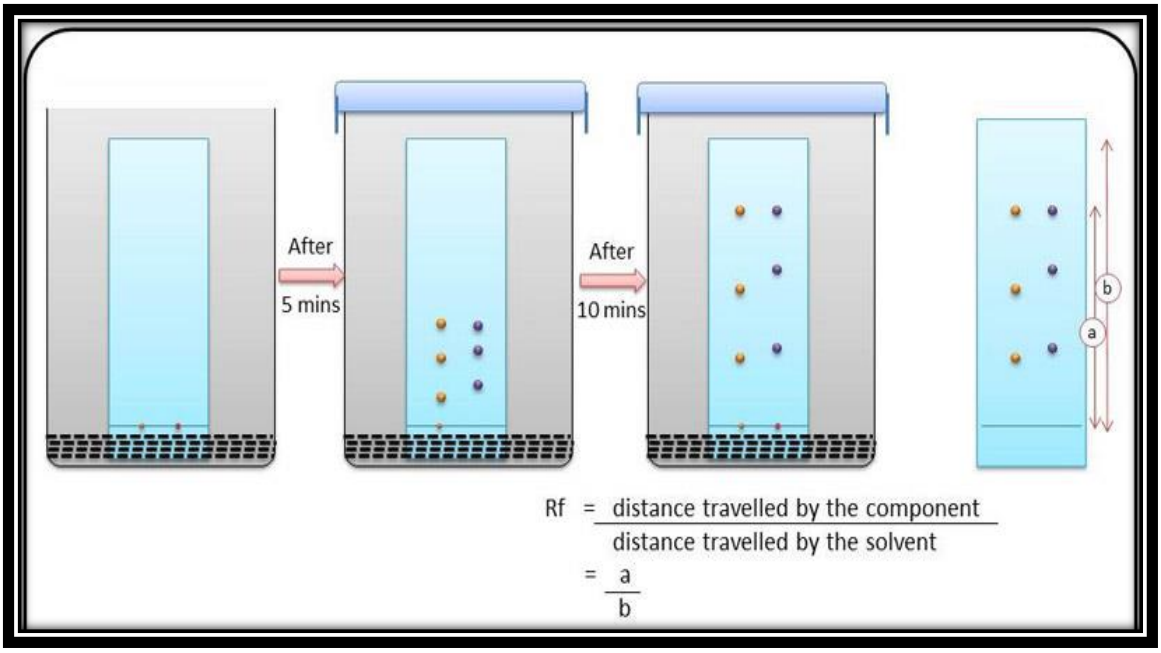

Figure (1.8) Thin-layer chromatography

(1.4.7)- Gas chromatograph [37-39]

Rather of using a gaseous or vaporous stationary phase, this technique makes use of a stationary phase ,which is liquid, that is adsorbed by an inert solid's surface in a column that is then inserted into the device. Chromatography using a gas as a mobile phase is known as "gas chromatography". The Helium or

Nitrogen gases make up the carrier phase. An inert gas (the mobile phase) is pushed throughout a column at elevated pressure. The analyzable sample is evaporated before being introduced to the mobile phase. Both the mobile& stationary phases on the solid support include components of the sample. Incredibly minute molecules may be separated using gas chromatography, which is a straightforward, flexible, highly sensitive, and easily implemented technology. Used for separating trace quantities of analyses Fig (1.9) .

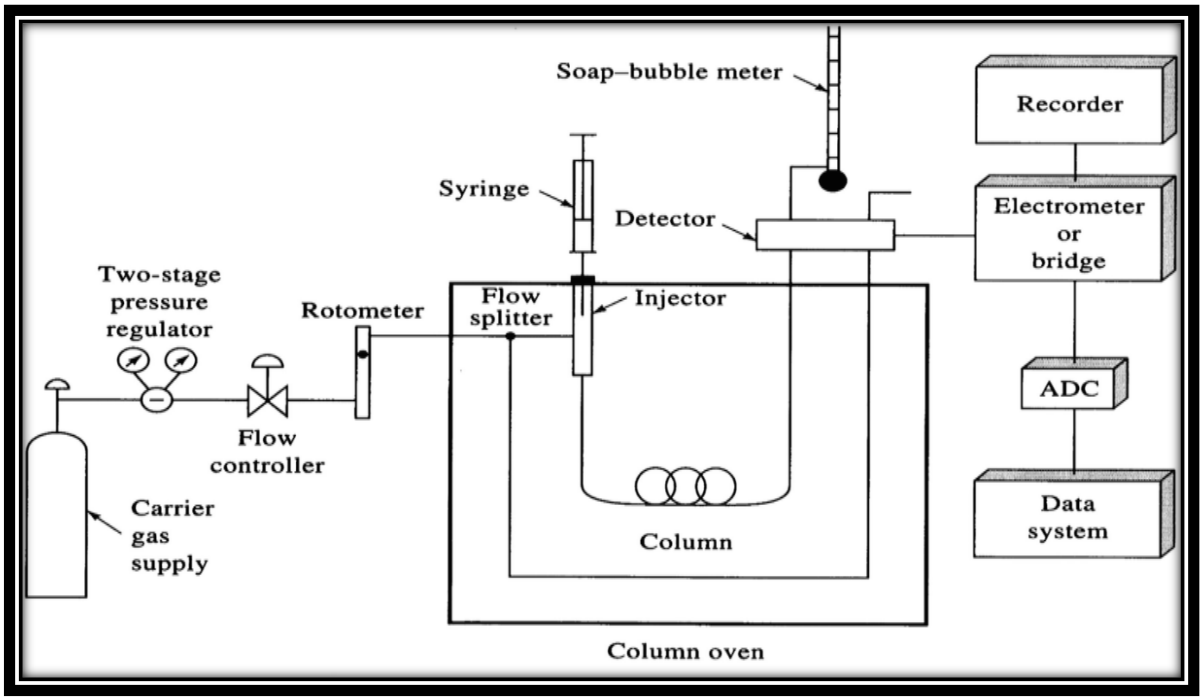

Figure (1.9)Gas chromatography

(1.4.8)- Dye- ligand chromatography [40,41] .

The capability of various enzymes to link purine nucleotides for Cibacron Blue F3GA dye was a major factor in the development of this method. Adsorbed proteins are isolated from the column due to their similarity to the planar ring structure of NAD, which contains negatively charged groups. Fig.(1.10).

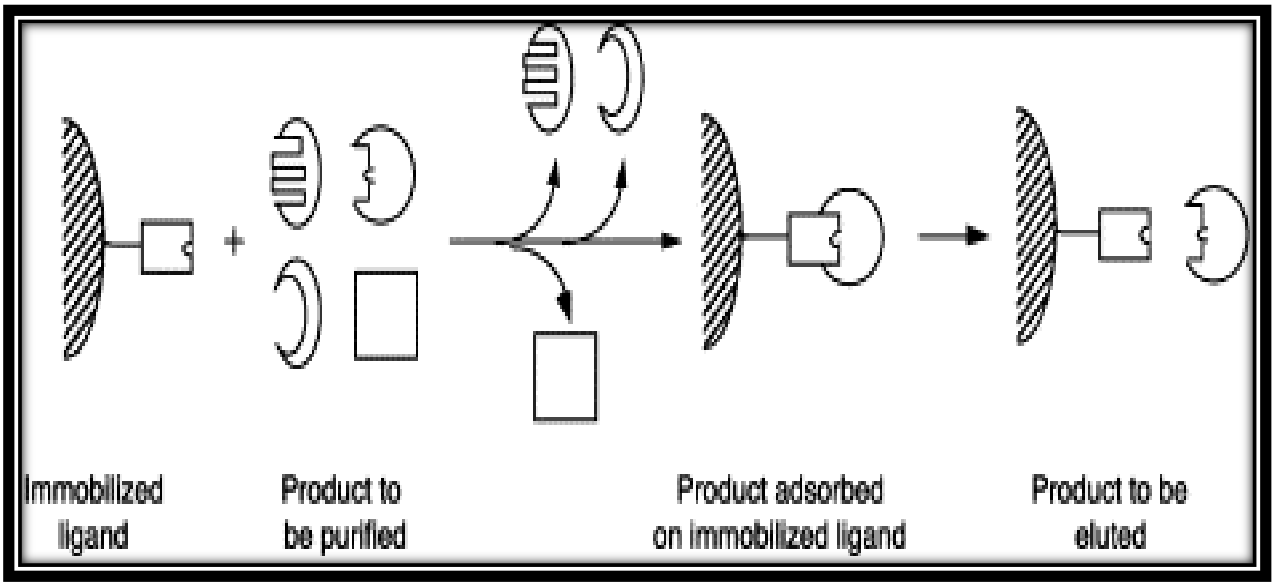

Figure (1.10)Dye- ligand chromatography

(1.4.9) - Hydrophobic interaction chromatography (HIC)

Affinity chromatography adsorbents designed for ligand linking are employed in this process. The hydrophobic interaction chromatography (a.k.a HIC) method relies on the reactions between side chains that are linked to a chromatography matrix. Fig(1.11)[42,43].

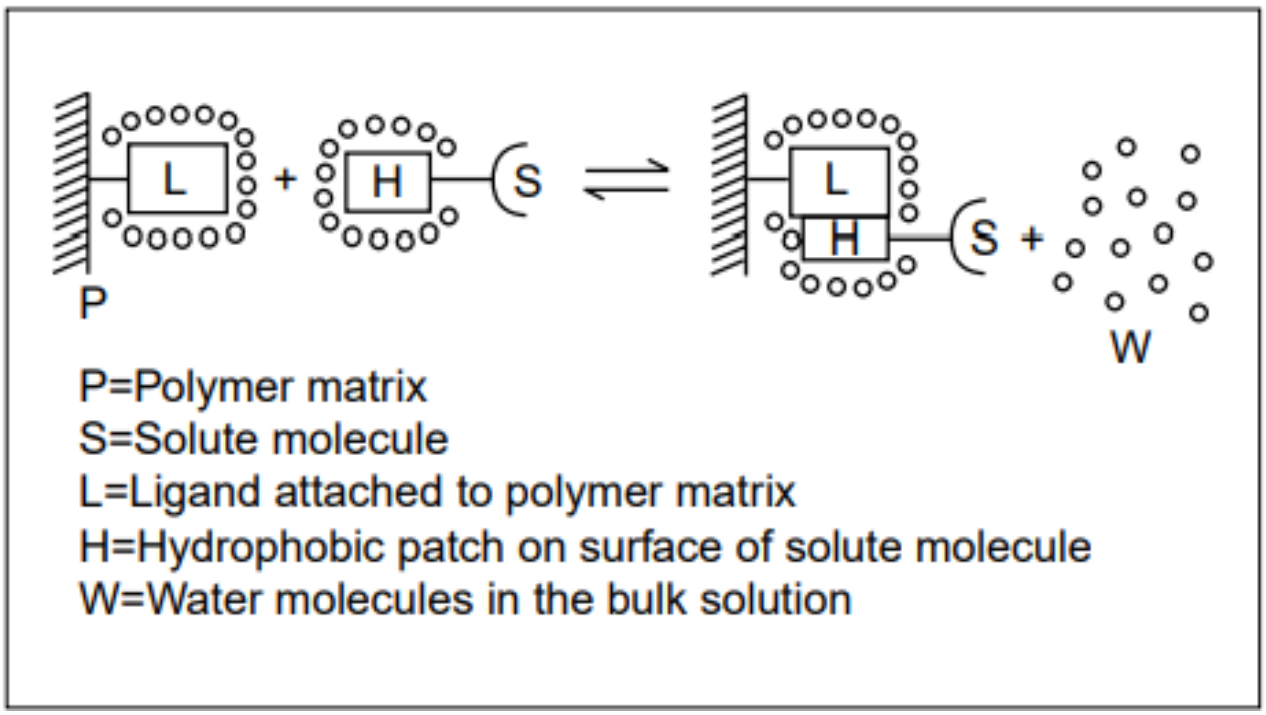

Figure (1.11) Hydrophobic interaction chromatography (HIC)

(1.4.10) -Pseudo affinity chromatography [44,45]

In particular, the affinity of chemicals like anthraquinone dyes and azodyes for , kinases,dehydrogenases, transferases and reductases makes them useful as ligands. IMAC (which stands for: Immobilized metal affinity chromatography) is the most common sort of this chromatography Fig(1.12).

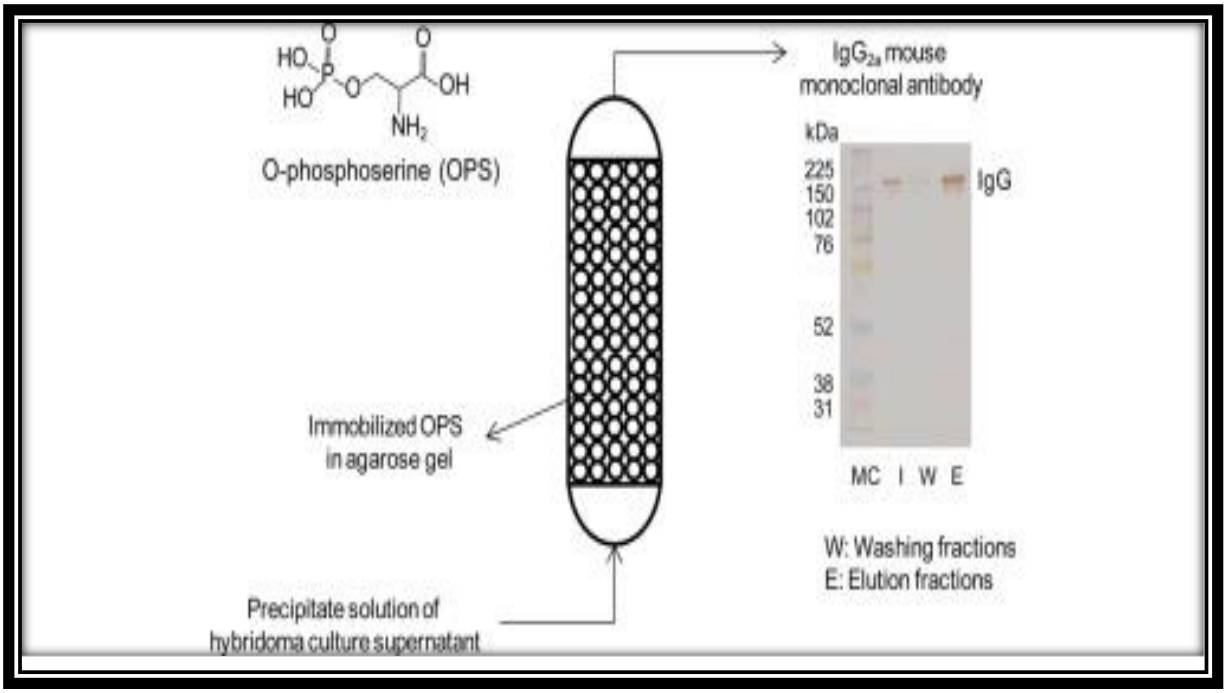

Figure (1.12) Pseudo affinity chromatography.

(1.4.11) - High-pressure liquid chromatography (HPLC) [46]

Chromatography using a liquid membrane to separate molecules. Method of achromatography in which a liquid mobile phase is used. High-performance liquid chromatography (HPLC) uses a liquid mobile phase to transport a liquid sample or a sample that is solid which has been dissolved in an appropriate solvent through a chromatographic column.Liquid–liquid partitioning, ion exchange,liquid–solid adsorption and size exclusion are examples of solute/stationary-phase interactions that play a role in the separation process. The instrumentation of a standard HPLC system is seen in Fig.(1.13).

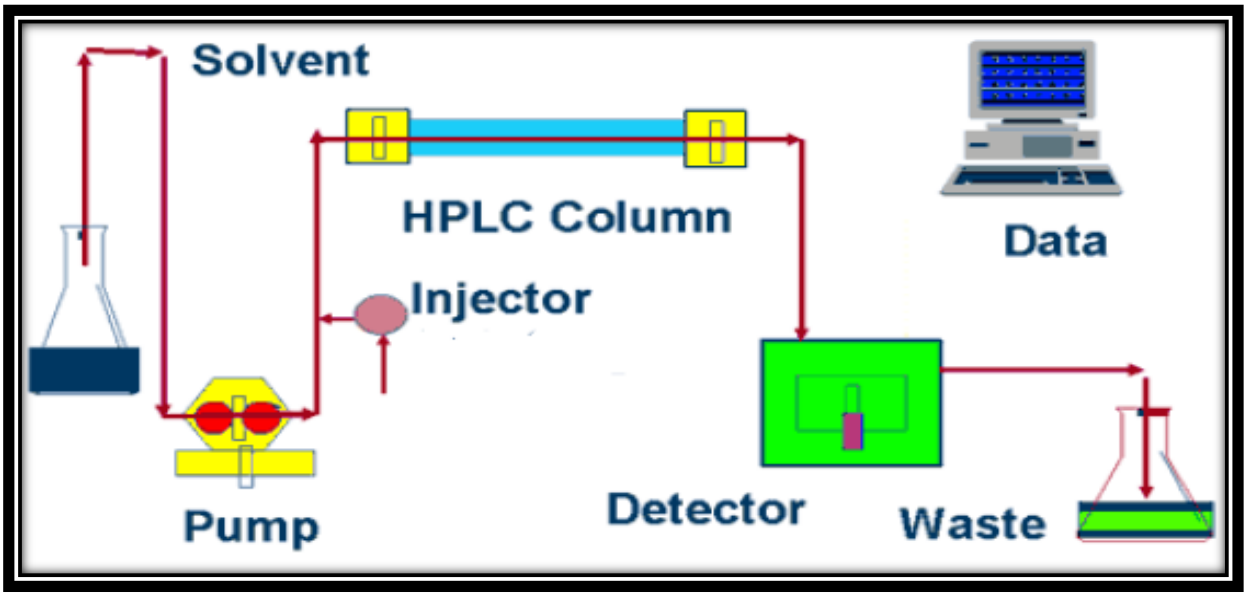

Figure (1.13) High-pressure liquid chromatography (HPLC)

(1.5) Chromatographic Resolution[47]

Chromatography's primary objective is to part sample constituents into distinct groups or peaks on their way down the column. Several characteristics, including retention duration, maximum width, maximum height and characterize a chromatographic peak. To further clarify, we might say that the following characteristics describe the resolution:

$$R_S = \frac{2\Delta t}{w_2 + w_1} \text{--------(1-1)}$$

where:
RS = resolution
Δt = difference between retention times of peaks 1 and 2
w_2 = width of peak 2 at baseline
w_1 = width of peak 1 at baseline .(fig.14 a ,b).

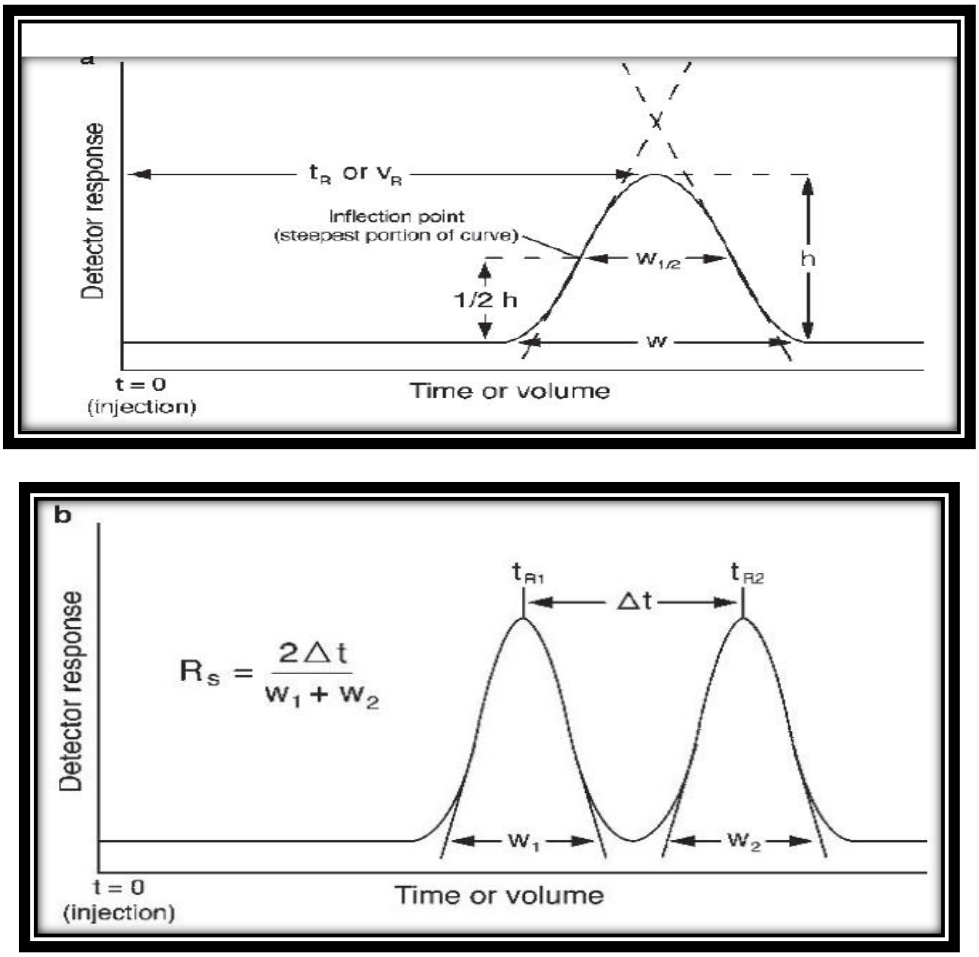

Figure (1.14) (a.one width ,b two width) for Chromatographic Resolution

(1.6) Flow Analysis

Flow analysis is the umbrella term for all analytical techniques that rely on the introduction of a sample into a flowing medium known as the carrier stream by aspiration or injection [48].

Two fundamental ideas can be used to classify flow analysis. The first is based on how samples are introduced, which can be continuous or discrete, and the second is based on the flowing medium, which can be segmented or unsegmented, as seen in[49,50] Fig. (1.15)

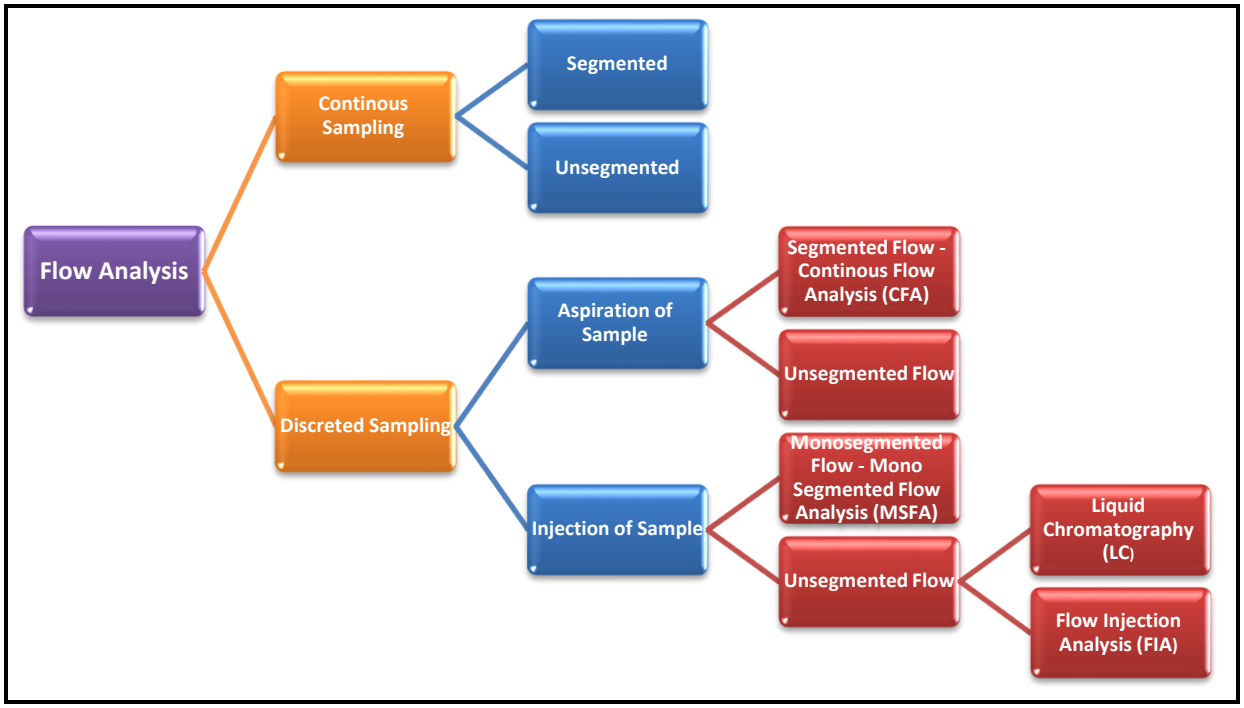

Figure (1.15) IUPAC classification of flow analysis methods

The reason for the appearance of the peak in the flow injection technique is due to the occurrence of two processes, one of which includes the formation of the dispersion phenomenon, which is a physical process, and the second includes a chemical process resulting from the interaction between the model and the detector after each of them is injected through the injection valve into an uninterrupted moving vector stream, and this causes a gradient in the concentration and gives the absorbance or the potential difference or any other

physical factor that changes as a result of passing the model through it, and thus the resulting signal is recorded in a peak form for each injection process .The processes that occur within any flow injection system can be described [51,52] Fig. (1.16).

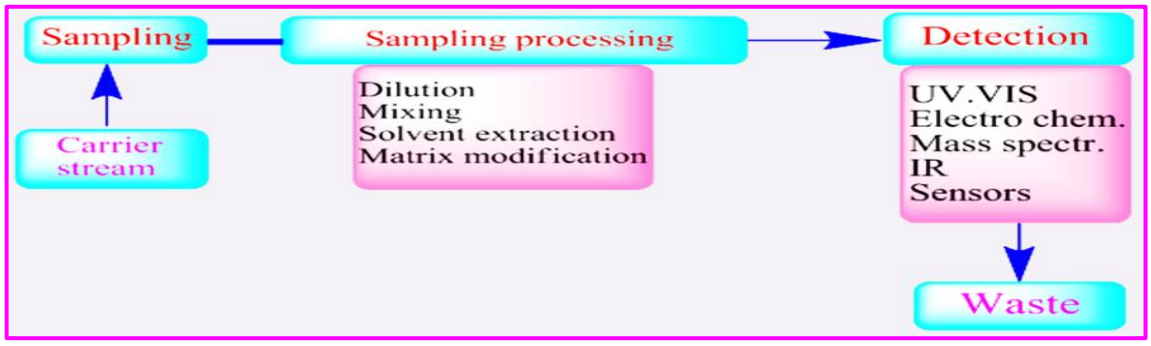

Figure (1.16) Description of the injection technique

(1.7) Flow-injection and HPLC[53,54]

Similarities between the flow injection technique and high-performance liquid chromatography, and among the similarities that were found is the ability to inject as the sample is entered by injection in both techniques, the possibility of using small volumes, the flow in the form of parts i.e. the nature of the mixture is laminar, and a comparison can be presented Simplified to show similarities between flow injection technology and high performance liquid chromatography Fig.(1.17).

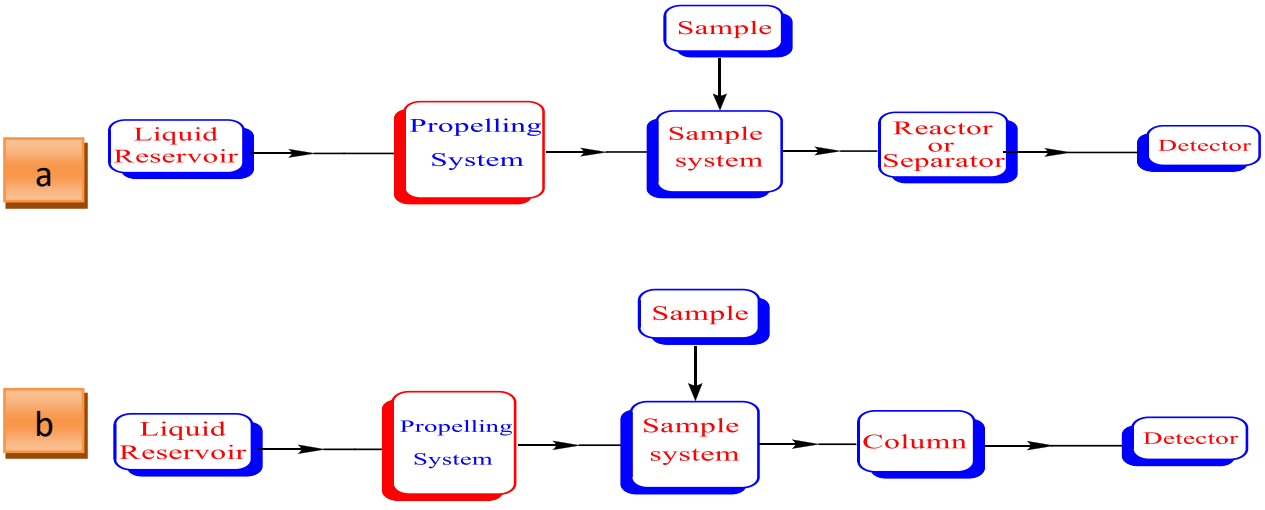

Figure (1.17) Similarities between a- FIA and b- HPLC

Despite the similarities between FIA and HPLC [55,56] , there are significant differences between the two techniques, as HPLC technology requires higher pressure than in flow injection, while FIA can work by about 1.5 atmospheres by using a simple peristaltic pump, also the liquid passes in HPLC technology, through a column tightly packed with materials, while in FIA, the liquid passes through the sample area from a narrow tube, in addition to the fact that HPLC is complex and designed to estimate several components in one sample, while FIA is characterized by its simplicity and estimation of one component in the sample, so that both (HPLC, FIA) are two different techniques due to the different principles of each[57] .

(1.8) HPLC-FIA COUPLING [58]

It takes 2 injection valves, a chromatographic column , 2 pumps, a reactor and an ongoing detector to make up a HPLC-FTA linked system, as well as reservoirs for the carriers, eluents and reagents. There are two ways to implement this relationship, both of which depend on the setting of the injection valve in the FIA subsystem (see Fig. 1.18): When the valve is located before the carrier's confluence with the chromatographic effluent (A) and when the valve’s located at the point of confluence (B). In order to stop air bubbles from poping up, restrictor coils’re frequently used. In analytical methods, these 2 modes're only utilised by a select few.

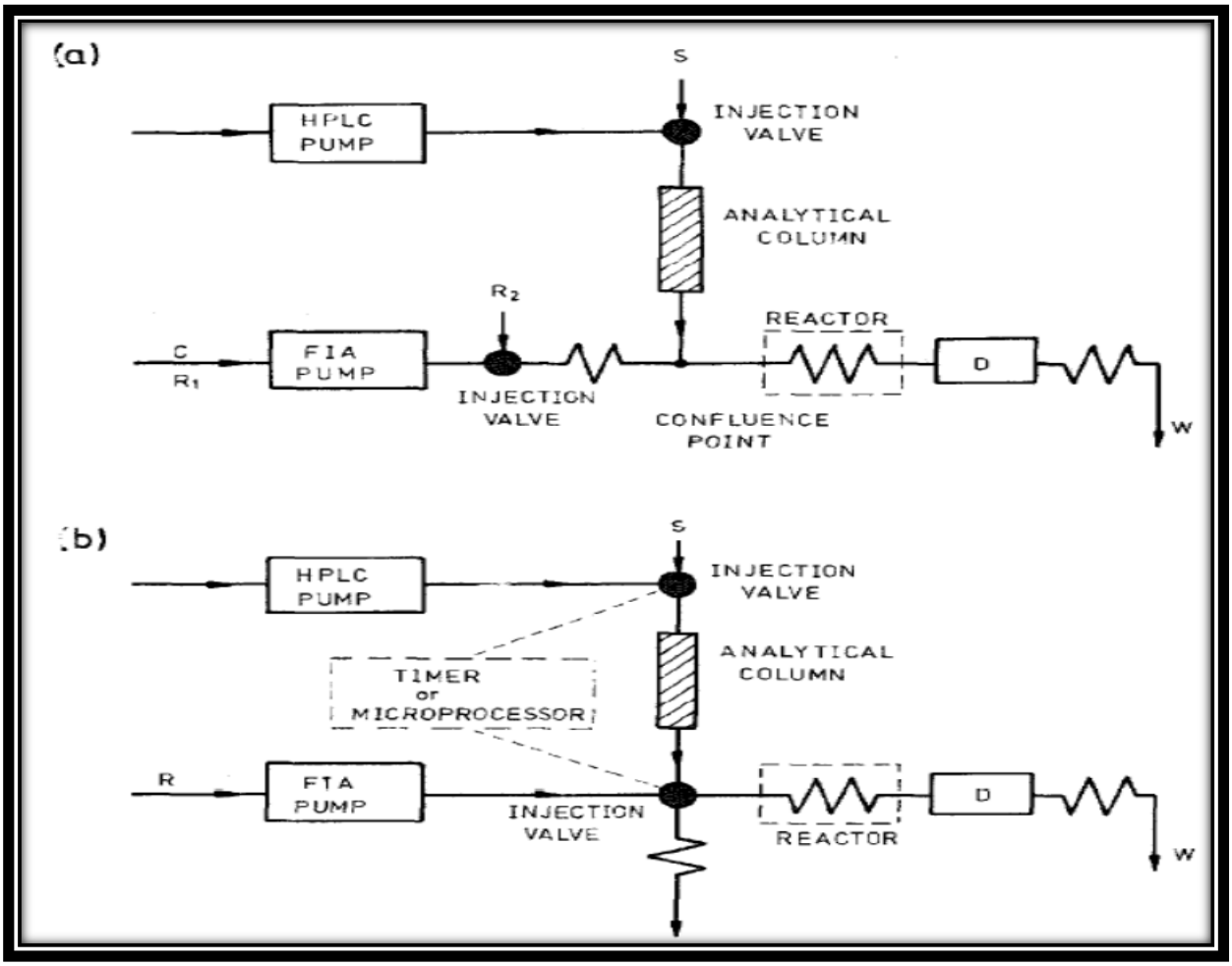

Figure (1.18) General arrangement of HPLC-FIA combination: (A) with FIA injection prior to the confluence with the chromatographic eluate; (B) with injection of the chromatographic eluate. C = carrier; R = reagent; S = sample; D = detector; W = waste.

The use of 2 valves in an on-line HPLC-FIA linked system is not the only option, as it was previously mentioned [59]. After the chromatographic process is complete, the effluent is pumped via a sampling valve's loop and periodically injected into the reagent flow. (Fig. 16B). In this case, automatic simultaneous operation of the two valves is required. Reducing sugar mixes were detected using a photometric detector, and amino acid mixtures were detected using an amperometric detector, both using this set up[60].

(1.9) Microfluidics

Microfluidics refers to technologies and methods for regulating and modifying fluid flows on a millimeter scale. Such fluid-related phenomena have long been studied as part of the fluid mechanical component of colloid science [61] and plant biology [62], and they depend on many fundamental features of viscous flow dynamics[63]. Ruzicka and Hansen described an unique microsystem

technique for the first time in 1984. The microconduits, microscopic potentiometric or optical detectors and gas diffusion or ion exchange units were all part of the integrated microsystem[59]. Another experiment involved using a tiny syringe instead of a peristaltic pump. Lab-on-Valve is a monolithic construction with a channel system, flow cell, and detector positioned over a multi-position valve. The channels diameters of the Lab-on-Valve system are measured in centimeters and fractions of millimetersFig.(1.19). ([64],[65])

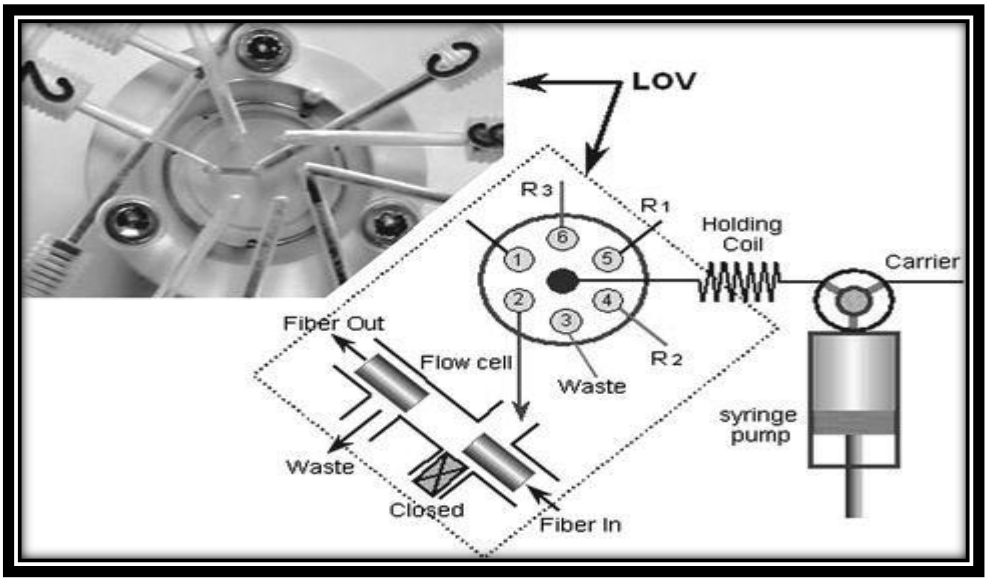

Figure (1.19) Lab-on-Valve system

Microfluidics was a word applied in the early 1990s to characterize microsystems. The sizes of channels in microfluidics were reduced to tens of micrometers, paving the door for the production of a complete Lab-on-a-chip or micro total analysis system (μTAS). As shown in Fig. (20 a,b) a microfluidic system comprises of a thin piece of glass or polymeric plate with microchannels and diameters of a few centimeters [66-68]

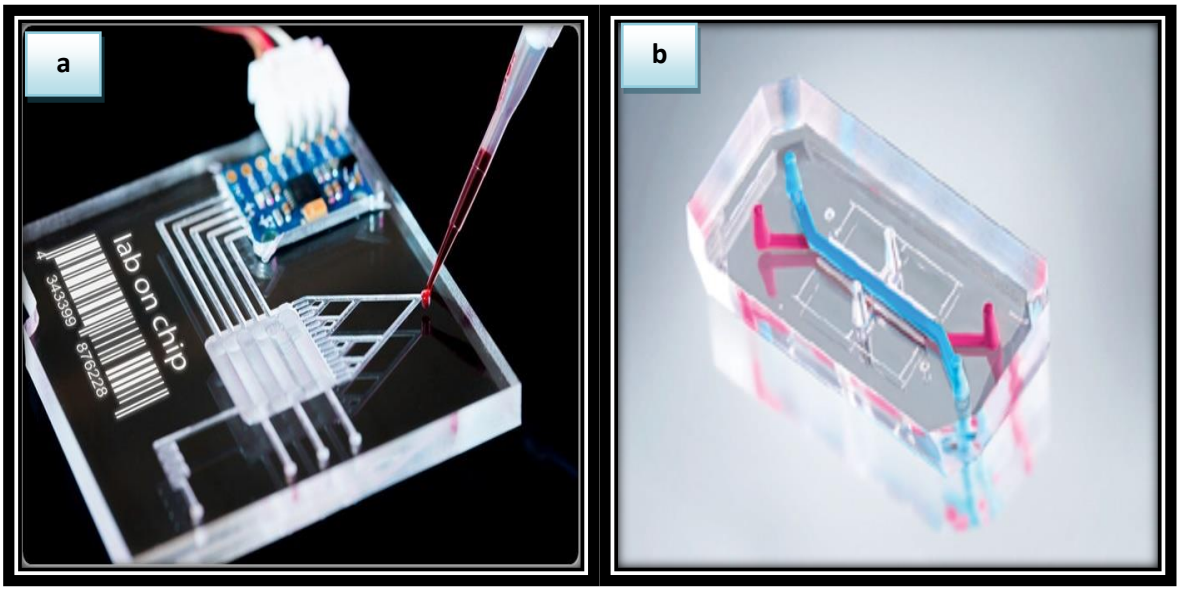

Figure (20 a, b): The micro channels of microfluidic systems

(1.10) Monolith

Innovations in column tech are a major force in the progress of separation research [(69)]. During HPLC's existence, silica particle materials packed columns were the gold standard. In 1973, the first commercially available columns containing 10m silica C18 particles were introduced. Since then, scientists have systematically decreased particle size to speed up and improve separation processes [(69,70)]. Because of the spherical packing, the external porosity of packed columns is fixed. As a result, column designs that allow for independent control of characteristic size (such as particle diameter) and porosity have the potential to produce intrinsically better chromatographic performance. As a result, polymer-monolith stationary phases have emerged as an appealing alternative for packed columns, with particular application in biomolecule analysis[(71,72).]

(1.10.1) Monolithic columns

In comparison to typical particle-packed columns, monolithic columns are comparatively easy to build, have great permeability,quick delivery of mass and high efficiency [(73)]. Organic monolithic columns that are based on polymer,

those based on silica are the two basic forms of monolithic columns. Inorganic/organic monoliths are mixtures of these two categories. However, they are frequently referred to as hybrids, and the term hybrid is used in a variety of contexts, such as for columns made from a mixture of tetramethoxysilane and methyltrimethoxysilane[69].

Heat- or photo-initiated free radical polymerization of appropriate monomers and cross-linkers in the presence of porogens is a typical method for creating organic-polymer-based monoliths inside the column [74]. Using a range of functional monomers and cross linkers, organic monolithic columns can give exceptional pH stability and tremendous flexibility in tuning monolithic chemical characteristics [75].Changing the porogenic solvents, the polymerization temperature and duration might also be done to vary their porosity and surface qualities. To make matters worse, organic monoliths have a shorter lifespan and an undesirable high variability in low retention due to swelling caused by organic solvents and a lack of mechanical stability. [68].

Silica-based monoliths have a larger surface area, mechanical stability, solvent resistance, and separation efficiency than organic monoliths, but surface functionalization of silica-based monolithic columns is labor-intensive and time-consuming. Fig.21. Depicts the structures of packed columns and monolithic columns[76].

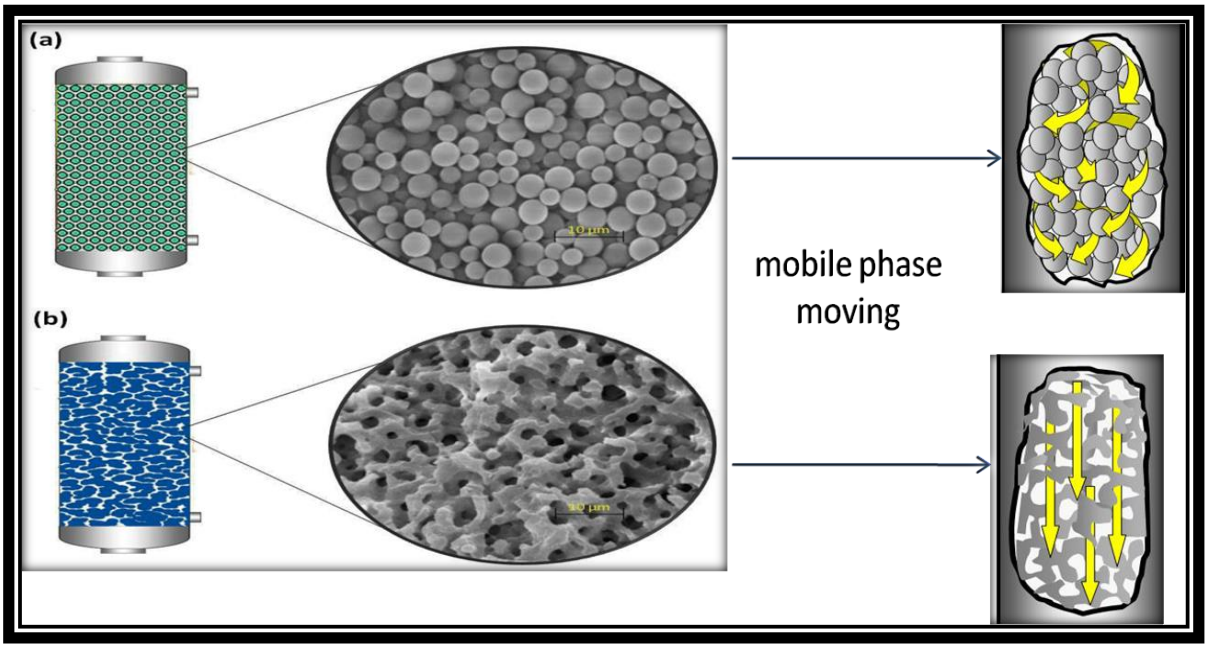

Figure (1.21)The difference in mobile phase movement in (a) packed column and (b) monolithic column

(1.10.2) Classification of monolithic columns

Monolithic chromatography columns have been made from **organic polymers such as:**(Polystyrenes, polymethacrylate and polyacrylamides-based) and **inorganic polymers such as:**(titania, zirconia, silica). Monolithic columns are classified as either inorganic-based (typically silica-based) or organic polymer-based monolithic columns[77]. released a research of the chemical composition and current uses of these various monoliths as replacements for conventional packed columns in capillary electrochromatography (CEC) and micro-high performance liquid chromatography (μ-HPLC)[78] .

Instead of the three main types of monolithic columns[81], carbon monoliths[72] might be used as an appropriate chromatographic phase, adsorbent[80], catalyst support[79] and porous electrode in constant flow conditions.

(1.10.2.1) Phases of Organic Monoliths

In 1967,at the time where organic monolith phases were in their infancy, (Kubin et al.)[82] developed a nonstop matrix of polymer enabling size-exclusion mode chromatographic separations employing a redox free-radical starting method. A solution,which is aqueous, of twenty two percent 2-hydroxyethylmethacrylate and zero point two percent ethylene dimethylacrylate was polymerized in a twenty five millimeter inner diameter glass tube at room temperature for twenty four hrs.

Svec and Frechet employed macro-porous polymer monoliths, which are physically more stiff, as an effective stationary phase for HPLC in 1997, & until now, they've been put to extensive utilisation in every conceivable chromatographic procedure. These monolithic polymer materials were made utilizing a simple moulding technique involving the polymerisation of a mixture containing monomers, initiators and porogenic solvents [83].

(1.10.2.2) Silica monolithic phases

In the seventies, Pretorious et al. [78] employed a continual porous foam,which is based on silica, as a "chromatographic support" for gas chromatography, describing one of the early attempts to create monolithic silica phases (GC). By hydrolyzing and gelating an alkoxysilane solution which contains poly(sodium styrenesulfonate), Nakanishi and Soga [84] in 1991 described a method for fabricating porous silica monoliths for use in high-performance liquid chromatography (HPLC).

Sol-gel processes can also be used to make inorganic silica-based monoliths [85]. This method of preparation, that happens in a mould, does, however, result in a reduction (shrinkage) of the entire silica structure. The diameters of the products are approximately four point six and seven milimeteres, respectively, when a mould with a diameter of six and nine millimeters is utilized. The silica monoliths ,which are produced as a result, should be coated with

polytetrafluoroethylene (PTFE) tubing or a PEEK resin to make a column for HPLC. Because the column length is limited to 15 cm, long, single and straight monoliths can’t be easily created using the sol-gel process.

Silica-based monolithic columns have also been created by loading fused silica capillaries with octadecylated 6 m particles and then thermally treating them. with dimethyloctadecylchlorosilane, the monolithic packing was reoctadecylated (C18 groups reattached to the monolith) in situ [86].

(1.10.2.3) Hybrid Organic – Inorganic Monolith

Organic-inorganic hybrids're substances that mix 2 or more integrating components at the molecular or nanoscale scale [89]. They are exceptional in a wide range of domains, like: adaptability, durability, biocompatibility, and mechanical qualities. This high level of efficiency is made possible by the uniform distribution of organic functional groups inside the inorganic matrix construction. Because they're versatile and simple to work with, hybrid materials have numerous potential applications in the chemical sciences [40]. Hybrid organic-inorganic monolith has gained significant interest as a possibly perfect material with a large surface area, great selectivity, superior mechanical strength&thermal stability. Hybrid organic-inorganic monoliths may be broken down into two distinct categories, one based on silica (hybrid silica monolith; HSM) and the other on polymers (hybrid polymer monolith; HPM) (HPM). The sol-gel technique is often used to make HSM, which is a monolith formed of a silica precursor incorporating organic moieties [89]. A colloidal solution serving as a precursor for an integrated network polymer is the starting point for most material fabrication using the sol-gel method [90]. Since the sol-gel technique only requires moderate conditions for the reaction and is highly flexible, it has a great deal of untapped promise as a method for creating hybrid inorganic-organic matrices [90,91]. Metal alkoxides and metal salts are common precursors that go through a variety of hydrolysis & polycondensation processes. Although silica-based monolithic materials may offer improved organic solvent tolerance

and mechanical stability, they are limited in their applications due to challenges like poor process control during production and a limited acidity operating range (pH: 2–8)as show on Fig (22).

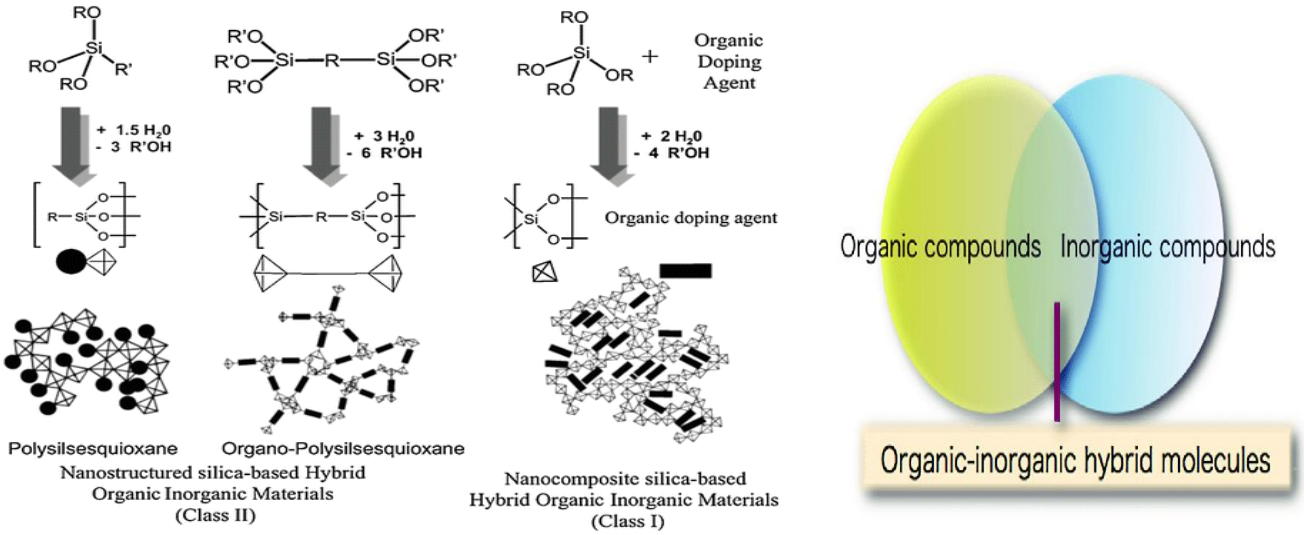

Figure (1.22)Different hybrid Organic – Inorganic Monolith

(1-11) Development of Monolithic Materials in Chromatography

Catalysis [92], filtration [93], electrochemistry [94], and separation sciences [95] are just a few of the applications for porous monolithic materials in science.

Since the 1970s, chromatographic monolithic materials have been created in a variety of shapes, including spheres, layers, rolls, irregular chunks, sponge pieces, tubes and cylinders[96]. These unique monolithic structures were created using a variety of materials, including cellulose is an example of an organic polymer, whereas synthetic polymers such as porous styrene-, methacrylate, acrylamide-based polymers and inorganic materials are examples of synthetic polymers (silica). A lot of focus has been granted to fluidic and surface properties, as well as the uses, of this range of monolithic materials. In LC (meaning liquid chromatography), various substances are separated using micro-particle packed columns (one – ten m), that have a wide surface area in order to react with the mobile phase solutes. In spite of the historical dominance of packed columns as chromatographic separation medium, a new spectrum of

monolithic materials has recently been produced, enabling alternate chromatographic performance and selectivity[96,97].

(1.11.1) Monolithic stationary phases for chromatography[98,99]

Chromatographic band expansion is caused by the following:

A- The existence of multiple flow paths, each with its own unique length and speed.

B- Phase equilibration occurs slowly, particularly in pores on the nanometer scale.

C- Solute diffusion with in fluid phase (mobile phase).

Columns with its particles packed with smaller particles (one-three μm) lead to quicker equilibration and thinner bands, as well as greater efficiency. This is because the contributions of components A and B to total band widening that are reduced (N). The primary drawback of this technique is a significant loss in pressure, which is inversley proportional to the square of the particle diameter. Total porosity of around eighty percent in monolithic columns is associated with much lower backpressures than compacted particle-based columns of around sixty five percent porosity. Therefore, it is assumed that the higher porosity of monolithic columns makes them suitable for strong flow rates. Using UHPLC (which stands for ultra high performance liquid chromatography) and sometimes very high temperatures are required when working with microparticle packed columns that create such high backpressures.[72].

(1.11.2) Monolithic columns have the following characteristics [100].

1. *A seamless, one-piece construction that is mechanically stable and doesn't rely on frits to keep its shape.*

2. *It is very permeable due to its high porosity.*

3. *The fast flow that could be achieved due to the presence of big through-pores and a thin skeleton may lead to quicker separation abilities***.**

Due to their great performance, miniaturization, and other desirable properties, monolithic materials have been implemented as HPLC phases and microfluidic chip columns (101). They were employed as high performance miniaturized columns for HPLC and phases within microfluidic chips, for instance, and a new thin monolithic disk technology based on a polymer monolith as a new stationary phase in the shape of a flat "membrane" which is suitable for protein separation was developed. This novel idea of using short monolithic rigid disks was put utilised in both theory [102] and practice[103].

(1.12) Chromatographic separation using glycidyl methacrylate copolymers as a mixed-mode monolith column.

condensing the carboxy group of methacrylic acid alongside the hydroxy group of glycidol produces glycidyl methacrylate, also known as (2,3-Epoxypropyl methacrylate), an enoate ester. Epoxide ester of enoate. From methacrylic acid and glycid, it is derived [104,105]as showing in Fig (23).

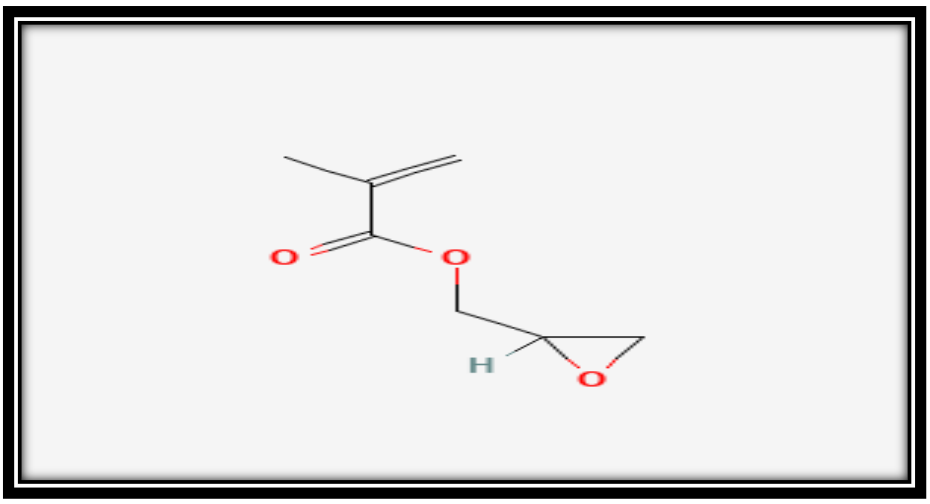

Figure (1.23) Glycidyl methacrylate(GMA)

The polymerization process of glycidyl methacrylate to form different polymer; therefore, PGMA is a one-of-a-kind structure that can be purified and stored in its homopolymer structure with a lot of control over the production procedure[106]. To further expand the spectrum of structures and applications of the final materials, co-polymerization with any other acrylate or methacrylate

monomer is feasible. 1–16 to obtain functionalised polymers, the epoxy side chains of PGMA can be treated to a nucleophilic ring-opening process under a variety of circumstances Fig (24). Because of the large range of chemistry accessible, the nature of the functional group and the manner of the ring-opening reaction can be arbitrarily chosen. PGMA's flexibility distinguishes it as a versatile and effective reactive scaffold in polymer chemistry[107].

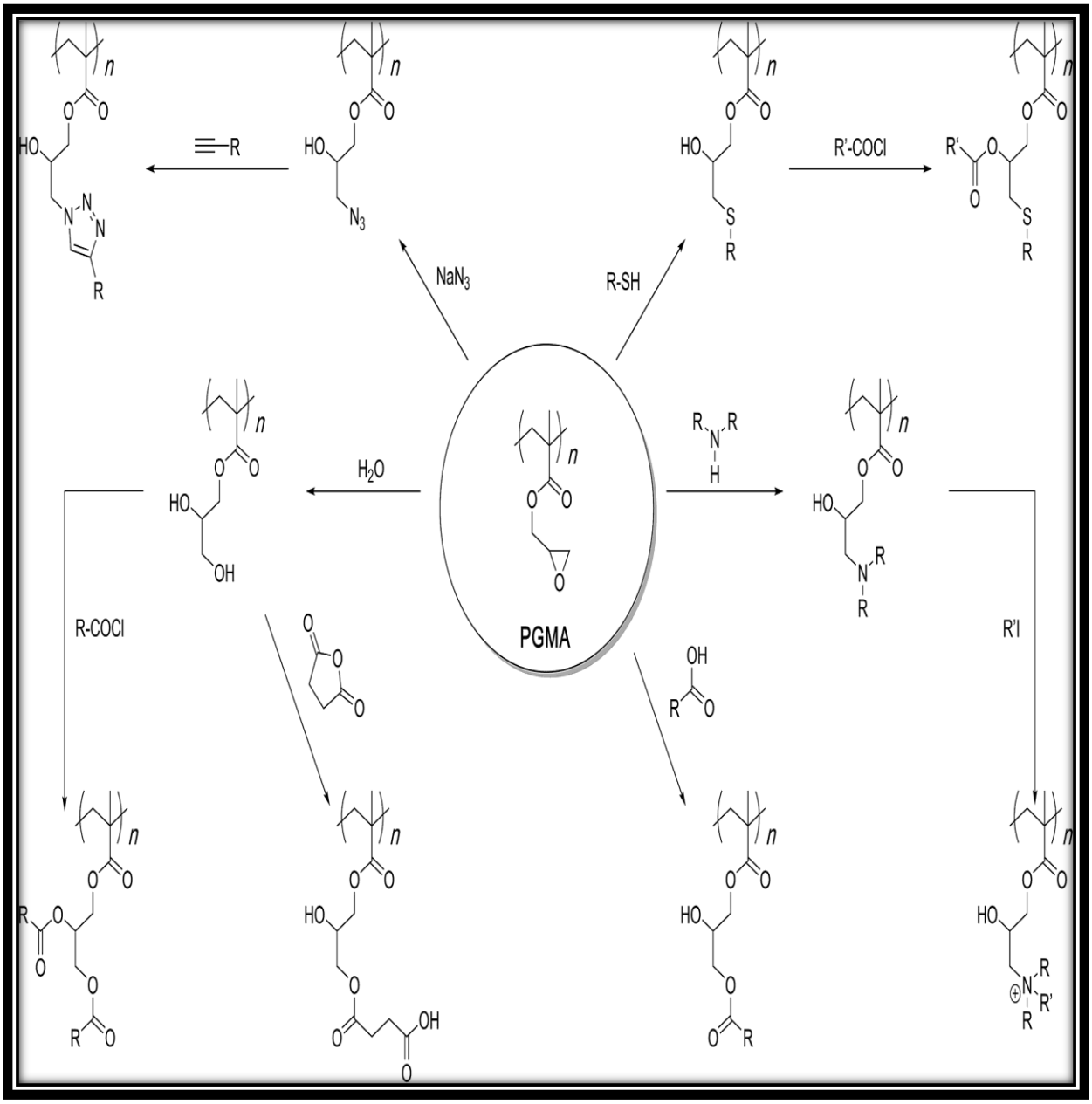

Figure (1.24) Scheme Polyglycidyl methacrylate post-polymerization modification processes.

(1.13) Different methods for various samples determination by Chromatography technique.

It is possible to analyze a wide variety of samples using chromatography. Chromatography and other techniques are given in tables (1.2) & (1.3), accordingly.

Table (1.2) Some of Chromatography techniques for the determination of different samples.

Seq.	Method	analytes	λ_{max} (nm)	Linear range	Detection limit	Application	Ref.
1	Online Column Switching Liquid Chromatography	clenbuterol (CLEN) and doxazosin (DOX)	250	75.0 ng/mL–200.0 µg/mL for CLEN and 37.5 ng/mL–100.0 µg/mL for DOX	8.47 and 25.66 ng/mL for CLEN and DOX	Pharmaceutical products	**108**
2	RP-HPLC and HPTLC	Ciprofloxacin Hydrochloride, Of loxacin, Tinidazole and Ornidazole	272.2, 292, 316.8, and 317.4 nm respectively.	y = 12.835x – 18.032, y = 33.788x – 47.343, y = 14.233x + 32.164, and y = 15.602x + 35.822, respectively	0.22 µg.mL-1, 0.40 µg.mL-1, 0.19 µg.mL-1, 0.37 µg.mL-1, respectively	Pharmaceutical products	**109**
3	RP-HPLC and HPTLC	Carve dilol	245	µg 200-10 mL^{-1} and 2.0-37.4 µg/spot	29 µg $mL^{-1}$and 0.05 µg/spot respectively .	Pharmaceutical products	**110**
4	(HPLC)	Amlodipine (AML)	465	2-30µg/mL	0.01µg/mL	Pharmaceutical products	**111**

5	RP-HPLC	Naproxen	254	0.5 to 80 ppm	10 ng/mL	Pharmaceutical products	**112**
6	capillary gas chromatography	Epichlorohydrin (ECH)	-------	0.6 to 3.4 µg/mL	0.15 µg/mL	Pharmaceutical products	**113**
7	RP-HPLC	Sertaconazole nitrate(SER)	260	10 to 500 µg/ml	0.1 µg/ml	Pharmaceutical products	**114**
8	Gas Chromatography	polycyclic aromatic hydrocarbons (PAHs)	----------	0.64×10^{-7} to 3.16×10^{-7}	(1×10^{-6})	Pharmaceutical products	**115**
9	RP-HPLC	Polythiazide	265	12.5–500 ng/m of prazosin and 6.25–250 ng/ml of polythiazide	0.0125 µg/ml of prazosin and 0.01875 µg/ml of polythiazide	Pharmaceutical products	**116**

Table (1.3): The other methods for determination the plant, biological and environmental samples by Chromatography technique.

Seq.	Method	Analytes	Part of Plant	Type of Elution/Mobile Phase	Conditions	Detector	Ref.
1	HPLC monolithic columns	quercetin, naringenin, ,naringin myricetin, rutin, kaempferol	tomatoes	/isocratic elution A: 50 mM phosphate buffer pH = 2.2)/ACN) ((75:25, v/v B: 2 mM formic acid/ACN (75:25, v/v)	1.0 mL/min/ 25 ◦C/one column	A: UV B: MS	117
2	TLC, HPLC, UPLC-ESI-QTOF-MS and LC-SPE-NMR	fingerprinting	aerial parts from Ipomoea aquatica	/gradient elution MeOH/H2O containing 0.05% TFA	1.0 mL/min/ 25 ◦C/two columns	UV	118
3	Ultrafast UPLC-ESI-MS and HPLC with monolithic column	vanillin, vanillic ,acid p-hydroxybenzoic ,acid p-hydroxybenzaldehyde	pods from Vanilla planifolia	isocratic elution/ACN/0.05 % TFA in H2O (12:88, v/v)	4.0 mL/min/ 35 ◦C/one column	PDA	119
4	LC columns.	glycyrrhizic and glycyrrhetinic acids	roots from Glycyrrhiza glabra	gradient elution/H2O/ACN both acidified with 0.05% TFA	2.5 mL/min/room temp./one column	PDA	120
5	(LC–MS)	proanthocyanidins	pea from Pisum sativu ,m lentil from Lens culinaris,faba bean from Vicia faba	/gradient elution H2O/ACN both with 1% acetic acid (v/v)	3.0 mL/min/ 30 ◦C/two columns	DAD	121
6	(HPLC-CE)	niaziridin and niazirin	leaves, pods, and bark from Moringa oleifera	isocratic elution MeOH/sodium dihydrogen phosphate–acetic acid buer (0.1 M, pH = 3.8) (20:80, v/v)	0.7 mL/min/ 25 C/one column	PDA	122
7	HPLC	geraniin, ellagic acid, gallic acid	rind from Nephel	isocratic elution/ACN/H2O	0.5 mL/min/room	UV–Vis	123

			ium lappaceum	(30:70, v/v)	temp./one column		
8	(HPLC-UV)	,rutin isorhamnetine-,3-O-rutinoside isorhamnetine-,3-O-glukoside ,quercetin isorhamnetin	berries from Hippophaë rhamnoides	gradient elution/H2O/ACN (both acidified with 1% acetic acid)	3.0 mL/min/ 40 Cº/one column ppm	UV	[124]
9	(HPLC-CL)	α -solanine and -chaconine	potato tubers	isocratic elution/20 mM phosphate buffer (pH = 7.8)/ACN (65:35, v/v)	0.6 mL/minone column	CL	[125]
10	centrifugal partition chromatography (CPC)	lysergol and chanoclavine	seeds from Ipomea muricata	isocratic elution ACN/0.01 M sodium dihydrogen phosphate buffer (with 0.2% (TFA (pH = 2.5) (15:85, v/v)	1.0 mL/min/ 25 Cº/one column	PDA	[126]
11	HPLC stationary phases of monolithic	vitamins K3, D3, E, and A	capsules and pediatric drops	isocratic elution /ACN/MeOH both with 0.1% (v/v) formic acid (pH = 2.6, 25: 75, v/v)	4.0 mL /min /room tem /one *colu*	DAD	[127]
12	LC-ESI-MS/MS	aspirin and dipyridamole	human plasma	isocratic elution/MeOH/0.1% formic acid in H2O (90:10, v/v)	1.0 mL/minone column	MS/MS	[128]
13	LC-MS/MS	codeine	human plasma	isocratic elution ACN/10 mM acetic acid (pH = (3.5 (50:50, v/v)	1.0 mL/min/ 25 Cº/one column	MS/MS	[129]
14	SPE-HPLC	Chloramphenicol	human blood	/isocratic elution mM 100 phosphate buffer (pH = 2.5)/ACN (75:25, v/v)	1.5 mL/min/ 28 Cº/one column	UV–Vis	[130]
15	(HPLC -UV)	cefadroxil, cefaclor, ,cephalexin cefotaxime, cefazolin, ,cefuroxime cefoperazone and ceftiofur	milk	gradient %0.1elution /formic acid MeOH/ACN (75:25 v/v)	1.5 mL/min/-/one column	PDA	[131]
16	LC-MS/MS	dapsone and N-	human	isocratic	0.8	MS/MS	[132]

		acetyl dapsone	plasma	elution/ACN/2 mM ammonium acetate in H2O (90:10, v/v)	mL/mino ne column		
17	(Ultra-HPLC)	retinol and -tocopherol	serum and human breast milk	100% MeOH	1.5 mL/min/ 50 Cº/one column	FL	[133]
18	(UV- monolithic column) off-line	Ni^{+2} and Cu^{+2}	Water waste	isocratic t Elution (pH = 8 for Ni^{+2} & pH = 4 for Cu^{+2} (30:70, v/v) (GMA-co-ACA co-AAM)	30µl/min 25 Cº/one column	UV and Atomic flam	research study
19	(FIA- HPLC monolithic column) On-line	Ni^{+2} and Cu^{+2}	Water waste	isocratic Elution (pH = 8 for N^{i+2} & pH = 4 for Cu^{+2} (30:70, v/v) (GMA-co-ACA co-AAM)	50µl/min 25 Cº/one column	UV and Atomic flam	research study
20	(FIA- HPLC microchip) On-line	Ni^{+2} and Cu^{+2}	Water waste	isocratic Elution (pH = 8 for Ni^{+2} & pH = 4 for Cu^{+2} (30:70, v/v) (GMA-co-ACA co-AAM)	50µl/min 25 Cº/one column	UV	research study

(1.14) Aims of Study

1. Investigation and preparation of chromatographic monolith columns .
2. Investigate different monomers and cross linker to form suitable monolith.
3. Off-line and online methods for incorporation ions with the monolith column.
4. Chromatography was connect to flow-injection and microfluidic injection techniques.U.V polymerization will be used to form desire polymer.
5. Implementing the plan on Al-Ma'amira heavy water treatment plant in Hilla.

2. Chemicals and Apparatus

(2.1) Apparatus

The table (2.1) illustrated the devices and their information, which are used in the present study.

Table (2.1): Devices and tools used in this study

Seq.	Device and tools	Manufacturer
1	**Electronic analytical balance with four decimal places**	**Denver Instrument, Germany**
2	**UV-Visible spectrophotometer, double-beam**	**Shimadzu (UV-1700), Japan**
3	**UV-Visible spectrophotometer, single-beam**	**PD-303UV APEL, Japan**
4	**Dual syringe pump**	**U.S.A (Kd Scientific)**
5	**intelligent HPLC pump**	**PU-980, Italy (JASCO)**
6	**Irradiation device**	**locally manufactured**
8	**Hot plate**	**Ardeas 51, Germany**
9	**3 way valve medical**	**German**
10	**Thermometer**	**Chine**
12	**valve with six different way Binary**	**Homemade**
13	**pH-meter**	**German**
14	**Water bath and shaker**	**M00/M01Memmert, Germany**
15	**Glass column (borosilicate tube)(60 mm)**	**Germany**
16	**polyetheretherketone (PEEK) tube**	**UK**
17	**Microfluidic chip with Monolith column**	**Homemade**
18	**Microfluidic chip**	**Homemade**
19	**Glass syringe**	**SGE 009760**
20	**stainless steel tubing HPLC throughout of ID=0.5 mm**	**Germany**
21	**Micropipettes (10-50)µl &(100-1000)µl**	**Chine**
22	**Sonicator ultra sonic bath**	**India**
23	**Valve HPLC (operate at pressures up to 17400 psi) multi-position valve, 6 ports**	**Germany**
24	**Atomic Absorption Spectroscopy**	**SHIMADZU AA-6300**
25	**Brunauer-Emmett-Teller (BET)**	**BEL, Model: BELSORP, Japan**
26	**Proton nuclear magnetic resonance**	**Model: Innova 5 Concole with an**

27	**(^{1}HNMR)** **Field Emission Scanning Electron Microscopy (FESEM)**	**Oxford 500 Magnet, Country: United state** **TESCAN, Model: Mira3, Czech Republic**
28	**Syringe pump**	**Bioanalytical System Inc., USA**
29	**FT-IR 380 spectra**	**Bruker**

(2.2) Chemicals

Table (2.2) shows the substances employed in the current study.

Table (2.2): Chemicals used in this study.

Seq.	Name	Formula	Molecular weight (g/mol)	Purity %	Supplier
1	3- (trimethoxysilyl) propylmethacrylate	$C_{10}H_{20}O_5Si$	248.35	98.00	Sigma-Aldrich
2	Glycidyl methacrylate	$C_7H_{10}O_3$	142.15	97.00	Sigma-Aldrich
3	Ethylene dimethacrylate	$C_{10}H_{14}O_4$	198.22	98.00	Sigma-Aldrich
4	2, 2-Dimethoxy-2-phenylacetophenone,(DAP)	$C_6H_5COC(OCH_3)_2C_6H_5$	256.30	99.00	Sigma-Aldrich
5	(2- diethylamino) ethyl methacrylate	$C_{16}H_{16}O_3$	256.30	97.00	Sigma-Aldrich
6	Acrylic acid	$C_3H_4O_2$	72.06	99.00	Sigma-Aldrich
7	Acrylamide	CH_2=CHCONH$_2$	71.08	≥98.00	GCC
8	Sodium sulfite	Na_2SO_3	126.04	≥98.00	BDH
9	Sodium bisulfite solution	$NaHSO_3$	104.06	40	BDH
10	Acetone	C_3H_6O	58.08	99.80	Sigma-Aldrich
11	Sodium hydroxide	NaOH	40.0	99.00	BDH
12	Hydrochloric acid	HCl	36.46	39.00	Fluka

13	1-Propanol	C_3H_8O	60.1	99.50	Merck
14	2-Propanol	C_3H_8O	60.1	99.70	Merck
15	Sodium sulphate	Na_2SO_4	142.04	99.00	BDH
16	2-Butanol	$C_4H_{10}O$	74.12	99.50	Riedel-de Haen
17	Methanol	CH_4O	32.04	99.50	BDH
18	Hexanol	$C_6H_{14}O$	102.17	99.85	BDH
19	Formic acid	HCO_2H	46.02	85.00	Thomas Baker
20	Benzene	C_6H_6	78.11	99.00	Sigma-Aldrich
21	Chloroform	$CHCl_3$	119.38	99.00	Scharlau
22	Dichloromethane	CH_2Cl_2	84.93	≥99.80	Sigma-Aldrich
23	Sulphuric acid	H_2SO_4	98.07	98.00	GCC
24	Diethyl ether	$(CH_3CH_2)_2O$	74.12	≥99.70	Sigma-Aldrich
25	N,N-Dimethylformamide(DMF)	$HCON(CH_3)_2$	73.09	≥99.80	GCC
26	Dimethyl sulfoxide(DMSO)	$(CH_3)_2SO$	78.13	≥99.90	GCC
27	2,6,8-Trihydroxypurine(Uric acid)	$C_5H_4N_4O_3$	168.11	≥99.90	Sigma-Aldrich
28	Nickel(II) nitrate	$Ni(NO_3)_2$	182.703	≥97.00	Sigma-Aldrich
29	Copper(II) nitrate trihydrate	$Cu(NO_3)_2 \cdot 3H_2O$	241.60	99-104	Sigma-Aldrich
30	Nitric acid	HNO_3	63.01	70.00	Himedia

(2.3) Fabrication of the monolithic column materials

The monolith was fabricated inside a 60 mm borosilicate tube with a (1.5 mm) inner diameter and a (3.0 mm) exterior diameter. The borosilicate tube was

connected to the polyetheretherketone (PEEK) tubing with a stainless reduction steel union 1/8" to 1/16" adapter, and the PEEK tubing was connected to the glass syringe with a microtight adapter. For the polymerization process, all solutions were pumped into the borosilicate tube using a syringe pump. A image of the experimental setup for fabricating the polymer-based monolith is shown in Figure (2-1).

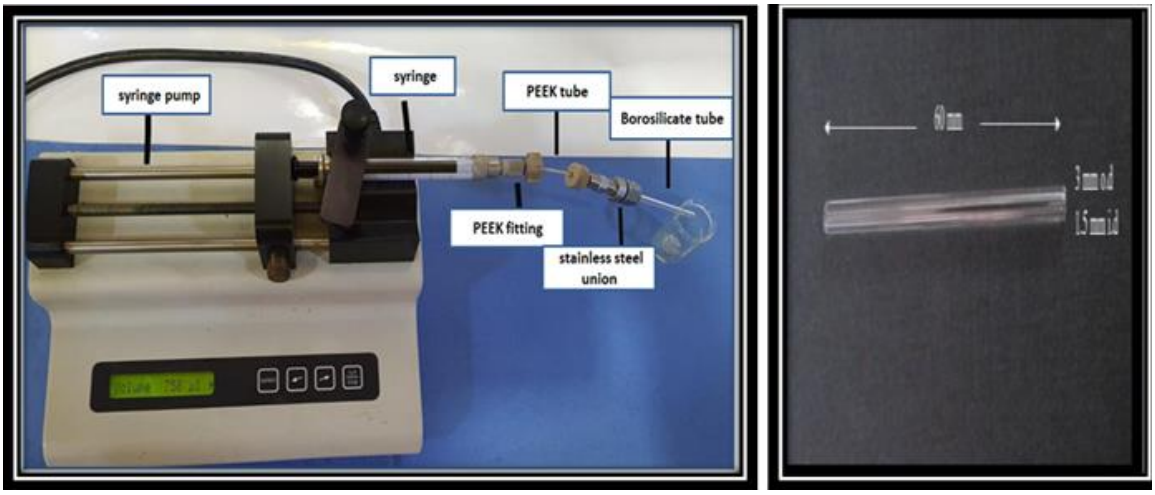

Figure 2.1 Photograph for fabrication of the polymer based monolith.

(2.3.1) Fabrication of the microchip for monolithic materials

The glass microchip has been produced, however it has two 1.5 mm diameter holes on the top layer that were drilled using typical glass drilling procedures for the intake and outflow of the mobile phase. The microchip was bonded to the PEEK tubes with epoxy glue, and the syringe pump for silanization was then linked to it as shown in Figure (2.2).

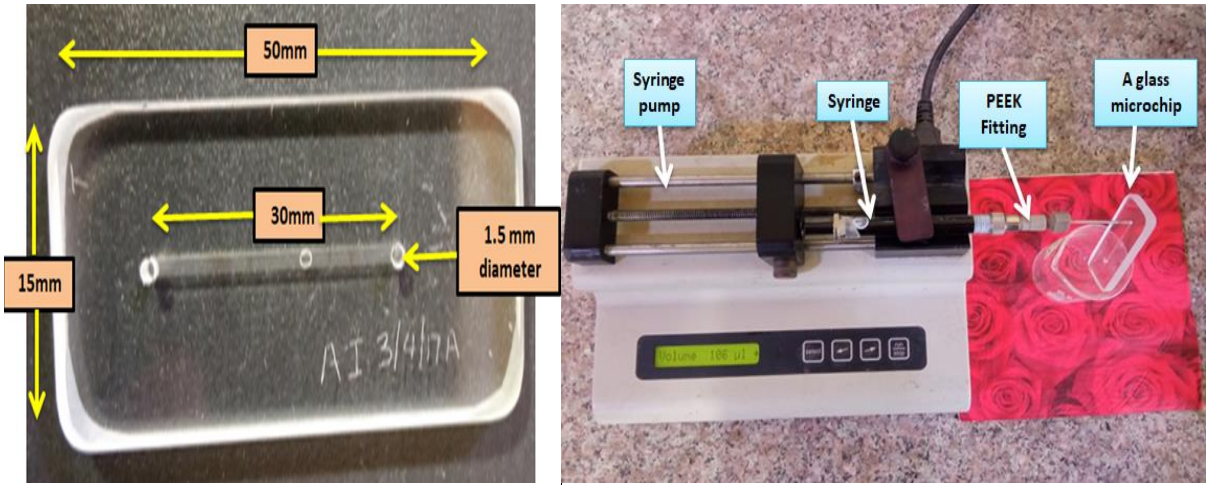

Figure 2.2 Microchip device design for LC separation.

(2.3.2) Silanization step to preparing the inner surface of the tube

To ensure that the polymer formed inside the glass tube does not come out or displace at different pumping rates, as well as to stabilize the bonding of the polymer formed inside the glass tube. This process is accomplished by washing the tube with acetone, then water, and then activating the inner surface of the borosilicate tube with a 0.2 M sodium hydroxide solution for 1 hour. After that, it was rinsed with water, then treated with a 0.2 M hydrochloric acid solution for 1 hour. After that, it was flushed with water, then ethanol, and lastly silanized with a 20 percent solution of 3-(trimethoxysilyl) propylmethacrylate in ethanol. After being dried with nitrogen gas, the borosilicate tube was ready for polymerization.

(2.3.3) Polymerization step

Based on the method of preparing the polymer made by (Ueki) with some modifications that fit the study.The monolith (GMA-co-ACA co-AAM) as (0.4 mL of GMA,0.2 mL of ACA a 0.3 mL AAM, 0.05 mL (EDMA) as a cross-linking agent and 2,2-Dimethoxy-2-phenylacetophenone (corresponding to 1 wt% of the amount of total monomers) was added to the monomer solution as an initiator. All these compounds were dissolved into porogenic solvent (1mL of

ehanol , 0.6 mL of hexanol). After purging with nitrogen for 5 min to remove the oxygen ,the monolith was synthesized by a free-radical polymerization. The distance between the lamp and the borosilicate tube was 10 cm. The monomer solution was immediately pumped inside the borosilicate and the two ends of the tube was closed using robber stopper . The polymerization process was left to proceed for 3min at UV light using UV lamp at 365 nm for anticipated irradiation time. The monolithic synthesized and washed with ethanol after with water to remove the porogenic solvent and remaining monomers present in the column. is shown in Fig (2-3).

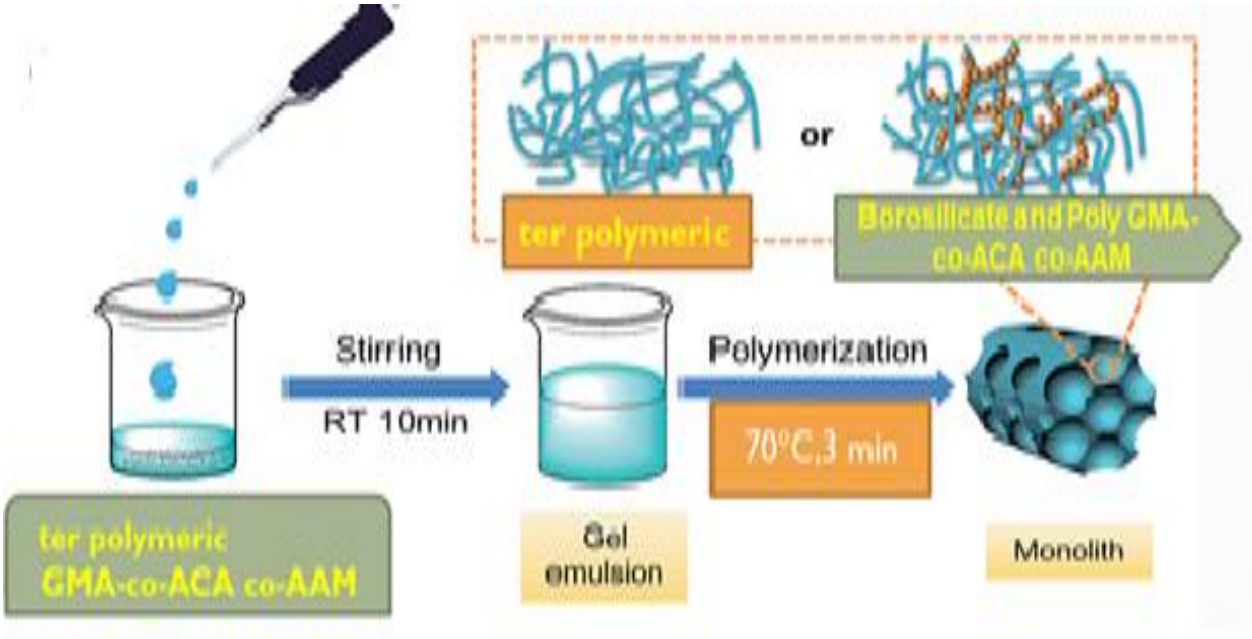

Figure 2.3. Photograph for Polymerization step.

(2.3.4) Preparation of monolithic column

The mixed mode monolithic columns were made using the procedures outlined in table 2.3. The monomers were studied in a variety of kinds and ratios, while the (v/v) ratio of monomers to cross-linker and initiators remained constant respectively (50 µl, 1%) .

Table 2.3 The monomers that are used to prepare the monolith column

					progen solvent	
NO.	Monomers ratio (v/v)	Monomer (GMA) mL	Monomer (ACA) mL	Monomer (AAM) mL	solvent (1) µL	solvent (2) µL
1	90---10	0.81	0	0.09	1-Propanol 1000	hexanol 650
2	10---90	0.09	0	0.81	1-Propanol 1000	hexanol 650
3	50----50	0.45	0	0.45	1-Propanol 1000	2-butanol 650
4	50----50	0.45	0.45	0	1-Propanol 1000	2-butanol 650
5	10---90	0.09	0.81	0	1-Propanol 1000	2-butanol 650
6	90---10	0.81	0.09	0	1-Propanol 1000	2-butanol 650
7	50----50	0	0.45	0.45	1-Propanol 1000	2-butanol 650
8	90---10	0	0.81	0.09	1-Propanol 1000	hexanol 650
9	10---90	0	0.09	0.81	1-Propanol 1000	hexanol 650
10	50--50--50	0.3	0.3	0.3	ethanol 1000	hexanol 650
11	60-20--10	0.6	0.21	0.09	ethanol 1000	hexanol 650
12	60-10--20	0.6	0.09	0.21	ethanol 1000	hexanol 650
13	40--20-30	0.4	0.2	0.3	ethanol 1000	hexanol 650

(2.3.5) Investigation of the irradiation distance

The influence of distance between the irradiation source at 5 to 25 cm , and the prepared separation column was investigated in order to determine the ideal distance for polymer formation inside the separation column.

(2.3.6)The effect of irradiation time

The irradiation time was investigated for each to prepare monolithic column that has high surface area and reasonable pore size, at using a variety of irradiation periods ranging from (1-6) min.

(2.3.7) Effect of porogenic solvents

The porogenic solvent can play an important role in the monolith formation, therefore, the composition of the porogenic solvent is by using (ethanol) besides other solvent that listed in.

(2.3.8)Limitation of Swelling Percentage

The swelling percentage of the monolith was measured using a variety of polar and non-polar solvents, including water, methanol, ethanol, benzene, and

acetonitrile, among others. Specific weights of the polymer were taken and submerged in the aforementioned solvents, and the weight of the monolith was then measured. The monolith of Swelling ratio was calculated according to equation:-

$$(\boldsymbol{Swelling\ ratio = Wwet - Wdry/Wdry \times 100} \qquad (\mathbf{1-2})$$

(2.3.9)Calculation chelating capacity for monolith column.

A capacity of the monolithic column was calculated by the following expression[133] :

$$(\mathbf{Q = (C * V)/W}) \qquad (\mathbf{2-2})$$

where Q is the chelating monolith column of adsorption capacity (mmol.g-1), V is the eluate of volume (L), C is the concentration of (M^{2+}) in the eluate (mmol.L^{-1}), and W is the dry weight of the monolith inside the column (g).

(2.3.10) Ring opening reaction of (GMA-co-ACA-co-AAM) monolithic column.

The epoxy ring in glycidyl methacrylate monomer was opened using reaction, sulfonation of the epoxy ring to form cationic/hydrophobic interactions using sodium sulfate.

The epoxy group was sulfonated by pumping a sulfonation solution using syringe pump that contained dimethyl sulfoxide (0.54 mol L-1.) as cationic surfactant and 2.52 g (1 mol L^{-1}) of sodium sulphite anhydrous was dissolved in 10 mL of distilled water ($NaHSO_3$/water/DMSO) =1/7/3 (weight ratio)for 2 hours at 5 μL min-1 in column block heater at 70 ºC. Then the monolith was washed with 10 mM HCL at 5 μL min-1 for 1 hour, finally washed with water for 2 hours.

2.4 Characterization of monolithic material

(2.4.1) (BET) Analysis & Scanning electron microscope (SEM).

The Brunauer-Emmett-Teller (BET) model analyser BJH (Barrett-Joyner-Halenda) model was used to evaluate the monolith of surface area and average pore size. To extract the monolith easily from the disposable plastic syringe, the monolith was created within (1 mL) a disposable plastic syringe following the procedure described in 2.3 without the silanization step. The unreacted components were then washed away using ethanol and water. The monolith was dried at 60 degrees Celsius in a column block heater. The surface area and average pore size of the monolith were determined using the BET isotherms of nitrogen adsorption and desorption at 77 K. A scanning electron microscope (Zeiss EVO 60) was used to characterize the morphology of the monolithic columns that have been prepared.

(2.4.2)Porosity measurement

The total porosity of the monolith was determined using the Fletcher et al. method, which involved weighing the monolith when it was dry (i.e., all pores contained only air) and then filling it with deionized water using a syringe pump for 3 hours to ensure that the monolith was completely filled with deionized water. Using the equation below, the porosity was calculated.

$$\boldsymbol{Ø_T = (W_M - W_T) / dLR^2 \pi} \qquad (\mathbf{2-3})$$

Where: $\boldsymbol{Ø_T}$= Total porosity **,** $\boldsymbol{W_M}$**=** Weights of the monolith when filled with water, $\boldsymbol{W_T}$**=** Weights of the monolith when dried **, d**=Density of water, **L**=Length of the monolithic column **,R**= the column's cylindrical radius.

(2.4.3)Permeability of the monolith

The backpressure generated by the HPLC system pump was used to test the monolith permeability. The pressure value was recorded once the pressure was stabilized.

(2.5)Synthesis of imidazole-azo ligand ((E)-2-((4 methoxyphenol)diazenyl)-4,5-diphenyl-1-Himidazole.

Dissolve 1.23 g (0.01 mol) of the compound (p-methoxy aniline) in a mixture of distilled water and hydrochloric acid (37%) (30 ml distilled water + 3 ml hydrochloric acid), cool to a temperature (0-5°C) and add to cold solution of sodium nitrite ($NaNO_2$) that prepared by dissolving (0.8 g) in (15 mL) distilled water and the mixture was left for 15 minutes to complete the denitrification process. After completing the denitrification process, a solution of diazonium salt was added gradually and very slowly with shaking.

The reagent solution was prepared by dissolving 2.2 g (0.01 mol) of the compound (5.4 diphenylimidazole) in 50 ml of ethanol. mixed with a solution consisting of dissolving 1 g of sodium hydroxide in 10 ml of distilled water, to give a red-orange color indication of the occurrence of the duplication process, and after completing the addition process, 100 ml of ice water was added, and then the acidity function was adjusted, and the mixture was left with stirring for half an hour, after which it was filtered and dried, and the precipitate was recrystallized with ethanol.

(2.5.1) (FT-IR) spectroscopy ,(C.H.N) and 1HNMR analysis for synthesis of Schiff base ligand.

To identify the presence of particular chemical groups in the ligand, FTIR was used in the transmittance mode. The 3500-1000 cm^{-1} spectral region was used to record the spectra. The proper metal to ligand ratio of the compounds was found using the elemental analysis (CHN) of the Schiff base and the complexes. The ^{1}HNMR spectra of the ligand was recorded in DMSO-

D6. The ^{1}HNMR spectrum of the ligand shows the following signals: phenyl multiples at (7.1 -8) δ range .

(2.5.2) Effect of new reagent concentration and pH buffer concentration.

The concentration of reagent was studied at the range ($1x10^{-6}$-$1x10^{-3}$) M. While the optimum pH range for the complex formation was examined using buffer solution consisting of 0.2M NH_4OH and 0.2M HCl at range (3.5-8).

(2.6) Stock solutions.

(2.6.1) 0.2 mol.$L^{-1}$of HCL.

This solution was prepared by adding 1.7 mL of concentrated hydrochloric acid to a volumetric flask filled with 100 mL of water (35% (w/w) purity hydrochloric acid and 1.18 g/mL specific gravity). The volume was then filled to the desired level. After standraztion for HCl it was titrated with sodium carbonate and using Methyl red as a guide, where (10) ml of the previously prepared 0.1 M sodium carbonate solution was taken and placed in a volumetric flask, to which two drops of the guide were added while the burette was filled with 0.1 M hydrochloric acid solution. The blunt was repeated three times, each time according to the volume of acid coming down from the burette needed to change the color of the solution from yellow to pink. Vaverage was

extracted and the following law was applied to calculate the exact molarity of the acid:(M X V) Na2CO3 = (M? X Vaverage) HCl

The smear results showed that the true molarity of the acid is 0.094 molar.

(2.6.2) 0.2 mol.$L^{-1}$of NaOH.

This solution was prepared by combining (0.8 g) of sodium hydroxide with (50 mL) of distilled water in a dry, clean beaker. Once the mixture had completely dissolved, it was transferred to (100 mL) of a volumetric flask, where the volume was then completed to the desired level. It was titrated using pre-titrated hydrochloric acid and phenonphthalein indicator, where (10) ml of 0.094 hydrochloric acid was taken and placed in a volumetric flask, to which two drops of the guide were added while the burette was filled with 0.1 M NaOH solution. The slurry was repeated three times, each time according to the size of the base coming down from the burette needed to change the color of the solution from colorless to pink. (V)average was extracted and the following law was applied to calculate the exact molarity of the base:

(M X V) HCl = (M? X V average) NaOH

The deformation results showed that the true molarity of the base is 0.132 molar

(2.6.3) 200 mg. L^{-1} of Nickel (II) Solution .

After adding 50 mL of distilled water to 0.1556 g of nickel (II) nitrate in a dry, clean beaker to dissolve it, the solution was transferred to a (250 mL) volumetric flask, and the volume was then filled to the mark with distilled water. Subsequently, several solutions were made with varying concentrations of the original solution.

(2.6.4) 200 mg.L^{-1} Copper (II) Solution .

After adding 50 mL of distilled water to 0.1900 g of copper (II) nitrate, the solution was dissolved. It was then transferred to a 250 mL volumetric flask and the volume was topped off with distilled water. Subsequently, a series of solutions were made with varying concentrations from the original solution.

(2.6.5) 100 mg.L^{-1} Neocuproine reagent .

Neocuproine, 0.01 g, was added to a dry, clean beaker along with 5 mL of ethanol, and when it had completely dissolved, the solution was transferred to a 100 mL volumetric flask where distilled water was used to bring the volume up to the desired level.

(2.7) Design and fabrication of microchip device for connected FIA-HPLC.

A glass microchip with the dimensions of 50 mm in length and 15 mm in breadth was created from B-270 crown glass (SKAN). It had two layers, each of which was 3 mm thick. Traditional glass drilling methods were used to make the two holes (each 1.5 mm in diameter) in the top layer, which serve as the mobile phase's inlet and outflow. The second layer was constructed up of the channel that was machined using a CNC machine; it had the following dimensions: 30 mm long, 1 mm wide, and 500 m deep. The two layers were then thermally fused for three hours at 585 °C to form the chip design. As soon as the chip was ready for use, the monolith was built inside it using the identical techniques shown in 2.3.1 , 2.3.2 and 2.3.3 .The chip was then linked to an FIA-HPLC system to study sample separation.

(2.8) Applications of (GMA-co-ACA-co-AAM) monolithic column.

(2.8.1) Waste water Samples Supplied from Al-Maimira station

These samples were injected after treatments by with HCl (0.2 M) for the determination of Cu (II), Ni (II) in water samples. After opening the glycidyl

methacrylate epoxy ring as described in (2.3.10) the monolithic column performance was investigated to separate diverse range of these ions and the samples were prepared by preparing a stock solution of each compound, then prepared the desire concentration from the stock solution.

(2.7) Lengths and Volumes of The Loops

(2.7.1) Stainless reduction steel and teflon loops

The volumes of stainless reduction steel and teflon loops were calculated depending upon their lengths according to the equation (2-4):

$$\boldsymbol{V = \pi r^2 L} \ldots\ldots (\mathbf{2-4})$$

Where, ***V***, the volume of loop per µL, ***r***, the radius, and ***L***, represents the height of cylinder (length of loop). Note that the diameter of loop is 1.00 mm & Stainless reduction steel diameter is 0.5mm.

Table (2.4): The loops' lengths

Seq.	loop's volume teflon loops (µL)	**loop's volume Stainless steel (µL)**
1	86.35	20
2	117.75	25
3	157.00	30
4	196.25	35
5	235.50	----
6	274.75	----

3. Results and Discussion

(3.1) Investigation and preparation of ion-exchange monolithic column.

The monolithic column was constructed within a borosilicate tube with a length of 60 mm and an inner diameter of 1.5 mm, while the outer diameter is 3 mm, as indicated in Figure (3.1), with the inner surface of the tube was prepared to utilize paragraphs (3.3), (3.2), and the polymerization process.

Chemical resistance, low thermal expansion coefficient, and usage at relatively high temperatures are all characteristics of borosilicate glass. It comes in various shapes and sizes, including rod, tube, and plate, as well as machined and hot-formed parts [134,135]. Therefore, it was chosen to prepare the monolith column.

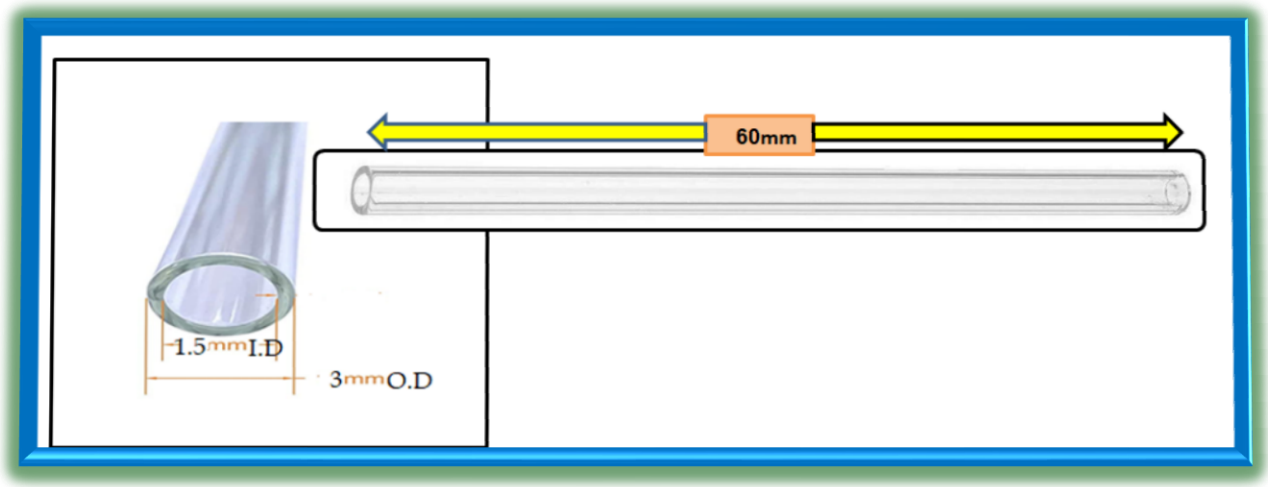

Figure 3.1 Diagram of a borosilicate tube before the siltation step.

(3.2) Preparing the inner surface of the tube (Silanization step)

Preparing the inner surface of the tube is the most crucial stage in forming the monolith within the borosilicate tube. 3-Trimethoxysilyl (propyl methacrylate) reacts with silanol groups (Si-OH) on the borosilicate tube's inner wall.

The process is to install the monolith on the inner wall of the tube and ensure that the polymer does not come out or dislodge when using a high pumping speed. As well as it helps prevent the shrinkage effect during the polymerization process. And avoid interactions that occur with silanol groups .The process of preparing the inner surface of the tube includes several steps. In each of these steps, the solutions necessary for the conditioning process are pumped into the borosilicate tube using a syringe and a flow rate of 5ml min^{-1} for one hour. The first step was to wash the inner wall of the tube using acetone to remove any organic matter, then rinse with distilled water to remove any acetone residue. Then a sodium hydroxide 0.2M solution was used to decompose the siloxane groups and increase the density of the silanol groups, then washed with distilled water to remove any remaining basic solution [(136)].

Furthermore, a hydrochloric acid solution of 0.2M was used to remove residual alkali metal ions; the borosilicate tube was then rinsed with distilled water to remove any residual hydrochloric acid, after which it was washed with ethanol to remove the distilled water. Finally, trimethoxysilyl (propyl methacrylate-3) was injected into a borosilicate tube and allowed to react for 1 hr, after which the tube was dried with nitrogen gas. Now the trimethoxysilane groups are attached to the silanol groups on the surface of the tube, while attached methacrylate groups will contribute to the polymerization reaction, linking the monolith to the inner walls of the glass tube[(137)]. The steps for preparing the inner surface of the tube are shown in the schema and figures (3-2) and (3-3).

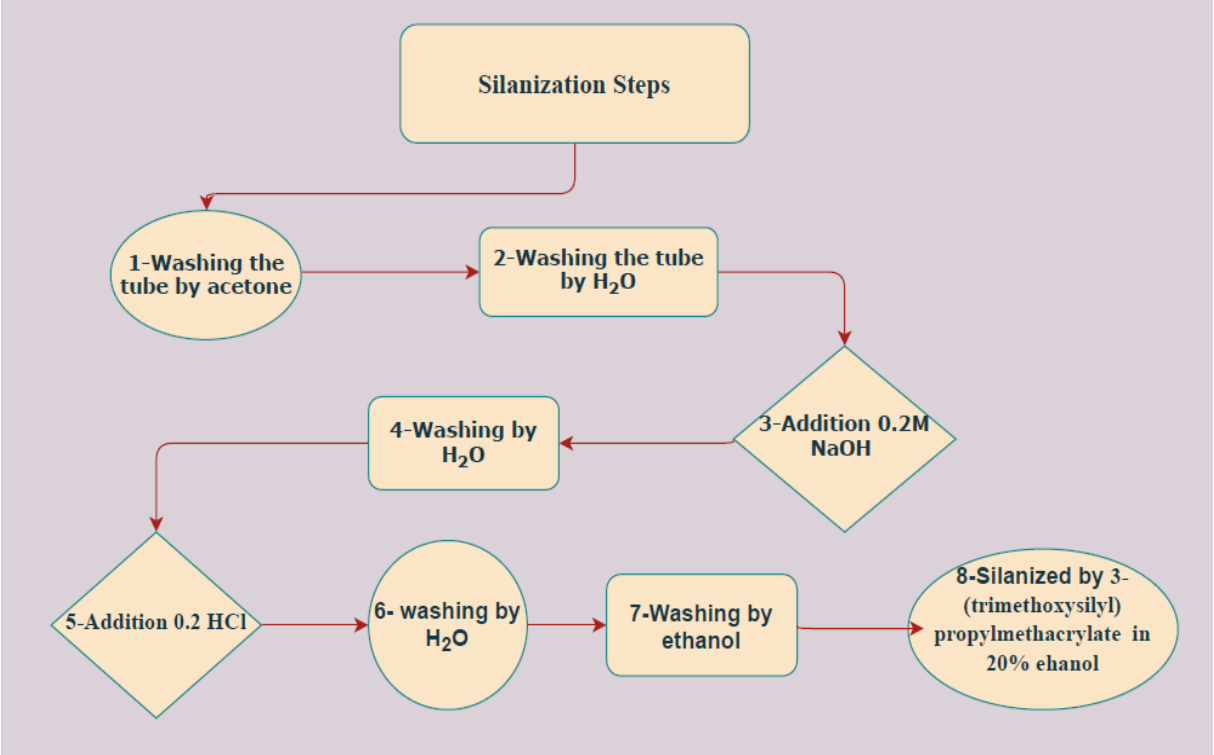

Fig. (3.2): Schematic diagram of the steps of the silanization process

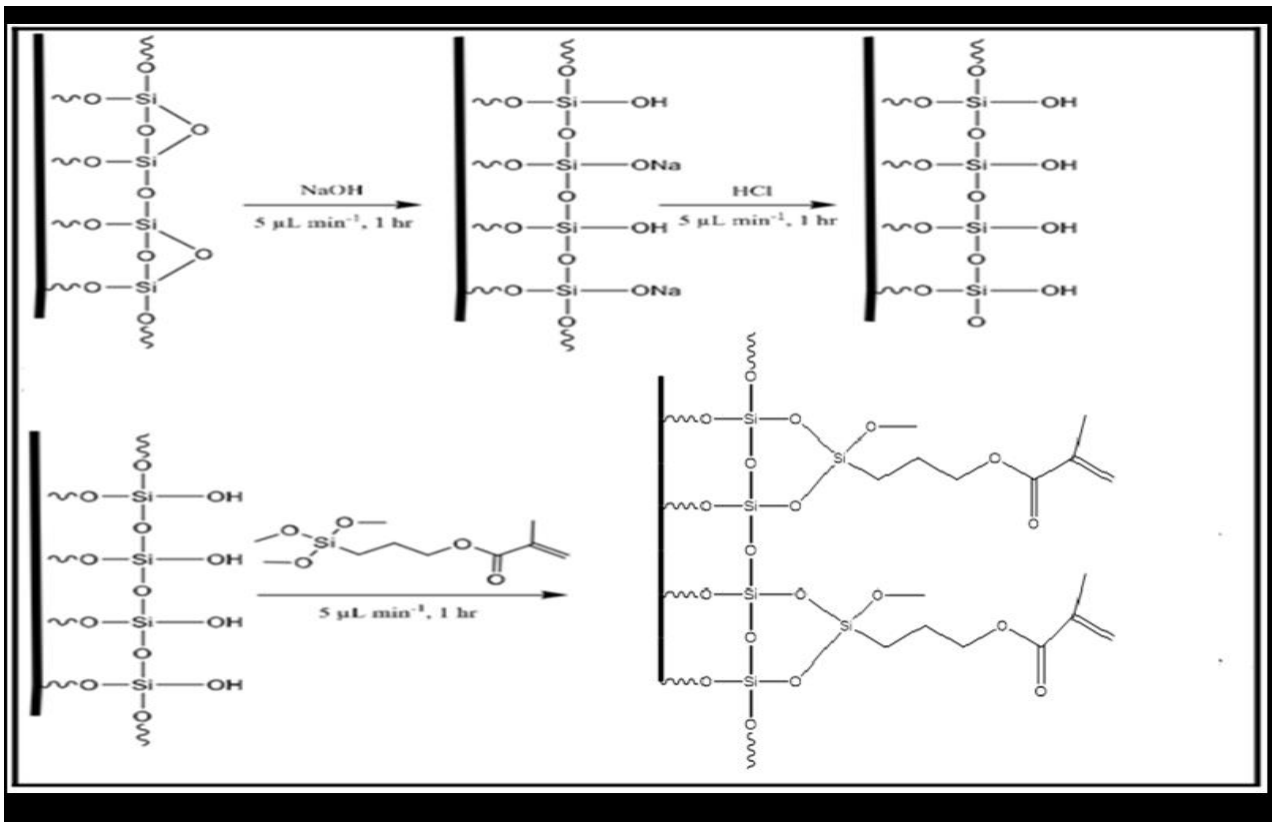

Figure (3-3) Silanization steps of borosilicate tube.

(3.3) The polymerization process

The polymerization process of the organic monolith is prepared from a mixture consisting of (Ter – monomers), glycidyl methacrylate(GMA), Acrylic acid (A. AC) and acryl amid (A.Am) were used to make monolithic columns via free radical polymerization.

(GMA) was chosen because it contains two functional groups, the double bond of methacrylate that participates in the photopolymerization reaction. Epoxide groups can be used in many chemical reactions, as in post-polymerization modification reactions, the production of different functional groups can provide multiple separation mechanisms [(138)]. The cross-linker, porous solvent, and initiator materials have vital in the polymerization reaction and final polymerization.

DMPA (2,2-dimethoxy-2-phenyl acetophenone) was used as an initiator instead of the more common initiator 2,2- azobisisobutyronitrile (AIBN); this was due to some defects when using (AIBN) and one of these defects is the formation of voids due to the rapid reaction and generation of N_2 gas during the polymerization process [(139)]. Ethylene glycol dimethacrylate (EDMA) is a common cross-linking agent to prepare large solid porous monolithic polymers [(140)]. The percentage of the cross-linker to the monomer must be constant because any change will affect the porous properties and the cross-linked chemical composition; for example, if the percentage of the cross-linker increases, the average pore size decreases due to the formation of high and fast-linking cross-linker microspheres, which are helpful in obtaining a monolith that has a large surface area. However, a monolith with a high surface area will have limited solvent permeability and increased back pressure, so the bond-to-monomer ratio should be constant [(141)].

A binary solvent consisting of (methanol and 1-hexanol) was used in the polymerization mixture. The primary role of this solvent is to dissolve the monomers, as well as the cross-linker and initiator, while it does not contribute to the dissolution of the polymer. The polymerization process was carried out by photopolymerization using ultraviolet rays to start the polymerization process of free radicals to form the monolith inside the borosilicate tube, as shown in Figure (3-4), because it has many advantages, such as controlling the pore size, short preparation time and avoiding high temperatures that lead to polymer cracking, controlling the position and length of the porous, and high mechanical strength [(142)].

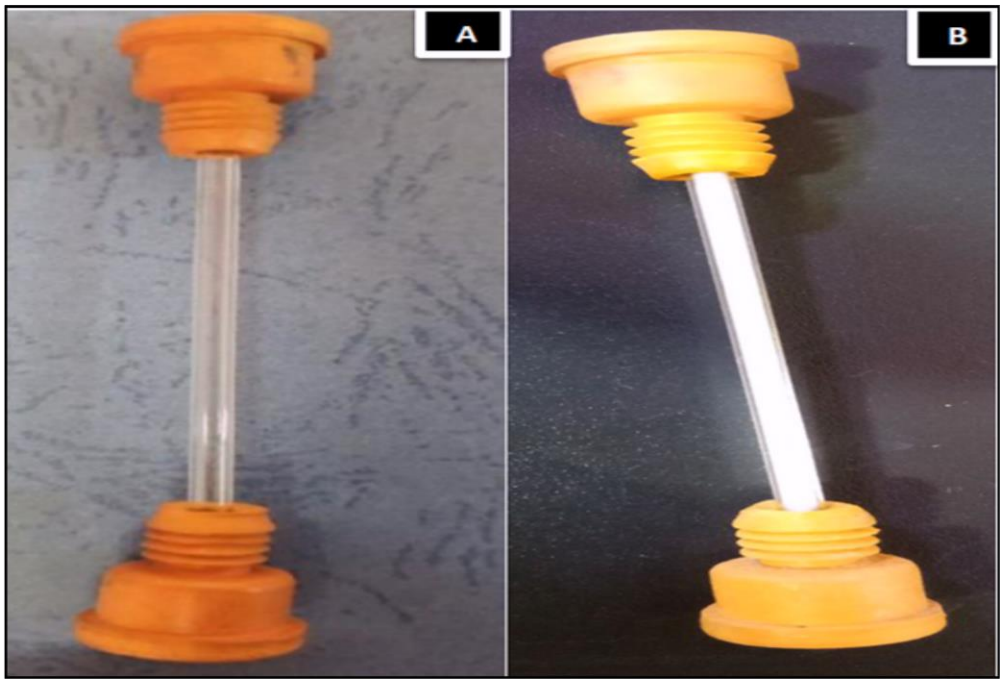

Figure 3.4 (A)The borosilicate tube after the silanization step, (B) the borosilicate tube after in-situ polymerization.

1-Initiation Step (Active species)

At this stage, the initiator cleavage divided into two free radicals. These free radicals attach to the monomers, forming active centres.

***I-I** is the initiator and **I**$^{\bullet}$ initiator radical.

R represents an atom or group of atoms such as –Cl, -CN, -C_6H_5, -OCH_3 or -CH_3; according to the type of substituent group R and the required polymer specifications, the kind of catalyst or initiator is selected.

2- Propagation Step (High molecular weight polymer)

At this stage, other monomers contribute to forming more free radical species.

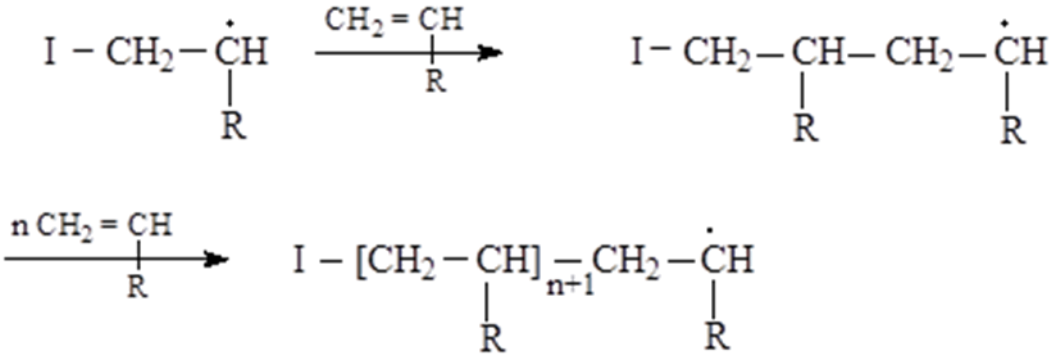

3-Termination Step (Disappearance of the active centres)

Termination of the active centres (radicals) nullifies their activity by:

a-Combination or coupling

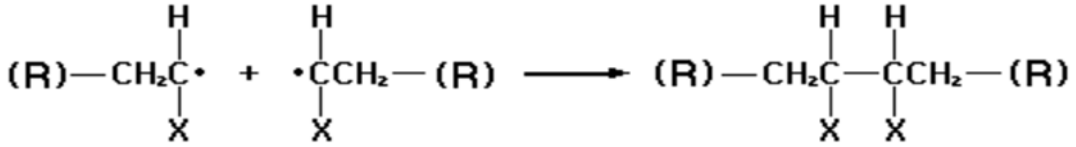

b- In the polymer chain, a hydrogen atom is cleaved from a carbon atom adjacent to the centre of the root (Disproportionation).

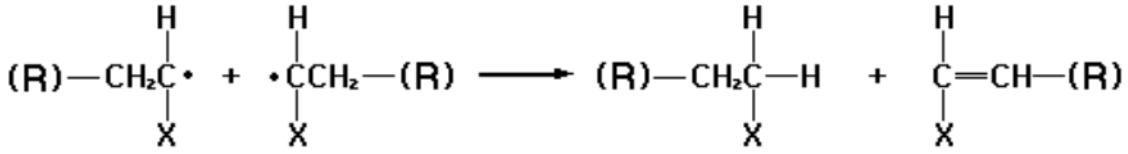

The free radical in the chain may move to the solvent, building block, or initiator, and the chain of growth ends. [143].

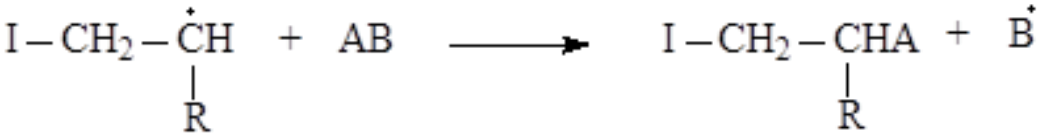

(3.4) Study the effect of the ratio for Ter – monomers.

The effect of the ratio for the monomers (GMA-co- ACA– co- AAM) at room temperature was studied, and the results are shown in Table (3-1).

From Table (3-1), it can be noticed that using the monomers (GMA-co- ACA - co- AAM) because GMA is an essential component, it contains the double bond that participates in the photopolymerization reaction and the epoxide ring, which gives the hydrophilic character of the compound. This ring can be entered in many chemical reactions to form groups used in the processes. When using the ratio of post-polymerization reaction (GMA) and (AAM) monomers (90:10,10:90,50:50) mL (v/v)%, the polymer forms quickly and in a high surface area, but with very high back pressure, and this is due to the small pores size, which causes the inability to load the ions inside the monolith, the ratio (GMA) and (ACA) monomers (50:50,10:90,90:10) mL (v/v)%, the polymer could not form effectively because it had large pores size and low back pressure, which might be owing to the low surface area of the sample, which results in limited contact between the sample and the solid phase.

While using the ratio (AAM) & (ACA) monomers (50:50,10:90,90:10) mL (v/v)% without (GMA) the polymer could not be formed because A well-mixed monomer was not formed.

Different ratios of monomers were used to obtain the exact percentage for the synthesis of monolithic column (50:50:50, 60:20:10, 60:10:20, 40:20:30); the ideal ratio was found 40:20:30 that the monolith is formed after 4 minutes in good shape with suitable back pressure and a suitable surface area.

Table (3-1). The use of different ratio monomers (GMA-co- ACA -co- AAM)

						progen solvent	
NO.	Monomers ratio (v/v)	Monomer (GMA) mL	Monomer (ACA) mL	Monomer (AAM) mL	Monolith formation time (min)	solvent (1) µL	solvent (2) µL
1	90--10	0.81	0	0.09	2	1-Propanol 1000	hexanol 650
2	10--90	0.09	0	0.81	2	1-Propanol 1000	hexanol 650
3	50---50	0.45	0	0.45	12	1-Propanol 1000	2-butanol 650
4	50---50	0.45	0.45	0	15	1-Propanol 1000	2-butanol 650
5	10--90	0.09	0.81	0	10	1-Propanol 1000	2-butanol 650
6	90--10	0.81	0.09	0	8	1-Propanol 1000	2-butanol 650
7	50---50	0	0.45	0.45	not formed	1-Propanol 1000	2-butanol 650
8	90--10	0	0.81	0.09	not formed	1-Propanol 1000	hexanol 650
9	10--90	0	0.09	0.81	not formed	1-Propanol 1000	hexanol 650
10	50--50--50	0.3	0.3	0.3	13	ethanol 1000	hexanol 650
11	60-20--10	0.6	0.21	0.09	6	ethanol 1000	hexanol 650
12	60-10--20	0.6	0.09	0.21	7	ethanol 1000	hexanol 650
13	40--20-30	0.4	0.2	0.3	4	ethanol 1000	hexanol 650

(3.5) Study the effect of the distance between the irradiation source and the separation column.

The impact of distance between the irradiation source and the prepared column was investigated to determine the ideal distance for polymer formation inside the separation column. The results were shown in Table (3-2) when the distance from the irradiation source was between 5 and 25 cm.

Table (3-2): The effect of the distance between the irradiation source and the separation column.

NO.	The distance (cm)	Result of the monolith column
1	5	The monolith is inside the separation column, but it cannot be washed because it is blocked
2	10	The monolith inside the separation column can be washed, but it is very difficult and with a very high back pressure
3	15	The monolith inside the separator column can be washed easily and with good back pressure
4	20	The monolith formed inside the separator column can be washed easily and with low back pressure
5	25	The monolith is inside the column but incomplete

Table (3-2) shows that the polymerization process cannot be controlled when the distance is between 5 and 10 cm, resulting in small pores size and the inability to wash the prepared column and use the process to re-concentrate the ions, while the polymerization process and polymer formation can be well controlled when using a distance of 15 cm, as the polymer is homogeneous and can be washed easily and with good back pressure, whereas when using a distance of 20-25 cm, the polymer is partially inside the separating column.

(3.6) The effect of irradiation time

The optimal irradiation period for polymer synthesis was investigated after optimizing the monomer ratio and distance between the irradiation source and the constructed column. The results were obtained using a variety of irradiation periods ranging from (1-6) min, as indicated in Table (3-3).

Table (3-3): Effect of irradiation time on monolith formation

Irradiation time (min)	Result of the monolith column
1	The polymer is not formed
2	The polymer is primitive (Emulsion)
3	The polymer is formed by low back pressure (White but soft)
4	The polymer is formed by good back pressure (Block white)
5	The polymer is formed by high back pressure (white rigid mass)
6	The polymer is formed by a very high back pressure (A very rigid white mass)

Table (3-3) shows that the irradiation time is one of the most crucial factors in converting a monomer mixture to a solid polymer; therefore, when using a long irradiation time of (5 min) or more, the polymer chains grow; as a result, the polymer branches grow rapidly, forming small pores as shown in Figure (3-4) (c), this is due to a dense cross-linked polymer network that is formed. When the irradiation time is less than (4 min), less polymerized material may form inside the borosilicate tube. The polymer will not form properly, affecting the performance of the prepared monolith as shown in Figure (3-4) (a); due to the growth, only a limited number of polymer chains grow from the surface,

whereas when the irradiation time is (4 min), back pressure and good surface area will be achieved as shown in Figure (3-5) (b) [144].

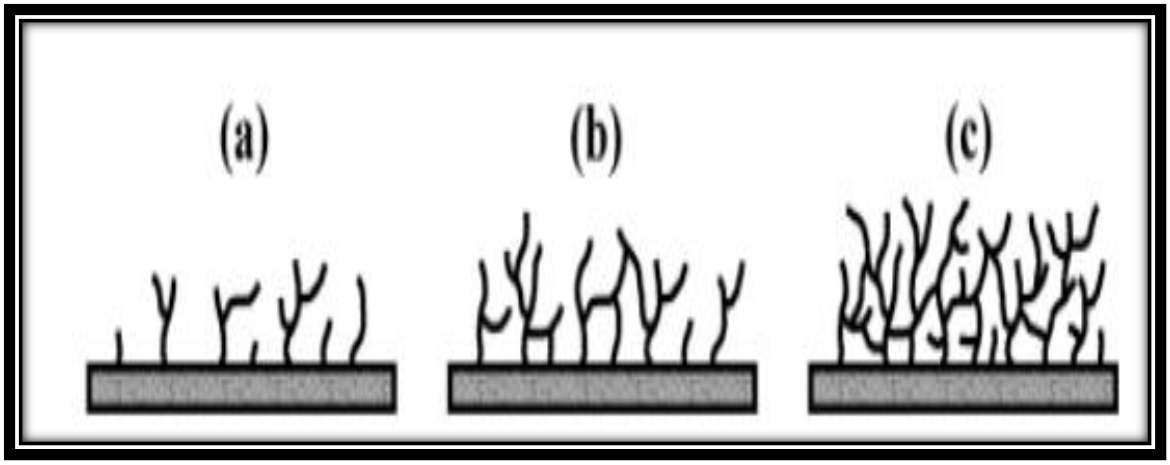

Figure 3.5: Growing polymer chains with increasing irradiation time from (a) to (c).

(3.7) Effect of porogenic solvents

The effect of the solvent type on the polymerization process was investigated to identify the optimal solvent that can be utilized in conjunction with (Ethanol) to produce a polymer with the desired surface area and pore size. Table (3-4) shows the findings of this experiment.

Table (3-4): The effect of porogenic solvents on polymer formation.

porogenic solvents		Result
solvent (1) µL	solvent (2) µL	
ethanol	1-hexanol	The polymer forms well and is easy to wash
ethanol	1-Propanol	Polymer forms, but with very large gaps.
ethanol	2-butanol	Polymer forms, but with very large gaps.
ethanol	Methanol	Polymer forms but with very small gaps
1-Propanol	1-hexanol	Polymer forms but it is blocked
Methanol	1-hexanol	The polymer is formed, but with very small gaps and difficult to wash
1-Propanol	2-butanol	No polymer formed

The kind of porogenic solvent substantially affects the porous characteristics of the polymer; it may be determined that the porous solvents' features significantly impact the polymer's porosity to get a high surface area and appropriate pore size. The influence of porogenic solvents on the formation of monoliths was investigated.

Compared to l-haxnol and MeOH, the monolith created by l-haxnol and ethanol is superior. MeOH, a polar porogen, produces materials with small surface areas, and 1-hexnol makes materials with low surface areas. However, washing off the prepared monolith is challenging due to the creation of a very small porous structure, which affects the prepared monolith's performance. Since all these studies were conducted at room temperature, low boiling point reagents can be utilized. The choice of solvent, therefore, relies on the type of polymer.

(3.8) Limitation of Swelling Percentage

Because solvent molecules disperse inside the crystal lattice of high molecular weight polymers, causing a change in size, cross-linked polymers expand, causing the polymer to collapse when subjected to mechanical stress or high pressure. It has a strong impact and drives the produced polymer to dissolve [145].

The percentage of swelling was calculated using the following equation:

$$\textbf{Swelling ratio} = \textbf{Wwet} - \frac{\textbf{Wdry}}{\textbf{Wdry}} \times \mathbf{100} \qquad (\mathbf{3-1})$$

Where (W wet) is the weight of the wet polymer, while (W dry) is the weight of the dry polymer, respectively [145].

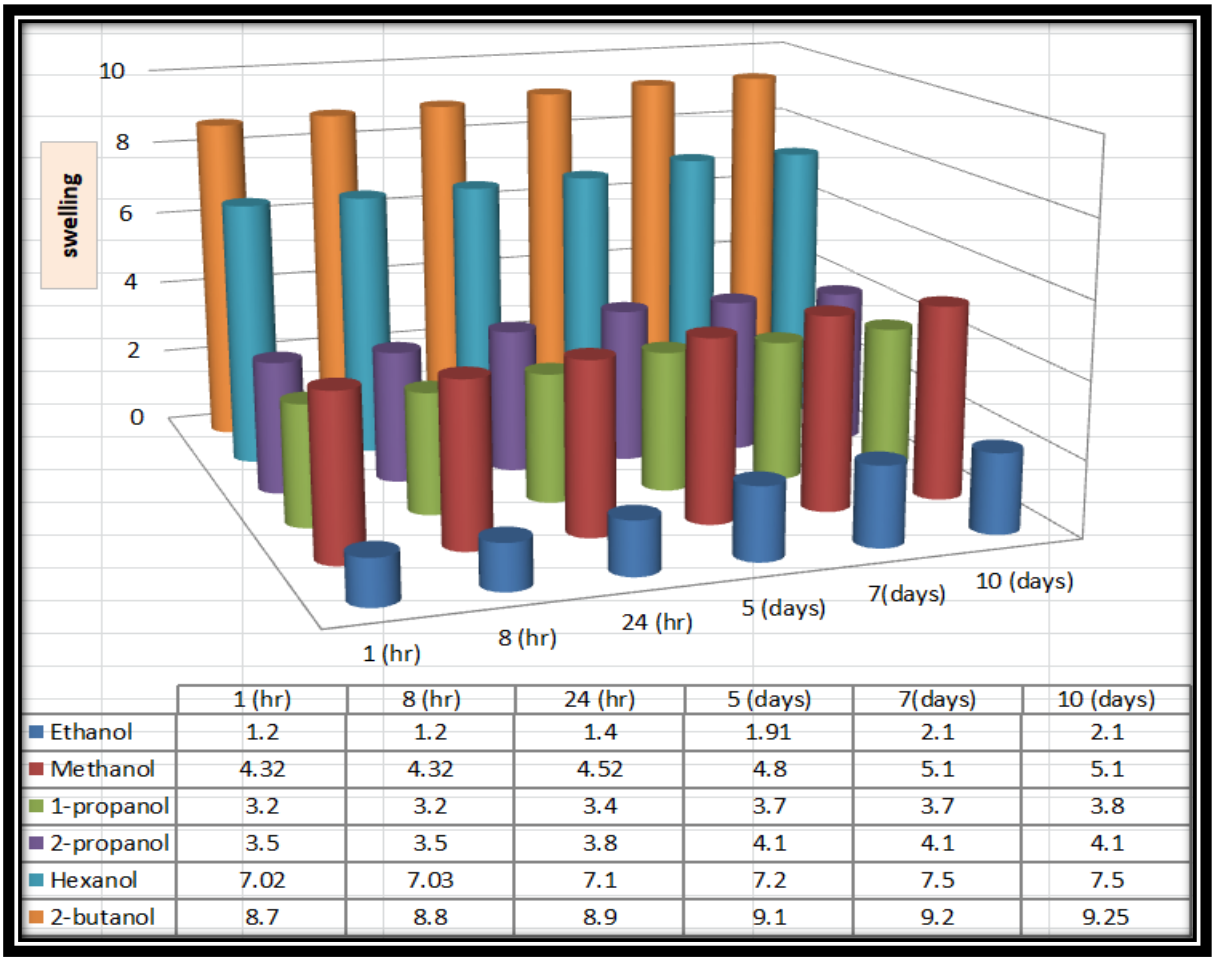

	1 (hr)	8 (hr)	24 (hr)	5 (days)	7(days)	10 (days)
Ethanol	1.2	1.2	1.4	1.91	2.1	2.1
Methanol	4.32	4.32	4.52	4.8	5.1	5.1
1-propanol	3.2	3.2	3.4	3.7	3.7	3.8
2-propanol	3.5	3.5	3.8	4.1	4.1	4.1
Hexanol	7.02	7.03	7.1	7.2	7.5	7.5
2-butanol	8.7	8.8	8.9	9.1	9.2	9.25

Figure (3.6)Variations of polymer swelling degree using different alcohol solvents

Figure(3.6) shows that when 2-butanol is used, the polymer swells significantly. It might be due to polymer saturated with the solvent and insoluble, as well as a lack of polymeric chain separation, resulting in micropores that decrease mechanical characteristics when using high-pressure rates and the inability to load ions while using high-pressure rates. Ethanol has the slightest swelling, allowing the produced polymer to have a porous structure.

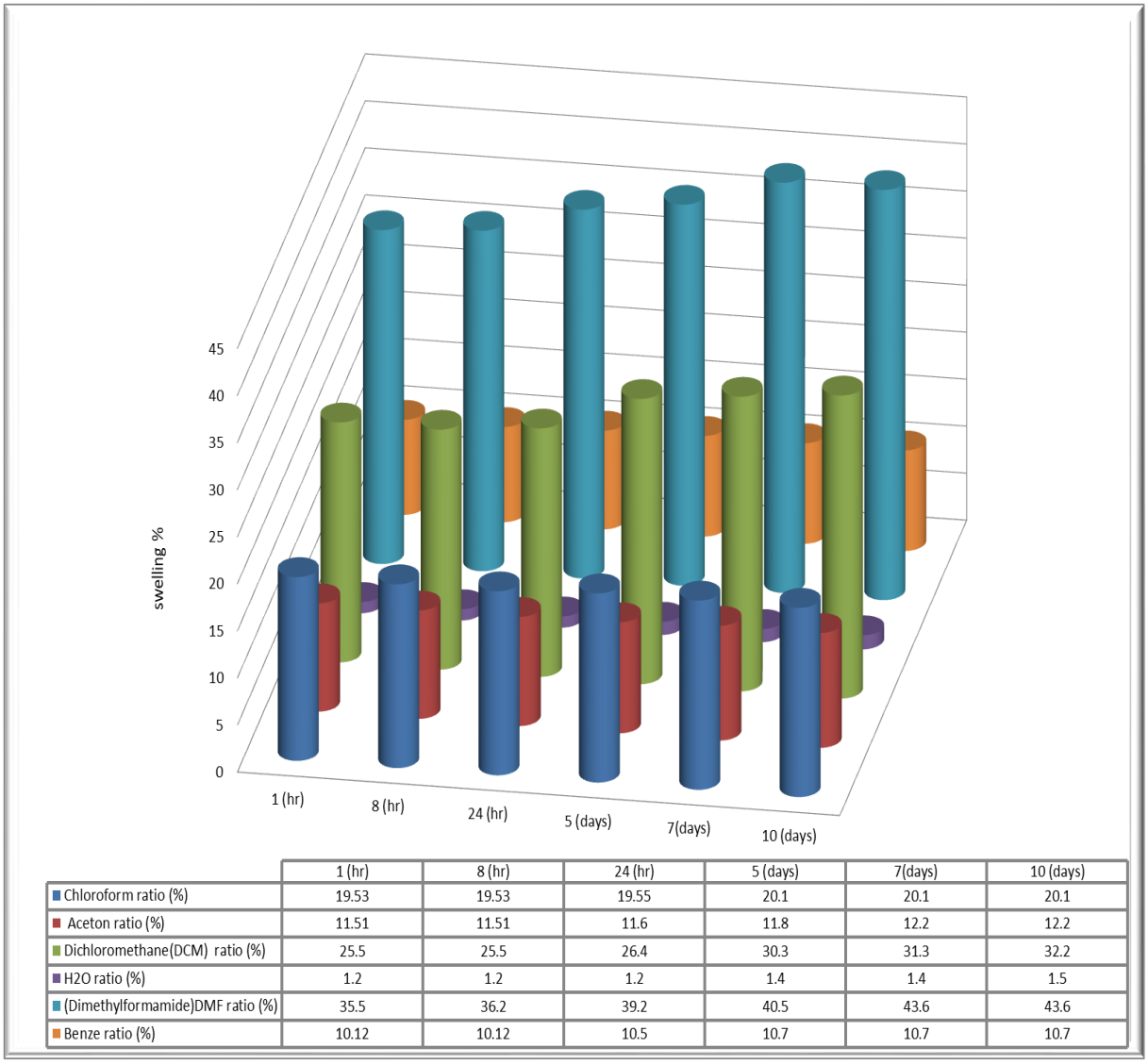

	1 (hr)	8 (hr)	24 (hr)	5 (days)	7(days)	10 (days)
Chloroform ratio (%)	19.53	19.53	19.55	20.1	20.1	20.1
Aceton ratio (%)	11.51	11.51	11.6	11.8	12.2	12.2
Dichloromethane(DCM) ratio (%)	25.5	25.5	26.4	30.3	31.3	32.2
H2O ratio (%)	1.2	1.2	1.2	1.4	1.4	1.5
(Dimethylformamide)DMF ratio (%)	35.5	36.2	39.2	40.5	43.6	43.6
Benze ratio (%)	10.12	10.12	10.5	10.7	10.7	10.7

Figure (3.7)Variations of polymer swelling degree using different polar solvents.

Figure (3.7) shows a high degree of polymer swelling when using DMF due to solvent saturation of the polymer, which can result in chemical decomposition, which can lead to cracking of the prepared monolith. In contrast, Figure (3.7) shows the lowest degree of swelling when using H_2O, which does not cause clogging of the polymer, obtains an excellent porous structure, and allows download ions.

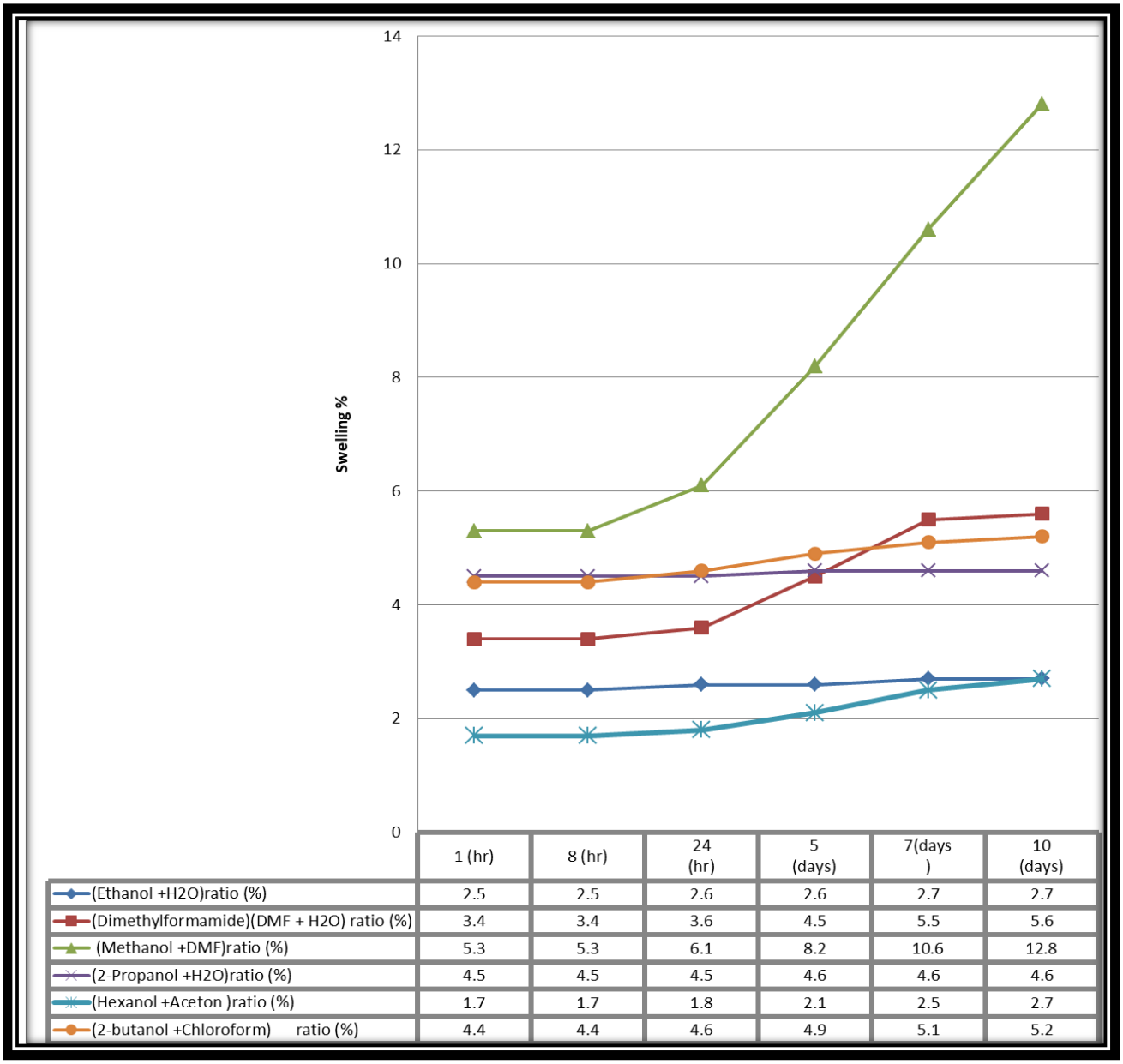

	1 (hr)	8 (hr)	24 (hr)	5 (days)	7(days)	10 (days)
(Ethanol +H2O)ratio (%)	2.5	2.5	2.6	2.6	2.7	2.7
(Dimethylformamide)(DMF + H2O) ratio (%)	3.4	3.4	3.6	4.5	5.5	5.6
(Methanol +DMF)ratio (%)	5.3	5.3	6.1	8.2	10.6	12.8
(2-Propanol +H2O)ratio (%)	4.5	4.5	4.5	4.6	4.6	4.6
(Hexanol +Aceton)ratio (%)	1.7	1.7	1.8	2.1	2.5	2.7
(2-butanol +Chloroform) ratio (%)	4.4	4.4	4.6	4.9	5.1	5.2

Figure (3.8) Swelling using a mixture of two different solvents.

As shown in figure (3.8), a high degree of swelling of the polymer occurs when a mixture of two solvents (Methanol + DMF) is used, which causes clogging of the polymer. In contrast, a mixture of (Hexanol + Aceton) does not cause clogging of the polymer. It allows the exchange of ions inside it and is used as a preservation solution.

(3.9) SEM analysis of Glycidyl methacrylate -co -Acrylic acid- co-acryl amid monolith column.

The scanning electron microscope (SEM) is a device that magnifies pictures to show microscopic-scale details about a specimen's size, shape, composition, crystallography, and other physical and chemical properties. Knoll and Theile [146]. They were the first to illustrate the SEM concept, with von Ardenne developing the first real SEM [147]. When an electron beam interacts with a specimen, two-electron products are produced:(A)backscattered electrons (BSEs), which are beam electrons that survive scattering and deflection by the electric fields of the atoms in the sample and retain a significant portion of their incident energy and (B) secondary electrons (SEs) are electrons that exit the specimen surface after being expelled from atoms in the sample by beam electrons. Despite the tremendous energy of the beam electrons, these secondary electrons have a poor kinetic energy transfer and hence depart the specimen surface with very low kinetic energies, as shown in Figure (3.9) [148].

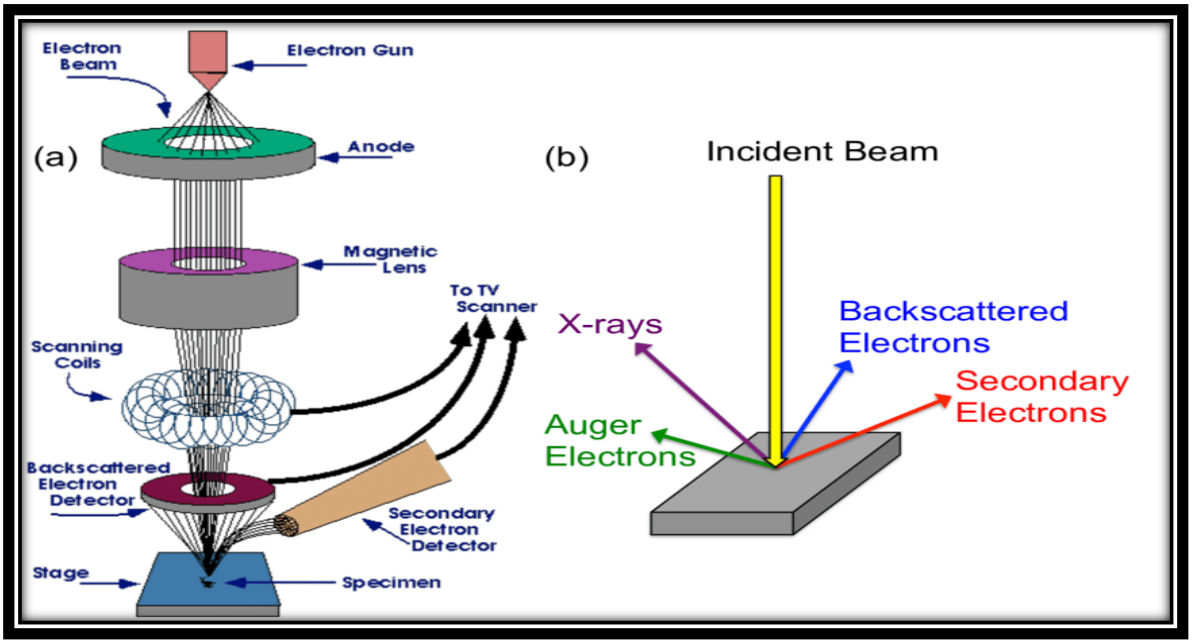

Figure (3.9) Schematic drawing of (a) the typical Scanning Electron Microscope (SEM) column and (b) sample-beam interactions within an SEM.

The morphology of the (GMA-co-ACA-co-AAM) monolithic column was characterized using (SEM) scanning electron microscopy. The monolith can be viewed as a network of interconnected channels with high flow through pores. The benefits of these pores exceed the monolith's surface area and increase the monolith's loading capacity, as in Figures (3-10). These pores allow the mobile phase to pass quickly through the monolith column, increasing Permeability and reducing back pressure. In addition, the monolith contains many medium and fine pores, and the composition of these pores is essential for expanding the monolith's surface area and the monolith's loading capacity. Furthermore, a high flow rate and modest back pressure allow quick extraction [(149)].

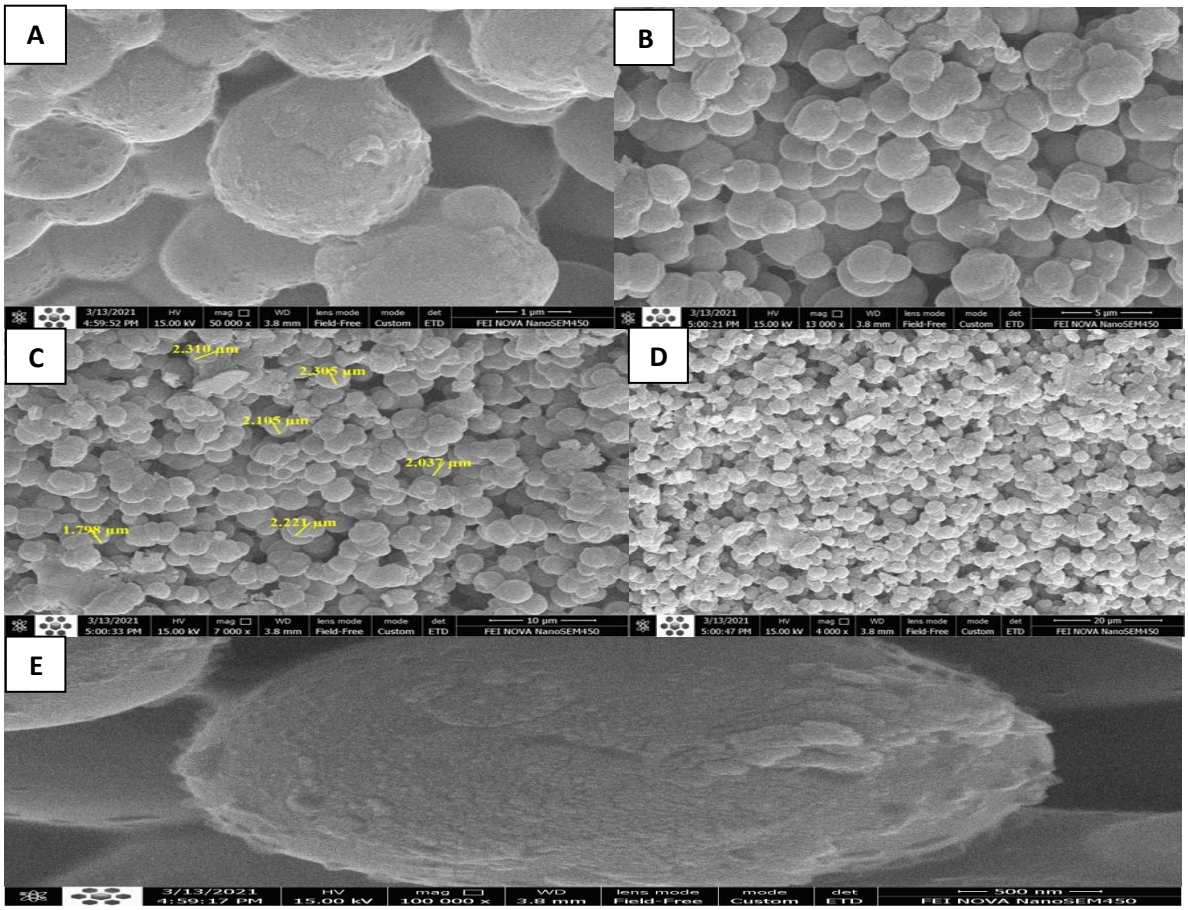

Figure (3.10) Scanning electron micrographs of monoliths((A) 1 µm ,(B) 5 µm,(C) 10 µm,(D) 20 µm and (E) 500 nm) at magnification.

(3.10) Brunauer-Emmett-Teller (BET) analysis for the (GMA-co-ACA- co-AAM) monolith column.

Brumauer, Emmett, and Teller discovered a method for determining a sample's specific surface area, including the pore size distribution of gas adsorption. The amount of gas adsorbed is determined by the exposed surface, temperature, gas pressure, and strength of the gas-solid interaction. Because of its excellent purity and strong reactivity with most materials, nitrogen is commonly utilized in BET surface area analysis. At the boiling point of nitrogen (-196C°), nitrogen is typically adsorbed on the surface of the particles. Because the nitrogen gas is below the critical temperature at this temperature, it will adsorb. The nitrogen gas is then progressively released into the sample cell from the particle surface [150]. The sample is removed from the nitrogen atmosphere and heated to release nitrogen adsorbed from the material. It quantifies its quantity when relative pressures less than atmospheric pressure that are attained by establishing partial vacuum conditions and creating adsorption layers. As illustrated in Figure (3-11) [151], the collected data is displayed as BET temperature, which defines the amount of gas adsorbed as a function of relative pressure.

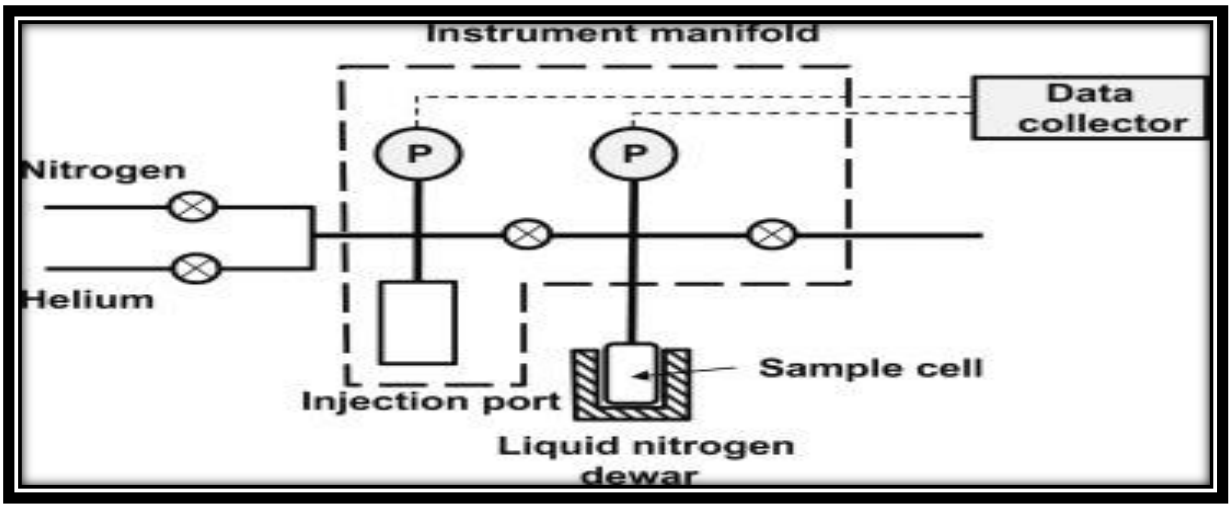

Figure (3.11) Schematic diagram of volumetric method apparatus.

The nitrogen gas adsorption/desorption isotherm was studied for the prepared monolithic column using (BET) analysis to investigate the average pore size and significant surface area for the prepared monolith. It can be seen that the average surface area and average pore size were (29.725 m^3/g and 13.5013 nm) desorption, respectively. These results could be a suitable preparation condition for an instant porogenic solvent that can contribute to tuning surface area and pore size. According to the IUPAC classification of adsorption isotherms, six types can be distinguished; the pores are classified as micropores (size < 2 nm), mesopores (2 nm < size <50 nm), and macropores (size > 50 nm), depending on their size [(152)].

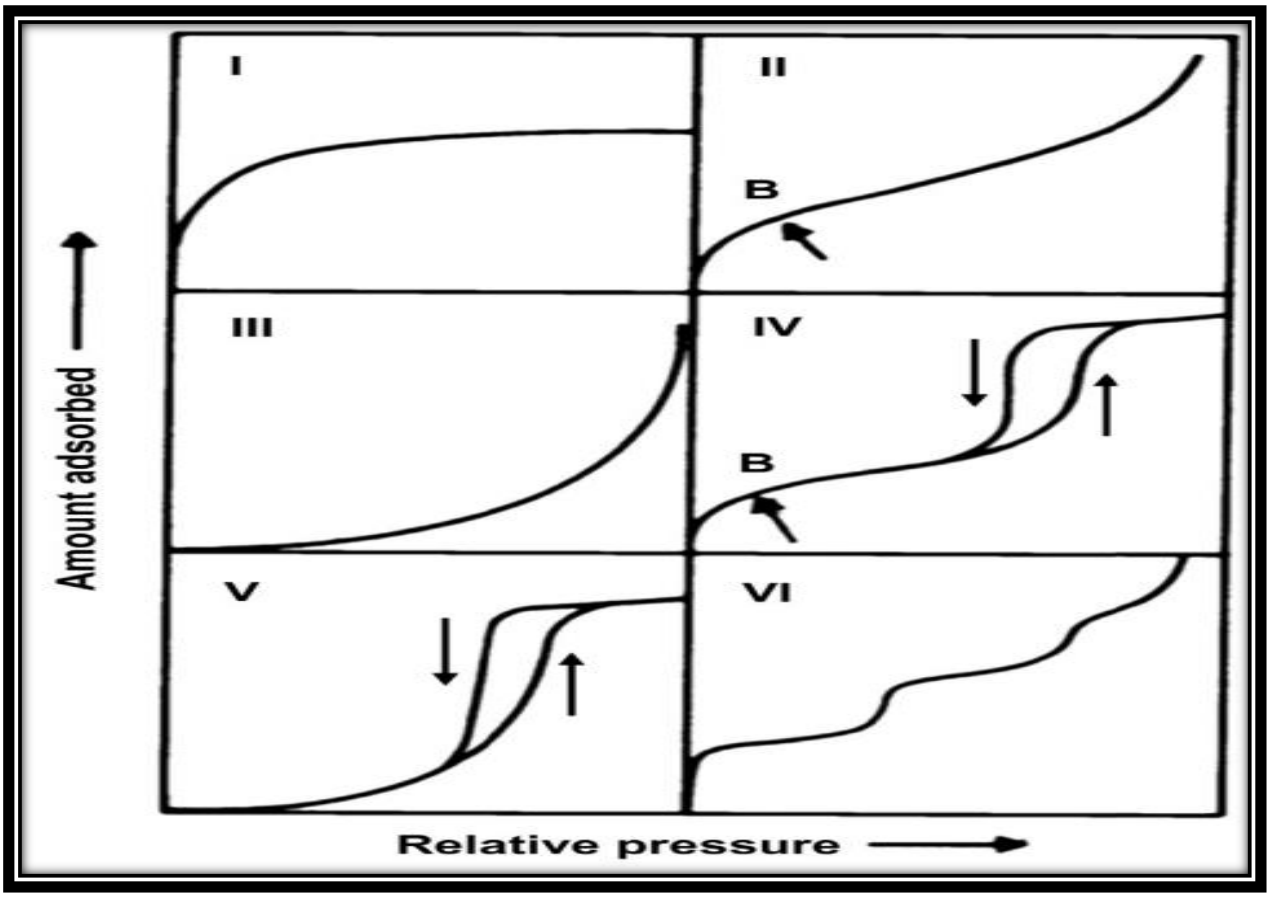

Figure (3.12)Six types of adsorption isotherm classified by IUPAC

(3.11) Study the effects of irradiation time on (GMA-Co-ACA-Co-AAM) monolith column formation.

Figure (3.13) demonstrates that an irradiation time of (4min) is requested to form a desired (GMA-co-ACA-co-AAM) monolith column surface area and pores size. An irradiation time between 0.5 and 8.8 min was applied. It can be noticed that a (5 min) irradiation time leads to a high surface because of a large number of monomers branch; irradiation times below 0. 5 min were not used since they were too low to achieve the polymerization of the monolith. Therefore, a photo polymerization time of 4 minutes was used for the monolith synthesis.

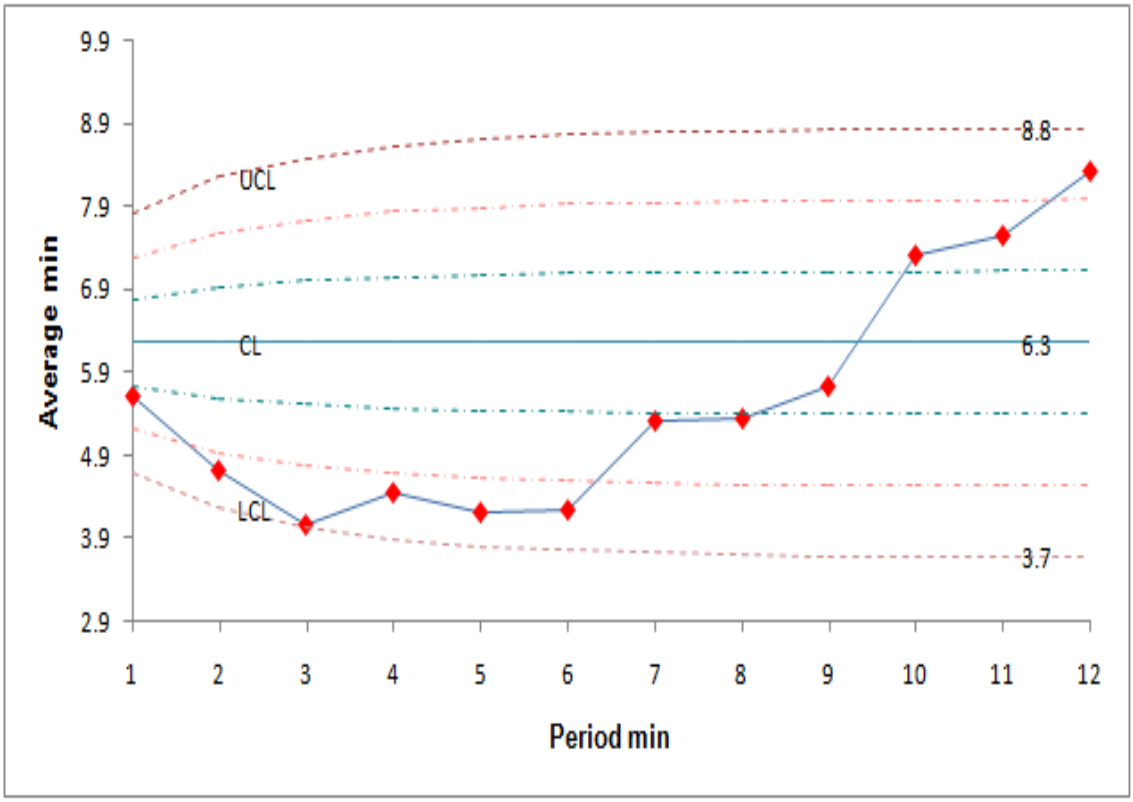

Fig.(3.13): Effect of increasing irradiation time on the monolith column.

(3.12) Permeability and the porosity of the monolith

The Permeability of the column was investigated by measuring the backpressure generated when pumping different flow rates using an HPLC pump, as in Figure (3.14). It was found that the pressure was increased from 55.103psi to 150.923 psi at a typical flow rate of 50µl/min (with different flow rates of 0.02-1.5 ml/min). The net pressure was calculated to be approximately 150.923 psi for the monolithic column at a flow rate of 1.5 mL/minas shown in Table (3-5) and Figure (3.15). After three measurements and the average is taken, it was found that the total porosity of the monolith is 0.8127.

Table (3-5) The Permeability of the (GMA-co-ACA co-AAM) monolith column.

No.	Flow rate(ml/min) n=3	Pressure(Psi) n=3
1	0.02	55.103
2	0.03	57.289
3	0.05	60.124
4	0.08	62.445
5	0.1	64.599
6	0.3	76.179
7	0.5	87.245
8	0.6	93.779
9	0.8	105.489
10	1	117.734
11	1.3	134.281
12	1.5	150.923

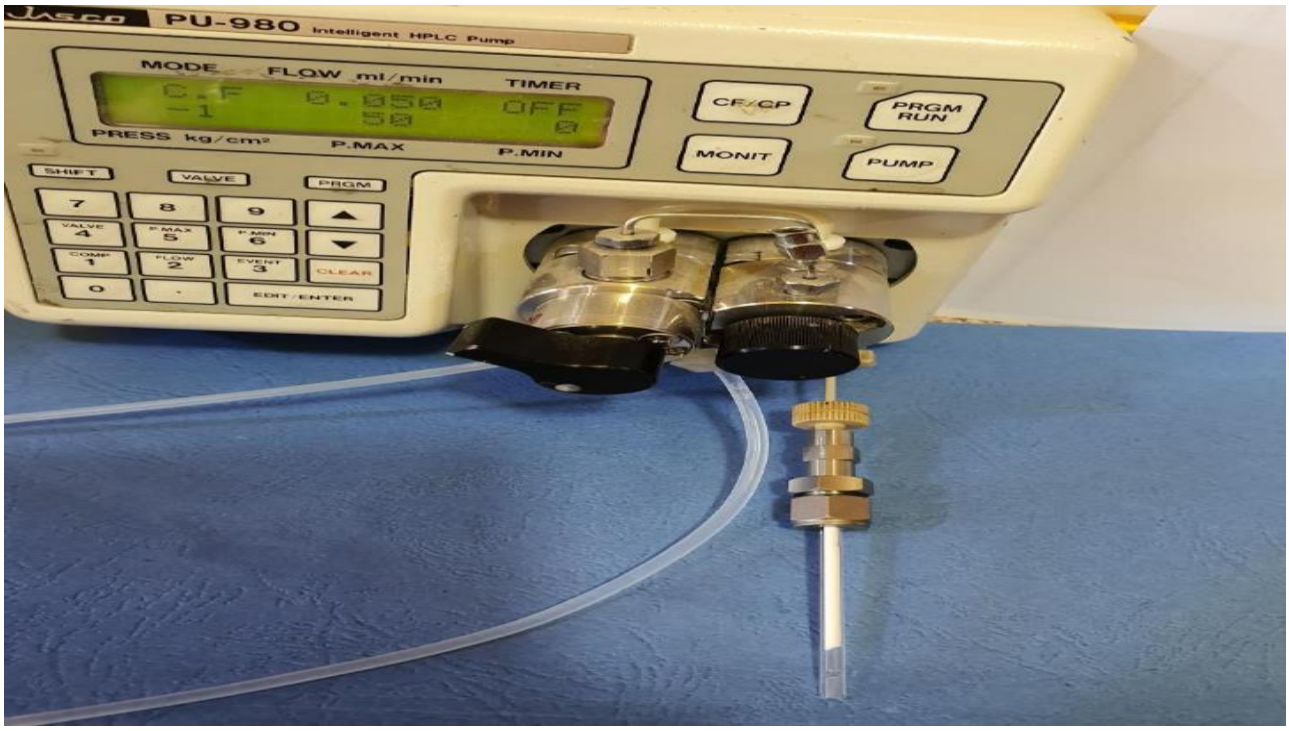

Figure(3.14)The HPLC pump measures the relationship of back pressure with flow rate.

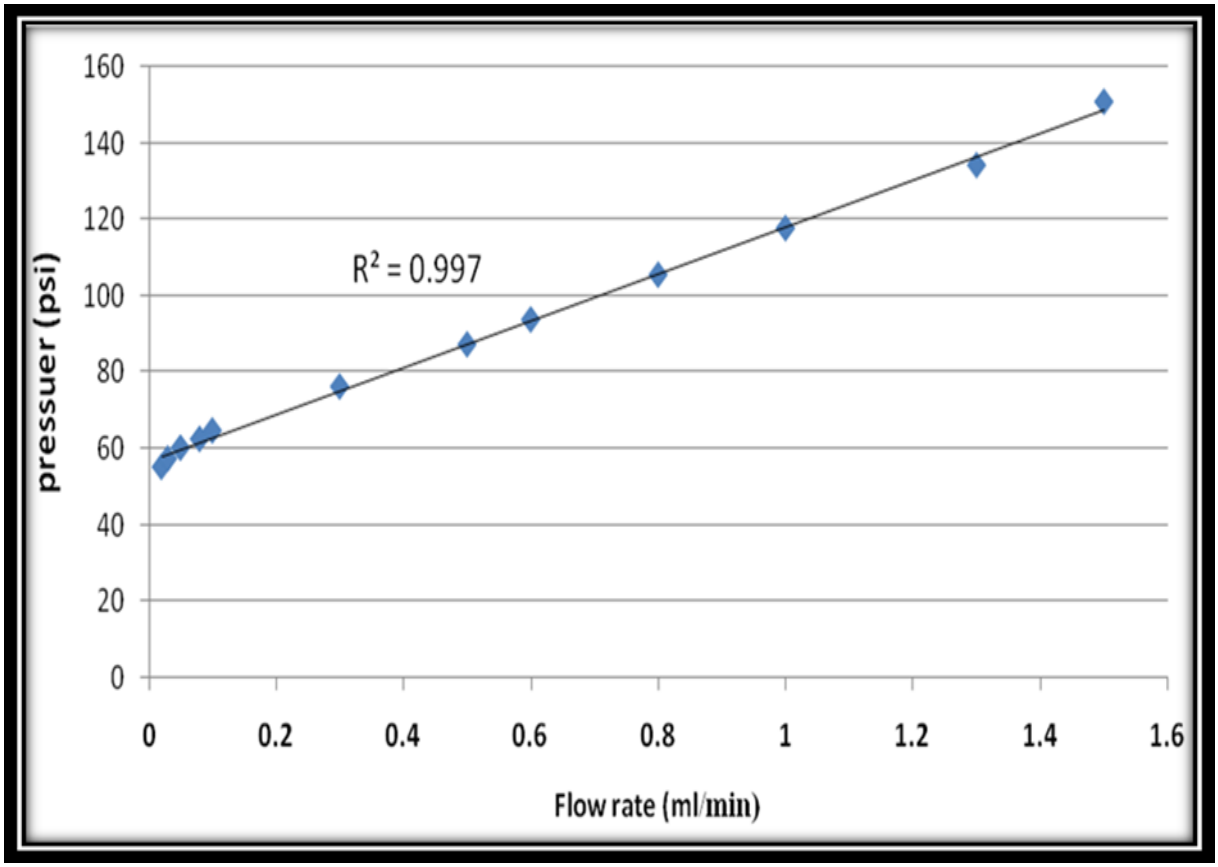

Figure(3.15).The Permeability of the (GMA-co-ACA co-AAM) monolith column.

(3.13) Investigation of polymer composition using FT-I.R.

Notably, significant differences between the prepared polymer and the monomers can be observed; some peaks have disappeared for the synthesized material.

(3.13.1) FT-I.R ATR Glycidyl methacrylate.

Figure (3-16) illustrates the glycidyl methacrylate. There are three essential bands. It belongs to the carbonyl group (C= O) at 1716.40 cm^{-1}, and absorption band at 1637.98 cm^{-1} back to (C = C) and the band at 907.70 cm^{-1} for to (C-O-C) (epoxy group). These three packages can be used for the polymerization reaction.

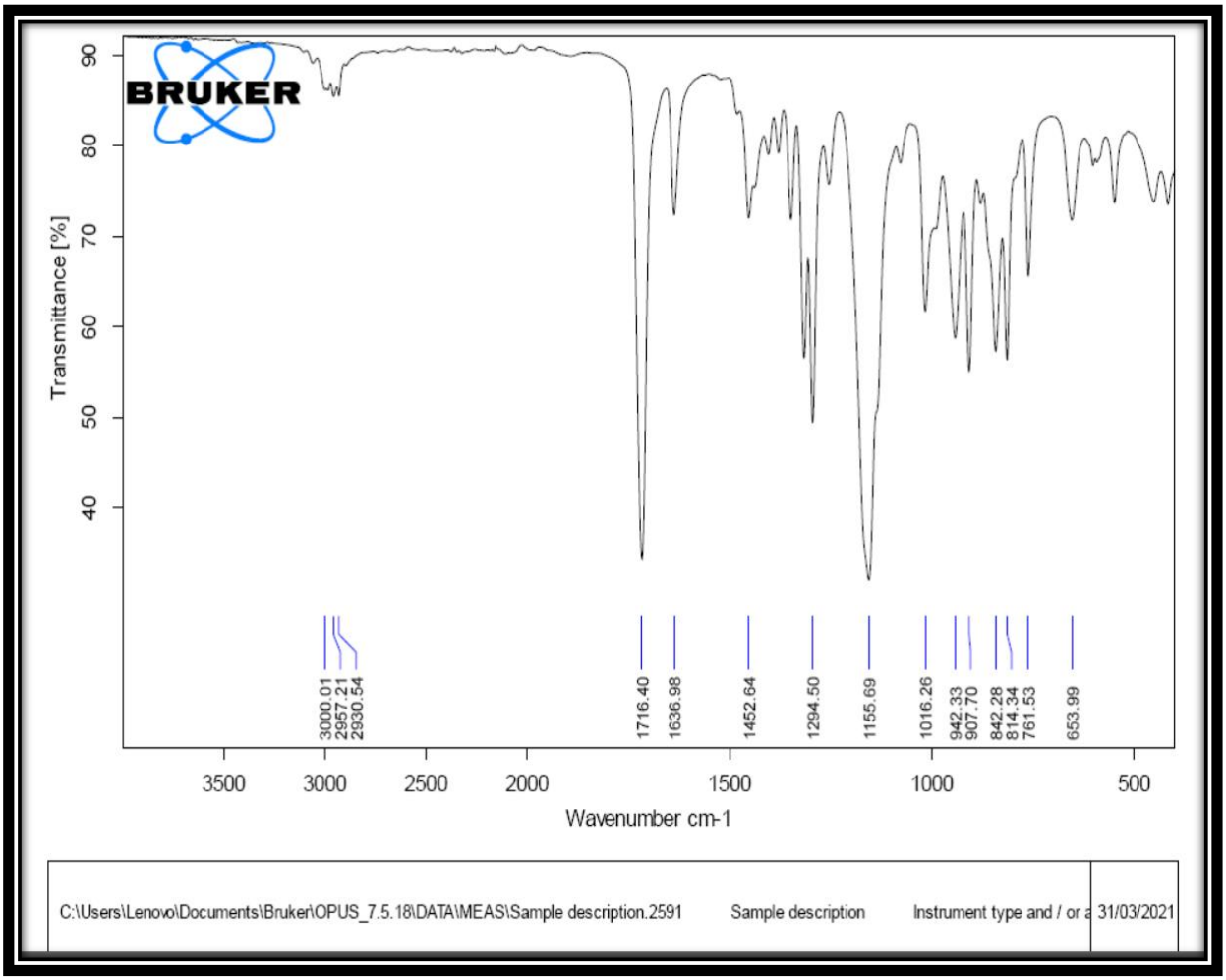

Figure(3.16) (FT-I.R) of the monomer for Glycidyl methacrylate.

(3.13.2) FT-I.R ATR Acrylamide Monomer.

The monomer acrylamide was identified using Fourier transform infrared (FT-I.R) spectroscopy, as shown in Figure (3-17); the results confirm the existence of the carbonyl, and amide peaks at (1666.02 and 3163.73 -3338.67)cm^{-1}, respectively.

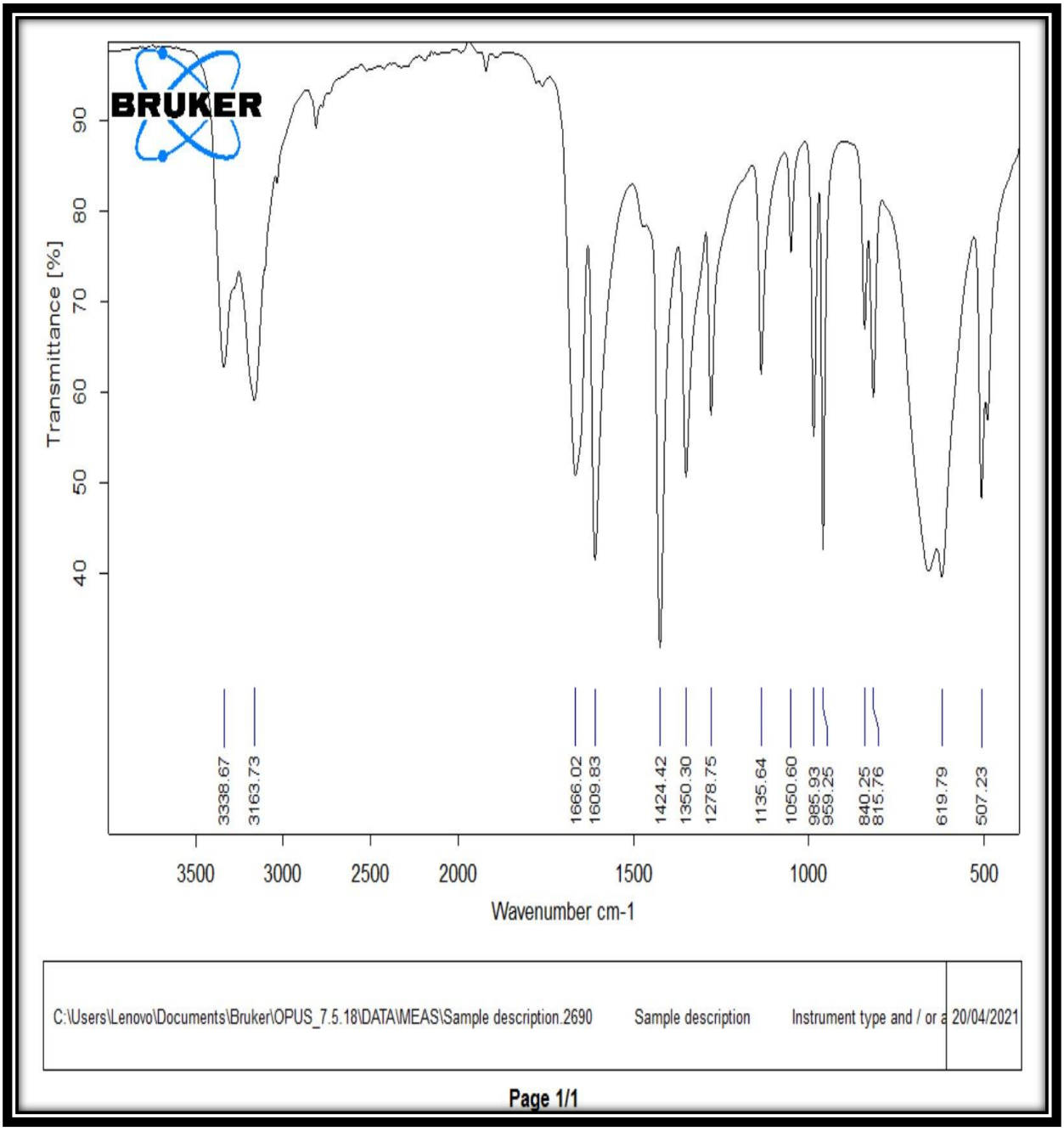

Figure(3.17) (FT-I.R) of the monomer for Acrylamide.

(3.13.3) FT-I.R Acrylic acid Monomer

Acrylic acid prominent peaks appeared at 1635.96 and 1716.21 cm^{-1}, which are C=C and C=O vibrations, respectively, as seen in Figure (3-18).

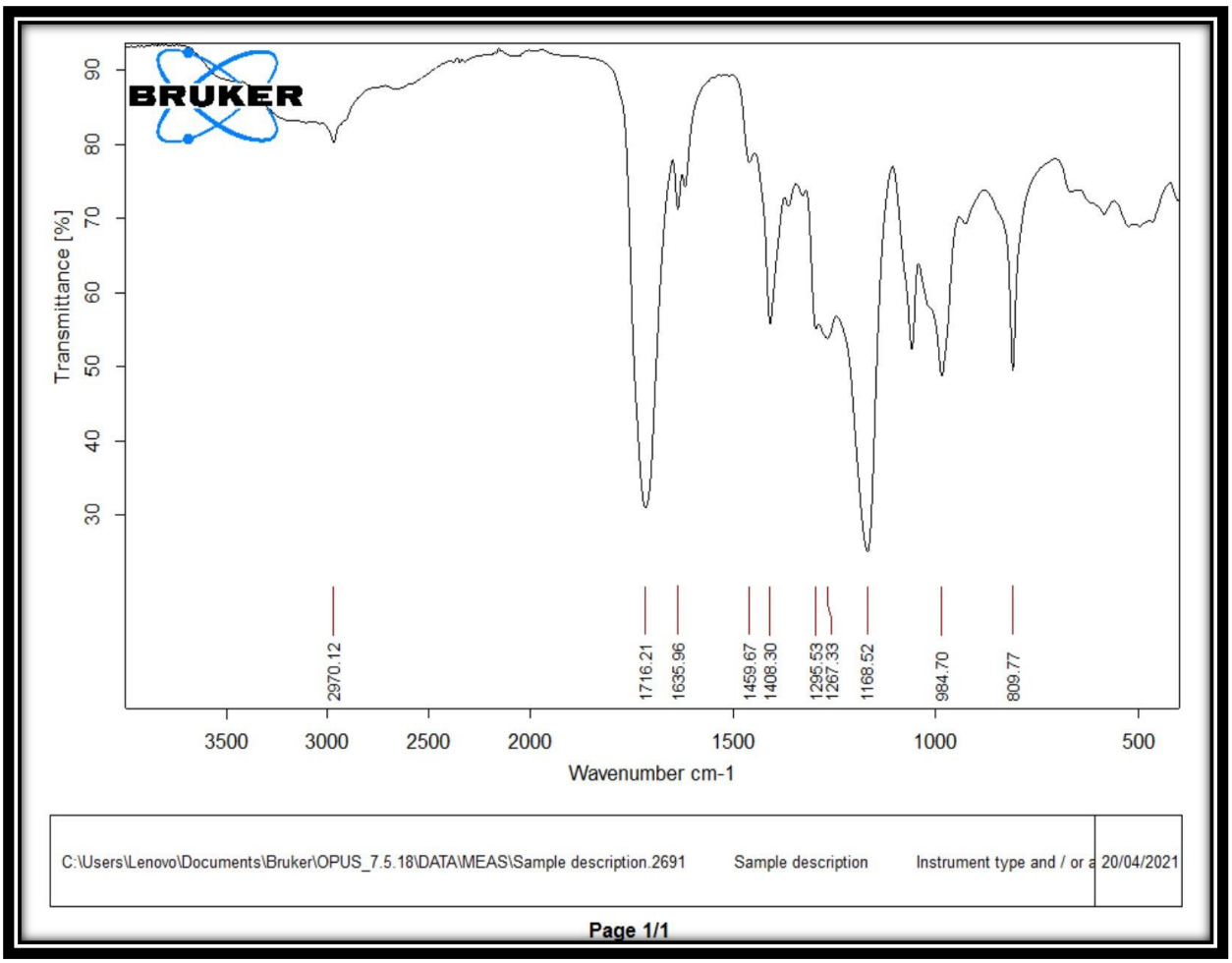

Figure(3.18) (FT-I.R) of the monomer for Acrylic acid.

(3.13.4) FT-I.R ethylene dimethacrylate

Infrared (FT-I.R) spectroscopy was used to identify the monomer ethylene dimethacrylate, as shown in Figure (3-19), which exhibits several absorption bands; the main peak are absorption bands at 1717.69 cm^{-1} for (C = O) and also emerged at 1636.85 cm^{-1}. For (C = C). These bands show that EDMA is involved in the polymerization reaction.

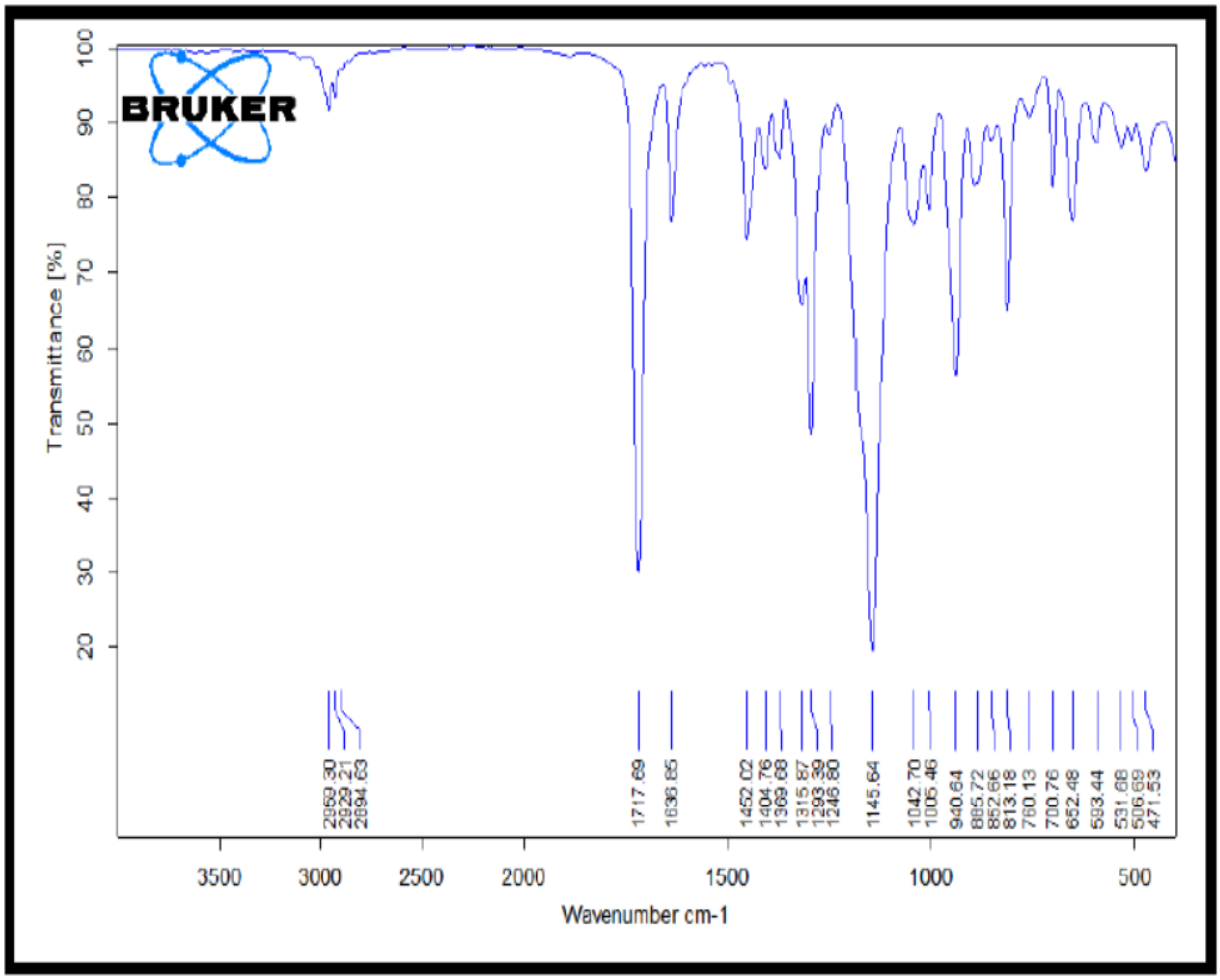

Figure(3.19) (FT-I.R) of the monomer for EDMA.

(3.13.5) (FT-IR) for the polymer before ring opening (GMA-co-ACA-co-AAM).

The carbonyl group absorption band in the prepared polymer was unchanged at C=O (1720.90 cm^{-1}). A slight shift in the epoxy group (C-O-C) towards 906.14cm^{-1}, while the disappearance of the 1636.85 cm^{-1}absorption bands belongs to (C=C), this is strong evidence of the polymer formation through the incorporation of both monomers and the cross-linker using the (C=C)as shown in Figure (3-20).

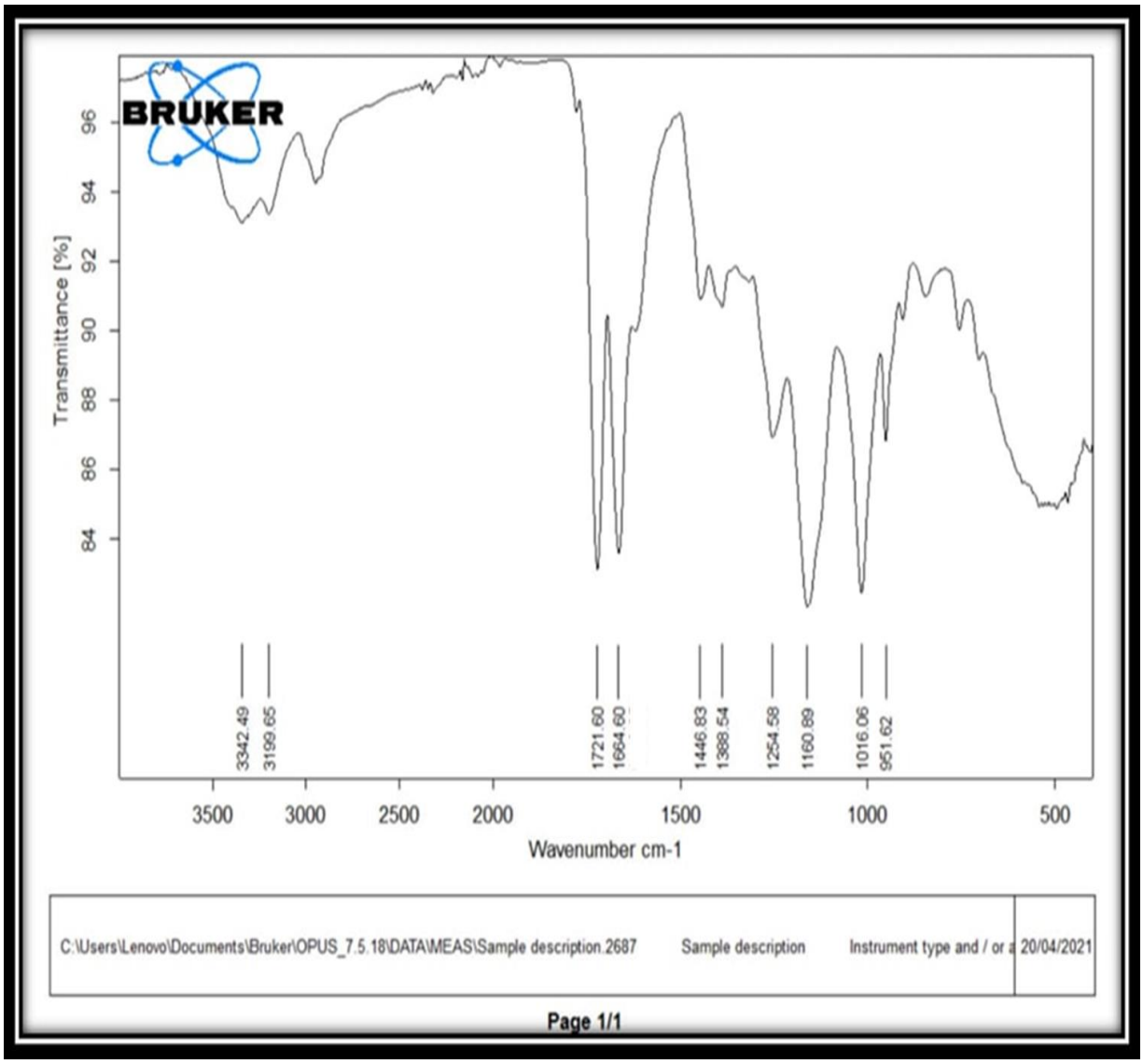

Figure(3.20) (FT-I.R) of the polymer (GMA-co-ACA-co-AAM).

(3.14) Process opening the epoxy ring of glycidyl methacrylate to form strong ion exchange monolithic columns.

Using a sulfonation process, the epoxy groups in GMA-co-ACA co-AAM monolithic columns can be opened by pumping a sulfonation solution, as described in section (2.5.2), using a syringe pump. Because sulfite groups have a stronger affinity for water than hydrophobic polymer chains suspended in water, direct sulfonation of epoxy groups with Na_2SO_3 solution was impossible.

Furthermore, the phase separation prevents the sulfite groups from accessing the epoxy groups in the polymers, which are required for the reaction. At 70 Cº, the sulfonate groups were implanted by reacting the GMA samples with Sodium sulfite in water–Dimethyl sulfoxide solution (Na_2SO_3 /water/DMSO) 1/7/3 (weight ratio))[155]. Figure (3.21) (3.22)

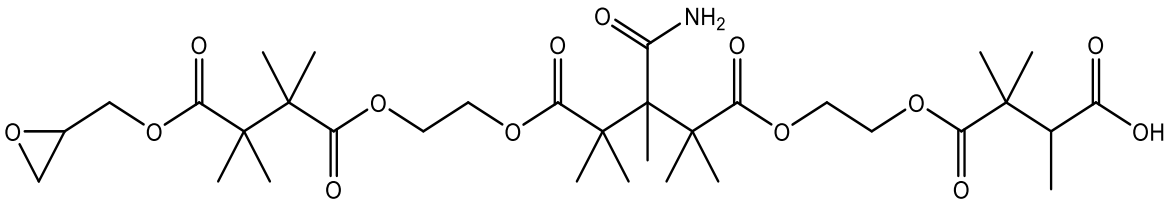

13-carbamoyl-4,4,5,5,12,12,13,14,14,21,21,22-dodecamethyl-1-(oxiran-2-yl)-3,6,11,15,20-pentaoxo-2,7,10,16,19-pentaoxatricosan-23-oic acid

Chemical Formula: $C_{33}H_{53}NO_{14}$

Molecular Weight: 687.78

Elemental Analysis: C, 57.63; H, 7.77; N, 2.04; O, 32.57

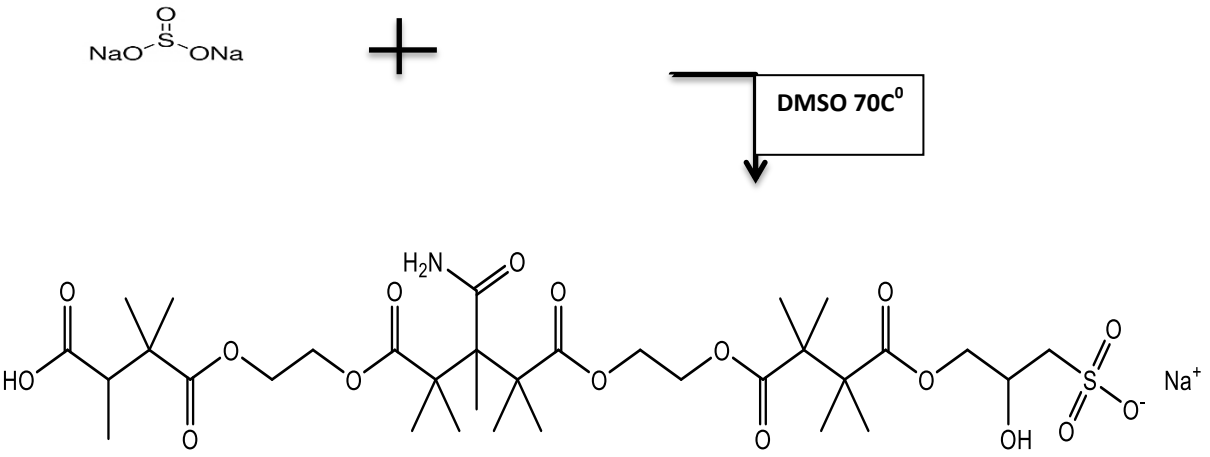

sodium 15-carbamoyl-24-carboxy-2-hydroxy-6,6,7,7,14,14,15,16,16,23,23-undecamethyl-5,8,13,17,22-pentaoxo-4,9,12,18,21-pentaoxapentacosane-1-sulfonate

Chemical Formula: $C_{33}H_{54}NNaO_{17}S$

Molecular Weight: 791.83

Elemental Analysis: C, 50.06; H, 6.87; N, 1.77; Na, 2.90; O, 34.35; S, 4.05

Figure (3-21) Principal scheme of sulfonation reaction of poly-GMA chains

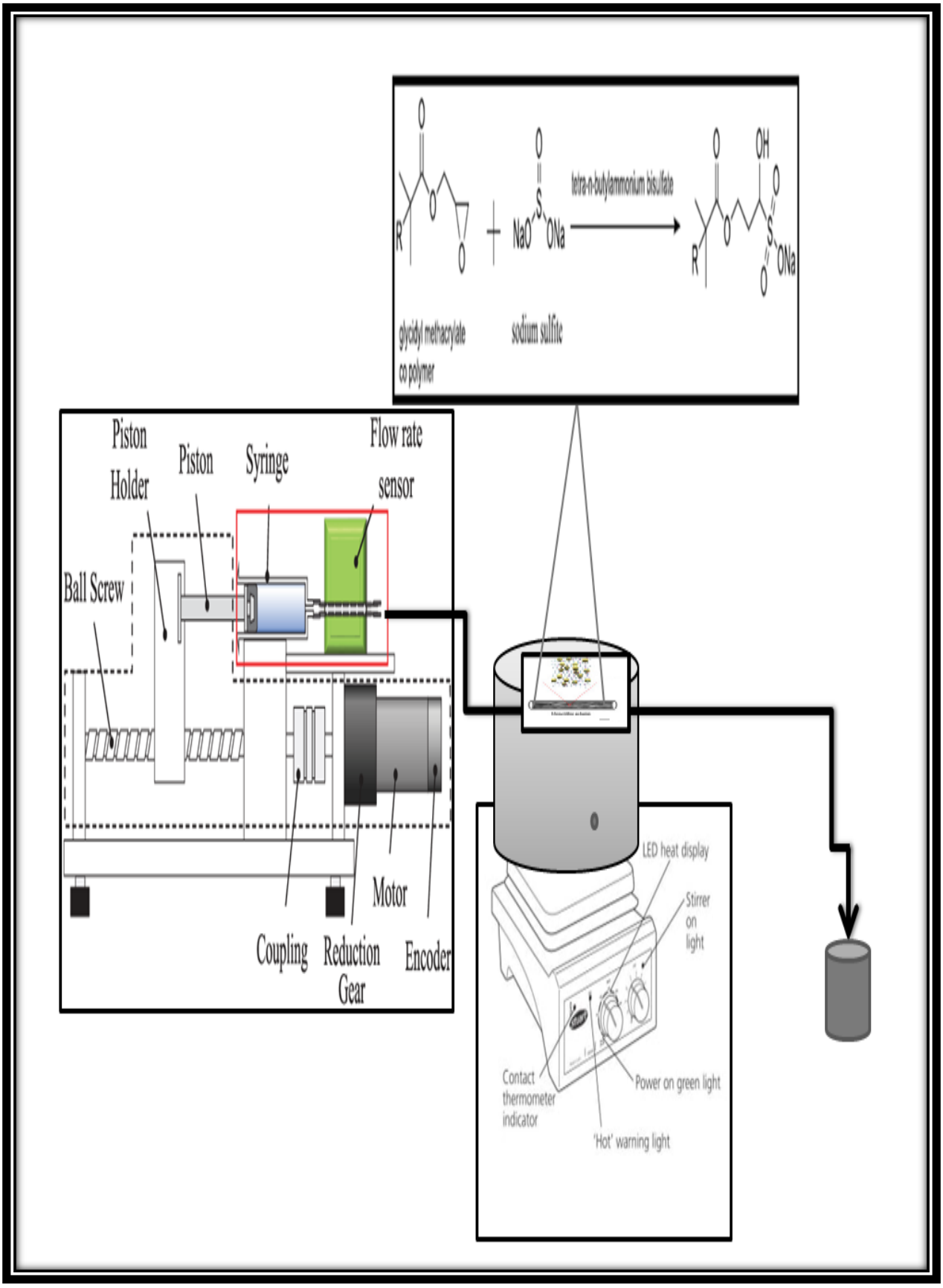

Figure (3.22) Opening the epoxy groups of the GMA in GMA-co-AC co-AAM monolithic columns by sulfonation reaction.

Figure (3.23) (A)Prepare work by connecting the syringe pump to the monolith column and using the sand bath heating mechanism at 70 Cº, (B) Dip the monolith column in hot sand,(C) Pumping the prepared solution to the sulfonation process.

(3.14.1) (FT-IR) spectroscopy for identification after ring opening (GMA-co-ACA-co-AAM) polymer.

The FT-IR spectra of the (GMA-co-AC co-AAM) monolith column shown in (Figure 3.24) were measured to evaluate the surface derivatization of the monolithic materials, the formation of a cationic exchange of the (GMA-co-AC co-AAM) monolith column. The results show that by changing the epoxy ring

to (-OH) and (R-SO3Na) groups from Figure (3.24), the peak at 906.14 $cm^{-1.}$ for epoxy groups of the GMA in the monolith that showed in Figure (3.18) disappeared, and there are two new peaks present, at 1016.06 cm^{-1} and 951.62 cm^{-1} for R-SO3 and S-O groups, respectively; in addition, a medium N-H stretching secondary amine 3342.49 -3199.65 cm^{-1} was observed, the peaks at 1721.60 cm^{-1} for C=O, and 1160.89 cm^{-1} for C-O ester groups are still unchanged due to non-participation of these groups in the sulfonation reaction[153,154].

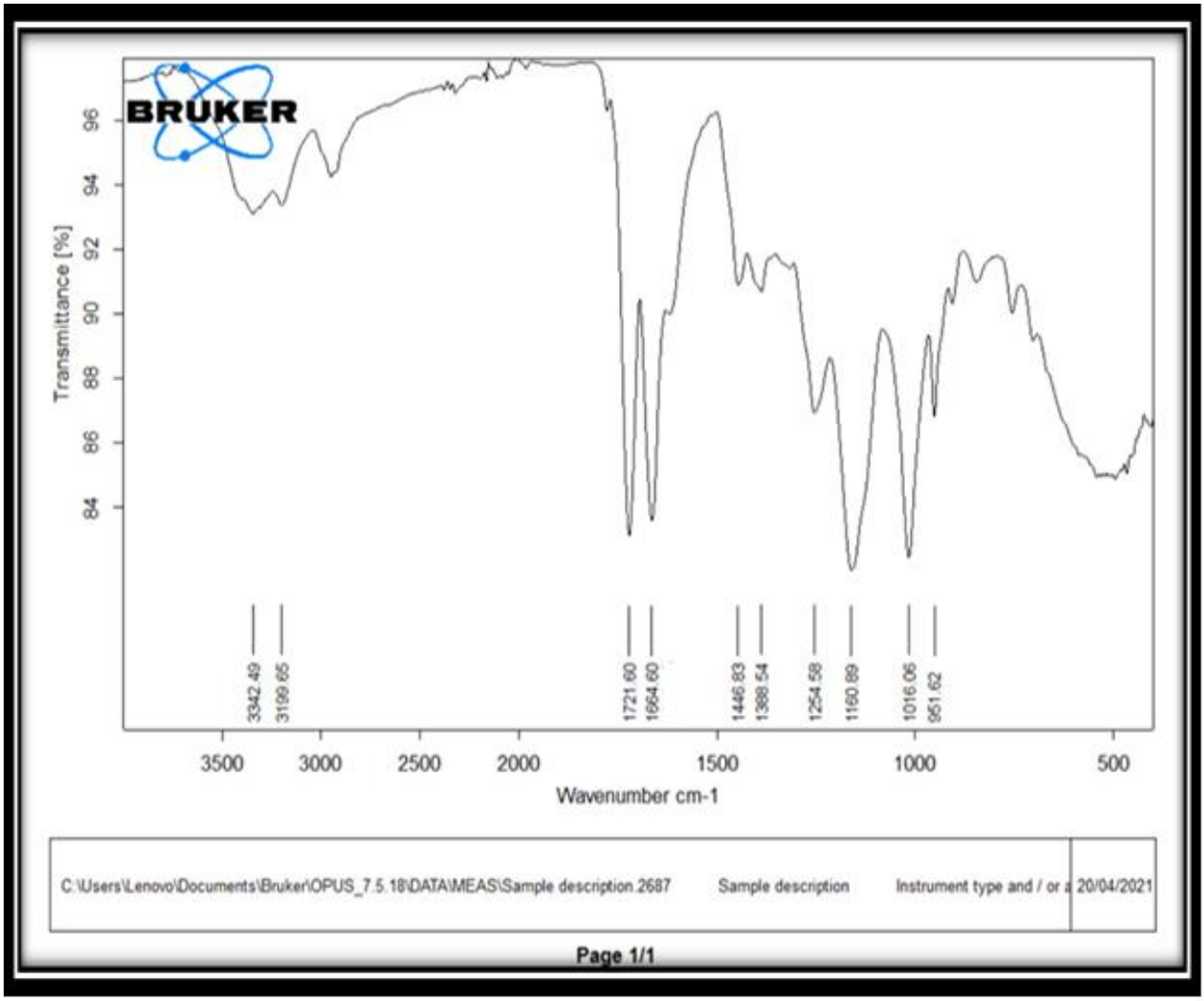

Figure (3.24) FTIR spectrum of the GMA-co-ACA co-AAM monolith after opening epoxy ring.

(3.15) ^{1}H- NMR spectrum.

^{1}H-NMR was used to examine the monolith formation **(GMA-co-ACA-co-AAM)**, which revealed several signals at (3.1-3.4) belonging to CH_2 groups, as well as a signal at 2.5 belonging to CH, while the bands belonging to CH_2 alkene, which at 6.4 were difference due to of polymer formation, vanished. Because this peak can only be detected in monomers (as shown in Figure) (3-25).

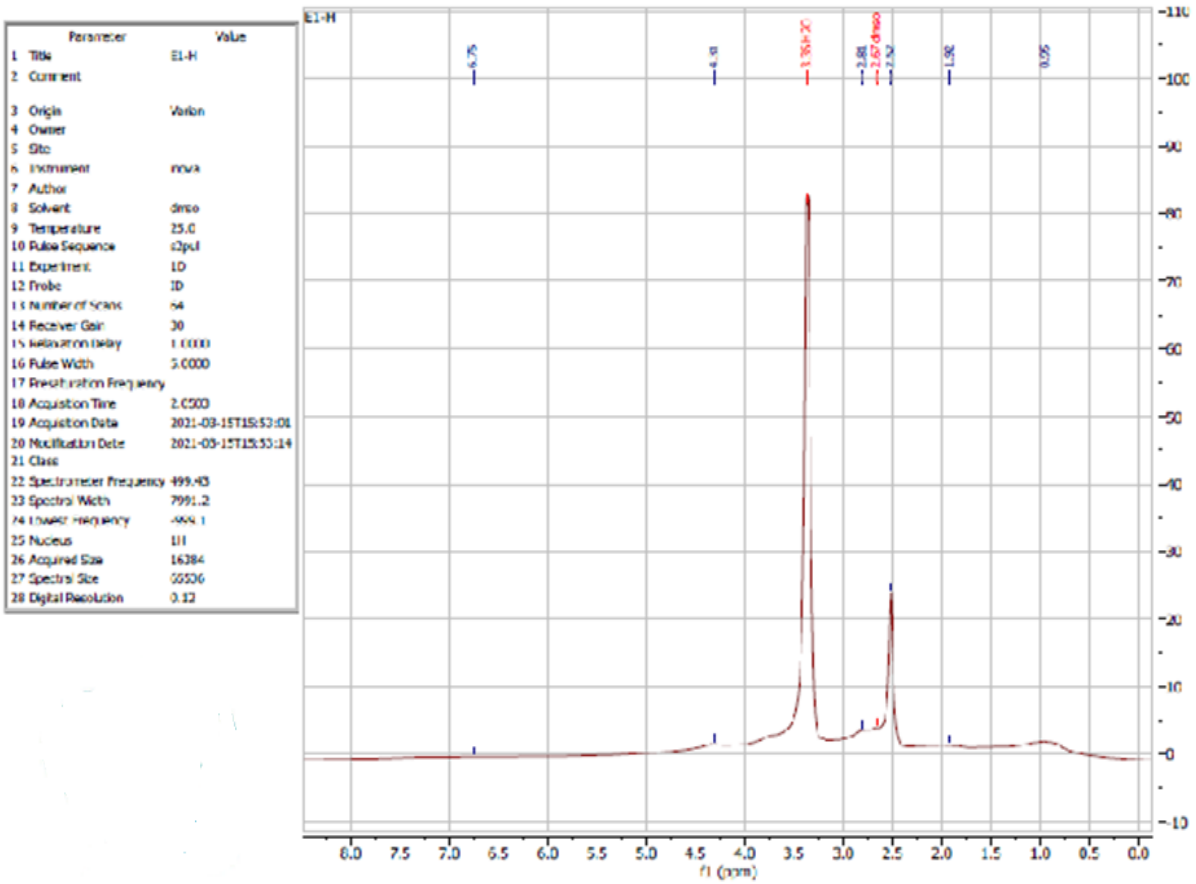

Figure(3.25) (^{1}H- NMR) of the polymer (GMA-co-ACA-co-AAM).

(3.16) Application for Off-line method for incorporation Copper ion with and without monolith column.

The monolith was washed with 2.5 mL of distilled water. Then 2.5 mL of a Cu^{+2} solution($Cu(NO_3)_2$ [2.5 $mg.L^{-1}$ and 3.5 $mg.L^{-1}$] was pumped through the monolith column at room temperature for 2 h, respectively. Then, 2.5 ml was pumped into the monolith column with distilled water to be washed. The two-in-one method was used to eluent the Cu ions reactivated the column by a pump of hydrochloric acid at a concentration of 0.2 M. The concentration of Cu^{+2} ion in the solution was determined (eluent) using colour absorption spectroscopy after it was reduced to (Cu^{+}) by Uric acid at 200 mg. L^{-1} and then prepared a series of standard concentrations using a specialized reagent (neocuprion hydrochloride) for the copper ion (Cu^{+}); this value was well compatible with that obtained by atomic absorption as the concentration result was (2.34 $mg.L^{-1}$) and (3.47 $mg.L^{-1}$) respectively. After the Cu^{+2} ion concentration (eluent) was determined using atomic absorption spectroscopy for comparison. Figure (3.26) and Table (3-8) show that.

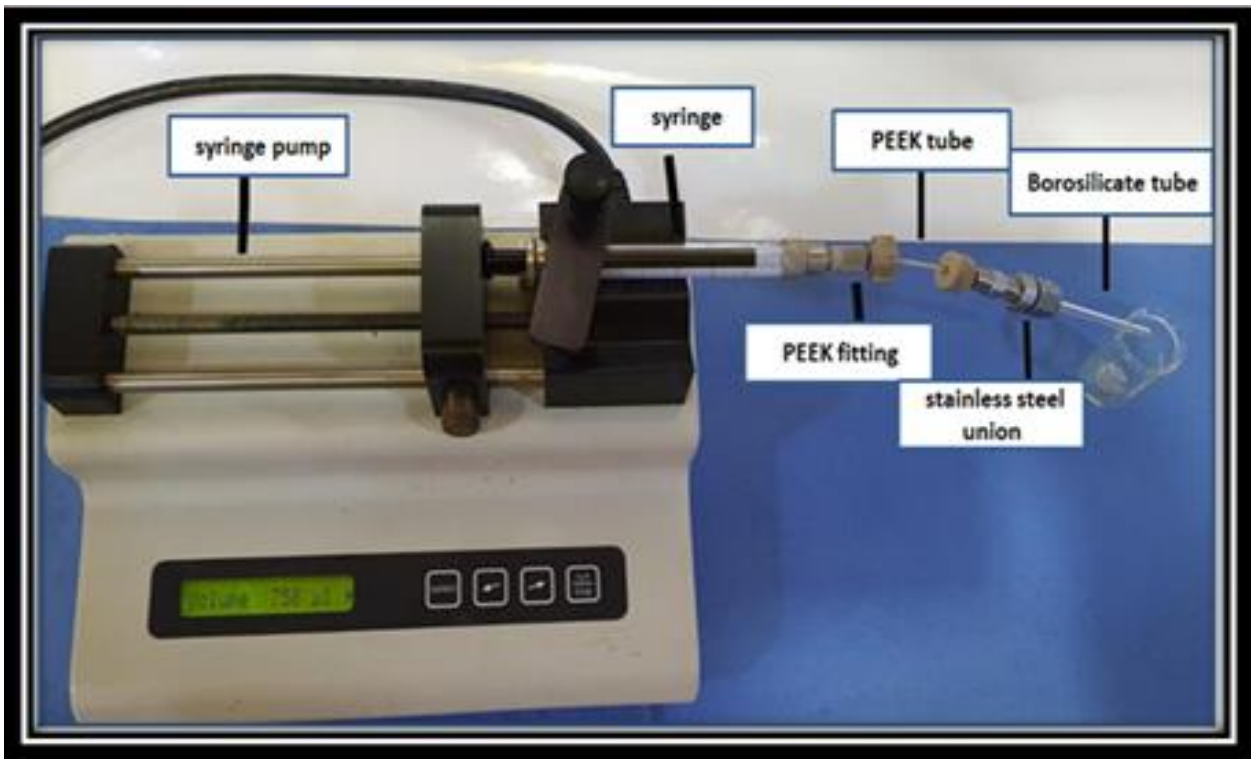

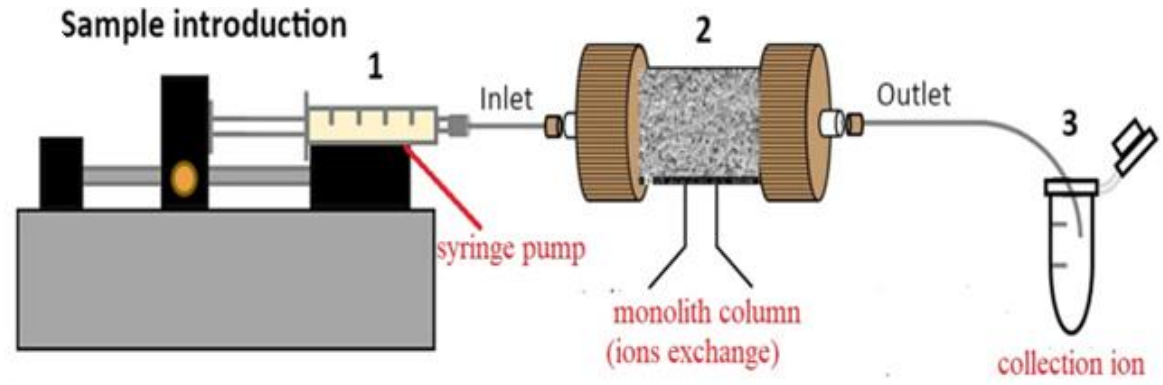

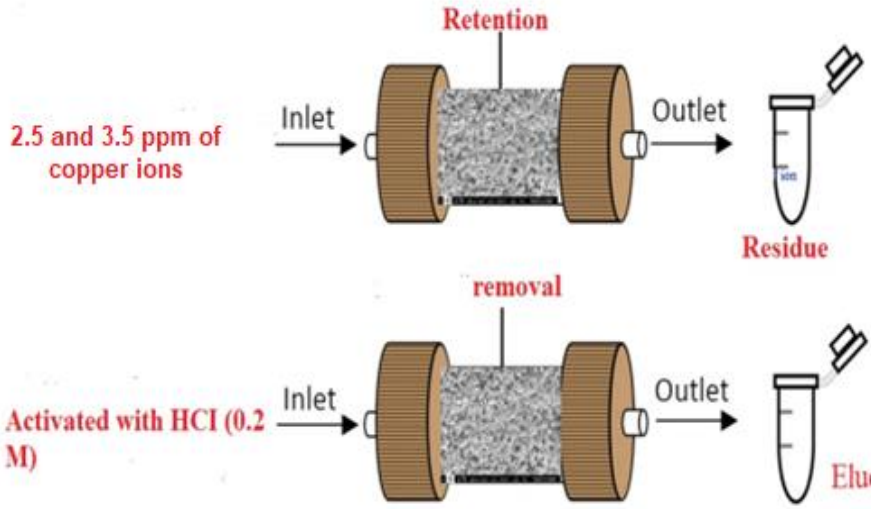

Figure (3.26) Off-line method for incorporation of Cu^{+2} ion with the GMA-co-ACA co-AAM

(3.17) The calibration curve for Cu^{+}.

Under the optimum parameters, a series of copper concentrations were prepared to study the calibration curve in the range of (1—35) $mg.L^{-1}$ from the calibration curve; it was found that the unknown concentration of the standard sample (8.5 $mg.L^{-1}$) injected through the monolith is equal (8.48 $mg.L^{-1}$) according to Figure (3-27). The result is shown in Tables (3.6) and (3.7).

Table (3.6): Calibration graph values at optimum conditions, including 200 ppm of Uric acid, neocuprion hydrochloride as reagent 100 ppm, and the temperature was 23±3 °C.

Conc. of Cu+ $mg.L^{-1}$	Mean Abc (n=3) $\bar{Y}$	S.D	R.S.D%	Recovery(%)	Mean of SD and RSD(%)
1	0.0120	0.001	4.681	100.00	$1.77*10^{-3}$ and 1.086%
3	0.0291	0.000	0.000	100.42	
5	0.0445	0.000	0.000	98.75	
10	0.0851	0.000	0.000	100.13	
15	0.1167	0.006	4.949	95.83	
20	0.1680	0.000	0.000	101.88	
25	0.2150	0.000	0.000	105.00	
30	0.2450	0.009	0.000	100.00	
35	0.3103	0.000	0.149	108.93	

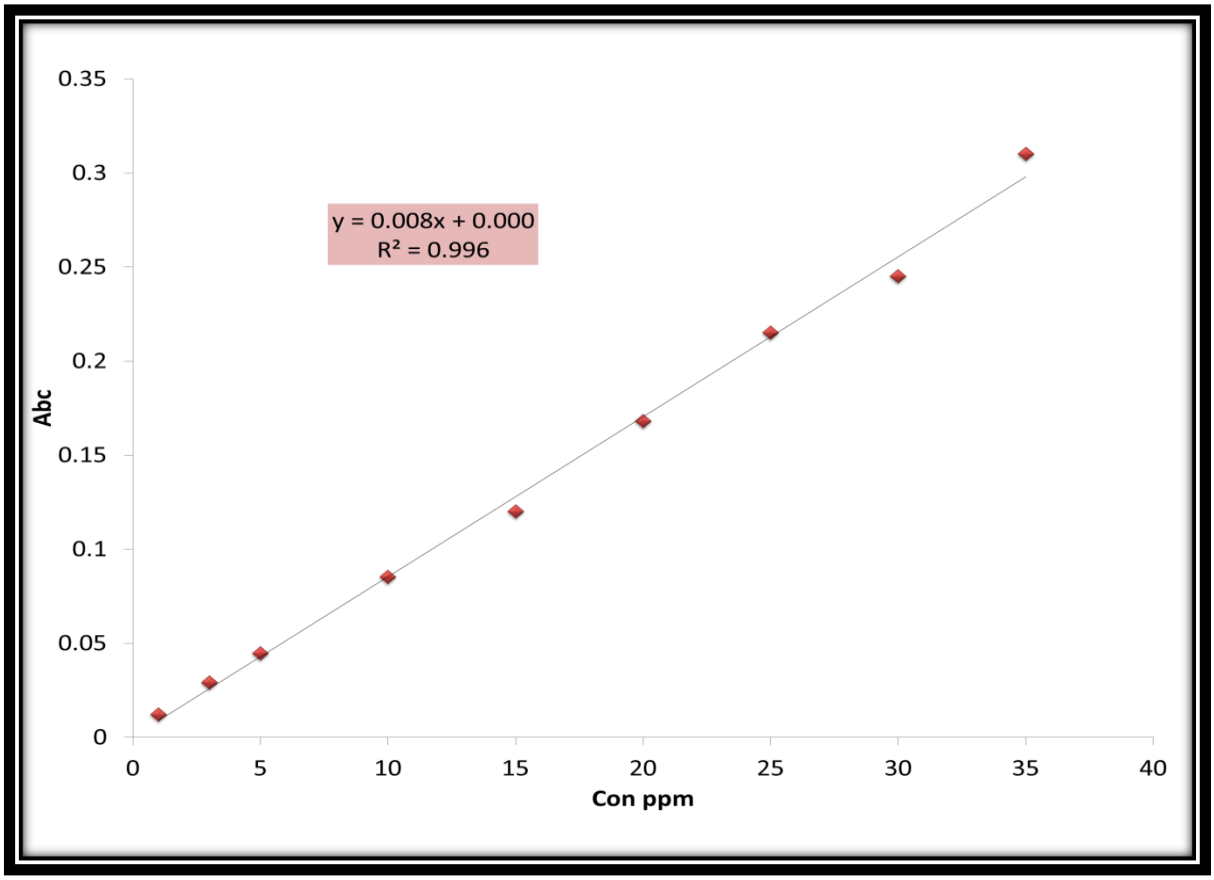

Figure (3.27) calibration curve for Cu+

Table (3-7) parameter of the calibration curve

Parameter	Value
Accuracy	99.825±5.9511
Regression Equation	y=0.0085x+0.0006
Slope	0.0085
Y-intercept	0.0006
Linearity Range	1—35 $mg.L^{-1}$
Correlation Coefficient	0.9980
SE Intercept	0.003
SD Intercept	0.010
LOD	0.269 $mg.L^{-1}$
LOQ	0.807 $mg.L^{-1}$
Average SD	0.001
Average RSD%	0.566 %

Table (3.8) shows the concentration of the standard solution before and after using the separation column, indicating the high separation effectiveness of the column. For the wastewater samples, it is evident that the column could separate (0.1213) $mg.L^{-1}$ from (0.3404) mg. L^{-1} copper ions were present in the water entering the station, and (0.0652) $mg.L^{-1}$ of (0.0771) $mg.L^{-1}$ copper ions were separated from the water leaving the station. This is because there was a presence of copper ions in the water entering the station. This is due to the fact of many other ions and copper ions. It also contains wastewater that was separated using the column.

Table (3-8) Application for Off-line method for incorporation Copper ion with & without monolith column.

Type of sample & position	Spectrophotometric determination n=3 In $mg.L^{-1}$			Atomic absorption determination n=3 In $mg.L^{-1}$		
	Before using column	After using column	RSD %	Before using column	After using column	RSD%
(Standard solution)	2.52	2.098	0.13	2.52	2.34	0.1
(Standard solution)	3.53	3.489	0.11	3.47	1.8676	0.03
Wastewater(inflow)	0.3404	0.1213	2.89	0.1301	0.0420	0.22
Wastewater (outflow)	0.0771	0.0652	0.44	0.0856	0.0260	0.67

(3.18) Synthesis of imidazole-azo ligand ((E)-2-((4 methoxyphenol)diazenyl)-4,5-diphenyl-1-Himidazole.

The reagent is an orange powder which is sparingly soluble in water. It is soluble in ethanol, methanol, acetone and chloroform and easily soluble in DMF and dimethyl sulfoxide (DMSO). It is red-orange in alkaline solution when reacted with nickel (II), as shown in Figure (3.28).

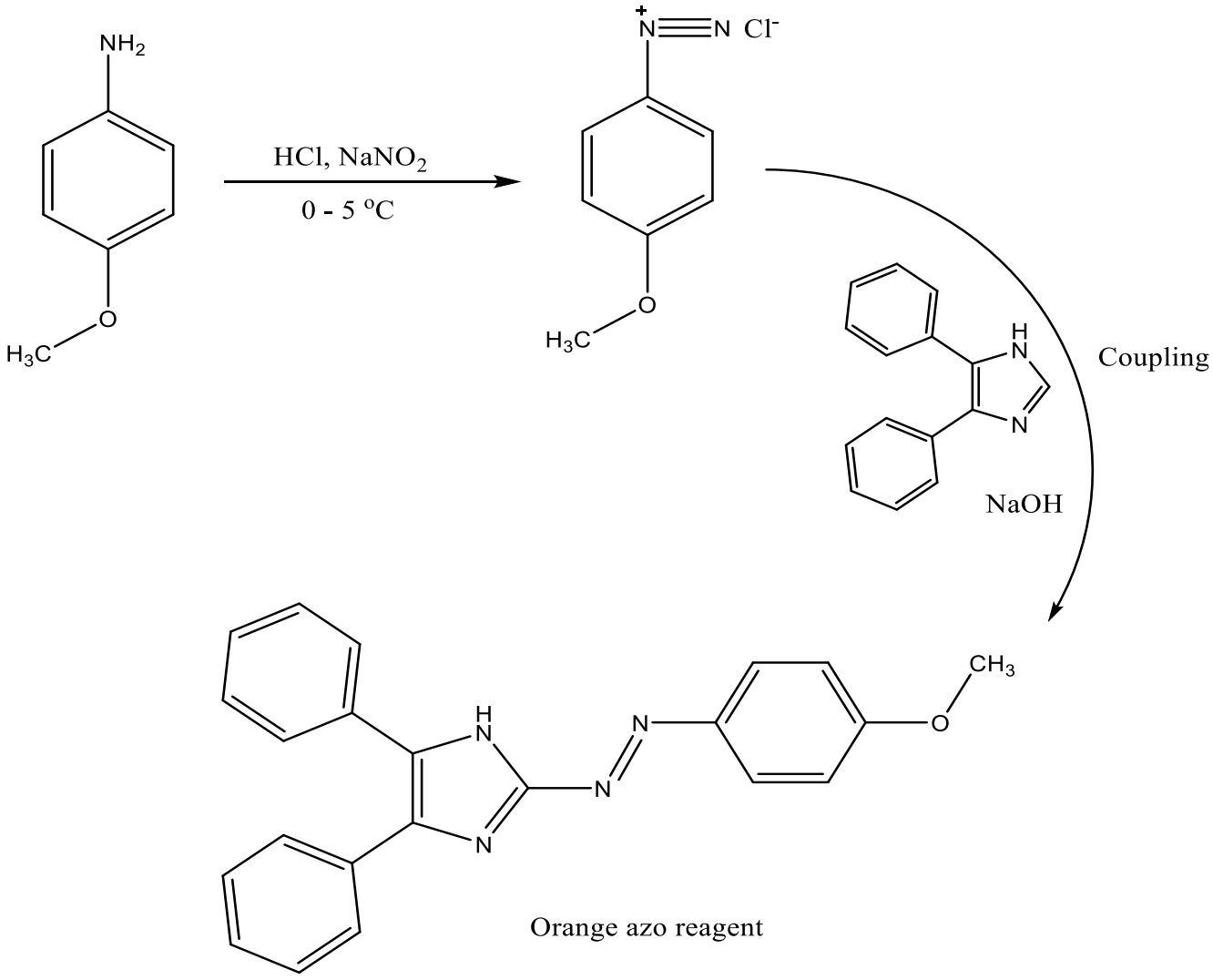

Figure (3.28) The scheme represents the reaction steps for synthesizing the ligand.

(3.19) Absorption spectrum of the complex

The absorption spectra of ((E)-2-((4 methoxy phenol) diazenyl)-4,5-diphenyl-1Himidazoleand its nickel complex under the optimum conditions is shown in Figure (3.29). It can be seen that the maximum absorption peak of the reagent is 415nm, while the absorption peak of the complex is 518nm. Therefore, due to the complex formation, the redshift (103 nm) accrued in the UV-Vis spectra.

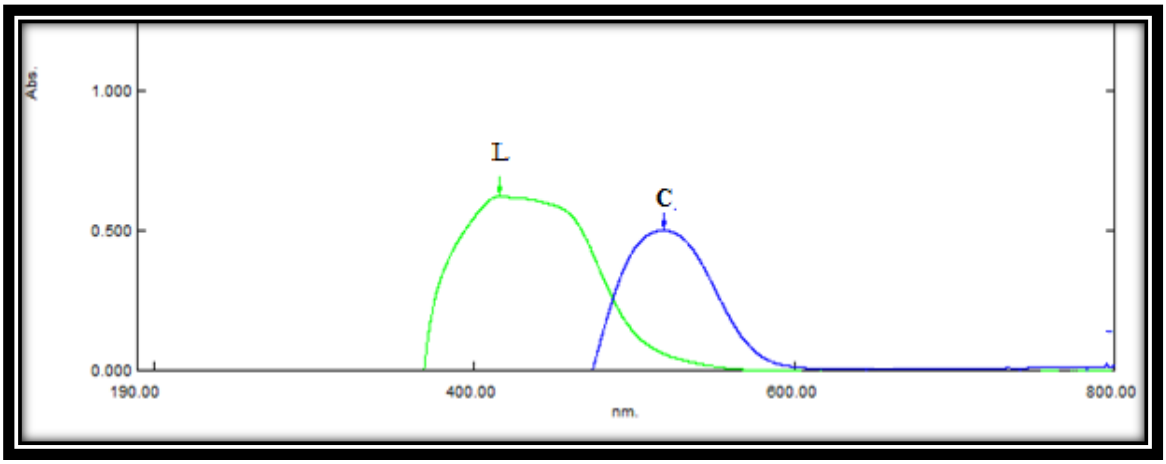

Figure (3.29). Absorption spectra of L: Reagent (MPDADPI)C:[Ni-(MPDADPI)]

(3.20) (FT-IR) spectroscopy and (C.H.N) analysis for ((E)-2-((4-methoxyphenol)diazenyl)-4,5-diphenyl-1-Himidazole reagent.

The FT-IR spectra of the((E)-2-((4-methoxy phenol) diazenyl)-4,5-diphenyl-1-Himidazole reagent is shown in Figure (3.30). The (C=C) group of the aromatic ring appears in the spectrum at 1672 cm^{-1}. The 1500 cm^{-1} and 1579 cm^{-1} frequencies are due to azo chromophore aromatic compounds because resonance increases the double bond beta [156]. 1298 cm-1 is due to C-N stretching (azo bond C-N) [157].

The N═N band appeared at 1463-1483 cm-1 [158]. The C-N absorption occurs at a higher frequency and widens the ring and the attached nitrogen atom[159]. The C-N stretching for tertiary amine appeared at 1174 cm^{-1} and 1144 cm^{-1}. The (C.H.N) analysis of the synthesized compound showed good agreement with found values calculated in Figure (3.31).

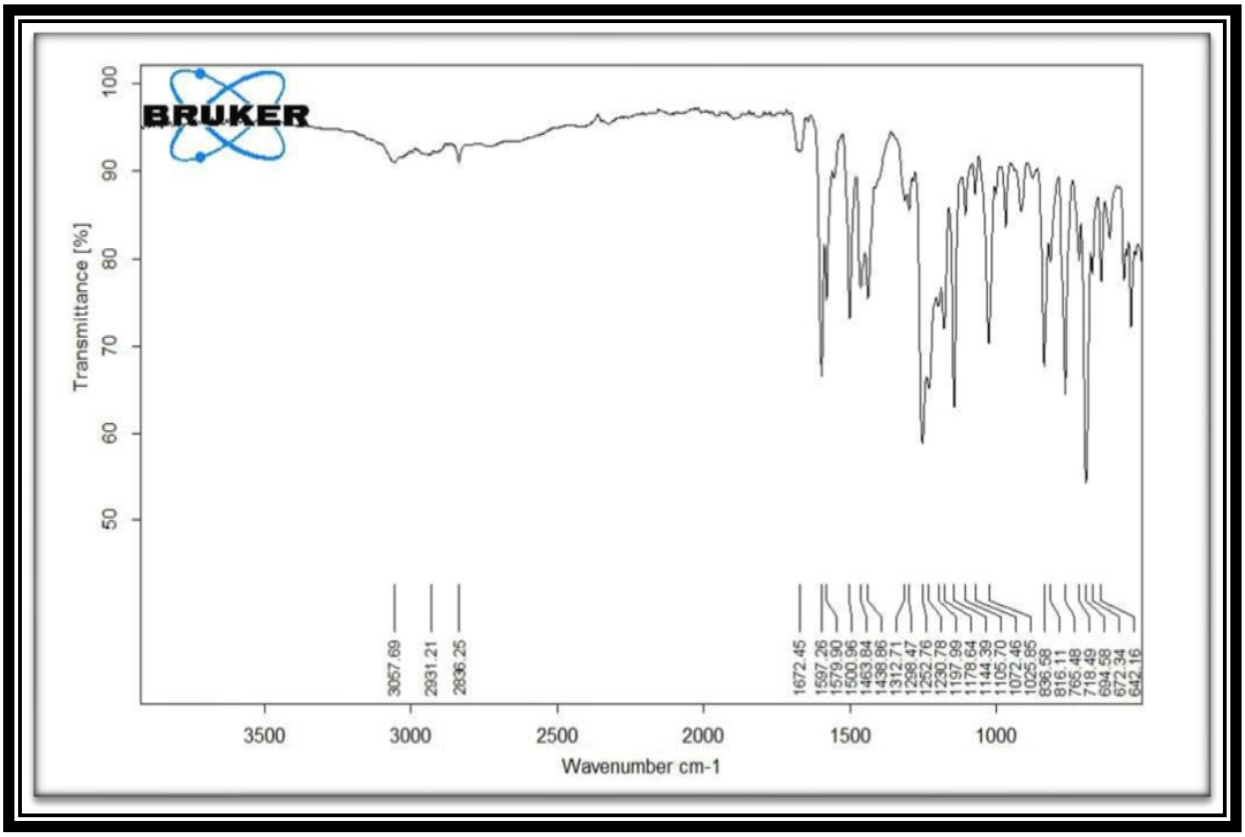

Figure (3.30) FT-IR spectrum of ((E)-2-((4-methoxyphenol)diazenyl)-4,5-diphenyl-1*Himidazol*e reagent.

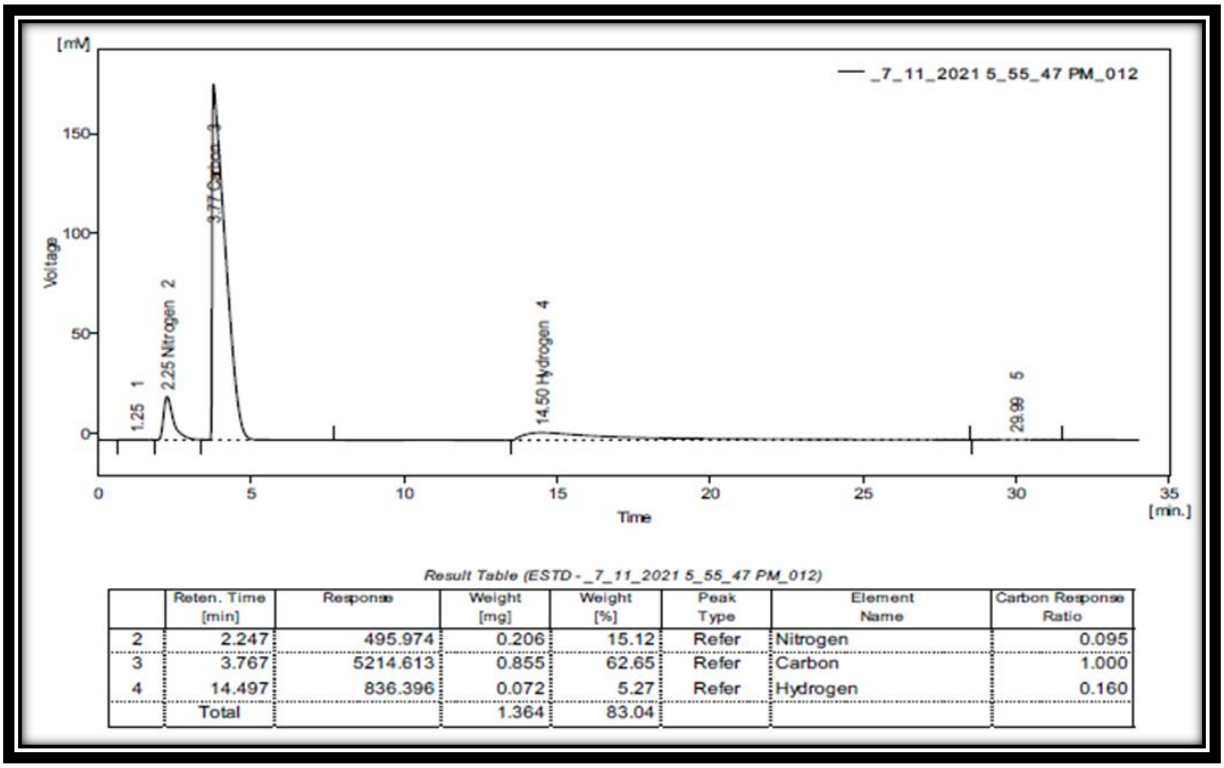

Result Table (ESTD - _7_11_2021 5_55_47 PM_012)

	Reten. Time [min]	Response	Weight [mg]	Weight [%]	Peak Type	Element Name	Carbon Response Ratio
2	2.247	495.974	0.206	15.12	Refer	Nitrogen	0.095
3	3.767	5214.613	0.855	62.65	Refer	Carbon	1.000
4	14.497	836.396	0.072	5.27	Refer	Hydrogen	0.160
	Total		1.364	83.04			

Figure (3.31) (C.H.N) analysis of ((E)-2-((4-methoxyphenol)diazenyl)-4,5-diphenyl-1*Himidazol*e reagent.

(3.21) ^{1}HNMR spectrum study

The ^{1}HNMR spectra of the ligand were recorded in DMSO-D6. The ^{1}HNMR spectrum of the ligand shows the following signals: phenyl multiples at (7.1 -8) δ range, -$OCH_3$of methoxy group at 3.2δ, -NH at 4.9δ, =C-CH3 at 2.2 δ rang[160] as shown in Figure (3.32).

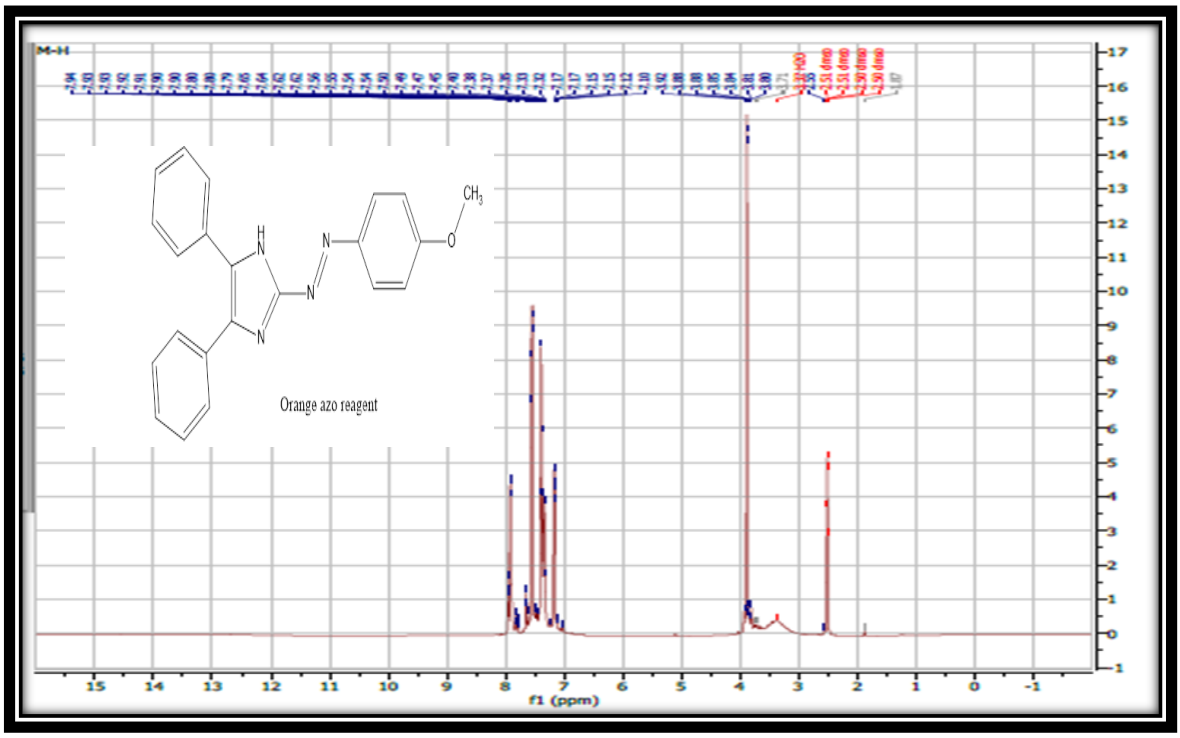

Figure (3.32)^{1}HNMR spectrum of the reagent.

(3.22). Effect of reagent concentration.

Ni(1I) solution concentration remained constant for optimization conditions; the reagent concentration was studied at the range ($1x10^{-6}$-$1x10^{-3}$) M. The reagent concentration of $5x10^{-5}$M was chosen as the optimum value.

(3.23).Effect of pH buffer concentration.

The optimum pH range for the complex formation was examined using a buffer solution consisting of 0.2M NH_4OH and 0.2M HCl; the result is shown in Figure (3.33). At a pH lower than 3.5, the complex was not formed due to the protonation or the electron pair of nitrogen atoms that prevent the nickel cations

from coordinating with the reagent. On the other hand, when the pH is increased over 3.5, the nickel ions will compete with the hydrogen ions to occupy the electrons pair and form a coordination complex, showing significant absorbance values in the range (3.5-8). After that, the absorbance values were decreased due to the precipitation of nickel as $Ni(OH)_2$. Therefore, the optimum pH was **8**.

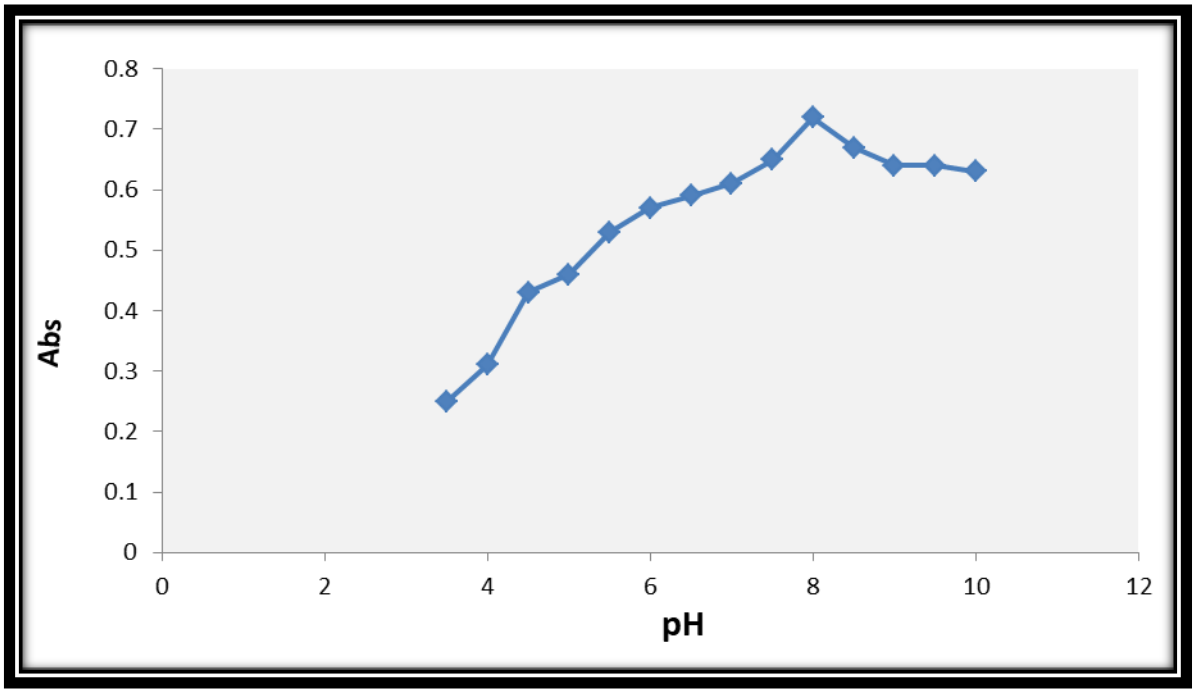

Figure (3.33). Effect of pH range

(3.24) Continuous Variation to the Stoichiometry of (M-L) Complexes.

Job's method of continuous variation was used to determine the stoichiometry of molecular complexes (M-L). It offers the potential advantage of determining the stoichiometry of complication in a single experiment without determining the absolute concentration of the bound ligand.

The continuous-variation method uses the concept that a limiting reactant lowers product yield and that there exists a mole ratio of reactants, r, which produces the highest product yield [161]. A series of solutions were prepared to contain variable concentrations of the two components, M and L, provided that the total concentrations were constant using (0.05 M of nickel (II) metal and 0.1 M of the

prepared ligand) the molar fraction is obtained from the top and is equal to 0.5 it mean (1:2) molar ratio for the complex (M-L). Figure (3.34) and Table (3-8) show. The formation constants (K_f) of the studied imine complexes formed in solutions were obtained from the spectrophotometric measurements using the continuous variation method according to the following relation[162].

$$Kf = \left(\frac{A/Am}{\left(1 - \frac{A}{Am}\right) 2C} \right) \qquad (3-1)$$

Where Am is the absorbance at the maximum formation of the complex (0.5), A (0.3) is the arbitrarily chosen absorbance value on either side of the absorbance mountain col (pass), and C (10 $mg.mL^{-1}$) is the initial concentration of the metal; therefore the formation constant(K_f) was (0.0375).

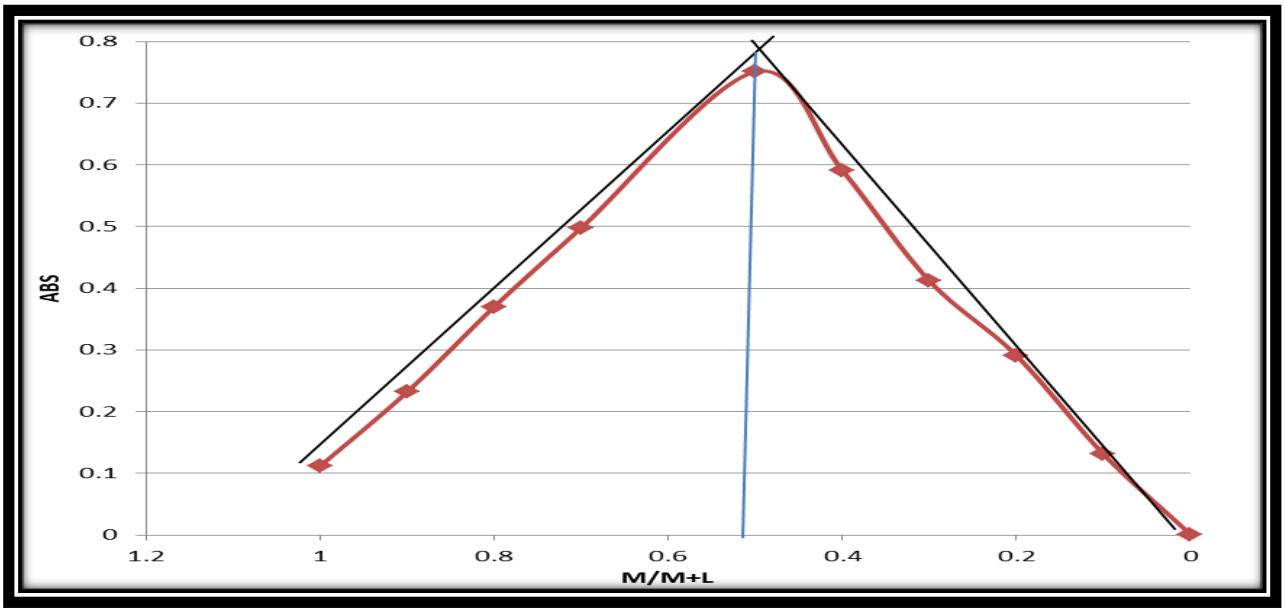

Figure (3.34) Continuous Variation to the Stoichiometry of (M-L) Complexes

Table (3-9). Continuous Variation to the Stoichiometry of (M-L) Complexes

Srq.No.	Volume of metal (ml) with 0.05 M	Volume of ligand (ml) with 0.1M	volume(M+L)(ml)	volume(D.W)(ml)	Total volume(ml)	ABS	mole fraction (M/(M+L)
1	10	0	10	15	25	0.001	0.0
2	9	1				0.131	0.1
3	8	2				0.541	0.2
4	7	3				0.859	0.3
5	6	4				0.7743	0.5
6	5	5				0.652	0.6
7	4	6				0.478	0.7
8	3	7				0.361	0.8
9	2	8				0.242	0.9
10	1	9				0.112	1.0

(3.25) Off-line method for incorporating Ni^{+2} ion with the GMA-co-ACA co-AAM monolith column using (MPDADPI) reagent.

The investigation of nickel ions was carried out for the prepared monolith. Firstly, it was washed with 2.5 mL distilled water, and after that, 2.5 mL Ni (II) as($Ni(NO_3)_2$. Four solutions (2.5, 3.5, 2 and 2.5) $mg.L^{-1}$for standard solution and wastewater (in & out flow) treatment station in Al-Maamera were pumped separately through the monolith column for these solutions (2 hrs), respectively. At room temperature, 2.5 mL was pumped into the monolithic column with distilled water to be rewashed, and then the column was activated with hydrochloric acid (0.2 M). The Ni^{2+} ions concentration in the eluent was determined spectrophotometrically, using a specialized reagent (MPDADPI) for the nickel ion (Ni^{+2}). The results were compatible with that obtained by atomic absorption as the concentration result was (1.899, 1.340,0.042 & 0.0260) $mg.L^{-1,}$ respectively. After the Ni^{2+} ion concentration was determined (eluent) by using atomic absorption spectroscopy for comparison, as shown in Figure (3.35) and Table (3.10)

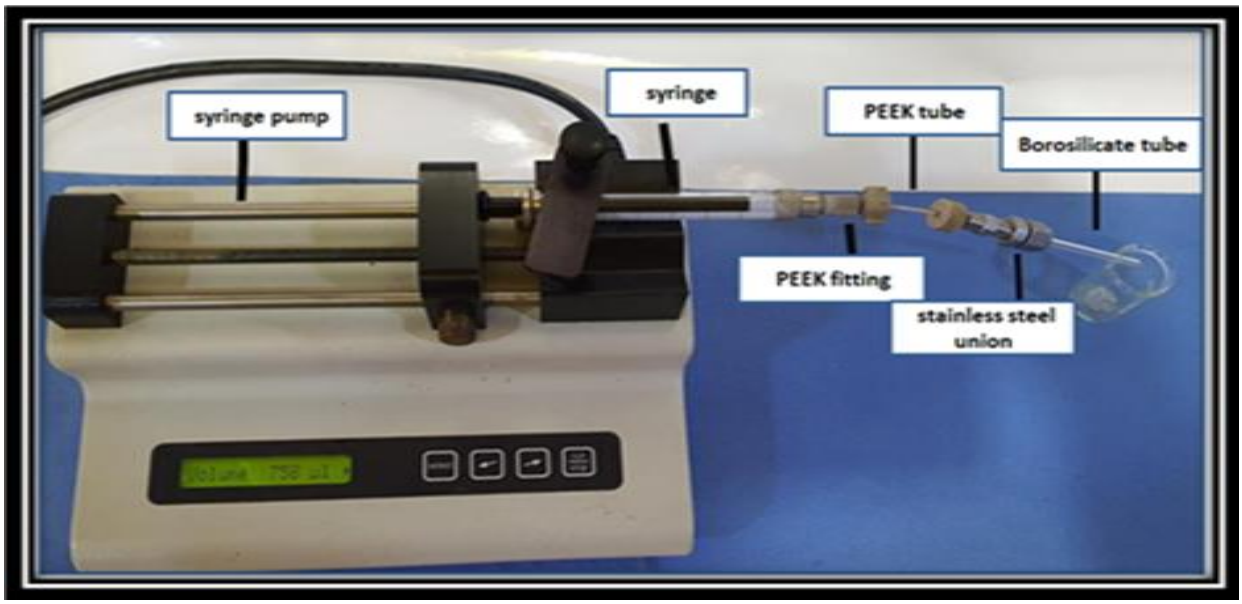

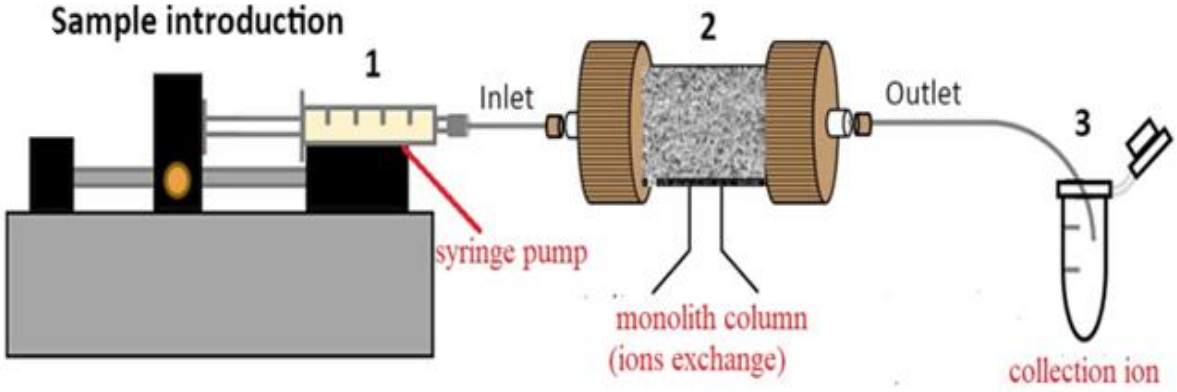

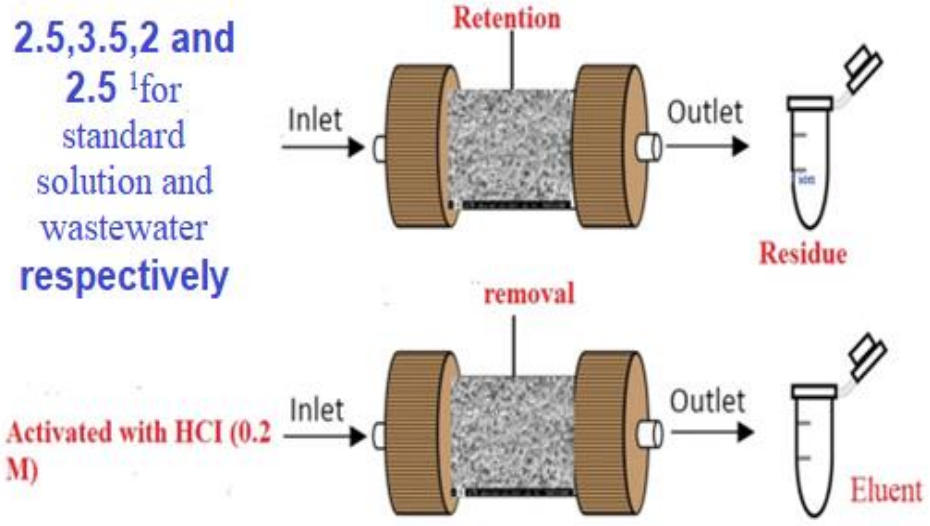

Figure (3.35) Off-line method for incorporation of Ni^{+2} ion with the GMA-co-ACA co-AAM

Table (3-10) Application for Off-line method for incorporation nickel ion with and without monolith column.

Type of sample& position	Spectrophotometric determination n=3 In $mg.L^{-1}$			Atomic absorption determination n=3 In $mg.L^{-1}$		
	Before using column	After using column	RSD %	Before using column	After using column	RSD %
(Standard solution)1	2.50	1.975	0.17	2.499	1.899	0.05
(Standard solution)2	3.50	2.933	0.21	2.98	1.340	0.05
Wastewater(inflow)	2.0	0.987	2.79	0.1521	0.0420	0.22
Wastewater (outflow)	2.50	0.789	0.74	0.0956	0.0260	0.67

(3.26) The calibration curve for Ni^{+2}.

After optimizing the optimum conditions, a series of Ni (II) concentrations were prepared to construct the calibration curve. The linear range of calibration curve was (0.5-32 mg. L^{-1}) (R^2=0.9987), as shown in Figure (3.36).

Table (3.11): Calibration curve values at optimum conditions, including $5x10^{-5}$M (MPDADPI) as reagent pH was 8, and the temperature was 23±3 °C.

Conc. of Ni(II) $mg.L^{-1}$	Mean Abc (n=3) $\overline{Y}$	S.D	R.S.D%	Found Con. ppm	Recovery(%)
0.5	0.013	0.001	0.907	0.486	97
1	0.019	0.001	0.093	0.714	71
1.5	0.025	0.001	2.341	1.143	76
2	0.041	0.001	2.439	2.286	114
4	0.075	0.001	0.773	4.714	118
8	0.143	0.040	0.196	7.929	99
12	0.182	0.001	0.549	12.357	103
16	0.232	0.001	0.497	16.000	100
20	0.299	0.001	0.193	20.714	104
24	0.342	0.002	0.446	23.786	99
28	0.411	0.001	0.281	28.643	102
32	0.452	0.001	0.128	31.643	99

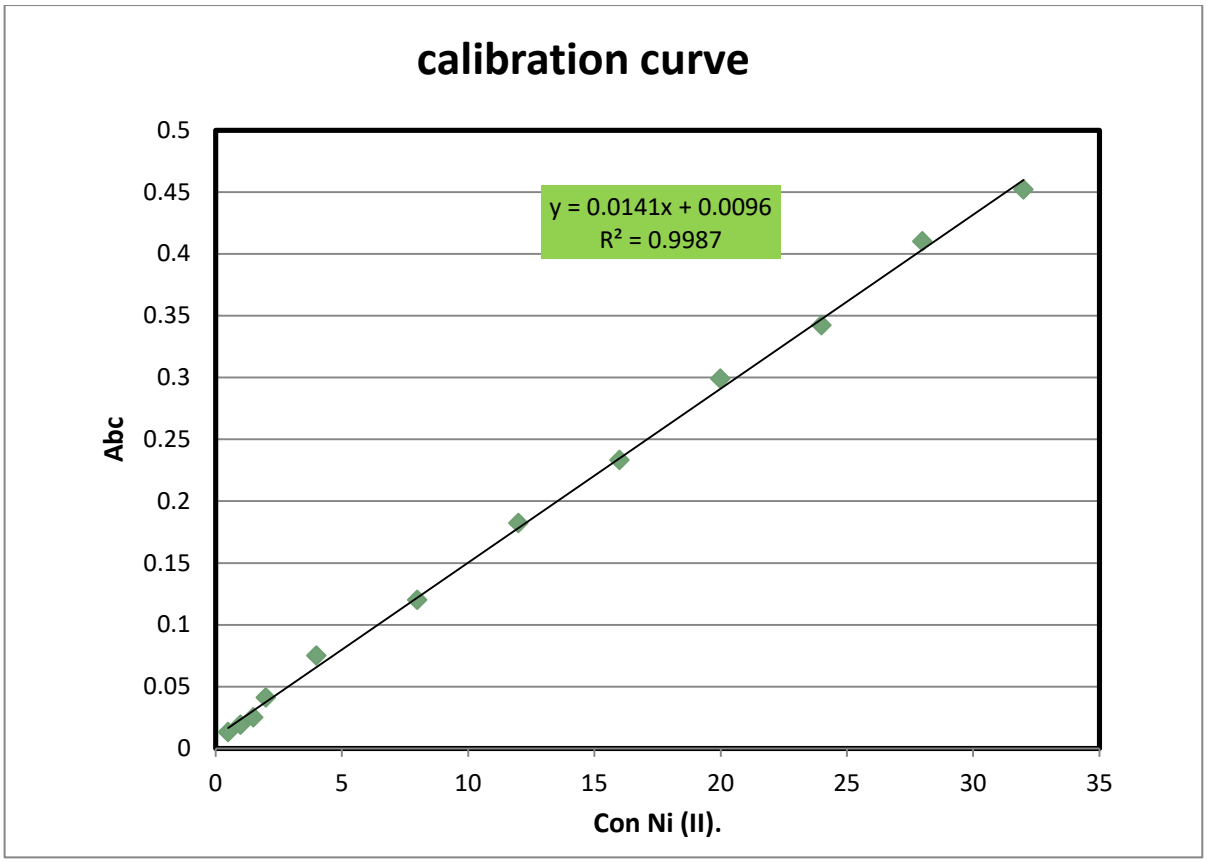

Figure (3.36) calibration curve for nickel ion

Table (3-12) parameter of the calibration curve

Parameter	Value
slope	0.014
Intercept	0.009
Linearity Range	0.5-32 mg/L
Correlation Coefficient	0.9987
LOD	0.3 $mg.L^{-1}$
LOQ	0.9 mg.L-1
Average SD	0.377
Average RSD%	0.370

(3.27) Distribution coefficients and capacity for monolith column

Distribution coefficients of Cu^{+2} ion with the GMA-co-ACA co-AAM monolith column were calculated as explained by the following (Eq.) (3-2) [163].

$$\left(\mathbf{Kd} = \frac{\mathbf{Ci} - \mathbf{Cf}}{\mathbf{Cf}} \times \frac{\mathbf{v}}{\mathbf{m}}\right) \qquad (\mathbf{3-2})$$

Where K_d represents the distribution coefficient; C_i (5 ppm) and C_f (3.5) are initial and final concentrations of metal ions, respectively. V (2.5 ml) is the volume of the solution (mL), and m is the mass of the monolith used (0.577g), where K_d was found to be (1.8).

The capacity of the monolithic column was calculated by the following Expression[164] :

$$\left(\mathbf{Q} = \frac{\mathbf{C} * \mathbf{V}}{\mathbf{W}}\right) \qquad (\mathbf{3-3})$$

Where Q is the chelating monolith column's adsorption capacity ($mmol.g^{-1}$), V is the eluate's volume (L), C is the concentration of (M^{2+}) in the eluate ($mmol.L^{-1}$), and W is the dry weight of the monolith inside the column (g). The total capability was found to be (6.49 $mg.L^{-1}$).

(3.28) Online method Cu^{+2} ion determination using the GMA-co-ACA co-AAM monolith column.

(3.28.1) Design (1) of HPLC-FIA system to determine copper ions.

The HPLC-FIA system has been designed for the determination of copper ions. The basis of this project is to connect and prepare the main parts through which to access the new system, which are:

1- The step of connecting the electronic pump (The Jasco PU-980 Intelligent HPLC Pump has built-in program that allows high and low pressure operation, gradient of one or two pumps. HPLC pump covers glow rate, gradient elution, solvent selection, and time-based programs. This pump also covers a wide flow rate range as well as precision,therefor the choosing of Jasco PU 980 Intelligent HPLC Pump Module is in excellent condition as shown in figure (3.37).

Figure (3.37) Jasco PU 980 Intelligent HPLC Pump Module

2- The stage of manufacturing the flow-injection valve or the so-called (injection unit): The valve consists of 3-way plastic secondary valves that can pass solutions in three directions by controlling them manually and can load two materials at the same time, and the third material as a carrier stream through using two connections, one for the detector and the other for the sample.

The valve was manufactured locally in the laboratory, characterized by its small size, as the loading connections were up to 5 cm in length. It was made of local materials, cheap and environmentally friendly in the case of damage and easy to control manually. Therefore, when any defect occurs in one of its parts, it can be easily disassembled and repaired without difficulty, comparable to the global valves used, which can load only one material, high price, very complex installation and the problem of dismantling them. This stage is represented by the entry of the sample (the copper ions) into the injection unit after the closure of the two ports of the carrier current and the monolith column, as the direction of filling the sample link is from the second valve (a) to the secondary valve (c) and then to the sample link and then to the secondary valve (b) then the excessive direction exit from the second valve (c) as shown in Figure (3-38).

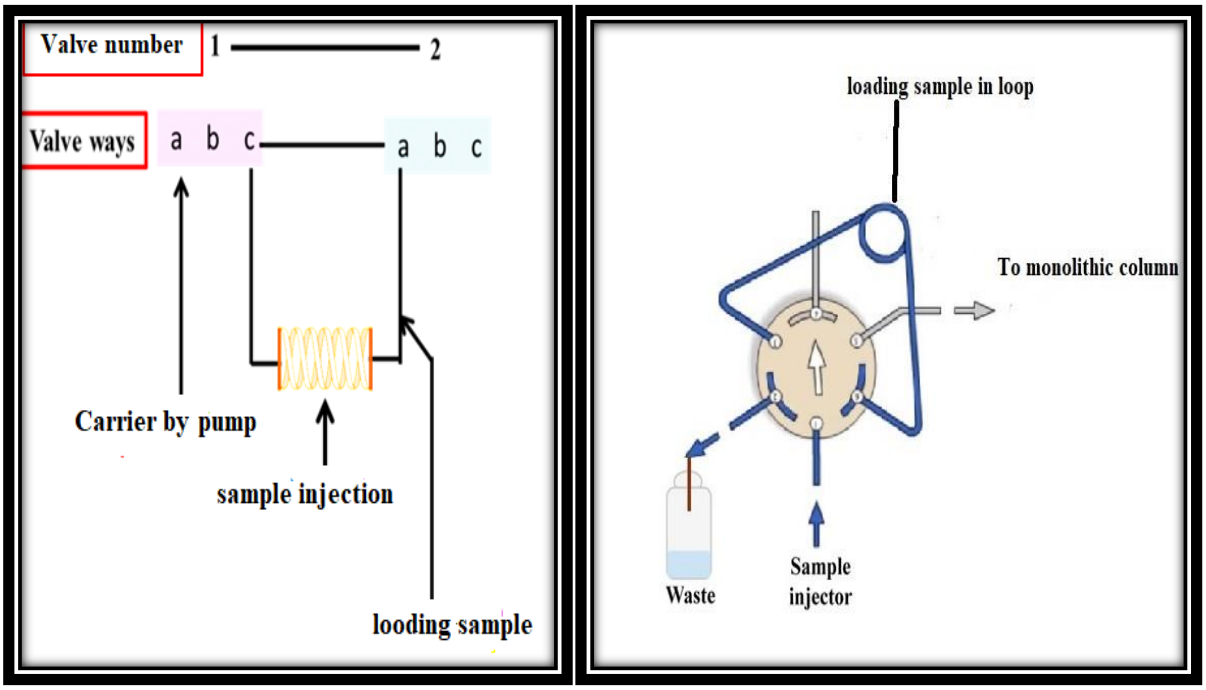

Figure (3.38) Home-made injection unit

3-The stage of connecting the prepared monolith column, the sample is separated by distributing the sample between two phases: mobile and stationary. A figure (3.39) illustrates it.

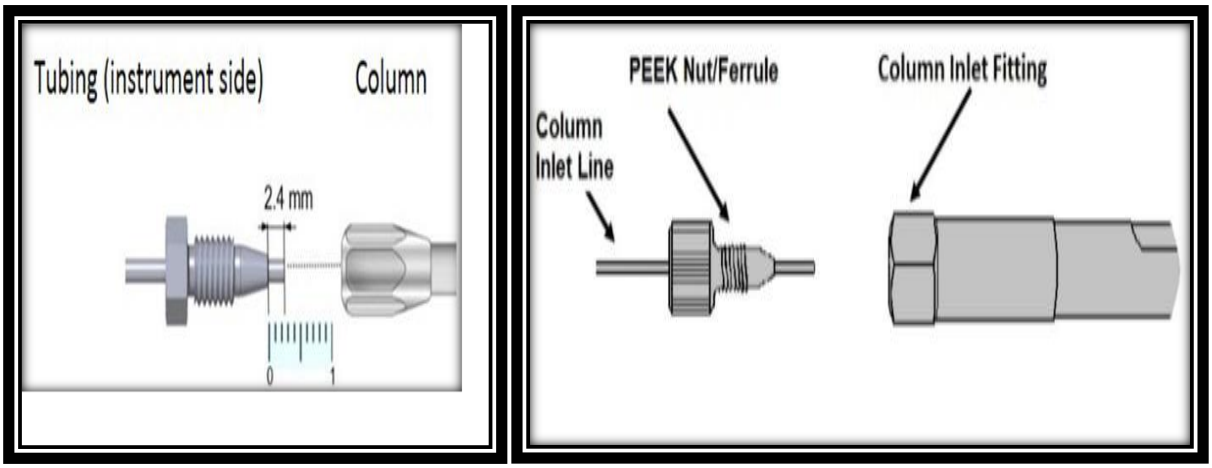

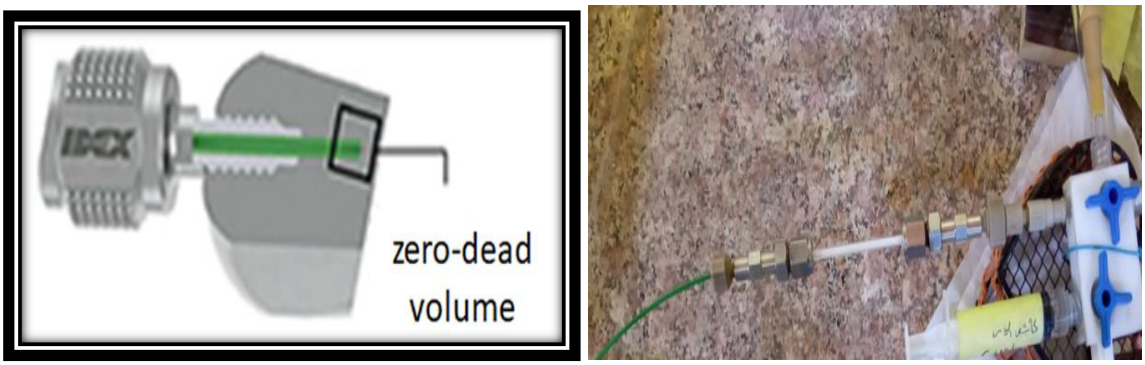

Figure (3.39) Connect the prepared monolith column at zero dead volume

4-The stage of designing and connecting the (reagent injection valve) with the monolith column, as the two-component valve was manufactured consisting of three plastic structures that are easy to control manually by changing their direction to inject the detector that interacts with the sample ,as shown in Figure (3.40)

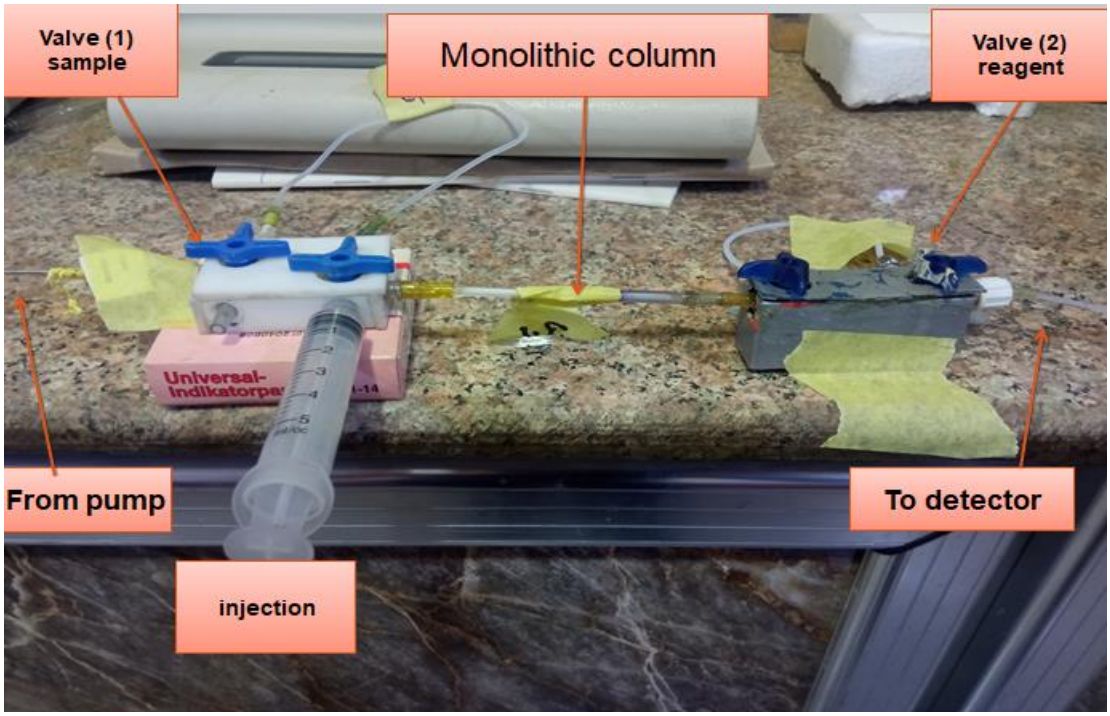

Figure (3.40) photo Connecting locally manufactured injection units

5-The stage of modulating the spectrophotometry device and using it as a detector by replacing the normal quartz cell with a flow cell where chemical

sensors depend on chemical reactions to obtain the response, which is one of the crucial parts of the system through which any physical variable can be sensed as a result of the chemical reaction if it has been modified as showing in Figure (3-41).

Figure (3.41) photo replacing the quartz cell with a flow cell in spectrophotometry device

(3.28.2) Injection Stage for the Reaction Components

The design of a completed unit for copper ion determination takes place in four stages, including pumping the carrier current into the system and injecting the sample into the load connection (copper ion loop). Thirdly "injection of the reagent to the detector injection valve through its load connection" (neocuprion loop), and fourthly pushing the reactants exposed to the parts of the system by the push carrier and the designed system are shown in Figure (3-42) and Figure (3.43).

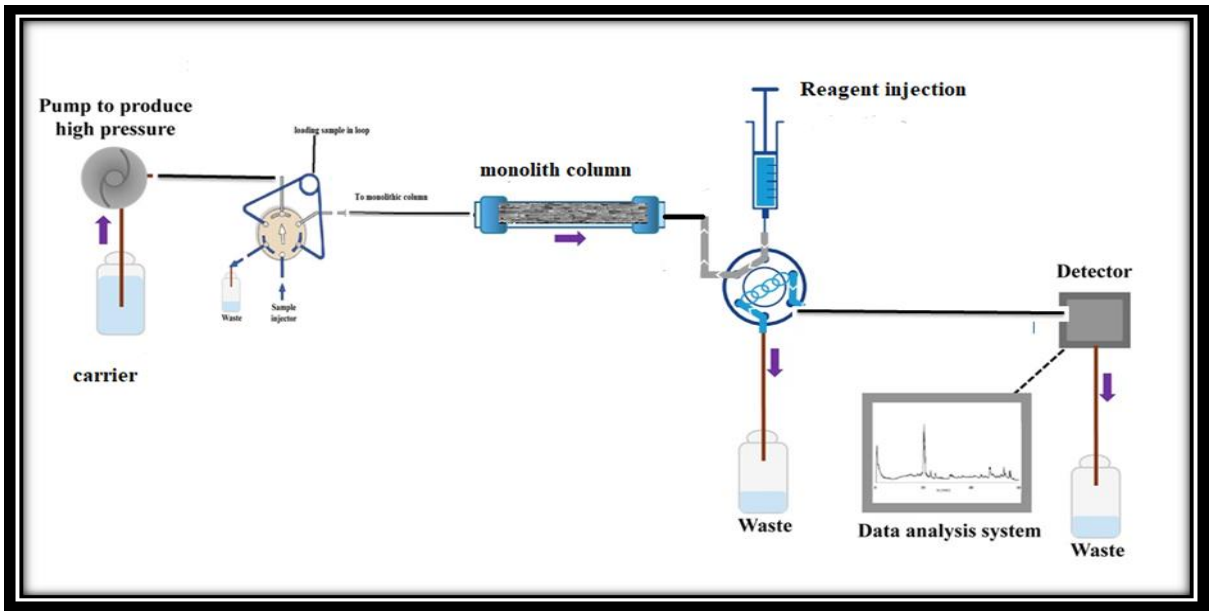

Figure (3.42): The designed(1) system online method

Figure (3.43): Photos of the designed(1) system online method

The first stage

It starts by operating the electronic pump (HPLC Pump), which works to pump the carrier represented by distilled water to the unit, passing through the injection valve sample (1), passing through the monolith column, and then to the reagent injection valve (2), ending with the injection cell, when the system's pipes and coils are filled with the carrier. The reading beeps after the carrier for reference (blank), as in Figure (3-44).

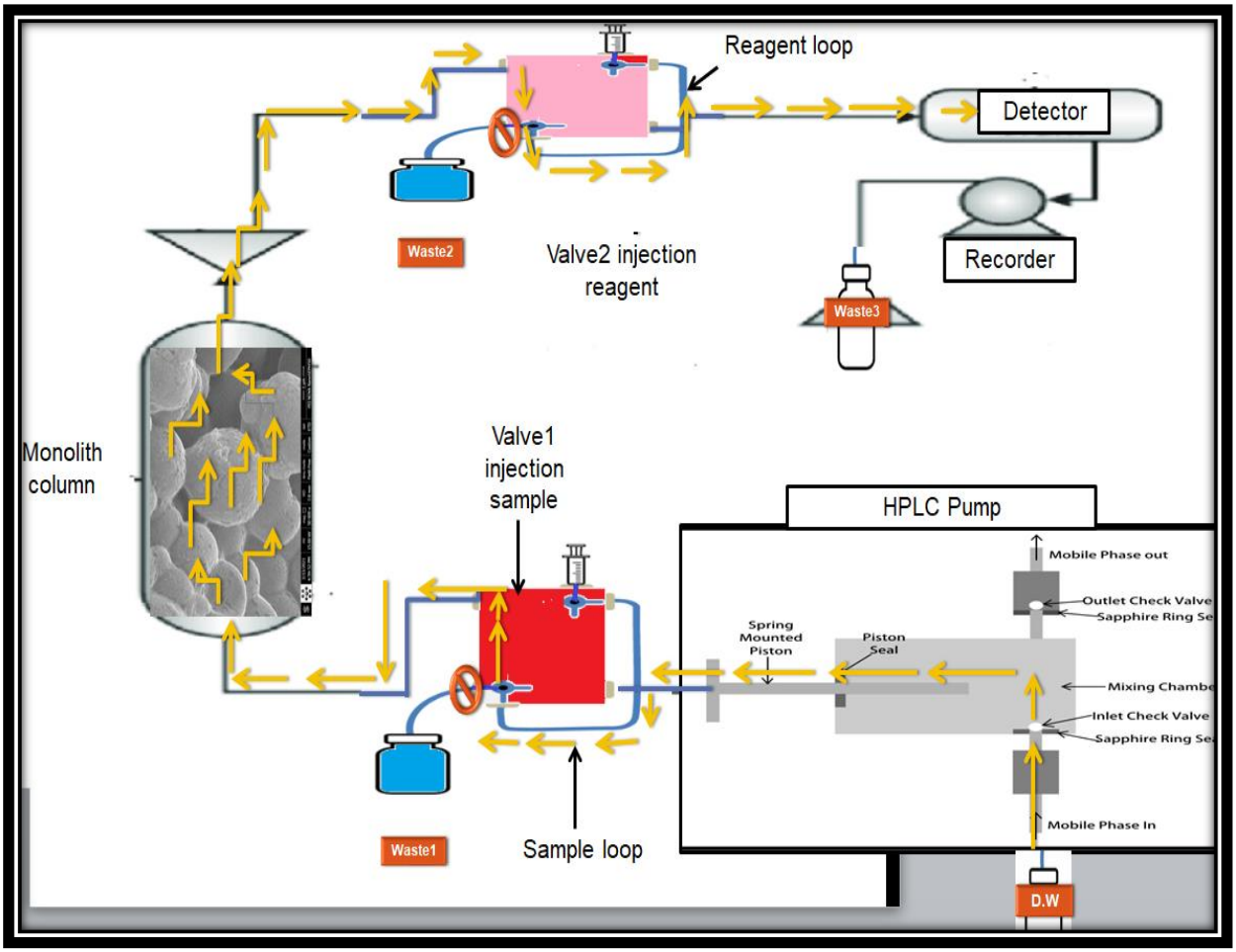

Figure (3-44) the process of flow of the carrier in all parts of the system

The second stage

This stage is represented by interring the sample (copper ion) into the injection unit after closing the two ports of the carrier and the monolith column, as the direction of filling the sample link is from the secondary valve (a) to the secondary valve (b) and then to the model linked and then to the secondary valve (c) after that In the direction of the overflow exit from the secondary valve (d) as in Figure (3-45) .

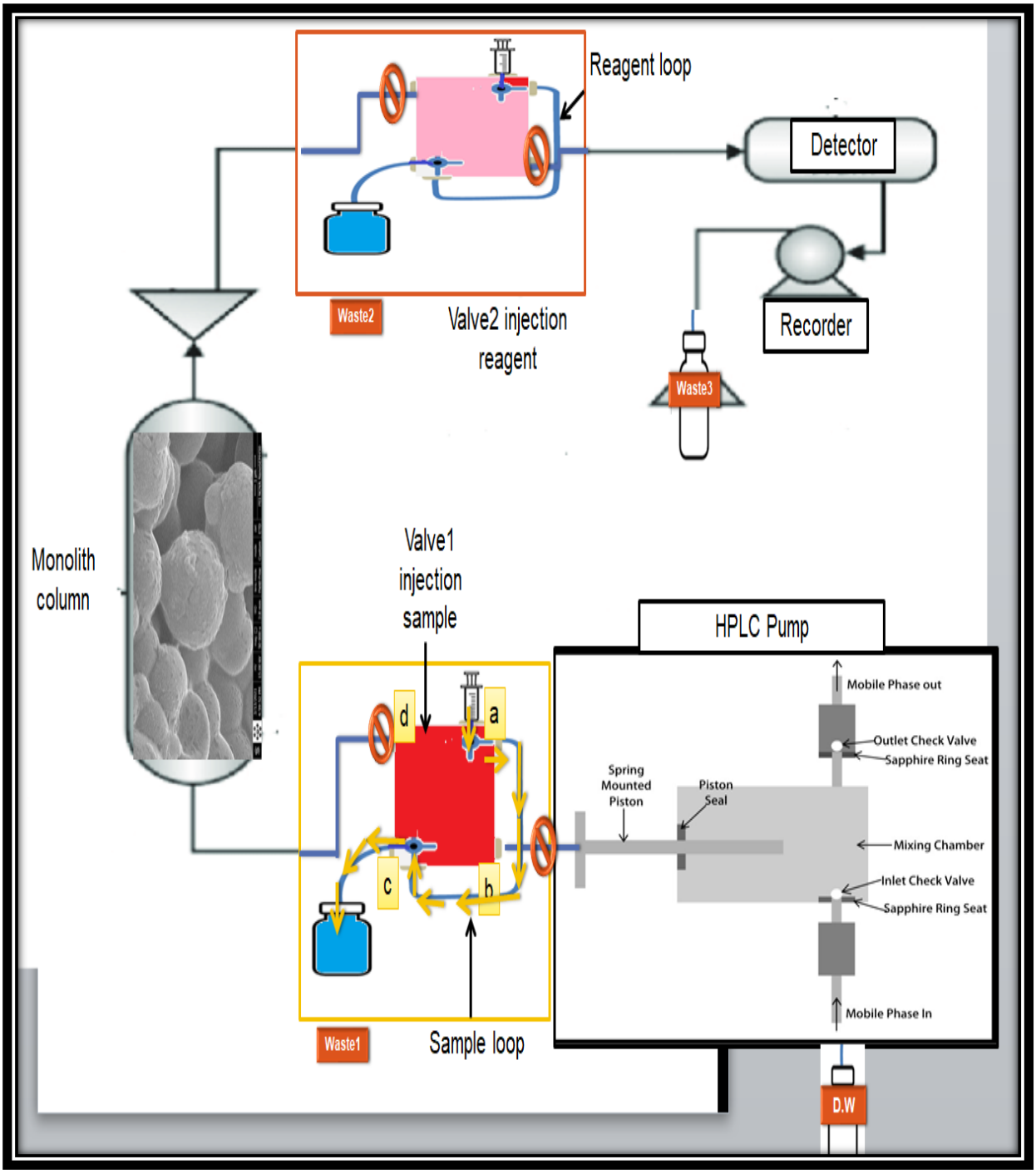

Figure (3-45) The Process of loading samples into the injection unit.

The third step

This stage is represented by injecting the reagent (neocuprion) into its valve (2) after closing the ports of the detector direction and the monolith

column, as the direction of filling the model connection is from the secondary valve (a) to the secondary valve (b) and then to the detector connection after that towards the exit of the surplus from Secondary valve (c) as in Figure (3-46)

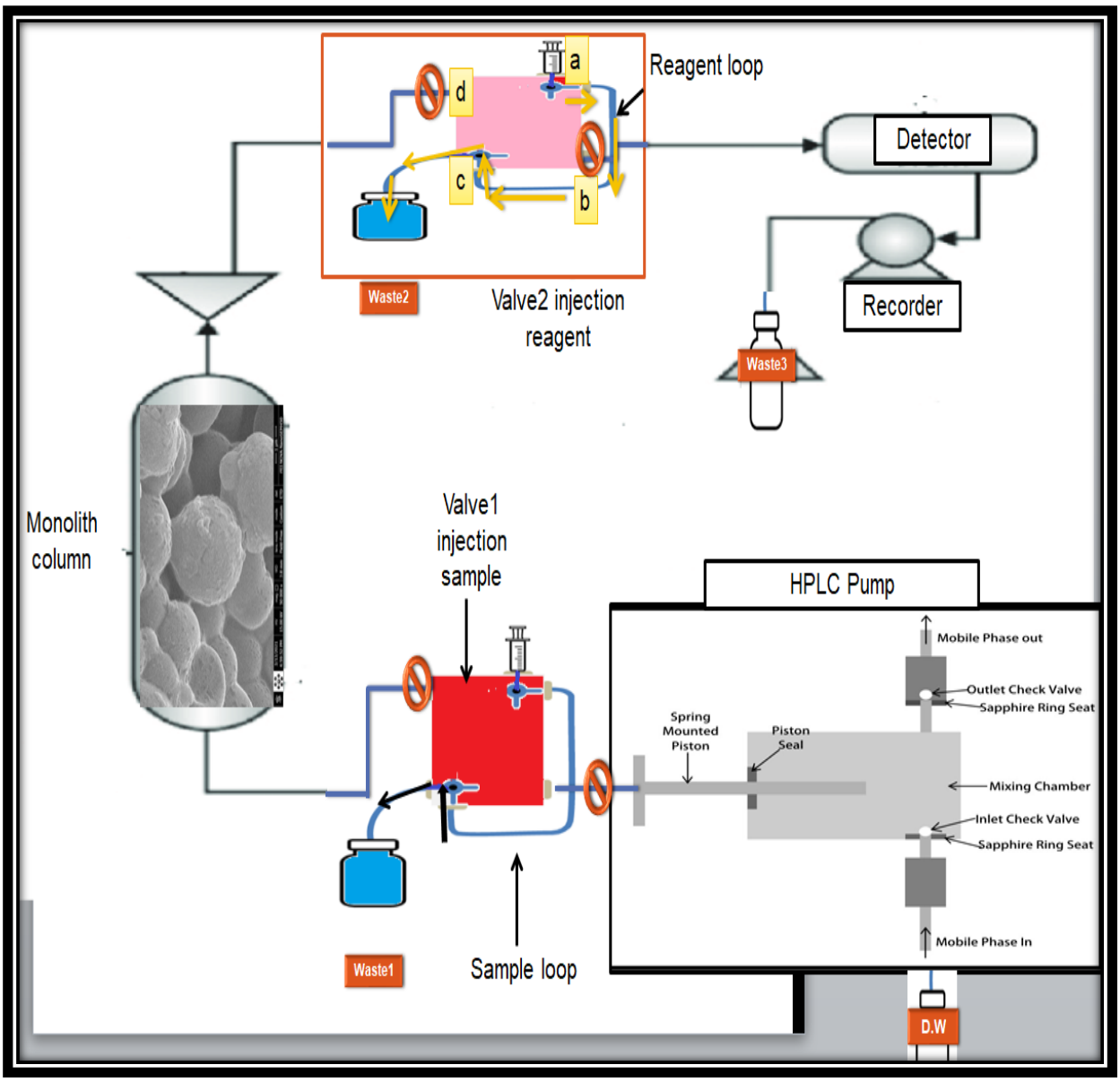

Figure (3-46) The Process of loading reagent into the injection unit

The fourth stage

After the completion of the process of loading the sample and the reagent to their respective loading connections in both valves (1,2), the direction of the

secondary valves (c) is changed in a way that leads to pushing [the sample by loading towards the monolith column as the separation of (cooper ion) occurs. The remaining product reacts with the reagent as in Figure (3-47).

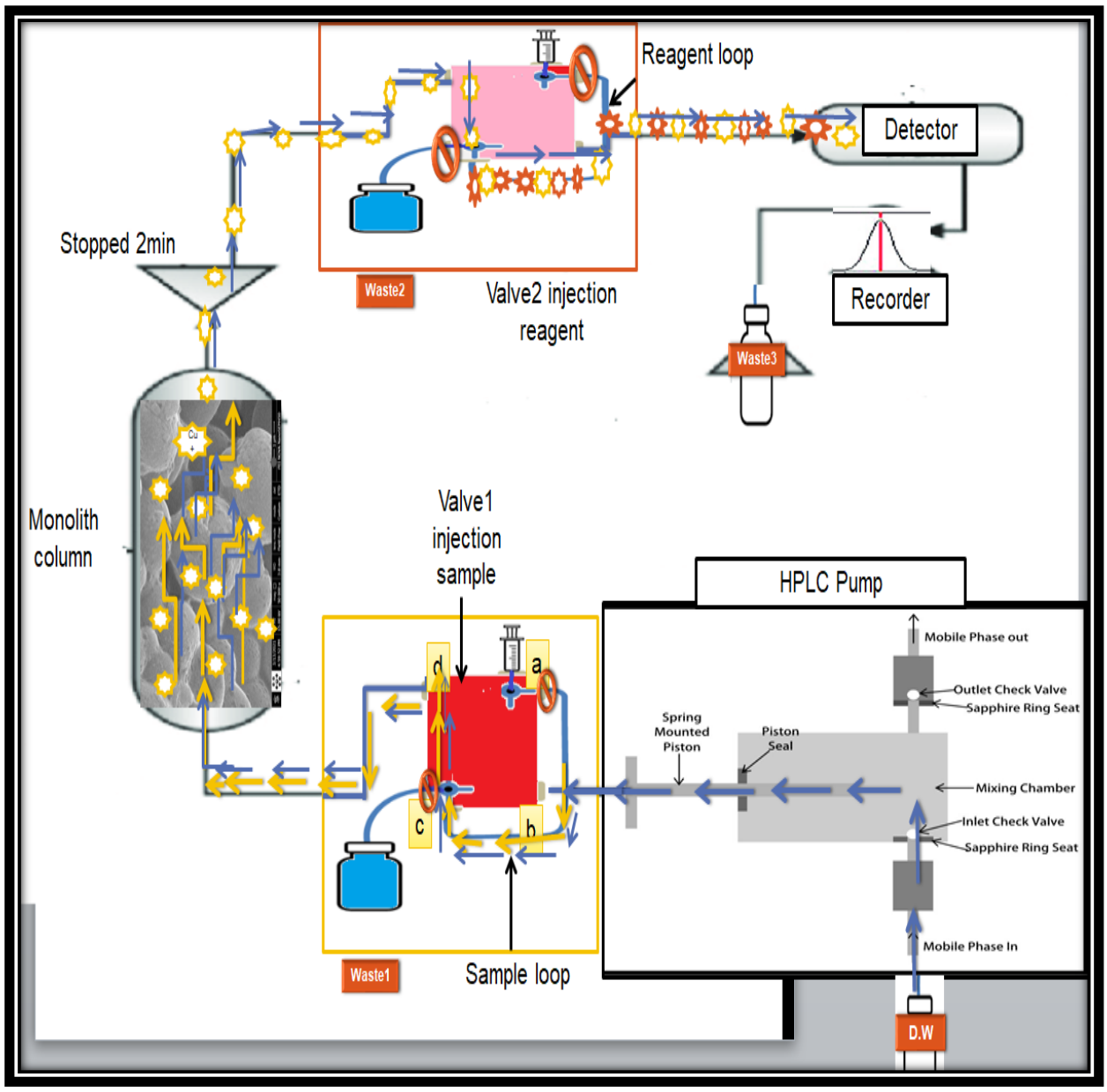

Figure (3-47) The Process of pushing sample by the carrier solution and separating it by the monolith column.

The last step

The process of passing hydrochloric acid at a concentration of (0.2 M) removes the trapped copper ions inside the monolith column and interacts with

the reagent injected into its valve (2). Then the direction of the two secondary valves (c) is changed in a way that leads to the payment of the trapped copper ions by loading, as it separates and removes element ions. They interact with the reagent, as shown in Figure (3-48).

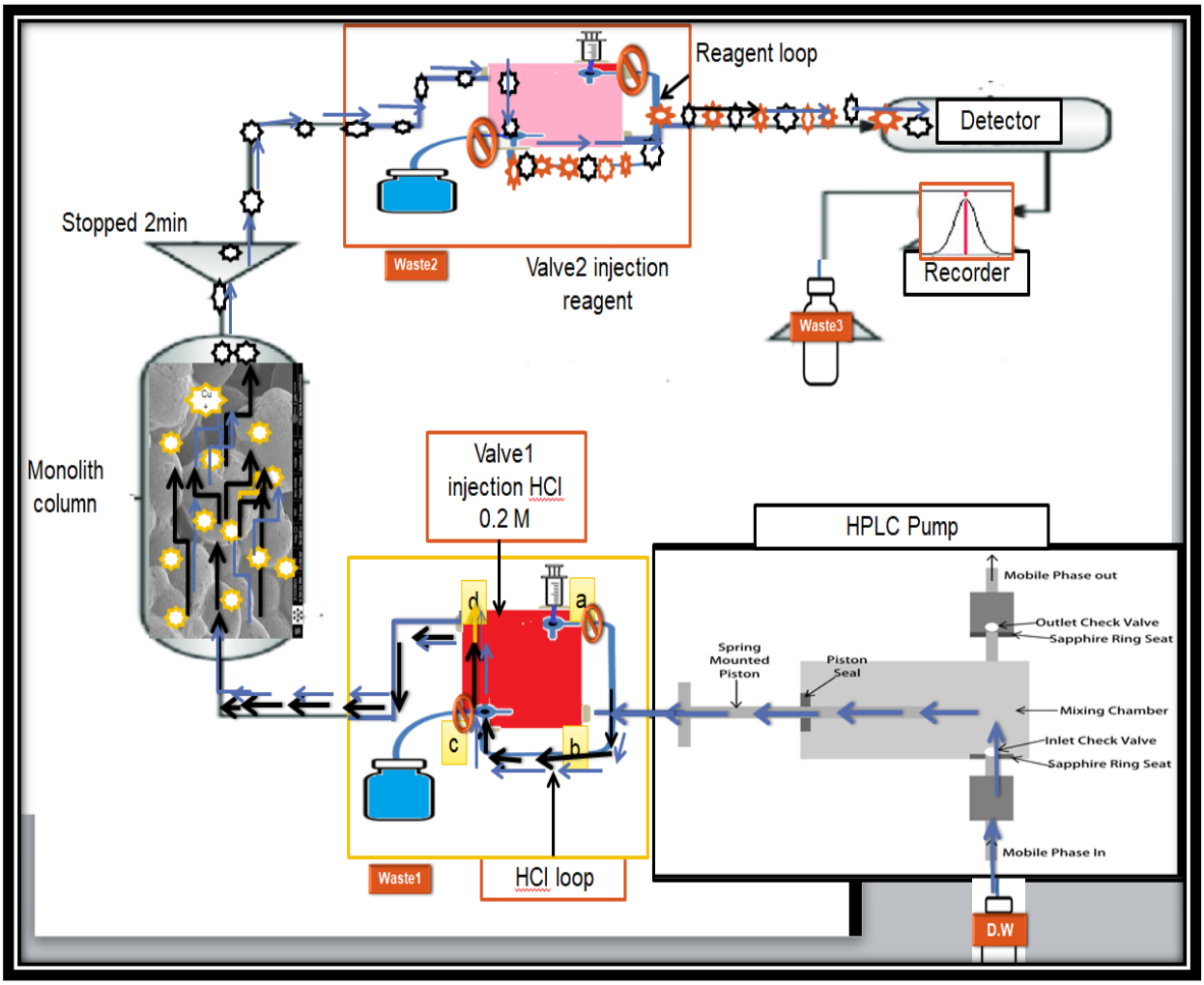

Figure (3-48) The Process of pushing a solution to remove the retained copper ions from the monolith column in the presence of the carrier.

(3.29)UV-Visible Spectrum

In this study, the test solution was prepared by adding 0.01 g of Neocuproine to (5 mL) from ethanol; when the dissolved done, the solution was transferred to (100 mL) volumetric flask and then completed the volume to the mark with distilled water to react with 100 µg.mL-1 of copper (II) to give a yellow-coloured complex using uric acid as an oxidizing agent by the process of reducing copper from the oxidation state (II) to the oxidation state (I) (figure 3.49). The results showed that the complex could absorb at λmax= 453 nm according to Figure (3.50) and this is agreed with the literature [168] .

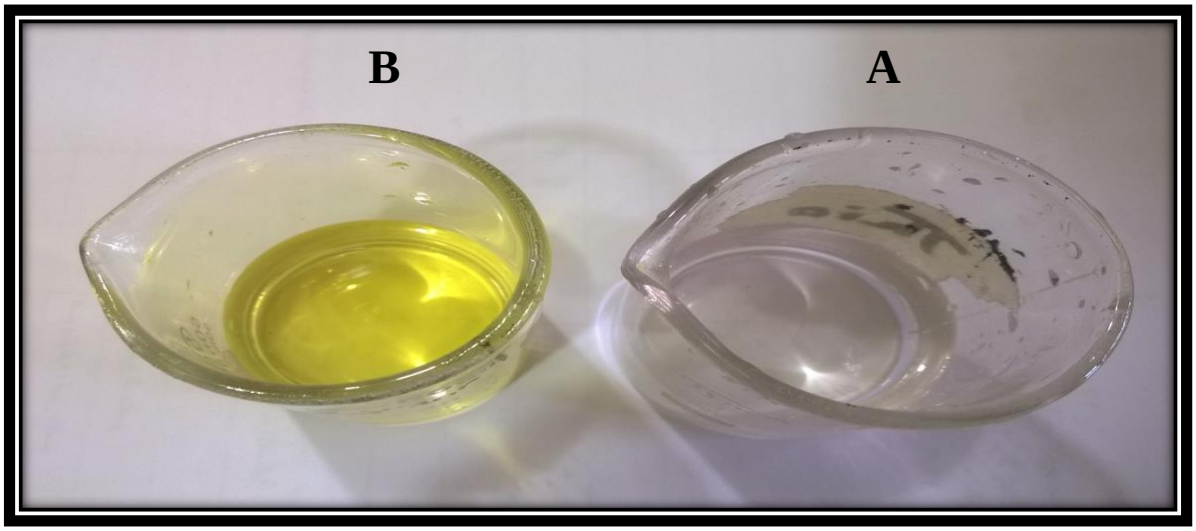

Figure (3.49): Formation of copper - Neocuproine complex, A, colourless solution of copper ion, B, yellow-coloured solution of the complex

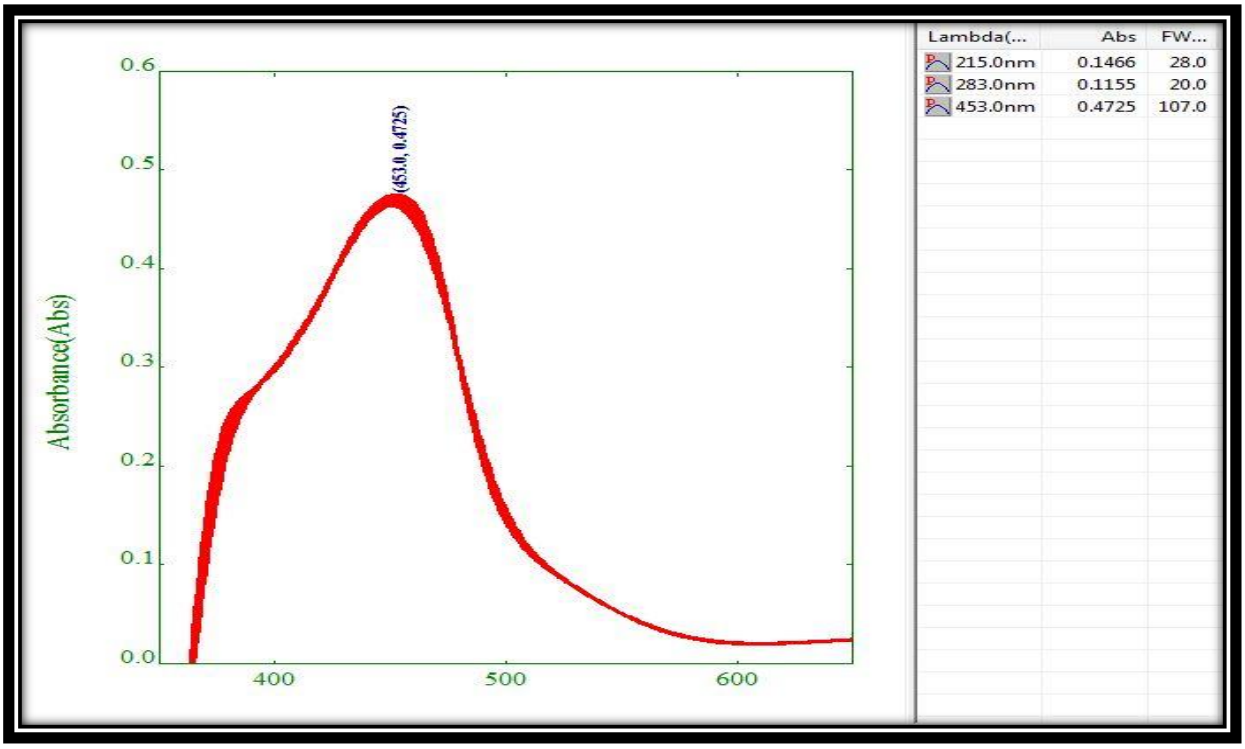

Figure(3.50): The UV-Visible spectrum of copper – Neocuproine complex

(3.30) Optimum Conditions

(3.30.1) Effect of Neocuproine Concentration

The effect of Neocuproine concentration on the peak height was studied in the range ($5*10^{-3}$-$5*10^{-9}$) M after removing by HCL. The preferred response was at the concentration ($5*10^{-5}$ M) of Neocuproine, according to the results in Table (3.13) and Figure (3.51).

Table (3.13): The relationship between Neocuproine concentration and peak height (mV). The conditions were 5 µg.mL^{-1} of Copper ion, D.W Carrier, the flow rate was 1.5 mL.min^{-1}, the net pressure was 150.923 psi for the monolithic column, 78.50 µL was the volume of both Copper ion and Neocuproine solutions, and the temperature was 23±3 °C.

Conc. of Neocuproine *5 M	Peak Height (mV)			Mean $\bar{Y}$	S.D	R.S.D%
10^{-9}	20	20	20	20	0	0.000
10^{-7}	27	29	27	27.66	1.154	4.175
10^{-5}	74	75	75	74.667	0.577	0.773
10^{-4}	35	34	34	34.33	0.577	1.682
10^{-3}	31	31	30	30.66	1.527	4.982

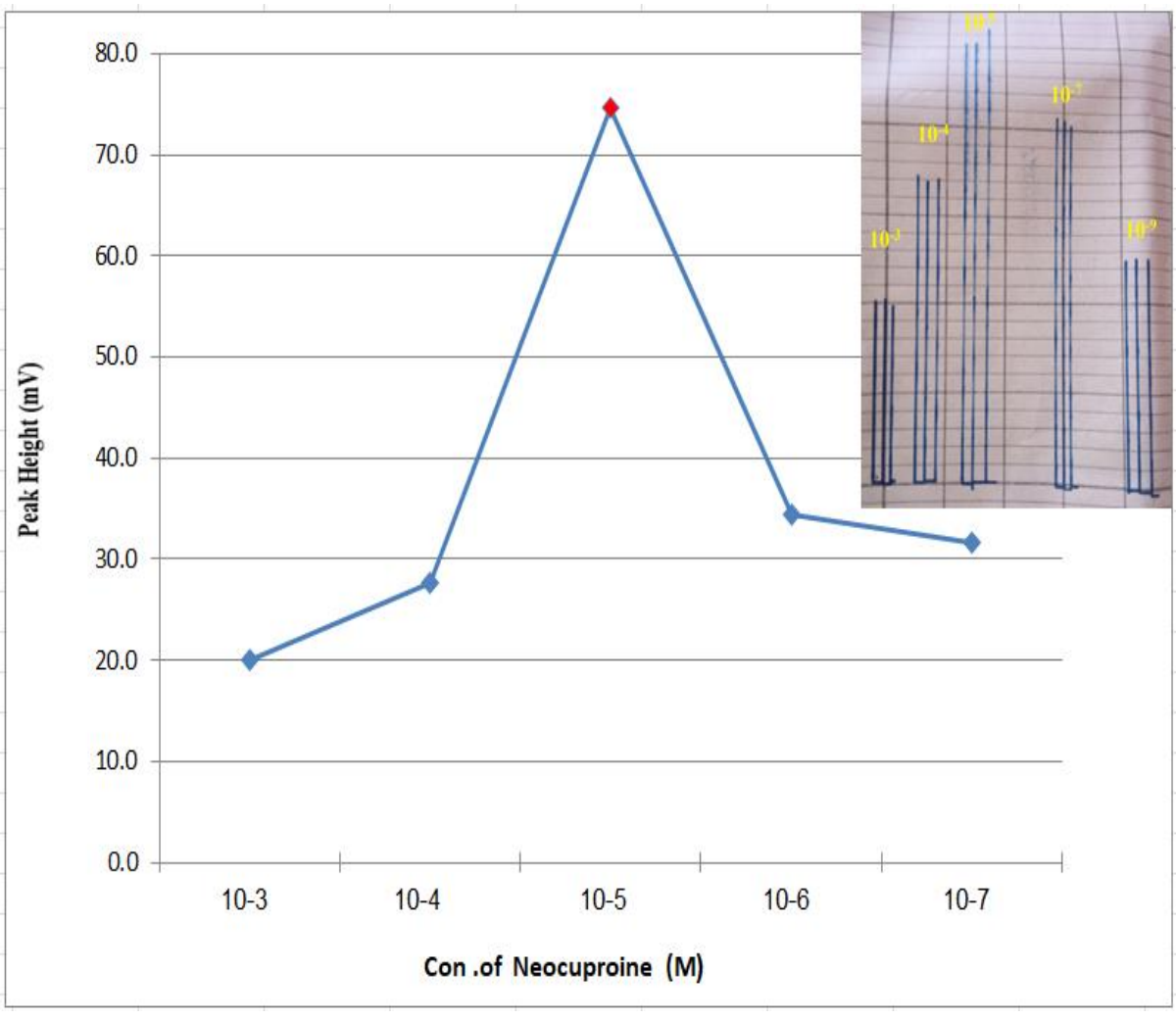

Figure (3.51): Effect of Neocuproine concentration on the peak height

(3.30.2.1) Effect of Reagent Solution Volume

The effect of Neocuproine solution volume on the form and response sensitivity was studied over the range (39.25 - 235.00) µL after removal by HCL. It was noticed that the highest peak is obtained at 78.50 µL of Neocuproine solution, as shown in Table (3.14) and Figure (3.52).

Table (3.14): The relationship between the volume of Neocuproine (µL) and peak height (mV). The conditions were 5 µg.mL^{-1} of Copper ion, 5*10^{-5} M of Neocuproine, D.W Carrier, the flow rate was 1.5 mL.min^{-1}, the net pressure was 150.923 psi for the monolithic column, 78.50 µL was the volume of Copper ion, and the temperature was 23±3 °C.

The volume of Neocuproine (µL)	Peak height (mV)			Mean $\bar{Y}$	S.D	R.S.D%
39.25	44	43	42	43.33	0.577	1.33
78.50	76	77	75	75.67	0.577	0.76
117.00	67	64	67	66.00	1.732	2.62
157.00	55	55	53	54.33	1.155	2.13
235.00	41	41	41	41.00	0.000	0.00

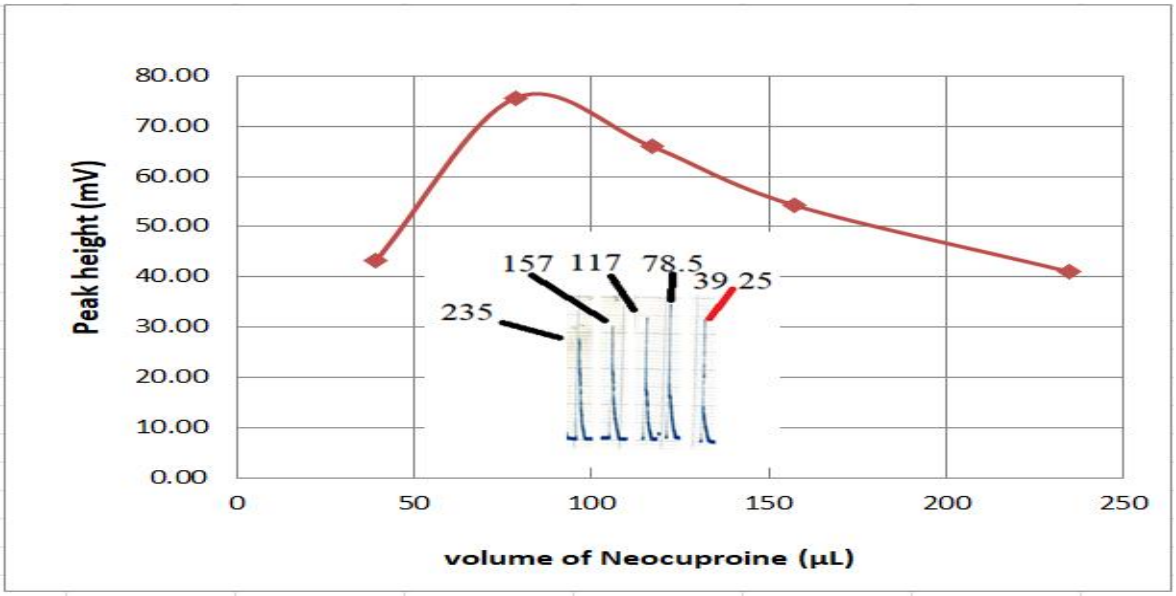

Figure (3.52): Effect of Neocuproine solution volume on the peak height

(3.30.2.2) Effect of Sample Solution Volume

The effect of sample solution volume was also studied using the optimum parameters. Variable sample volumes (39.25 - 235.00) µL were injected through the home-made injection valve, from the results in Table (3.15) and Figure (3.53).

Table (3.15): The relationship between sample solution volume (µL) and peak height (mV). The conditions were 5 µg.mL^{-1} of Copper ion, 5*10^{-5} M of Neocuproine, D.W Carrier, the flow rate was 1.5 mL.min-1, the net pressure was 150.923 psi for the monolithic column, 78.50 µL was the volume of Neocuproine reagent, and the temperature was 23±3 °C.

The volume of sample (µL)	Peak height (mV)			Mean $\overline{Y}$	S.D	R.S.D%
39.25	41	42	40	41.00	1.000	2.439
78.50	75	75	75	75.00	0.000	0.000
117.00	40	44	40	41.33	2.309	5.587
157.00	38	38	38	38.00	0.000	0.000
235.00	29	28	29	28.67	0.577	2.014

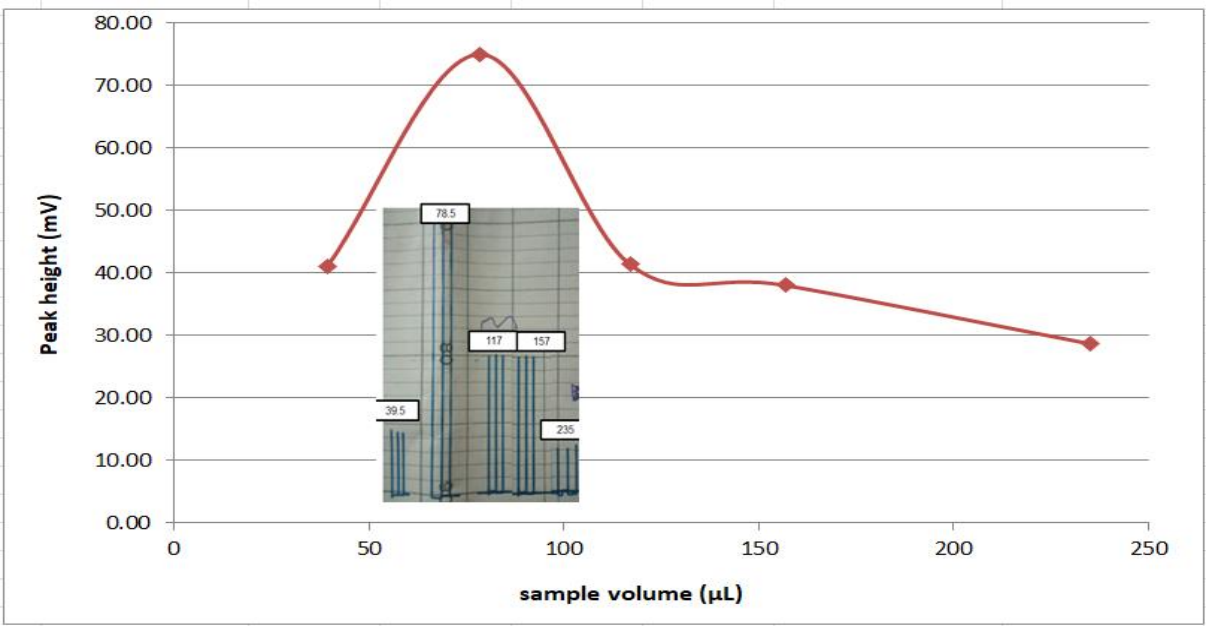

Figure (3.53): Effect of sample solution volume on the peak height

(3.31) Construction of Calibration Curve.

Under the optimum parameters in previous sections, a series of copper ion (I) concentrations were prepared to study the calibration curve. The calibration graph showed linearity over the range (0.05-17)mg.mL^{-1} (R^2=0. 0.9981), according to Figure (3.54) and Table (3.16) and (3.16).The limit of detection ((S/N=3) was 0.039 mg.mL^{-1} and the limit of quantification (S/N=10) was 0.117mg.mL^{-1}.

Table (3.16): Calibration graph values at optimum conditions, including 5*10^{-5} M of Neocuproine, D.W Carrier, the flow rate was 1.5 mL.min-1, the net pressure was 150.923 psi for the monolithic column, 78.50 µL was the volume of both Copper ion and Neocuproine solutions, and the temperature was 23±3 °C.

Conc. Of Cu(I) mg.mL^{-1}	Peak Height in (mV)			Mean $\bar{Y}$	S.D	RSD%	Found Con. mg.mL^{-1}	Recovery %
0.05	3.5	3	3	3.17	0.289	1.116	0.05	100.00
0.5	6	6	6.5	6.17	0.289	4.681	0.48	95.76
1.0	10	11	10	10.33	0.577	3.587	1.08	108.48
3.0	23	23	24	23.33	0.577	2.474	3.05	101.82
5.0	37	37	35	36.33	1.155	3.178	5.18	103.52
7.0	46	45	45	45.33	0.577	1.274	6.54	93.42
9.0	63	64	64	63.67	0.577	0.907	9.12	101.28
13.0	87	87	86	86.67	0.577	0.666	12.75	98.09
15.0	100	100	100	100.00	0.000	0.000	14.72	98.14
17.0	117	117	119	117.67	1.155	0.981	17.30	101.75

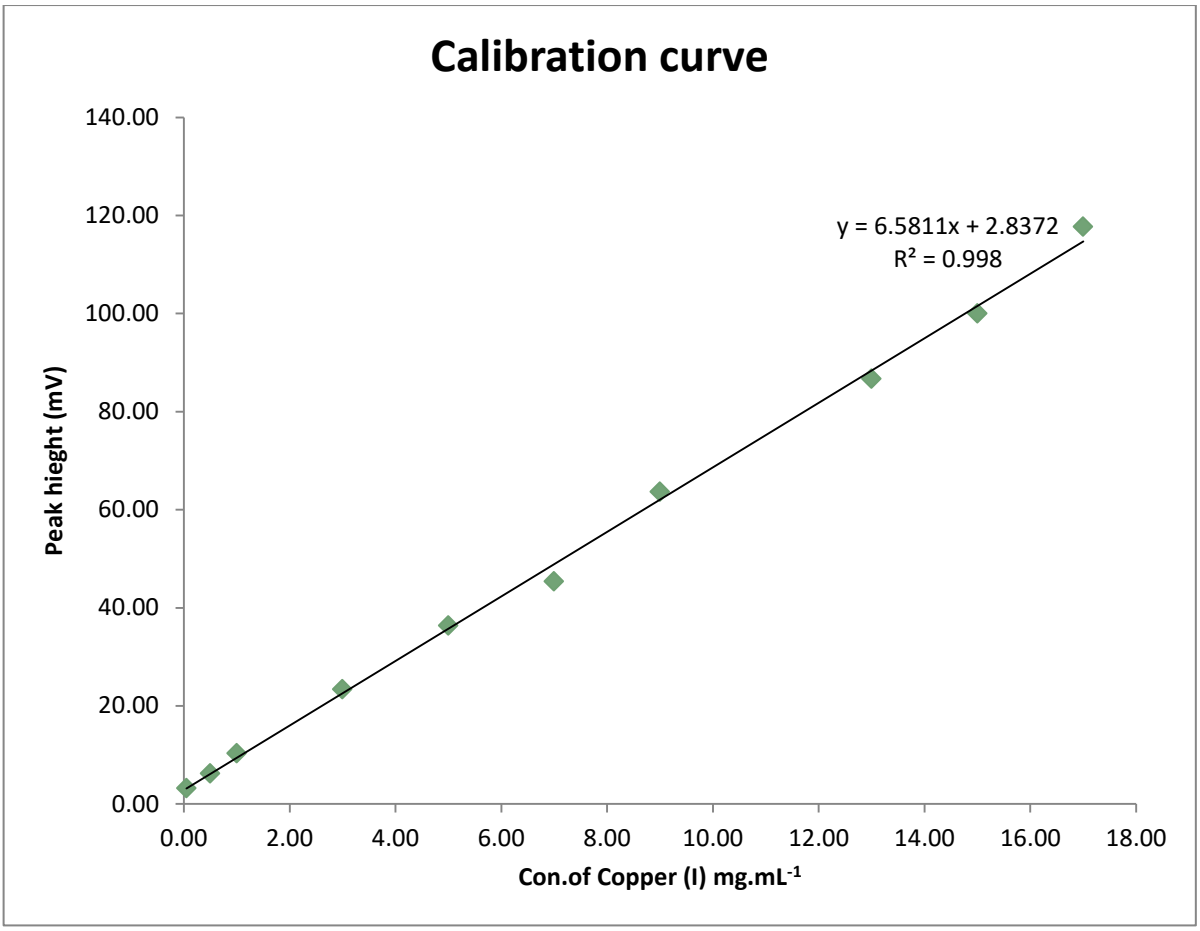

Figure (3.54). Calibration curve for copper (I)

Table (3-17) parameter of the calibration curve

Slope	**6.5811**
Y-intercept	**2.8372**
Linearity Range	**0.05-17 mg.mL^{-1}**
Correlation Coefficient	**0.9981**
LOD	**0.039**
LOQ	**0.117**
Average SD	**0.577**
Average RSD%	**2.886**

(3.32) Applications

The proposed online -HPLC-FIA design(1) was successfully applied for the determination of Cu(I) in standard samples and water samples (table 3.1) .The water sample was taken from the (Al-Muamira station), and the exact location was the wastewater (inflow) and (outflow) of the station. The relative error and recovery percentage were calculated using equations (3.5) and (3.6), respectively.

$$\mathbf{R.E.\%} = \frac{\mathbf{Actual\ value - Measured\ value}}{\mathbf{Known\ value}} \times \mathbf{100} \qquad \textbf{(3-5)}$$

$$\mathbf{Recovery\%} = \mathbf{100} \mp \mathbf{R.E.\%} \qquad \textbf{(3-6)}$$

Table (3.18): Determination of Cu (I) in standard samples and environmental samples by using Online- HPLC-FIA design(1) with two different levels

Sample	Before using mono concentration mg.mL^{-1}	Found concentration mg.mL^{-1}	S.D	R.S.D%	E_r%	Recovery%
standard samples	1.00	1.18	0.03	2.17	2.0	98.0
	5.00	5.24	0.06	2.04	0.8	99.2
Wastewater(inflow)	1.00	1.00	0.00	0.00	0.0	100
	5.00	5.10	0.03	0.84	2.0	98.0
(outflow)	1.00	1.05	0.00	0.00	5.0	95.0
	5.00	5.07	0.00	0.00	1.4	98.6

(3.33) Design (2) of HPLC-FIA system online method for incorporation Ni(II) ion with the GMA-co-ACA co-AAM monolith column.

Figure (3.55) shows an overall view of the new HPLC-FIA system. The system consists of left to right an electrical pump for the production of high pressure, flow injection one-valve(universal valve) for allowing a discrete amount of sample only, a monolith column to separate ions, flow injection one-valve (home-made) for allowing a discrete amount of reagent to be introduced into carrier stream, the spectrophotometer is used as a detection device after simple modification by replacing the normal cell with the flow cell. The detector senses the gradient of sample concentration at 518 nm, and the recorder measures the response. The steps of connecting the system are shown in Figure (3.56)

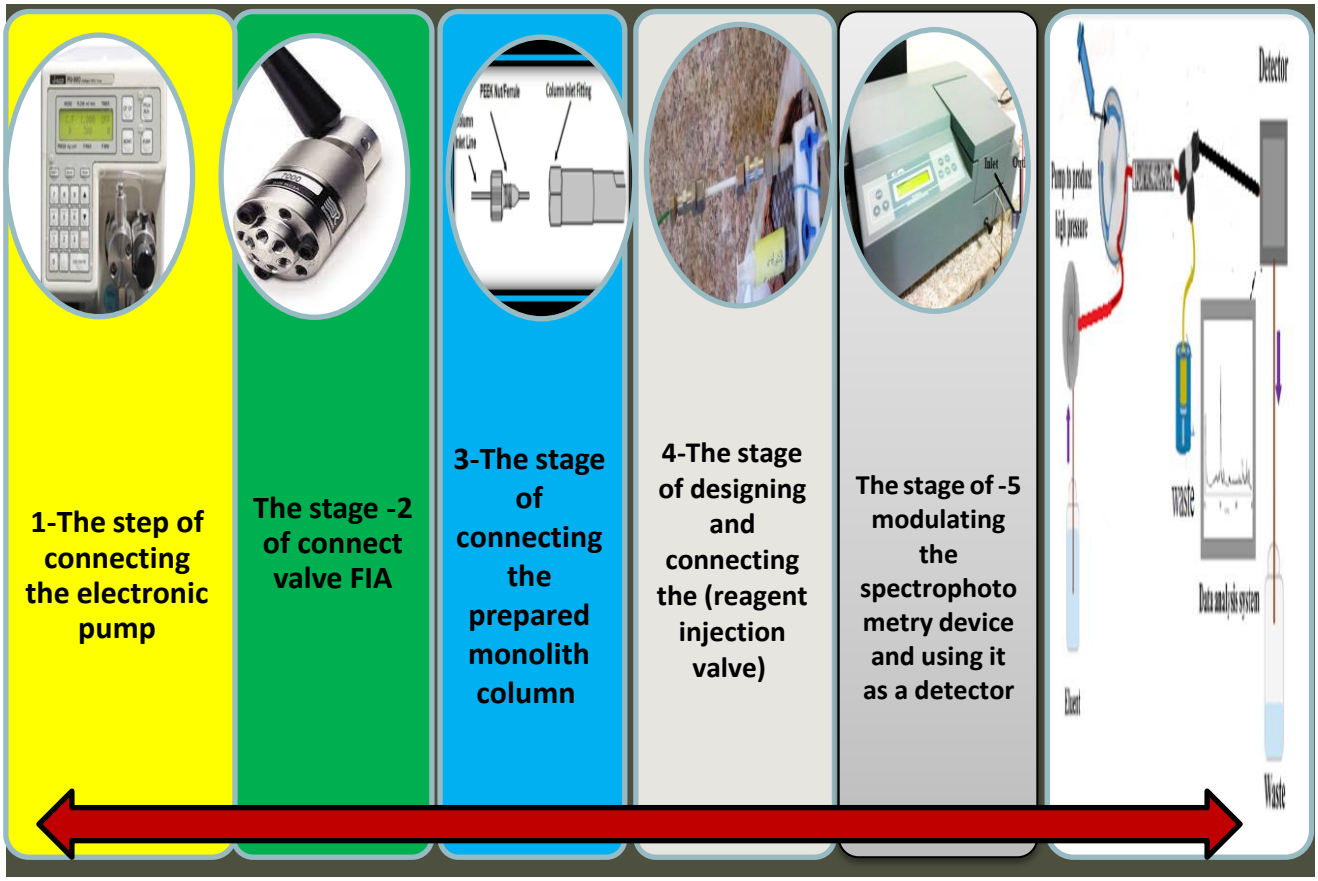

Figure (3.55) Scheme of steps design of HPLC-FIA system

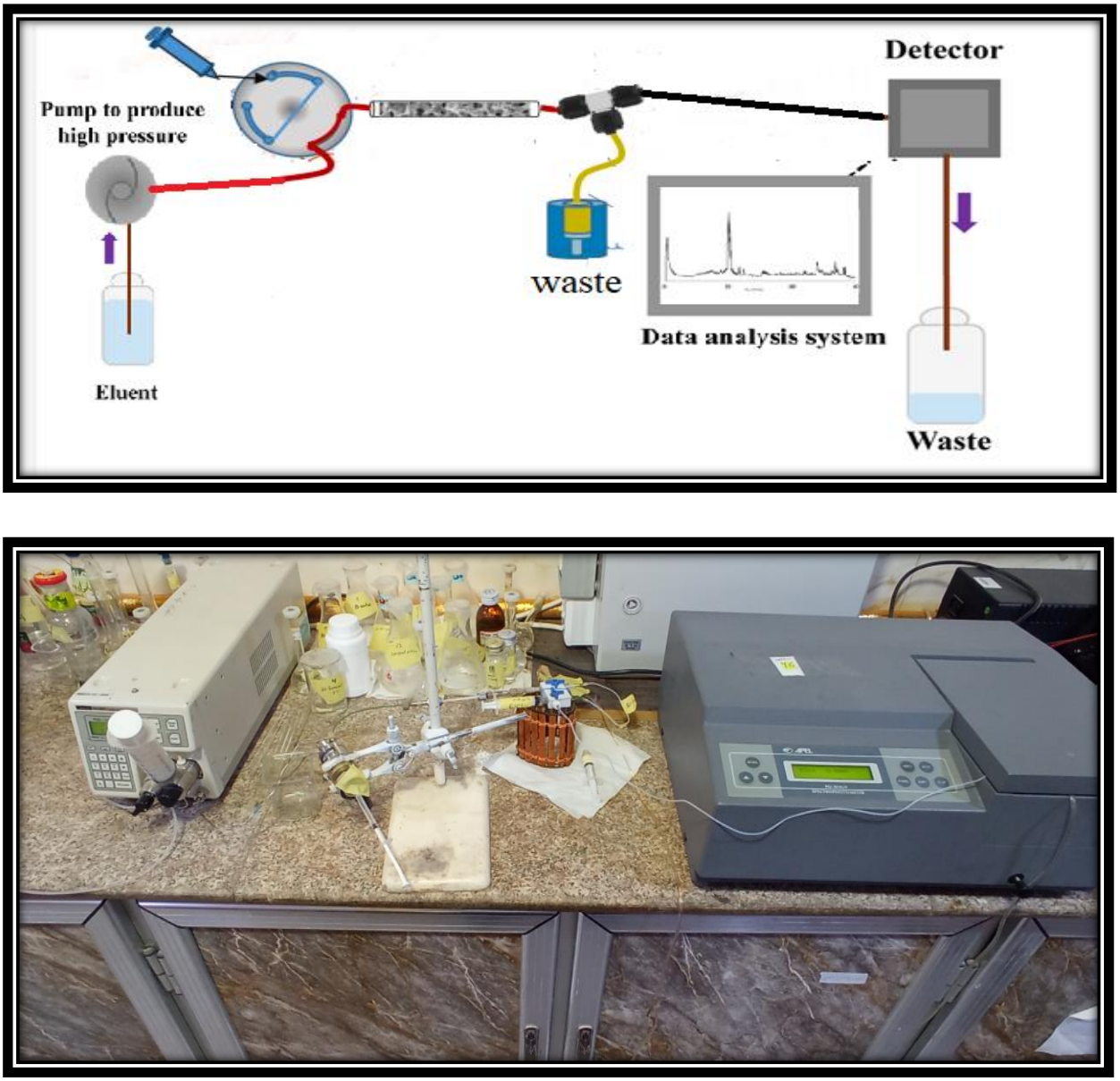

Figure (3.56): The designed(2) system online method

(3.33.1) Injection Stage for the Reaction Components

Firstly, pumping distilled water (HPLC Pump) in all the systems passing through the one-valve(universal valve), passing through the monolith column, one-valve (home-made), and the detector. As in shown in Figure (3-57).

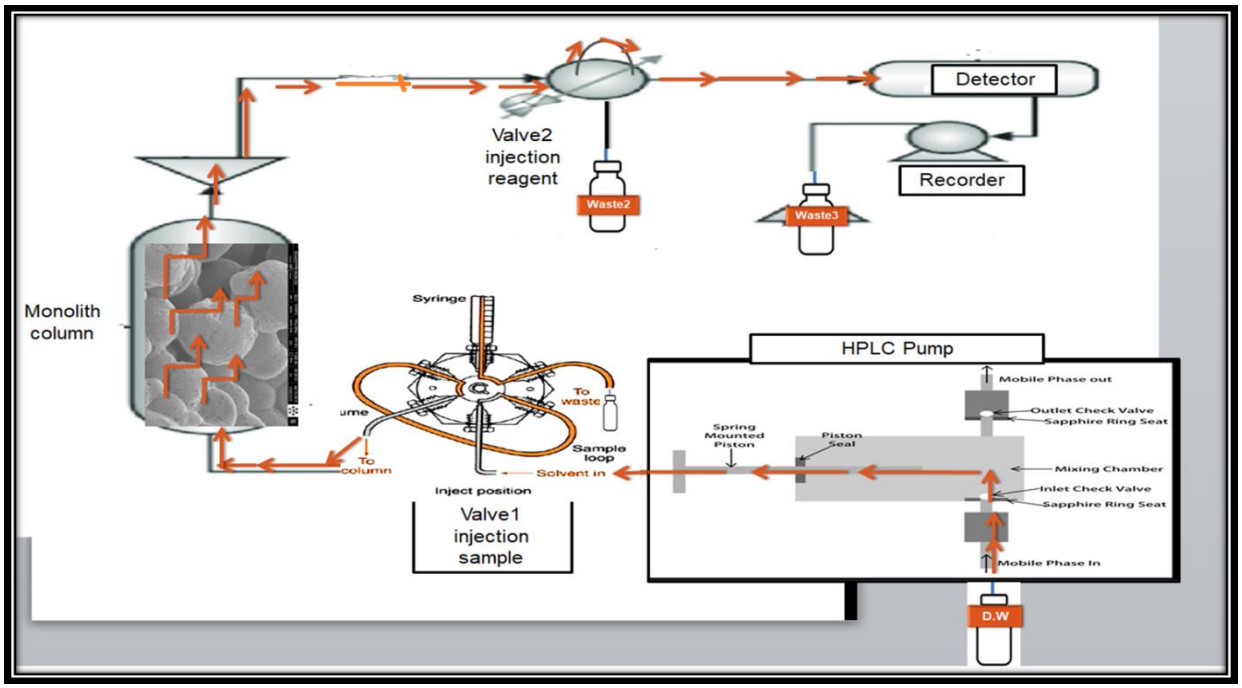

Figure (3.57) the process of flow of the carrier in all parts of the system

Secondly, Figures (a,b,c) (3.58) and Figure (3.59) show manual injection of the sample (nickel ion) into the injection unit and as a first step it is called (loading sample) at load position (No.4 position to No.1 position) by special needle (injection syringe) and the waste comes out of position No. 6. In contrast, site No. 2 and 3 continue to pump towards the monolith column and up to the detector.

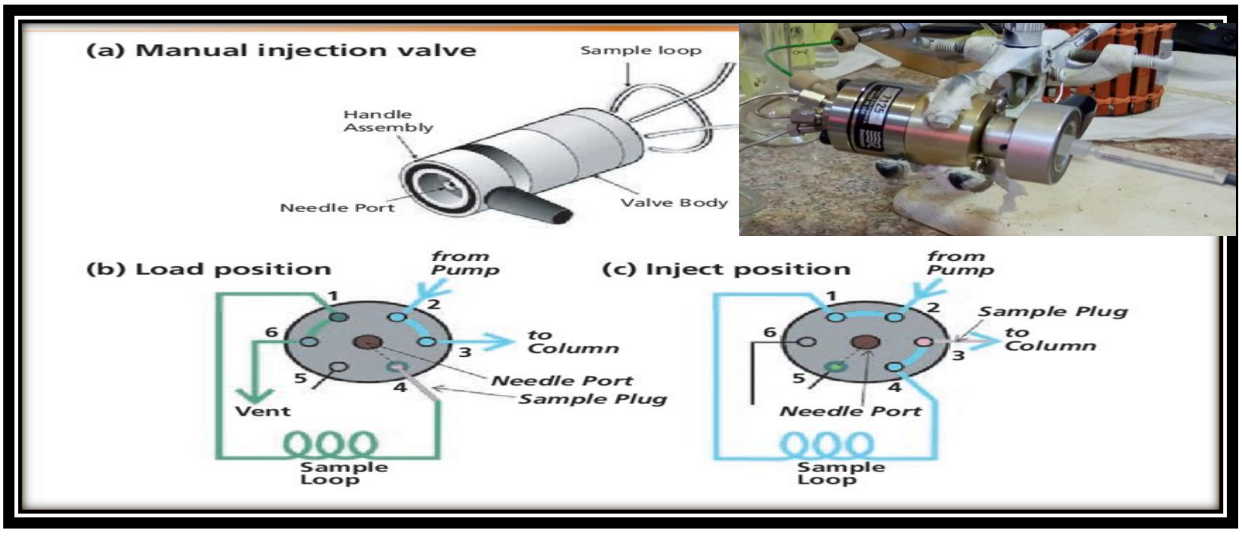

Figure (3.58) Manual injection process in injection unit universal valve.

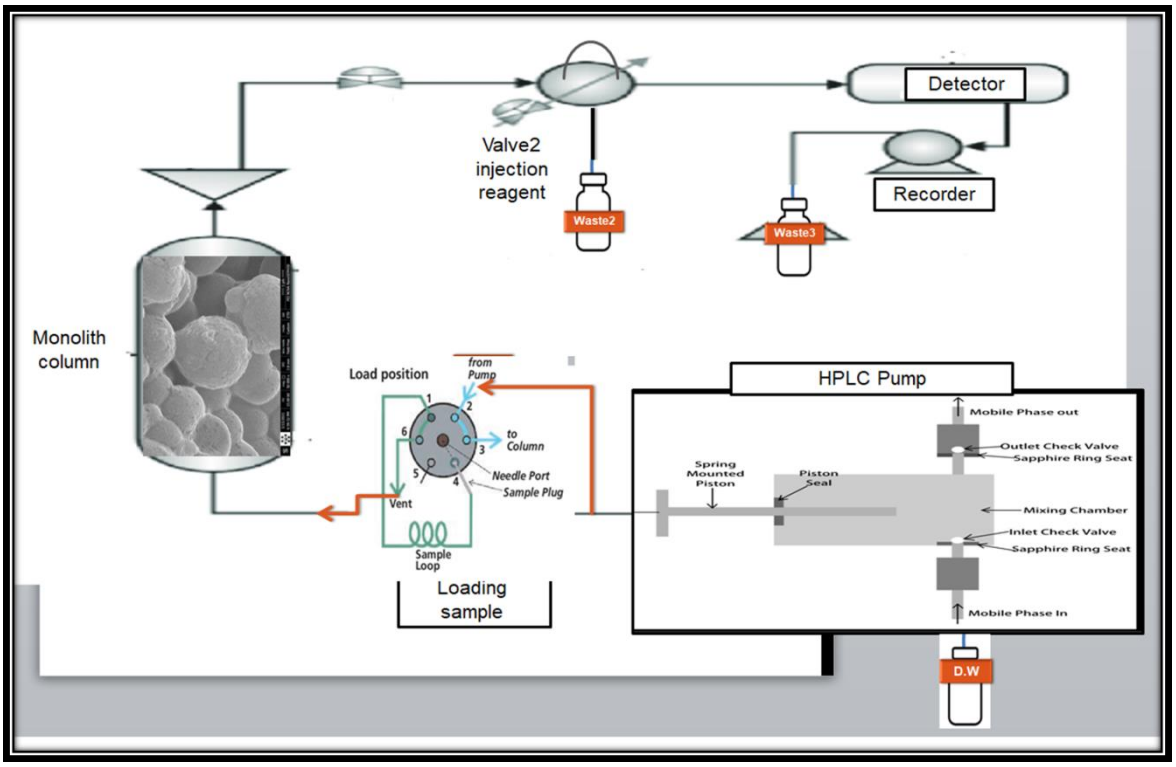

Figure (3.59) Loading (Ni^{+2} ions) into the injection unit.

Thirdly, manually injecting the new reagent (MPDADPI) into (home-made valve 2) after (1min), closing the ports of the detector direction and the monolith column, as in figure (3-60)

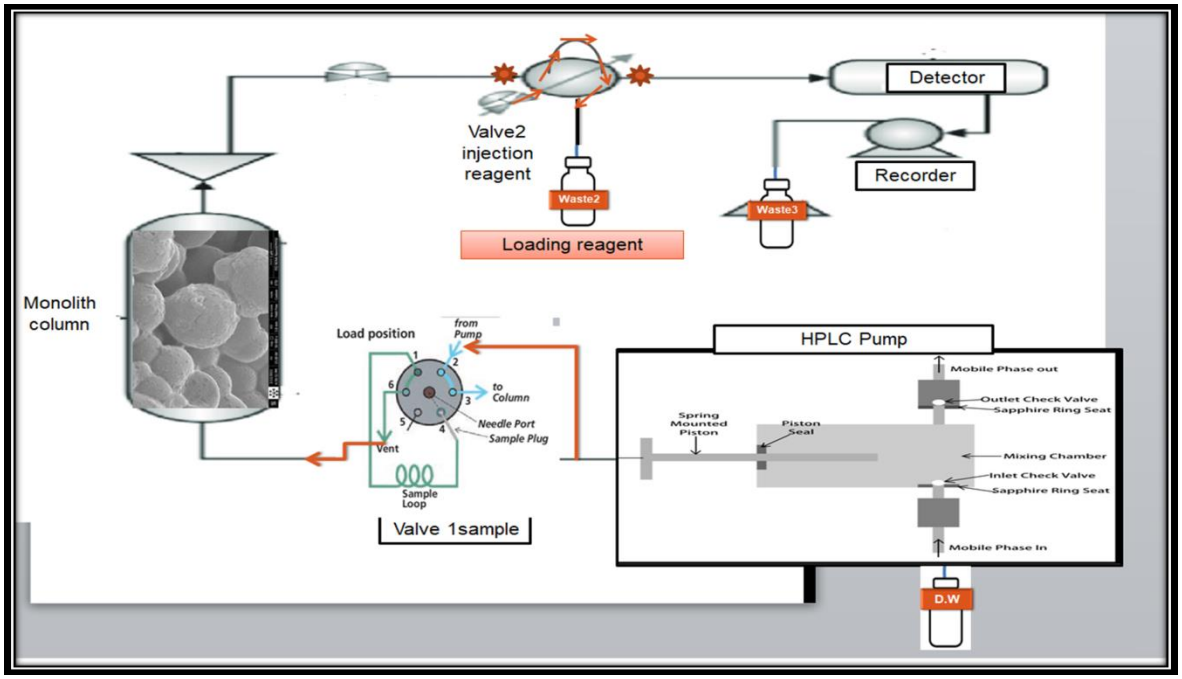

Figure (3.60) Loading (MPDADPI) as reagent into the injection unit

In the final stage, pushing elutes the nickel ions for the monolith column by loading towards separating (nickel ions) occurs. The remaining product reacts with the reagent and then passes (0.2 M) of HCL to remove the trapped nickel ions inside the monolith column and react with the reagent injected into its valve. Then the direction of the two secondary valves is changed in a way that leads to the payment of the trapped nickel ions by loading, as it occurs separation and removal of element ions. They interact with the reagent, as shown in Figure (3-61) and (3-62).

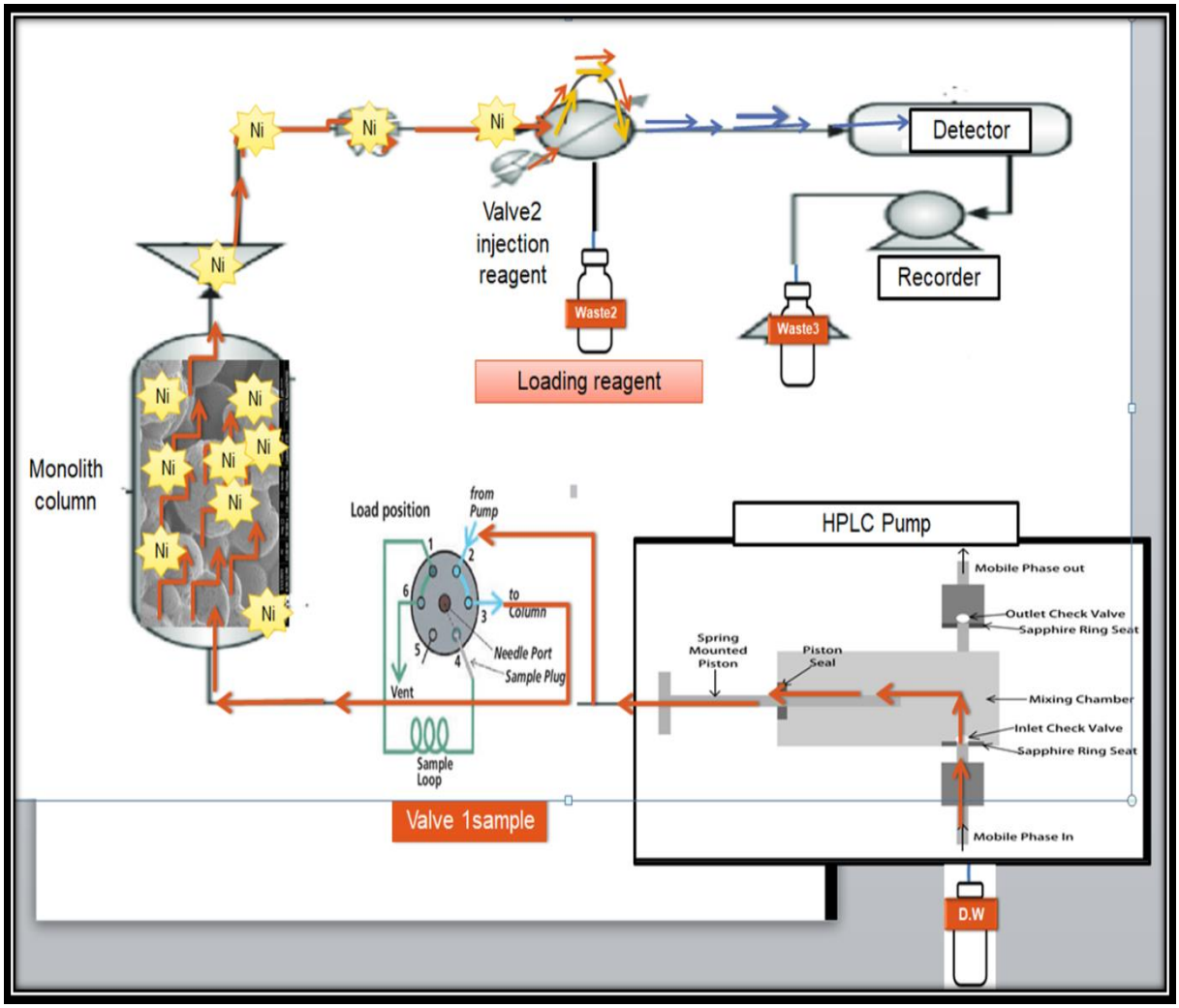

Figure (3.61) The process of pushing the sample by the carrier solution and separating it by the monolith column

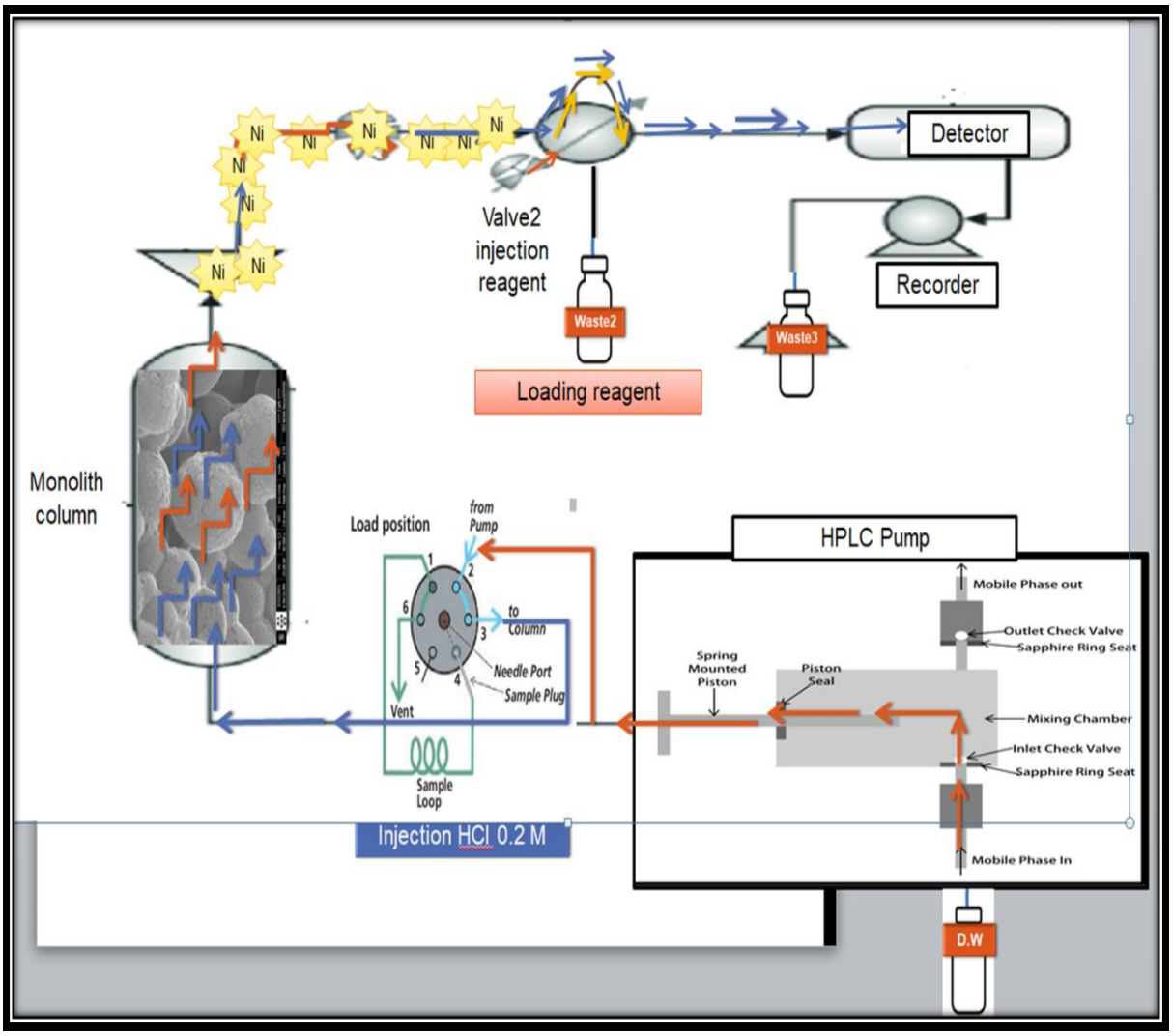

Figure (3.62) The Process of pushing a solution to remove the retained Nickel ions from the monolith column in the presence of the carrier.

(3.34) Construction of Calibration Curve

A series of Ni (II) concentrations were prepared to construct the calibration curve. The linear range of calibration graph was (0.005-2.90) $mg.L^{-1}$ (R^2=0.9995), as shown in Figure (3.63) and Table (3.18). The limit of detection (S/N=3) was $1ng.mL^{-1}$ and limit of quantification (S/N=10) was 1 $\mu g.mL^{-1}$.

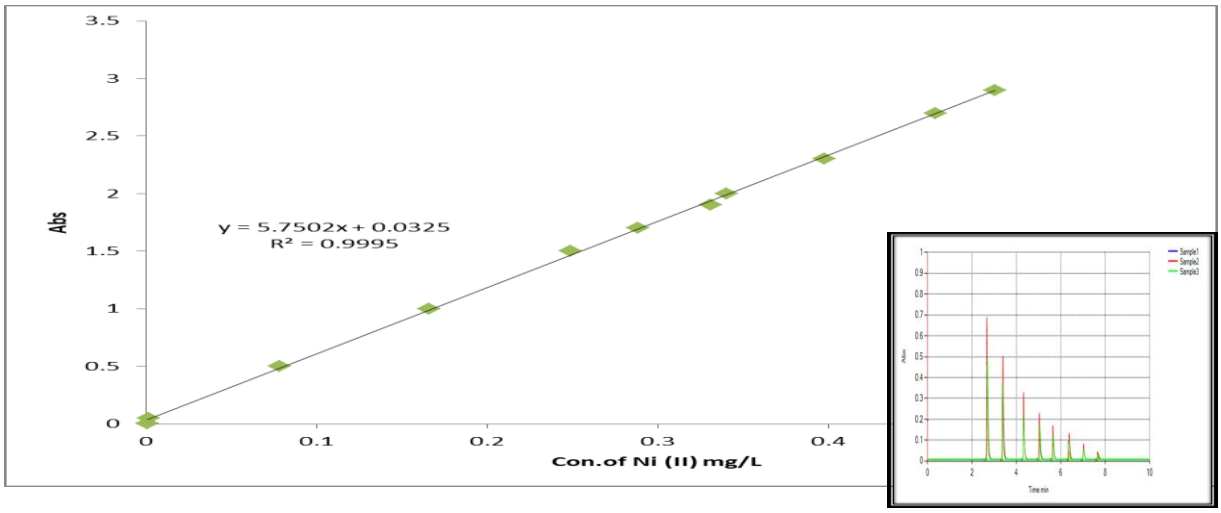

Figure (3.63): Calibration Curve for Ni (II).

Table (3.19): Calibration graph values at optimum conditions, including $5*10^{-5}$ M of(MPDADPI), D.W Carrier, the flow rate was 1.5 mL.min-1, the net pressure was 150.923 psi for the monolithic column, pH was 8, and the temperature was 23±3 °C.

Conc. of Ni(II) mg.L-1	Mean Abc (n=3) $\overline{Y}$	S.D	R.S.D%	Found Con. $mg.L^{-1}$	Recovery(%)
0.005	0.001	0	0	0.0047	94.00
0.050	0.002	0.000	3.149	0.0499	99.80
0.5	0.079	0.001	0.734	0.51	102.00
1.0	0.167	0.002	0.913	0.99	99.00
1.50	0.248	0.001	0.465	1.52	101.33
1.70	0.289	0.001	0.180	1.68	98.82
1.90	0.331	0.001	0.175	1.98	104.21
2.0	0.341	0.000	0.000	2.12	106.00
2.30	0.398	0.001	0.145	2.41	104.78
2.70	0.463	0.001	0.125	2.77	102.59
2.90	0.498	0.001	0.116	2.88	99.31

(3.35) Innovative Design and fabrication of monolithic columns inside microchip device for Separation Ni(II) ion.

A glass microchip had two layers, each 3 mm thick. The chip's length and width were 50 mm and 15 mm, respectively. For the inlet and outflow of the mobile phase, two holes (each 1.5 mm in diameter) were drilled into the top layer of glass using conventional drilling methods. The second layer was the CNC-milled channel, which had the following dimensions: 30 mm long, 1 mm wide, and 50 m deep. The two layers were thermally fused, and design of the chip is shown in figure (3.64)

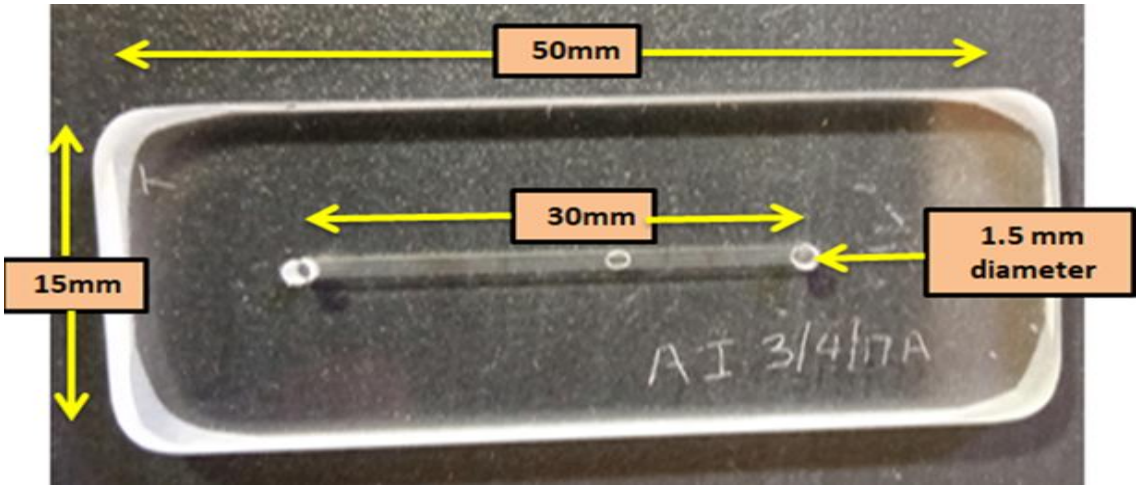

Figure (3.64): A glass microchip photograph used to separate Ni^{+2} ions.

(3.36) Preparing the inner surface of the chip (Silanization step), polymerization process & opening the epoxy ring GMA.

When the chip was ready for use, the monolith was constructed inside the chip using the identical techniques shown in (3.2),(3.3),(3.14) and (3.30); the results appeared that the net pressure was calculated to be approximately 64.599 psi for monolith inside the microchip at a flow rate of (0.1) mL/min, the effect of sample solution volume and reagent solution was (25.0 µL) and $7*10^{-5}$ M concentration of (MPDADPI). The chip was then connected to an HPLC system

to study sample separation**,** as shown in Figure (3.65- 3.67) detailed diagram showing the basic steps of microchip configuration and its readiness for use with the HPLC-FIA system.

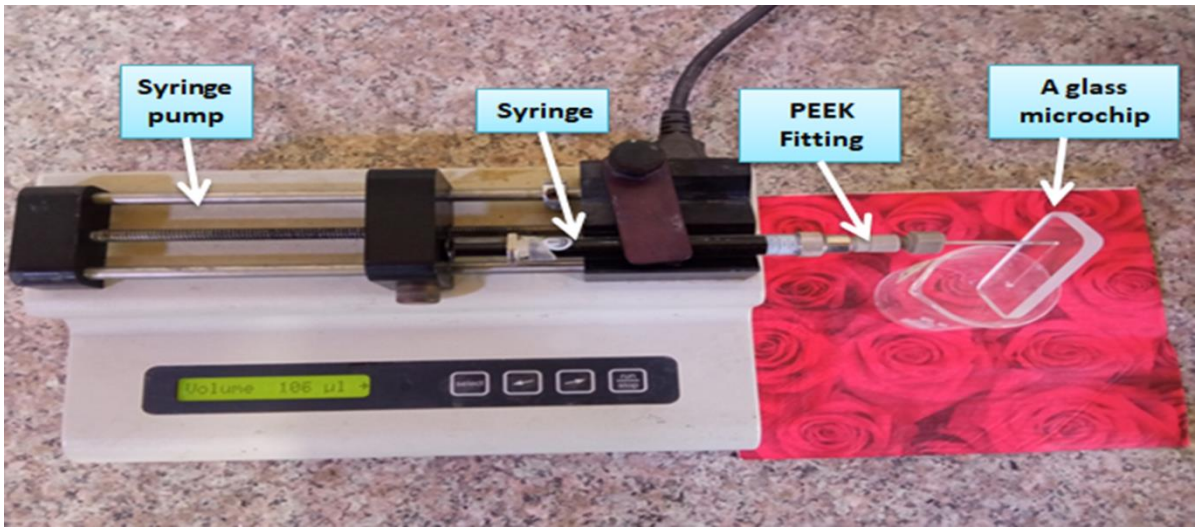

Figure (3.65): photo silanization processes

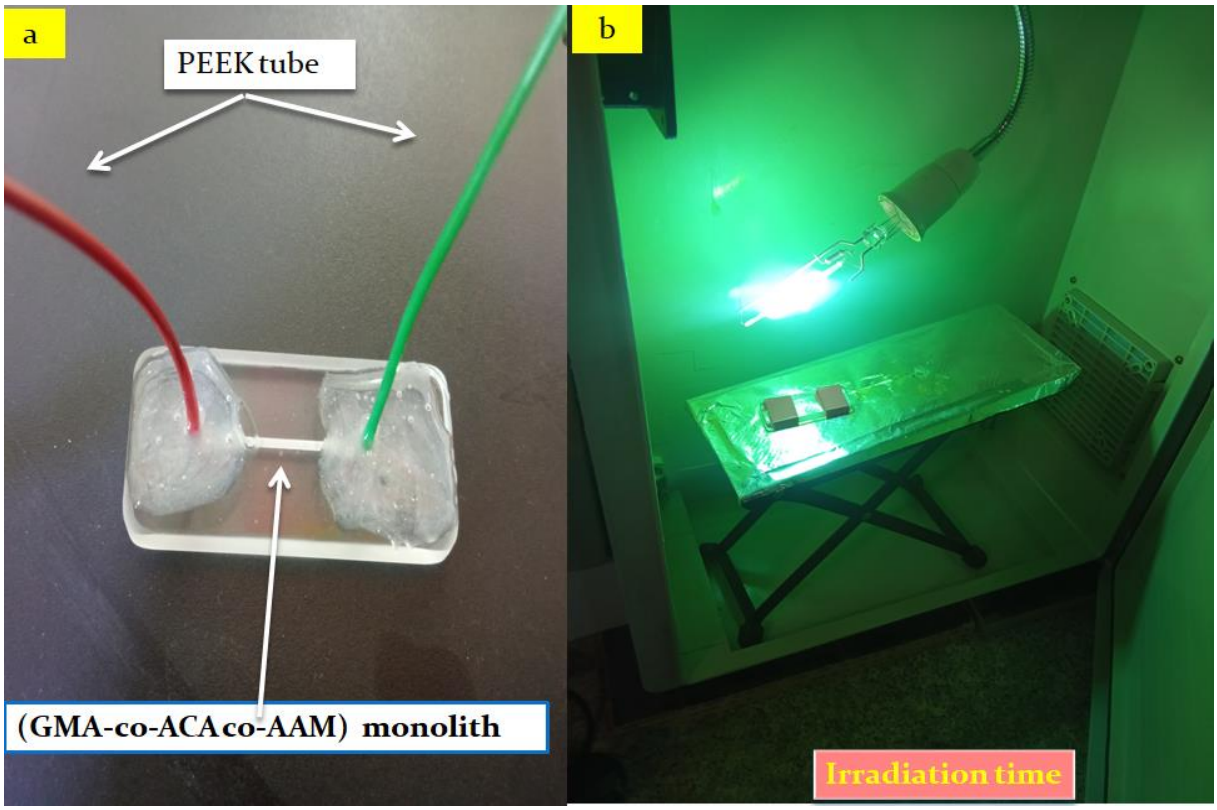

Figure (3.66): (a) A photograph of the microchips device; on the left, the microchip after the silanization step, (b) On the right, the irradiation time cabin

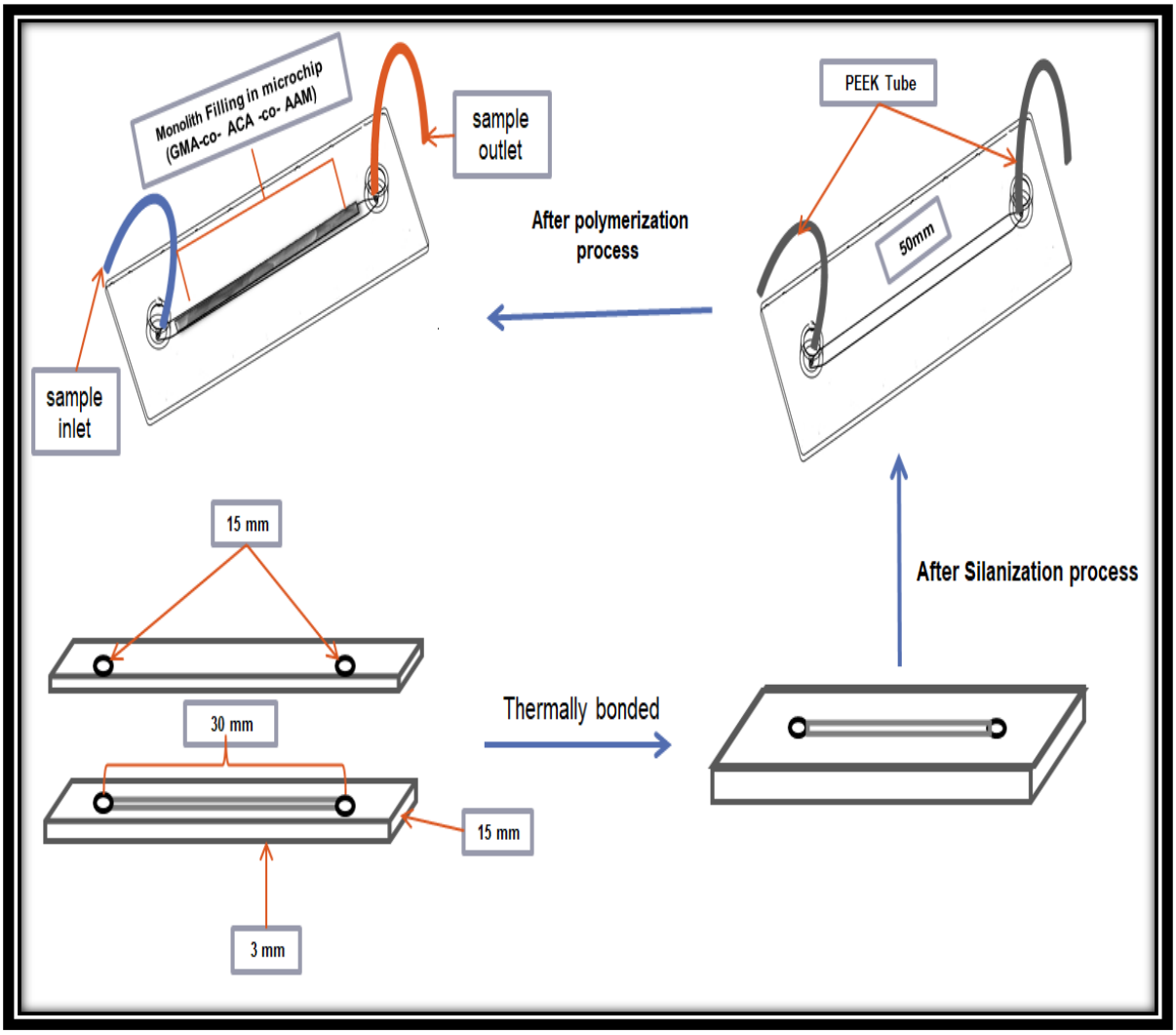

Figure (3.67): scheme stages of designing the microfluidic chip.

(3.37) HPLC Detector.

HPLC Detectors is used instead of a spectrophotometer, and it is used as a detector because it has the advantages of variable wavelength UV -Vis, high sensitivity, and a selection of flow cells; the Model 1050 detector is ideal for liquid chromatography applications.

A direct mechanical drive on the unit's front panel sets the desired wavelength. The standard deuterium lamp covers UV wavelengths; an optional tungsten lamp is available for visible wavelengths. The lamps are prealigned, readily

accessible, and can be easily changed [169]. So it has been modified as shown in Figure (3.68).

Figure (3.68): UV/Vis Detector.

(3.38) Data Acquisition System

In order to optimize the characteristics of the design system in terms of performance, handling capacity and cost, the relevant sub-systems can be combined by a data acquisition system (D.Q.S), which consists of individual sensors with the necessary signal conditioning, data conversion, data processing, multiplexing, data handling and associated transmission, storage and display systems. Analog Data Acquisition System is generally acquired and converted into digital form for processing, transmission, display and storage. Data may be transmitted over long distances (from one point to another) or short distances (from the test centre to a nearby PC). [170] . as shown Figure (3.69) .

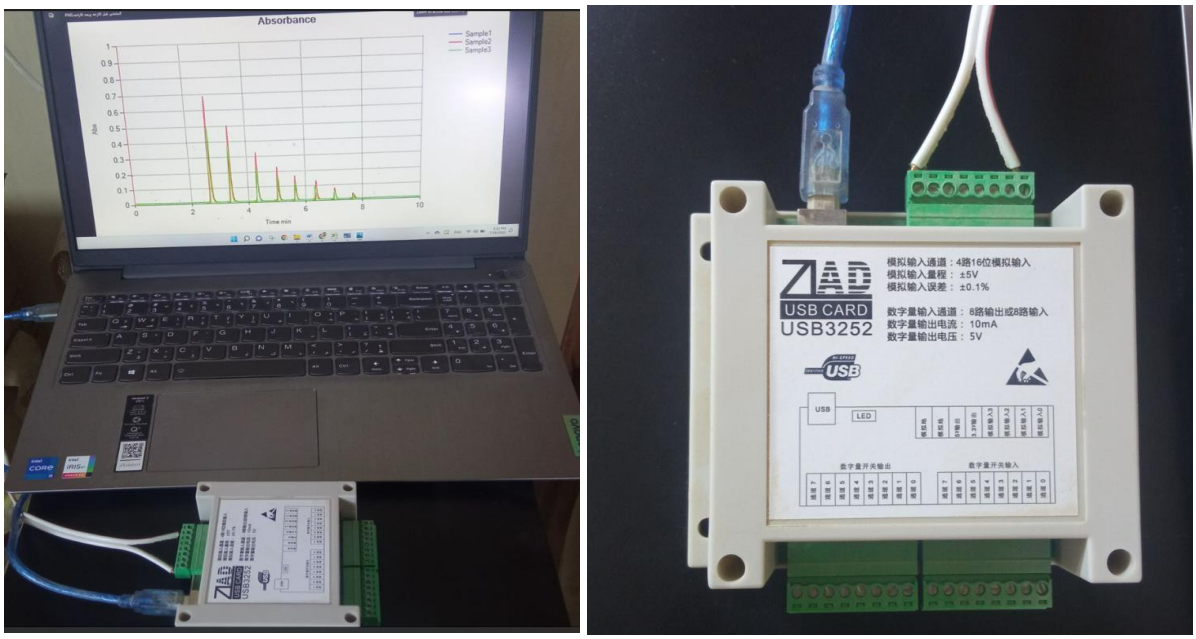

Figure (3.69): data Acquisition System.

(3.39) Distribution coefficients, total capacity for monolith microchip device.

Calculation of equations within (3.2) and (3.3) was applied, and the results were that the total capability of the microchip was found to be (10.831 ppm) distribution coefficients of Ni^{+2} ion (4.333).

(3.40) Work Stages for microchip design.

(3.40.1) Sample injection Stage.

After the pumping of D.W by (HPLC Pump) for all systems, the injection process of Ni (II) is (1.5 $mg.L^{-1}$) in one-valve (universal valve) manually in two steps; the first step is called (loading sample) at load position (No.4 position to No.1 position) by needle HPLC (injection syringe). The waste comes out of position No. 6 and the second step pushes the sample toward the microchip, as shown in the figures (3.70 a),(3.70 b) and (3.70c).

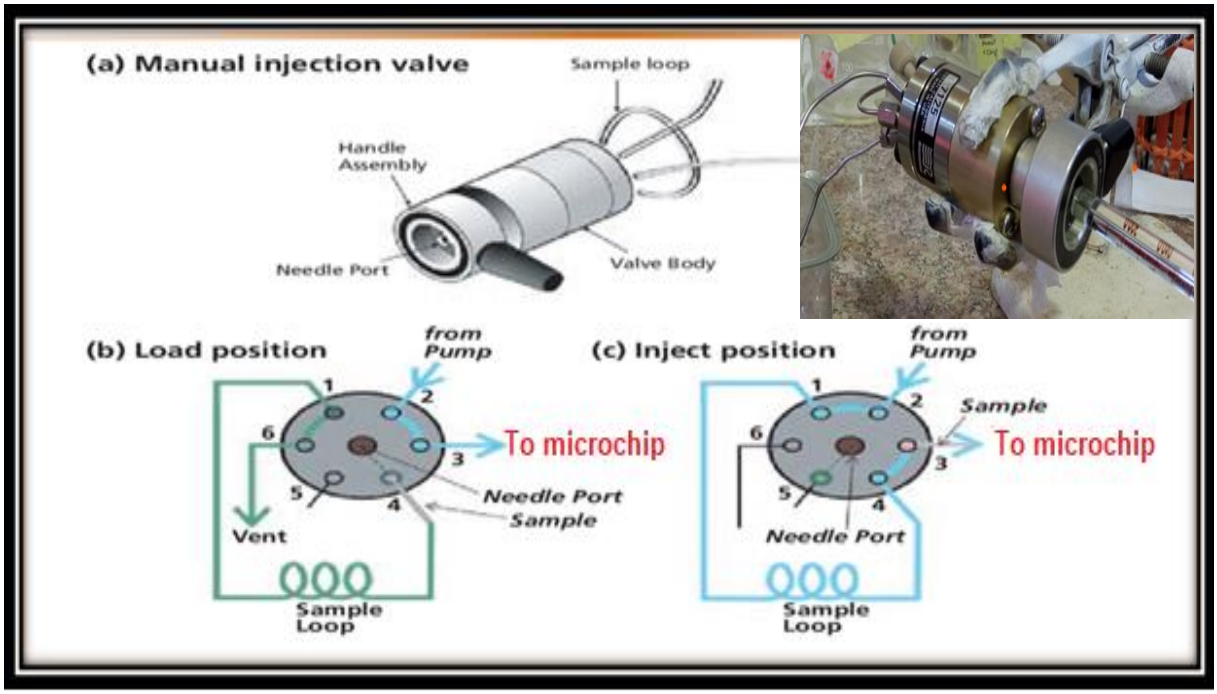

Figure (3.70) : (a) Manual one-valve (universal valve) and (b,c) loading and injection process of the sample, respectively.

(3.38.2) Reagent injection Stage.

After the injection and loading process of the sample, the reagent was injected fixed size injection syringe (25µl) in a sub-valve (3-way) tied and installed after the monolith microchip waiting only (30 seconds). as shown in Figures (3.71).

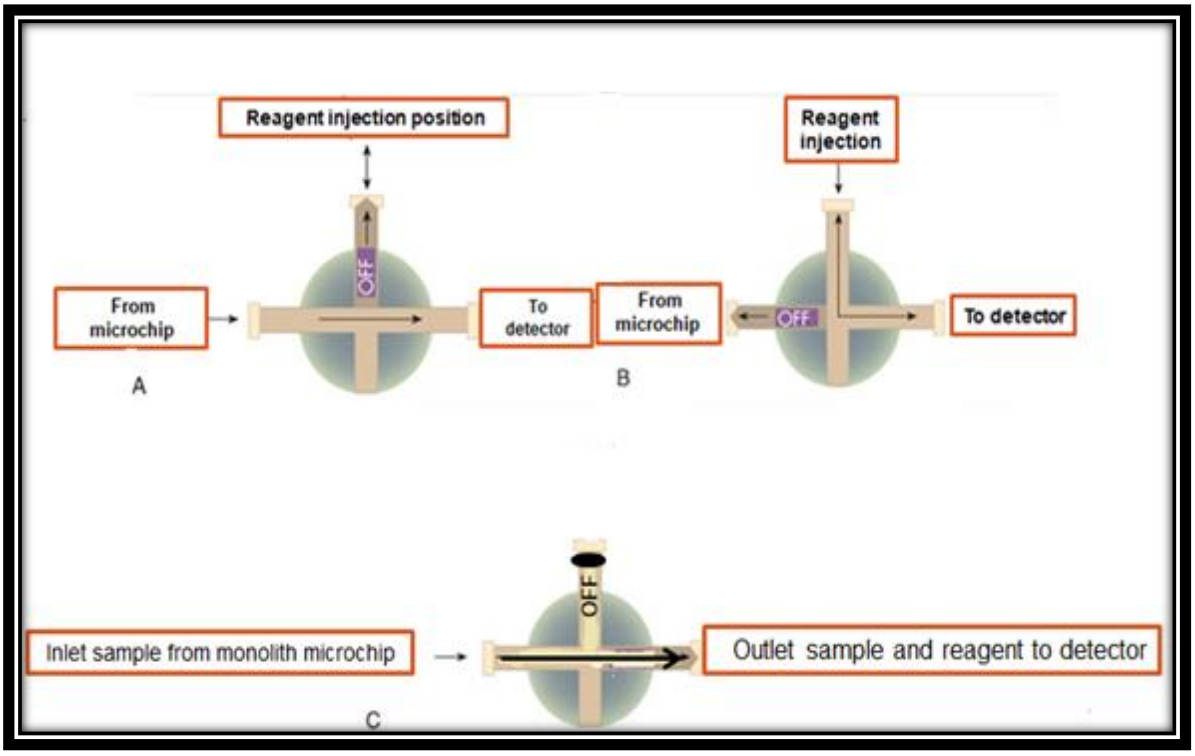

Figure (3.71) (A, B, C): Stages of injection and pushing reagent toward the detector

(3.40.3) Removing by injection Stage for HCL.

0.1 mol.L^{-1} of HCL was fixed as the optimal chemical conditions to remove the eluent of nickel ions (II) in monolith microchip by injection in one-valve (universal valve) manually and to push by (HPLC Pump); these ions from the monolith microchip meet with the second reagent injection and head towards the detector to draw the signal. Note that the concentration of Ni (II) was 1.5 mg.L^{-1}. as shown in Figures and Photo (3.72) A and B.

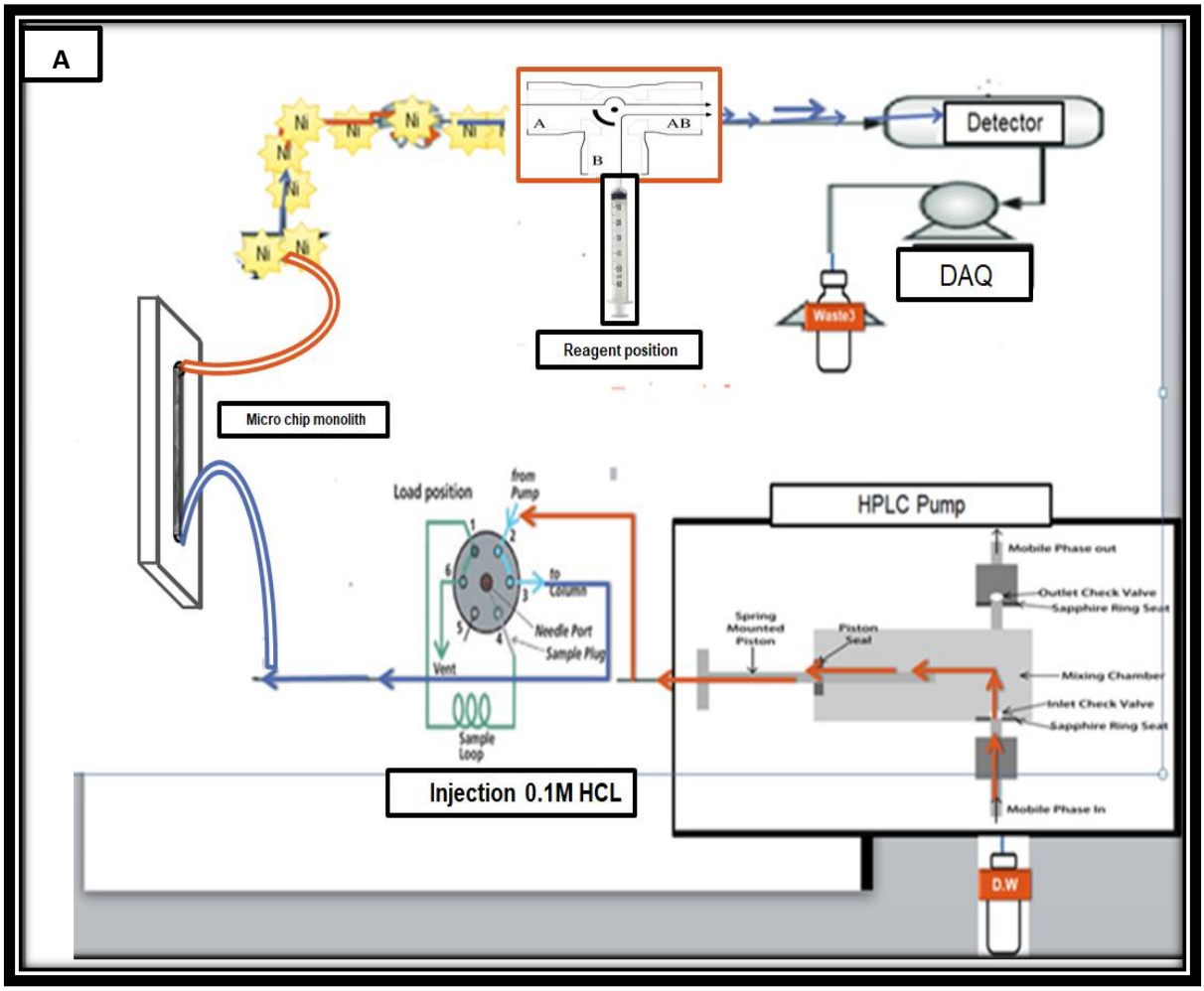

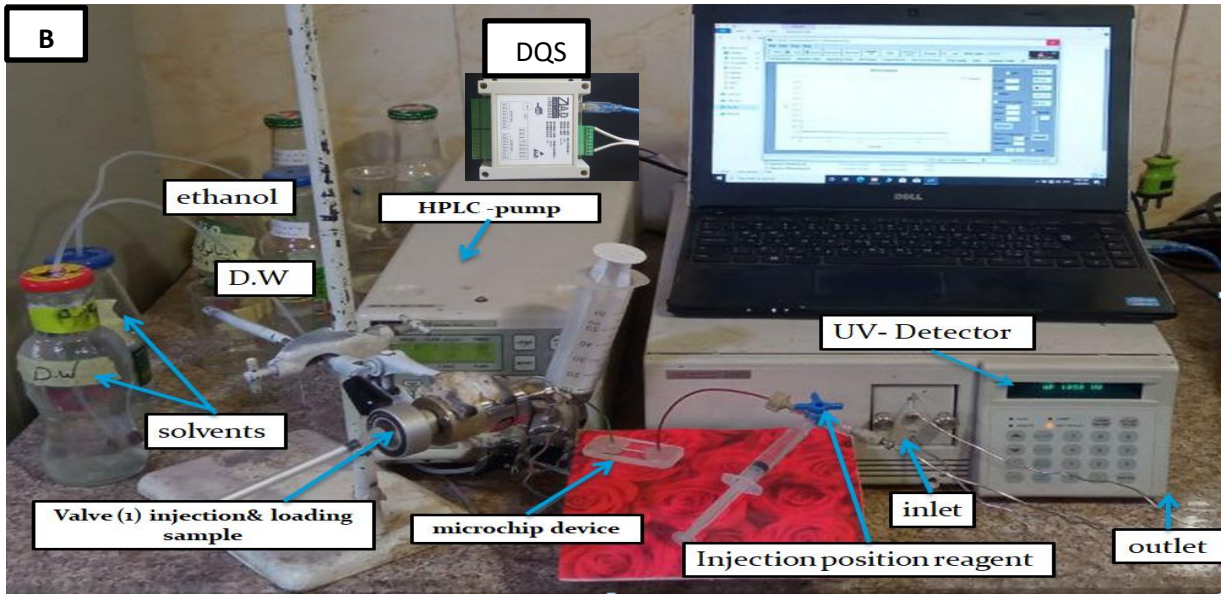

Figure (3.72) A, B: Schematic shape and photo connection of monolith microfluidic chip to the other parts of the system.

(3.41) Calibration Curve

Ni (II) concentrations were prepared over the range (0.001-3.5.) μg.mL^{-1} to construct the calibration curve. The coefficient of determination (R^2) was 0.9977, according to the results in Table (3.19) and Figure (3.73). The limit of detection (S/N=3) was 0.87 ng.mL$^{-1,}$ and the limit of quantification (S/N=10) was 0.087 μg. mL^{-1}.

Table (3.20): Calibration curve values at optimum conditions, including 7*10^{-5} M of(MPDADPI) 0.1 mol.L-1 of HCL, D.W Carrier, the flow rate was 0.1 mL.min^{-1}, the net pressure was 64.599 psi for monolith microchip, the effect of sample solution volume, reagent solution was (25.0 μL), pH was 8, and the temperature was 23±3 °C.

Conc. of Ni(II) μg. mL^{-1}	Mean Abc (n=3) $\bar{Y}$	S.D	R.S.D%	Found Con. μg. mL^{-1}	Recovery(%)
0.001	0.009	0.001	0.639	0.0011	90.91
0.005	0.015	0.001	4.133	0.0049	102.04
0.5	0.070	0.001	1.657	0.51	98.04
1	0.142	0.00	0.00	1.39	71.94
1.5	0.218	0.003	1.376	1.52	98.68
2	0.304	0.005	1.621	2.01	99.50
2.5	0.360	0.003	0.735	2.50	100.00
3	0.423	0.006	1.316	2.98	100.67
3.5	0.493	0.021	4.220	3.49	100.29

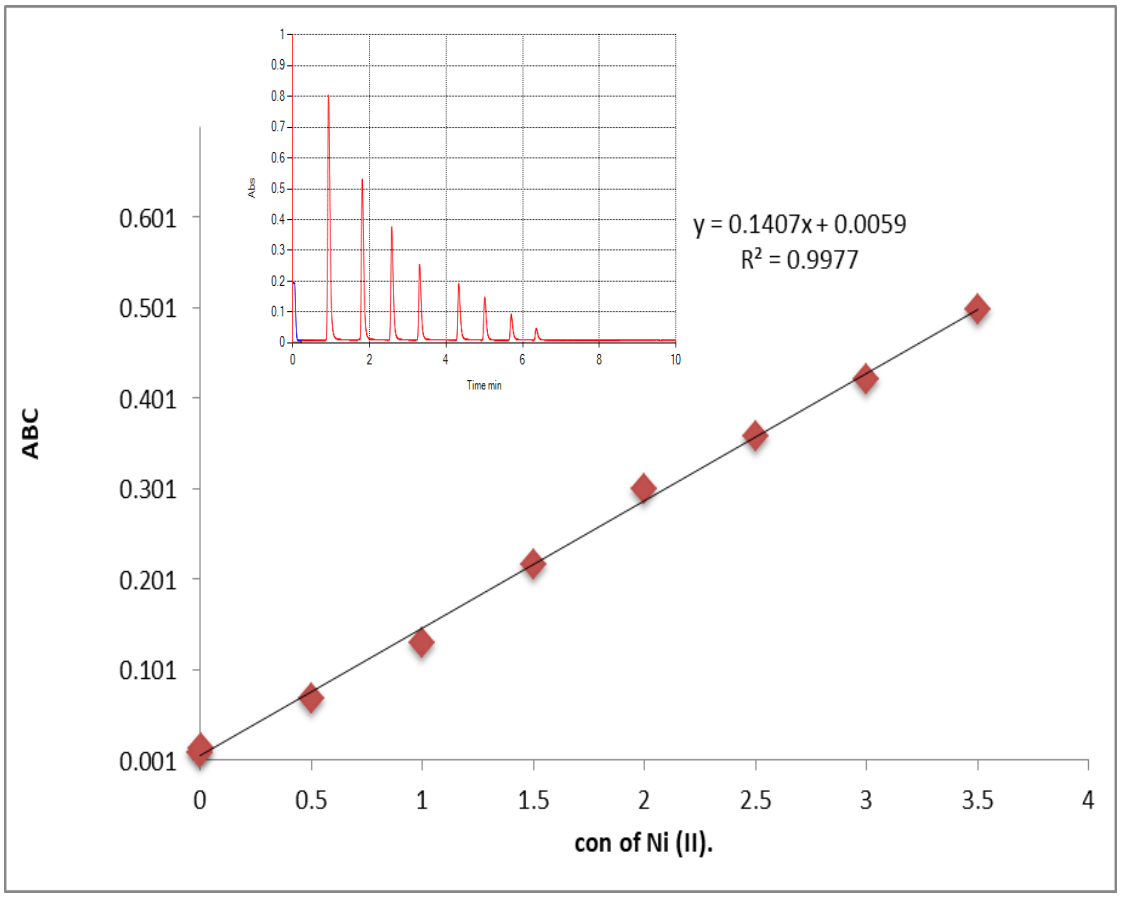

Figure (3.73): Calibration curve for Ni (II)

(3.42) Summary of Innovative Systems

The monolithic column and microchip are used to determine elements (Ni^{+2} and Cu^{+2}) under study properties measured using the new innovative systems are summarised in Table (3.20).

Table (3.21): Work summary of innovative Systems

Seq.	Measured Property	Off-line method for incorporation Cu^{+2}	Off-line method for incorporation Ni^{+2}	On-line method for incorporation Cu^{+2}	On-line method for incorporation Ni^{+2}	On-line method for incorporation Ni+2 using microchip
1	λ_{max} (nm)	453	518	453	518	518
2	Conc. of reagent	100 mg.mL^{-1} of Neocuproine	$5x10^{-5}$M of MPDADPI	mg.mL-1 of 100 Neocuproine	5x10-5M of MPDADPI	7x10-5M of MPDADPI
3	Volume of sample (µL)	----------	-------	78.5	39.25	25
4	Volume of reagent (µL)	---------	----------	78.5	78.5	25
5	Length of monolithic column (mm)	60 mm	60mm	60mm	60mm	microchip device (30mm)
6	Flow rate mL.min^{-1}	1.5	1.5	1.8	1.8	0.1
7	Linear range	1–35 mg/L	0.5-32 mg/L	0.05-17 mg.mL-1	0.0005-0.5	0.001–3.5 µg.mL-1
8	Correlation coefficient (r)	0.998	0.9987	0.9981	0.9995	0.9977
9	Slop (b)	0.0085	0.014	6.5811	5.75	0.1407
10	Intercept (a)	0.0006	0.0096	2.8372	0.0321	0.0059
11	L.O.D	0.269 mg/L	0.3 mg/l	0.039mg.mL-1	0.003	0.00087 µg.mL-1
12	L.O.Q	0.807 mg/L	0.6mg/l	0.117mg.mL-1	0.091	0.00261 µg.mL-1

Table (3.22): Comparing the work with some prepared monolithic columns

Reaction	Length of monolithic column	Flow rate	Analyte	Technique	RF
Poly(glycidyl methacrylate-co-ethylene methacrylate) A polymerization mixture consisting of 25.5% GMA, 17.5% EDMA, 40% 1-dodecanol, 17% cyclohexanol, and 1% AIBN (with respect to monomers) (all percentages w/w) was purged with nitrogen for 10 min.	100m	0.25 µL/min	A mixture of ovalbumin,chymotrypsinogen,cytochrome c, ribonuclease A and lysozyme	anion-exchange mode capillary system	171
Then capillary column rinsed with acetone for 0.5 h and dried with steam nitrogen gas for 0.5 h. The polymer precursor solution prepared from0.002 g AIBN (polymerization initiator), 0.09 mL glycidyl methacrylate (monomer), 0.03 mL ethylene dimethacrylate (cross-linker), 0.105 mL 1,4-butanediol, 0.06 mL decanol, and 0.015 mL water (porogen).	2-3 mm	(4 µL/min)	iodate,bromate, nitrite, bromide, and nitrate.	ion chromatography capillary system	172
prepared by co-condensation of (3-chloropropyl)-trimethoxysilane (CPTMS) and tetramethoxysilane (TMOS) , and then N-methylimidazole was bonded to the CP-silica column via the chloropropyl group.	33.5 cm	(0.01 mL/min)	benzene, naphthalene, anthracene, chrysene	Capillary electrochromatography (CEC)	173
An IonPac AS9-HC separation column with an AG9-HC pre-column and an ASRS-ultra II 4 mm suppressor used ina chemical mode of operation	100mm	1 mL/min	fluoride, nitrite, nitrate and phosphate	ion chromatography	174
prepared by Poly(ethylene glycol) (0.88 g) and urea (0.9 g) were dissolved in 10 mL of 0.01 mol/L acetic acid. Tetramethoxysilane was added to this solution (35/65, v/v)	70 cm	41 nL/min	proteomic analyses	Silica-Based Monolithic Columns	175
prepared by dissolving (NPOE) 2-Nitrphenyl octyl ether (2.0 mL), (PVC) Poly (vinyl chloride) (0.4 g), (TDAB)Tetradodecylammonium bromide (0.1554 g) and (TFPB)Sodium tetrakis [3,5-bis(trifluoromethyl)phenyl] borate (0.0886 g) in 10 mL of tetrahydrofuran (THF) in a beaker.	1480 cm	4.17 µL/s	SO4 2- , Cl- , NO2 - , Brand NO3 - ions. F- , HPO4 2- and CH3COO	A sequential injection chromatography (SIC) constructed from a short monolithic column	176
prepared by poly(glycidyl methacrylate-co-ethylene dimethacrylate)The 40: 60 v/v mixture of monomers (GMA and EDMA, 75: 25 vol%) and porogenic diluents (cyclohexanol and dodecanol, 90: 10 vol%), in which AIBN (1% w/v with respect to monomers) was dissolved, was purged with nitrogen for 15 min	7.9 mm	1.0 mL/min	proteins	weak cation exchange chromatography	177
prepared by poly(glycidyl methacrylate-co-ethylenedimethacrylate) 900 mL of GMA and 300 mL of EDMA were dissolved in a ternary porogen of 1050 mL of 1,4-butanediol, 600 mL of 1-propanol and 150 mL of water. Twelve milligrams of AIBN was added to the mixture as a polymerization photo-initiator (1 wt% relative to the monomers). Prior to irradiation, dissolved oxygen in solution was degassed by sonication for 15 min.	100 mm	2 mL/min	bromate,nitrite and nitrate	anion-exchangechromatography	178
poly(GMAPEGDA) by reaction of the epoxy groups with DEA.PEGDA was chosen as the only crosslinker because of its effectiveness in reducing non-specific adsorption of proteins on the monolith. Then the polymer precursor was prepared by mixing monomer, crosslinker, porogens,	10 cm	0.15 µ L/min	proteins	anion-exchange capillary liquid chromatography	179
phosphate monolith was prepared by the reaction mixture consisting of ethylene glycol methacrylate phosphate (80 µL, ~100 mg), bisacrylamide (60 mg), dimethylsulfoxide (270 µL), dodecanol (200 µL), N,N′-dimethylformamide (50 µL), and AIBN (2 mg) was sonicated for 20 min to obtain a homogeneous solution and then purged with nitrogen for 10 min	7 cm	21 µL/min	proteins	strong cation exchange	180
prepared from a mixture consisting of (Ter – monomers), glycidyl methacrylate(GMA), Acrylic acid (A. AC) and acryl amid were used to make monolithic columns via free radical polymerization (AAM). DMPA (2,2-dimethoxy-2-phenylacetophenone) as an initiator instead of the more common initiator 2,2- azoisobutyronitrile (AIBN) this was due to some defects when using (AIBN) and one of these defects is the formation of voids due to the rapid reaction and generation of N2 gas during the polymerization	microchip device (30mm) &60mm	(0.1 &1.5)mL/min	Ni (II) and Cu(II)	strong cation exchange	The work

4. Conclusions and Future forecast

(4.1) Conclusions

1. A new glycidyl methacrylate-co- Acrylic acid -co-acryl amide monolithic column was successfully prepared and characterized.
2. The polymer was optimized as a strong cation exchange column by converting the epoxy group to sulfonate groups reaction.
3. Moreover, the chelating capacity was calculated to find out the number of ions that can be exchanged between the column and sample solution.
4. The new innovative (design) were characterized with simplicity, rapidity, high efficiency and sensitivity.
5. The sensitivity of response and limit of detection were improved by using the microfluidic chip with interfered conduits.
6. The column was successfully applied to determine the Cu (II) and Ni (II) concentration accuretly by compering the result that obtained using spectrophotometric method with the result that gained using atomic absorption method.
7. The results show that the ion –exchange chromatography method is more sensitive and faster when compared with the methods traditional.
8. The proposed methods were applied for the determination of Ni(II)and Cu (I) in various samples.

(4.2) Future forecast

1. The prepared monolithic columns or microchip can be used in sample analysis such as blood, urine and pharmaceutical .

2. Simple reconfiguration of the manifold can be implemented for the determination of With other elements (II) when pH changes with ((E)-2-((4 methoxyphenol)diazenyl)-4,5-diphenyl-1Himidazoleand (Orange) by using the HPLC-FIA system.
3. 3-Other detection devices can be used to improve the sensitivity of measurement and other characteristics, such as, chemiluminescence, fluorescence, etc. with HPLC-FIA technique.

4. 4-The prepared study can be used in community service as an application through the university's relationship with the ministry, for example, health or water resources, in order to purify the water from heavy, harmful elements with concentrations higher than the permissible limit.

Chapter One

Introduction

1. Introduction

(1.1) Chromatography

The discovery of chromatography is generally credited to Tswett [1]. Chromatography is an important biophysical technique that enables the separation, identification, and purification of the components of a mixture for qualitative and quantitative analysis [2].

All chromatographic systems have a mobile phase that transports the analytes through the column and a stationary phase coated onto the column or on the resin beads in the column[3]. The stationary phase loosely interacts with each analyte based on its chemical structure, resulting in the separation of each analyte as a function of time spent in the separation column[4].

Chromatography differs from other methods of separation in that a wide variety of materials, equipment, and techniques can be used[5].

Four separation techniques based on molecular characteristics and interaction type use mechanisms of ion exchange, surface adsorption, partition, and size exclusion. Other chromatography techniques are based on the stationary bed, including column, thin layer, and paper chromatography [2].Column chromatography is one of the most common methods of protein purification[6].

Based on this approach three components form the basis of the chromatography technique.

1-Stationary phase: This phase is always composed of a “solid” phase or “a layer of a liquid adsorbed on the surface a solid support”.

2-Mobile phase: This phase is always composed of “liquid” or a “gaseous component.”

3-Separated molecules [4-7].

As illustrated in scheme Classification of chromatography methods according to various applied techniques. Fig (1) [5,8].

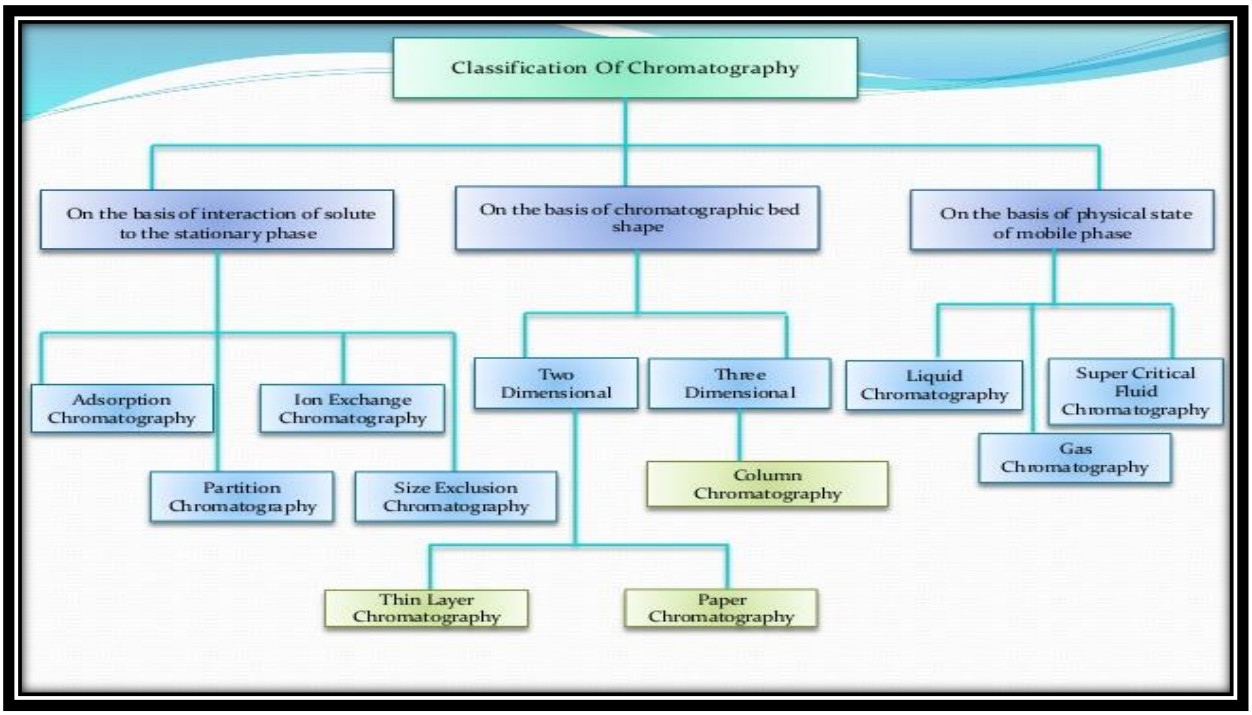

Figure (1.1) A scheme for subdividing the field of chromatography, according to various applied techniques.

(1.2) Classification based on the physical state [8]:-

The first method based on the physical state of the mobile phase and the stationary phase. They fall into four categories , Such as

1. Gas-liquid
2. gas-solid
3. liquid-solid
4. liquid-liquid

(1.3) Classification based on contact between mobile phase and stationary phase[8,9]:-

1. Liquid-solid chromatography (LSC)
2. Liquid-Liquid chromatography (LLC)

3. Gas-Solid chromatography (GSC)
4. Gas-Liquid chromatography(GLC)

(1.4) Classification of chromatography based on Chemical or physical mechanism[9]:-

1. Column chromatography
2. **Ion-exchange chromatography**
3. Gel-permeation (molecular sieve) chromatography
4. Affinity chromatography
5. Paper chromatography
6. Thin-layer chromatography
7. Gas chromatography
8. Dye-ligand chromatography
9. Hydrophobic interaction chromatography
10. Pseudo affinity chromatography
11. High-pressure liquid chromatography (HPLC)

(1.4.1)-Column chromatography [10,11]

This technique is used for the purification of biomolecules. On a column (stationary phase) firstly the sample to be separated, then wash buffer (mobile phase) are applied (Fig.2). Their flow through inside column material placed on a fiberglass support is ensured. The samples are accumulated at the bottom of the device in a tme-, and volume-dependent manner .

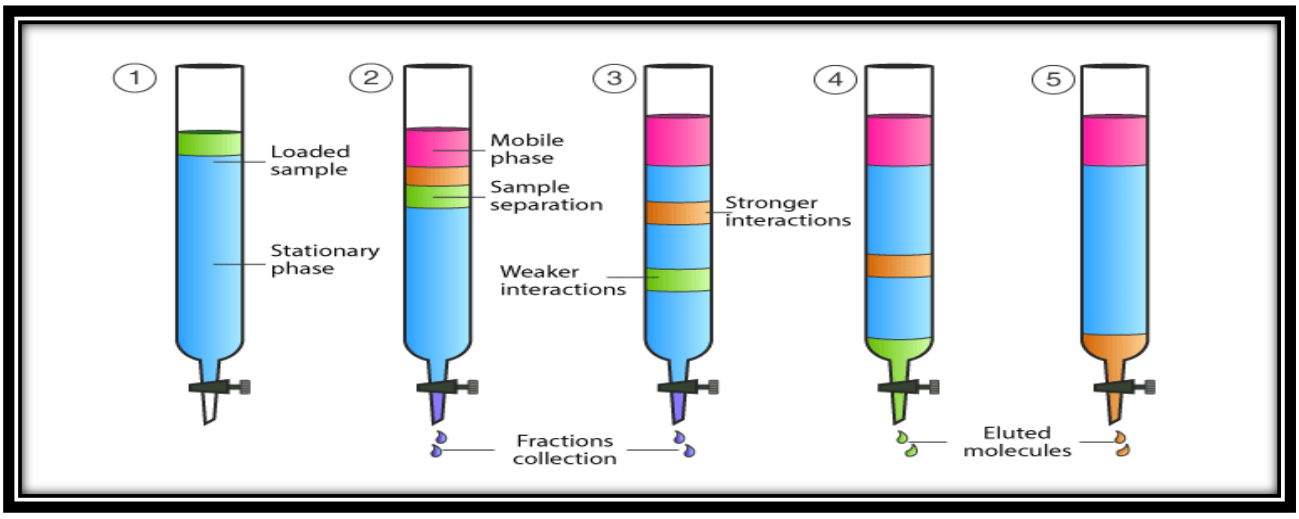

Figure (1.2).Column chromatography.

(1.4.2)- Ion- exchange chromatography [5,6]

Electrostatic interactions between charged protein groups and solid support material are used in IEC. Proteins are separated from the column by adjusting the pH, ion salt concentration, or ionic strength of the buffer solution. Anion-exchange matrices are positively charged ion-exchange matrices that adsorb negatively charged proteins. Cation-exchange matrices, on the other hand, are made up of negatively charged groups and adsorb positively charged proteins. (Fig.3).

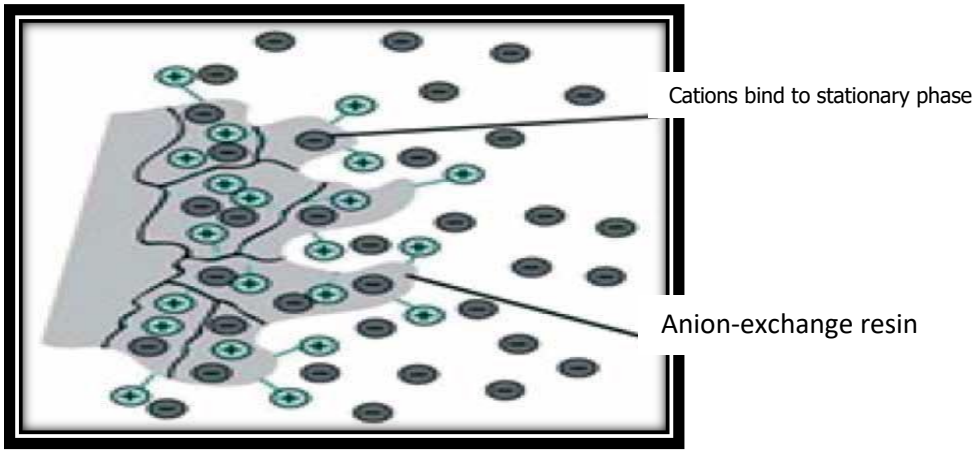

Figure (1.3) Ion- exchange chromatography.

In ion-exchange chromatography the stationary phase is a cross-linked polymer resin, usually divinylbenzene cross-linked polystyrene, with covalently attached ionic functional groups[12,15,14].

The counterions to these fixed charges are mobile and can be displaced by ions that compete more favorably for the exchange sites.

Ion-exchange resins are divided into four categories: **strong acid cation exchangers; weak acid cation exchangers; strong base anion exchangers; and weak base anion exchangers.** As in scheme provides a list of several common ion-exchange resins [12,13].

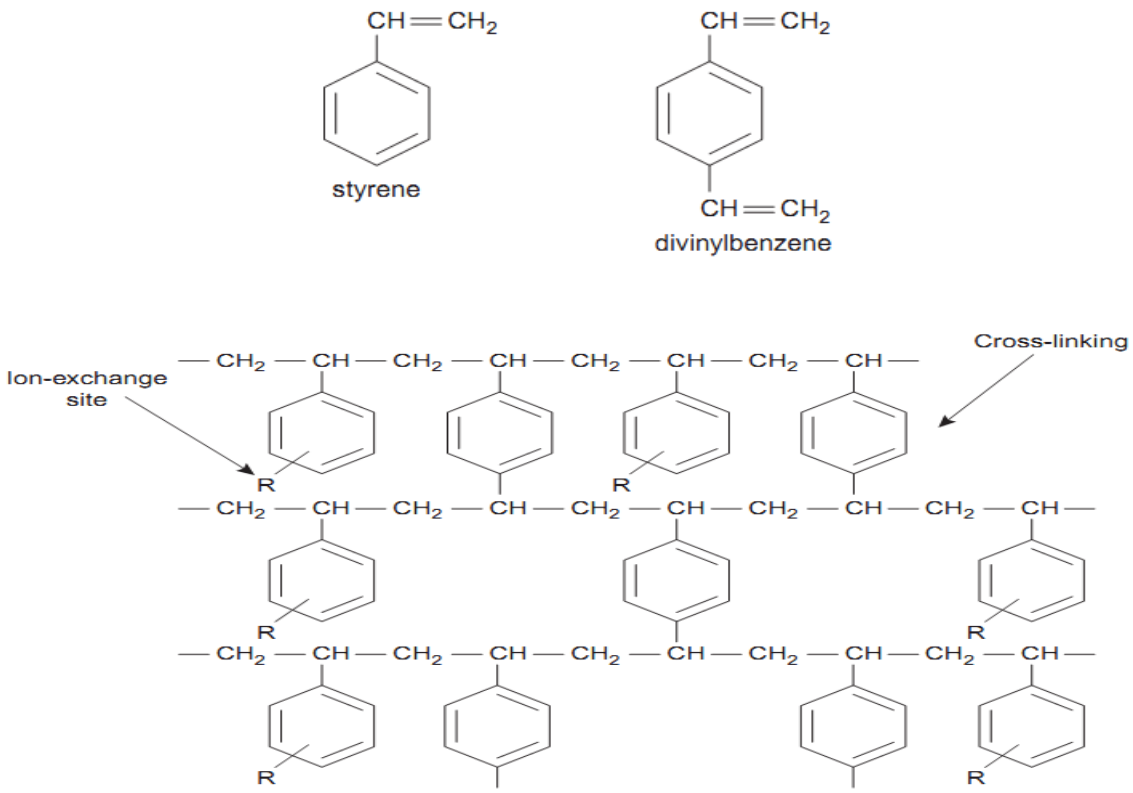

Figure (1.4) scheme provides a list of several common ion-exchange resins

Strong acid cation exchangers include a sulfonic acid functional group that retains its anionic form, and thus its capacity for ion-exchange, in strongly acidic solutions. The functional groups for a weak acid cation exchanger, however, are fully protonated at pH levels less than 4, thereby losing their exchange capacity.

The strong base anion exchangers are fashioned using a quaternary amine, therefore retaining a positive charge even in strongly basic solutions. Weak base anion exchangers, however, remain protonated only at pH levels that are moderately basic. Under more basic conditions, a weak base anion exchanger loses its positive charge and therefore, its exchange capacity[(8)]. Table (1.1) show types of function group ion- exchange.

Table (1.1) Types of function group ion- exchange.

Type	Functional Group	Examples
strong acid cation exchanger	sulfonic acid	$-SO_3^-$ $-CH_2CH_2SO_3^-$
weak acid cation exchanger	carboxylic acid	$-COO^-$ $-CH_2COO^-$
strong base anion exchanger	quaternary amine	$-CH_2N(CH_3)_3^+$ $-CH_2CH_2N(CH_2CH_3)_3^+$
weak base anion exchanger	amine	$-NH_3^+$ $-CH_2CH_2NH(CH_2CH_3)_2^+$

The ion-exchange reaction of a monovalent cation, M+, at a strong acid exchange site is

$$-SO_3^-\text{–}H^+(s) + M^+(aq) \rightleftharpoons -SO_3^-\text{–}M^+(s) + H^+(aq)$$

The equilibrium constant for this ion-exchange reaction, which is also called the selectivity coefficient, is

$$K = \frac{\{-SO_3^-\text{–}M^+\}[H^+]}{\{-SO_3^-\text{–}H^+\}[M^+]}$$

where the brackets { } indicate a surface concentration.

$$D = \frac{\text{amount of } M^+ \text{ in stationary phase}}{\text{amount of } M^+ \text{ in mobile phase}} = \frac{\{-SO_3^-\text{–}M^+\}}{[M^+]} = K\frac{\{-SO_3^-\text{–}H^+\}}{[H^+]}$$

D is a function of the concentration of H^+ and, therefore, the pH of the mobile phase(16,17).

Ion-exchange resins are incorporated into HPLC columns either as micron sized porous polymer beads or by coating the resin on porous silica particles. Selectivity is somewhat dependent on whether the resin includes a strong or weak exchange site and on the extent of cross-linking. The latter is particularly important because it controls the resin's permeability and, therefore, the

accessibility of the exchange sites. An approximate order of selectivity for a typical strong acid cation exchange resin, in order of decreasing D, is

$$Al^{3+} > Ba^{2+} > Pb^{2+} > Ca^{2+} > Ni^{2+} > Cd^{2+} > Cu^{2+} > Co^{2+} > Zn^{2+} > Mg^{2+} > Ag^{+} > K^{+} > NH_4^{+} > Na^{+} > H^{+} > Li^{+}$$

That highly charged ions bind more strongly than ions of lower charge. Within a group of ions of similar charge, those ions with a smaller hydrated radius or those that are more polarizable bind more strongly. For a strong base anion exchanger the general order is

$$SO_4^{2-} > I^{-} > HSO_4^{-} > NO_3^{-} > Br^{-} > NO_2^{-} > Cl^{-} > HCO_3^{-} > CH_3COO^{-} > OH^{-} > F^{-}$$

Again, ions of higher charge and smaller hydrated radius bind more strongly than ions with a lower charge and a larger hydrated radius. The mobile phase in IEC is usually an aqueous buffer, the pH and ionic composition of which determines a solute's retention time. Gradient elutions are possible in which the ionic strength or pH of the mobile phase is changed with time [18,19].

Ion-exchange chromatography has found important applications in water analysis [20] and in biochemistry [21]. Ion-exchange chromatography also has been used for the analysis of proteins[22] , amino acids[21], sugars, nucleotides, pharmaceuticals, consumer products, and clinical samples[23,24].

(1.4.3)-Gel- permeation (molecular sieve) chromatography

The basic principle of this method is to use dextran containing materials to separate macromolecules based on their differences in molecular sizes. This procedure is basically used to determine molecular weights of proteins, and to decrease salt concentration of protein solutions . In a gel- permeation column stationary phase consists of inert molecules with small pores. The solution containing molecules of different dimensions are passed continuously with a constant flow rate through the column[6,25].

Molecules larger than pores cannot permeate into gel particles, and they are retained between particles within a restricted area. Larger molecules pass through spaces between porous particles, and move rapidly through inside the column. Molecules smaller than the pores are diffused into pores, and as molecules get smaller, they leave the column with proportionally longer [26–28] as shown Fig 5.

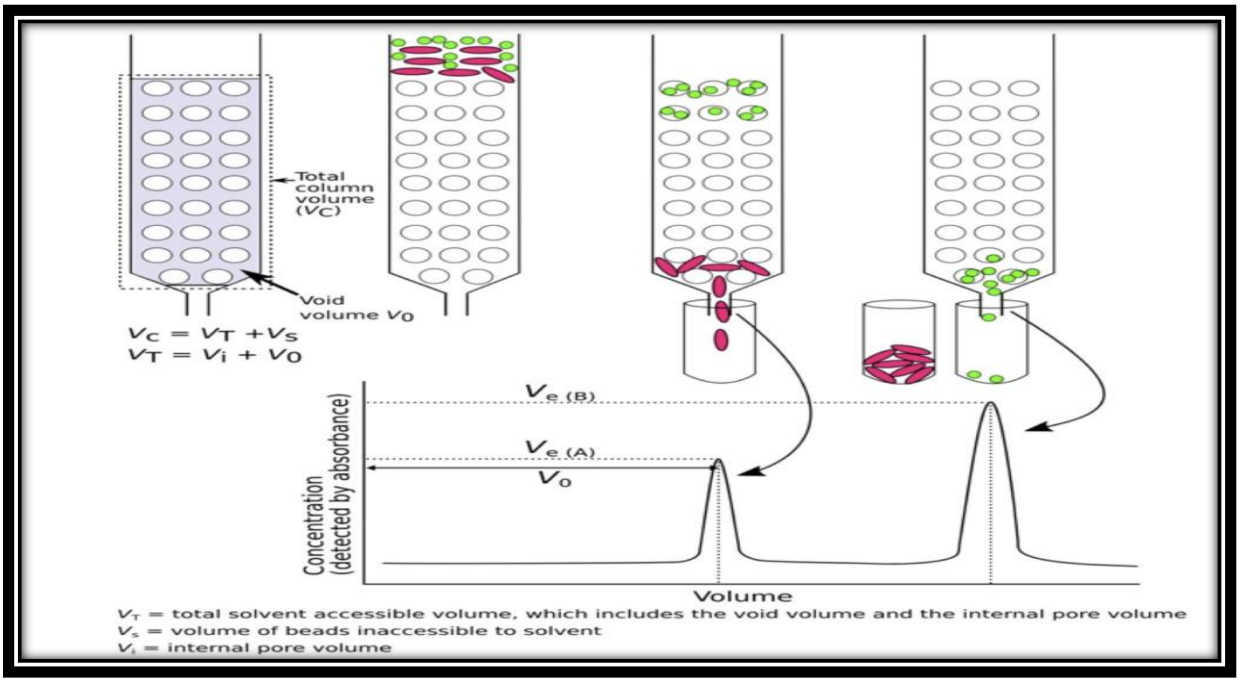

Figure (1.5) Technique gel- permeation chromatography

(1.4.4)-Affinity chromatography [29,30] .

This chromatography technique is used for the purification of enzymes, hormones, antibodies, nucleicacids, and specific proteins . A ligand which can make a complex with specific protein (dextran, polyacrylamide, cellulose etc) binds the filling material of the column. The specific protein which makes a complex with the ligand is attached to the solid support, and retained in the column,while free proteins leave the column. Then the bound protein leaves the column by means of changing its ionic strength through alteration of pH or addition of a salt solution (Fig.6).

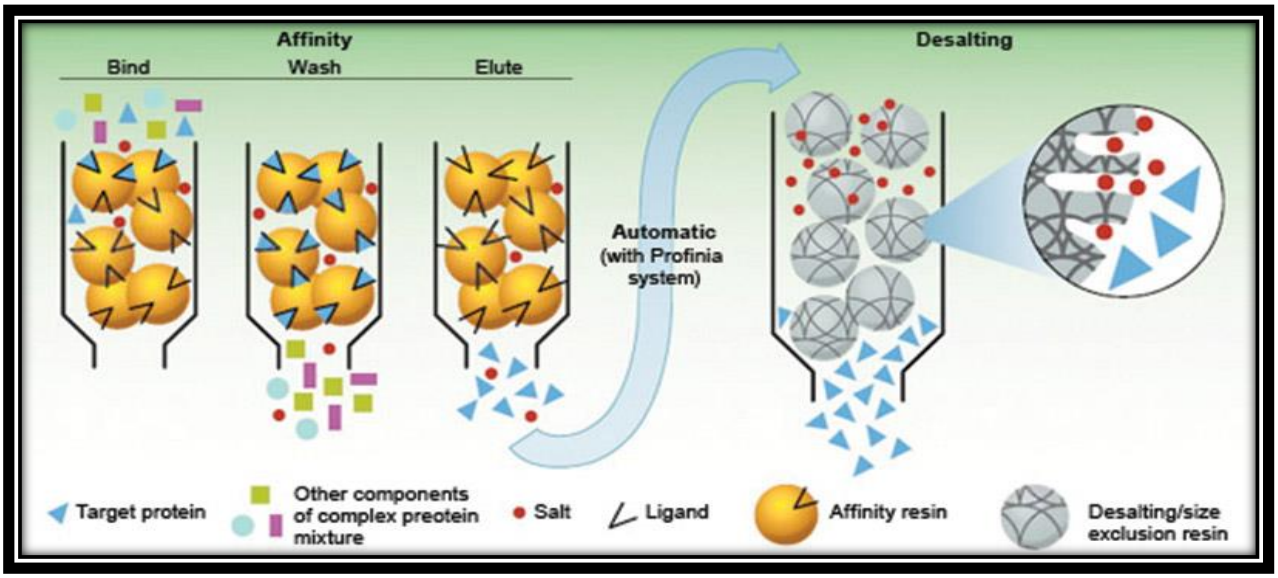

Figure (1.6) Affinity chromatography.

(1.4.5)-Paper chromatography [31-33]

In paper chromatography support material consists of a layer of cellulose highly saturated with water. In this method a thick filter paper comprised the support, and water drops settled in its pores made up the stationary "liquid phase." Mobile phase consists of an appropriate fluid placed in a developing tank. Paper chromatography is a "liquid-liquid" chromatography Fig .7.

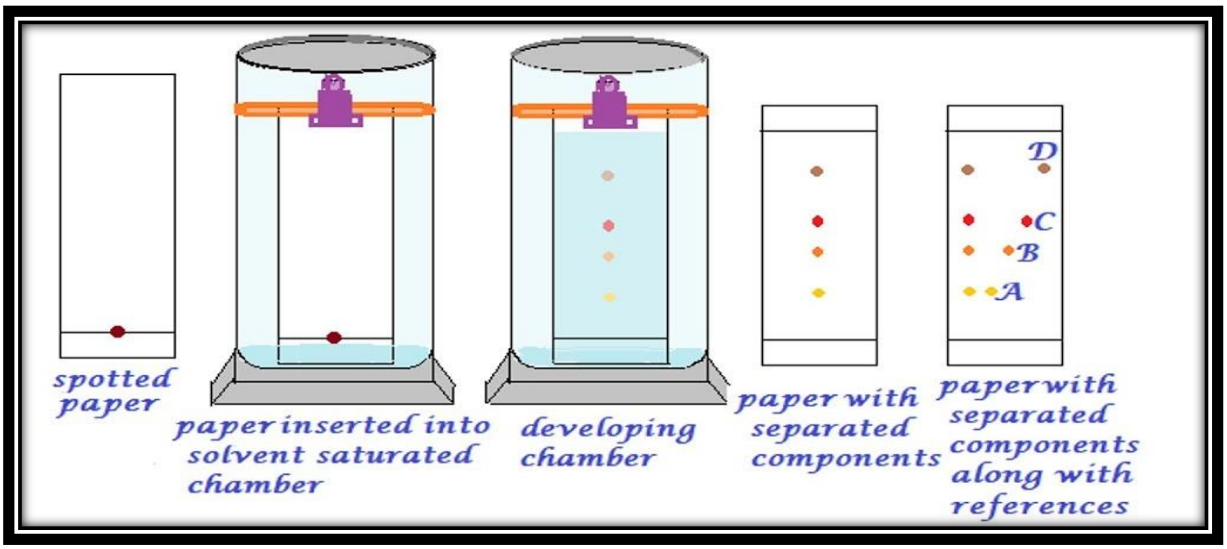

Figure (1.7) paper chromatography

(1.4.6)-Thin-layer chromatography [34]

Thin-layer chromatography is a "solid-liquid adsorption" chromatography. In this method stationary phase is a solid adsorbent substance coated on glass plates. As adsorbent material all solid substances used. In column chromatography (alumina, silica gel, cellulose) can be utilized[35]. In this method, the mobile phase travels upward through the stationary phase The solvent travels up the thin plate soaked with the solvent by means of capillary action. During this procedure, it also drives the mixture priorly dropped on the lower parts of the plate with a pipette upwards with different flow rates. Thus the separation of analytes is achieved. This upward travelling rate depends on the polarity of the material, solid phase, and of the solvent [36]. Fig.8

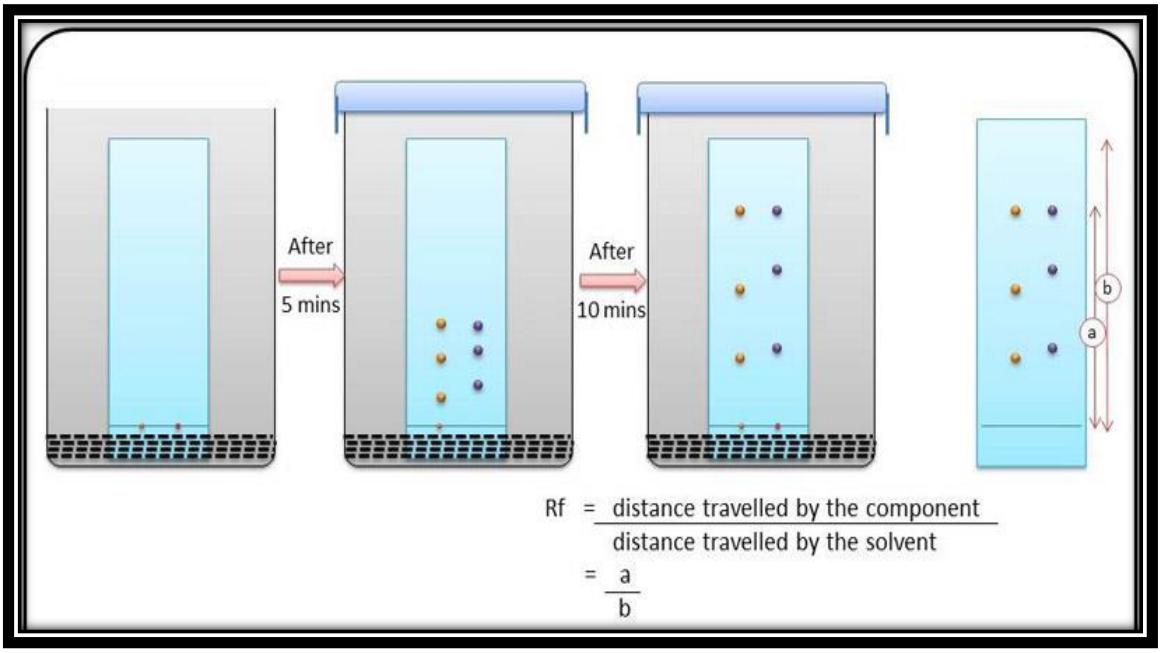

Figure (1.8) Thin-layer chromatography

(1.4.7)- Gas chromatograph [37-39]

In this method stationary phase is a column which is placed in the device, and contains a liquid stationary phase which is adsorbed onto the surface of an inert solid. Gas chromatography is a "gas-liquid" chromatography. Its carrier phase consists of gases as He or N_2. Mobile phase which is an inert gas is passed

through a column under high pressure. The sample to be analyzed is vaporized, and enters into a gaseous mobile phase . The components contained in the sample are dispersed between mobile phase, and stationary phase on the solid support. Gas chromatography is a simple, multifaceted, highly sensitive, and rapidly applied technique for the extremely excellent separation of very minute molecules. It is used in the separation of very little amounts of analyses. Fig 9 .

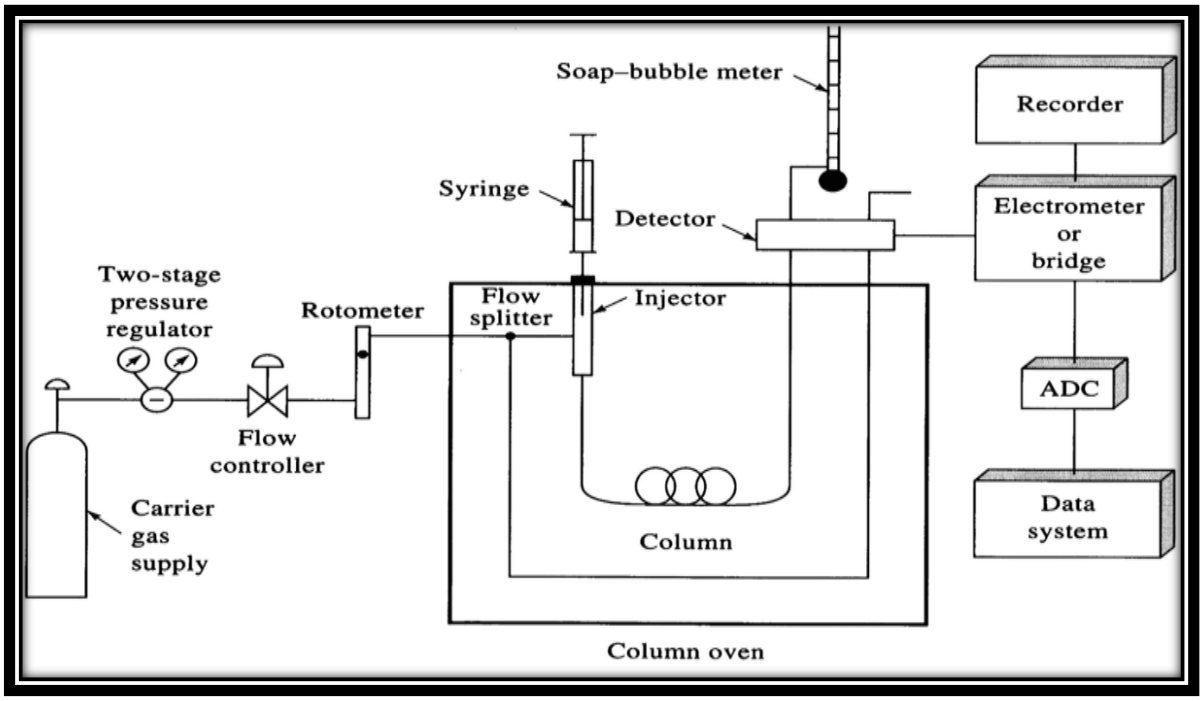

Figure (1.9)Gas chromatography

(1.4.8)- Dye- ligand chromatography [40,41] .

Development of this technique was based on the demonstration of the ability of many enzymes to bind purine nucleotides for Cibacron Blue F3GA dye . The planar ring structure with negatively charged groups is analogous to the structure of NAD., the adsorbed proteins are separated from the column. Fig.10

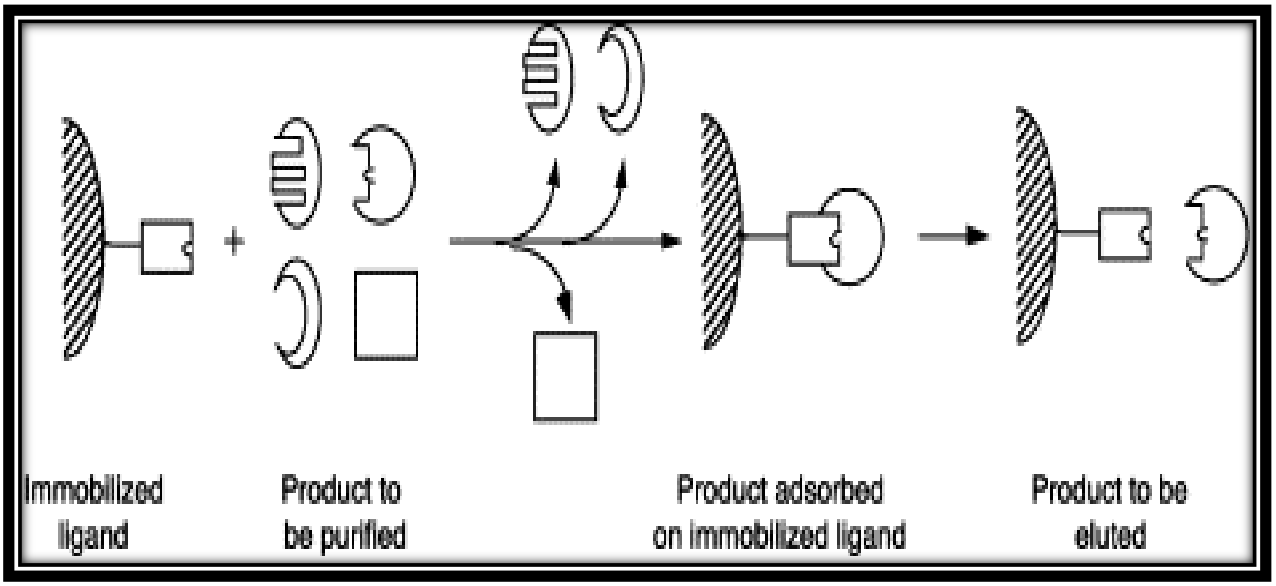

Figure (1.10)Dye- ligand chromatography

(1.4.9) - Hydrophobic interaction chromatography (HIC)

In this method the adsorbents prepared as column material for the ligand binding in affinity chromatography are used. HIC technique is based on hydrophobic interactions between side chains bound to chromatography matrix [42,43]. Fig(11)

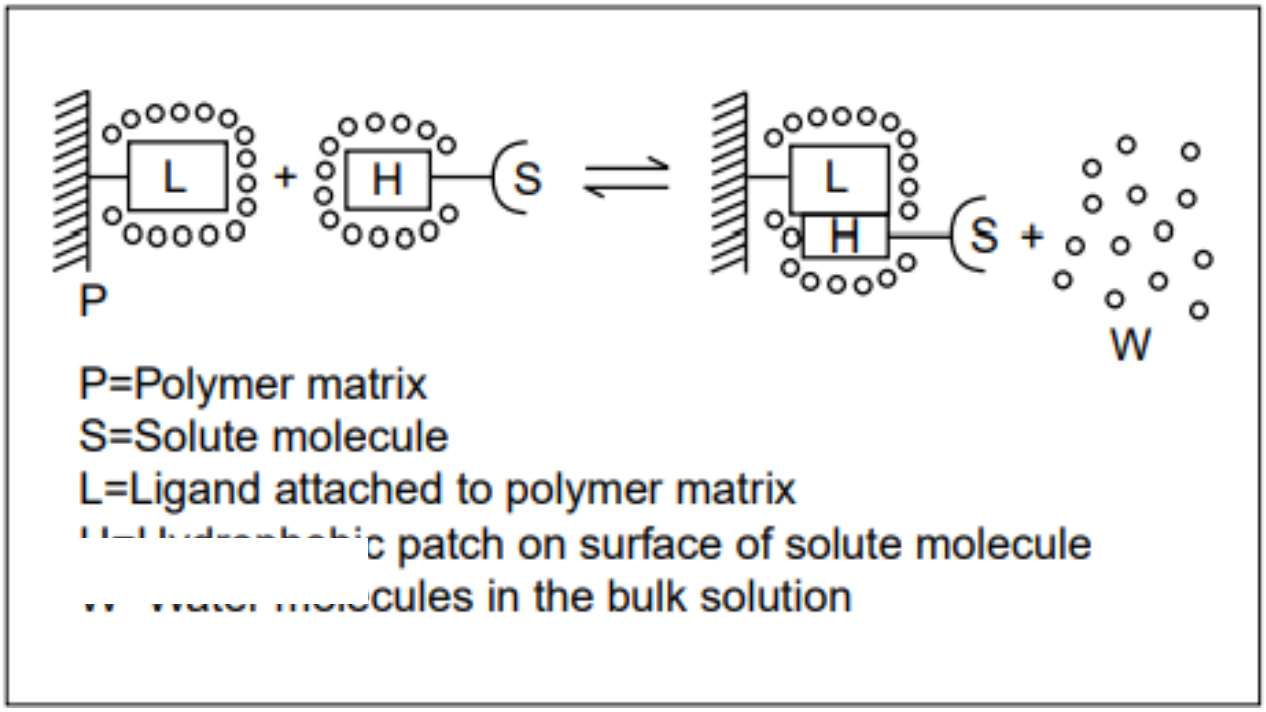

Figure (1.11) Hydrophobic interaction chromatography (HIC)

(1.4.10) -Pseudo affinity chromatography [44,45]

Some compounds as anthraquinone dyes, and azodyes can be used as ligands because of their affinity especially for dehydrogenases, kinases, transferases, and reductases The mostly known type of this kind of chromatography is immobilized metal affinity chromatography (IMAC) Fig12.

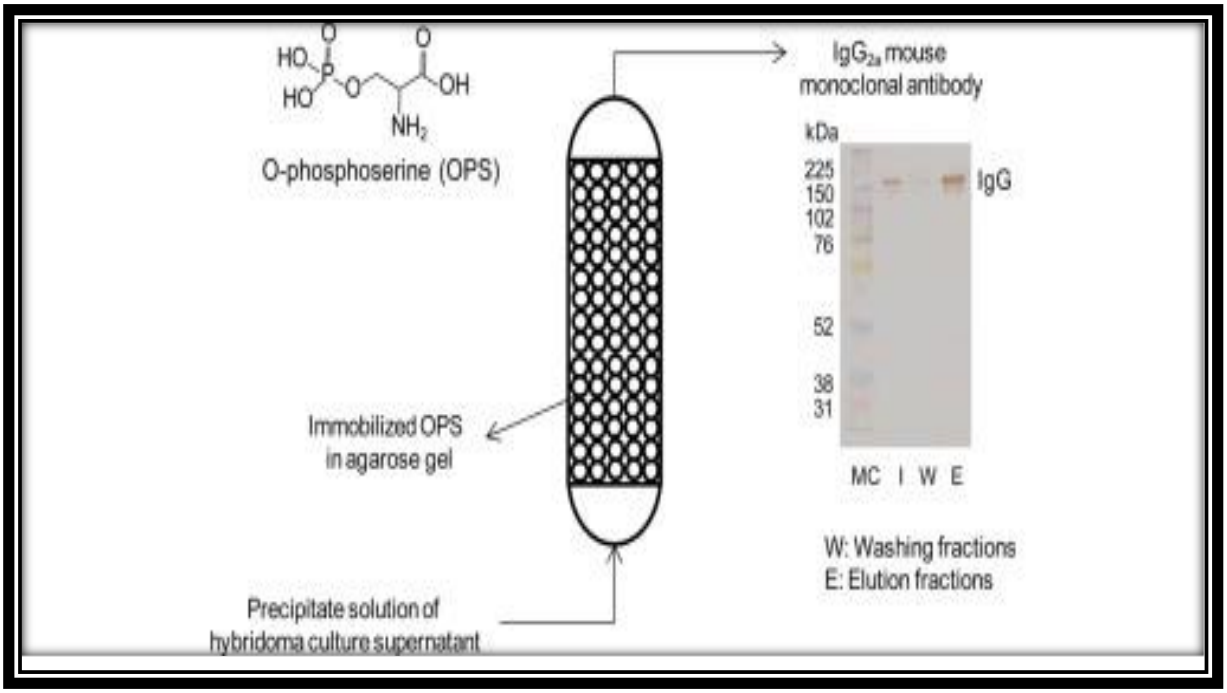

Figure (1.12) Pseudo affinity chromatography.

(1.4.11) - High-pressure liquid chromatography (HPLC) [46]

High-performance liquid chromatography "HPLC".Achromatographic technique in which the mobile phase is a liquid. In HPLC, a liquid sample, or a solid sample dissolved in a suitable solvent, is carried through a chromatographic column by a liquid mobile phase. Separation is determined by solute/stationary-phase interactions, including liquid–solid adsorption, liquid–liquid partitioning, ion exchange and size exclusion. A schematic diagram of a typical HPLC instrument is shown in Fig .13.

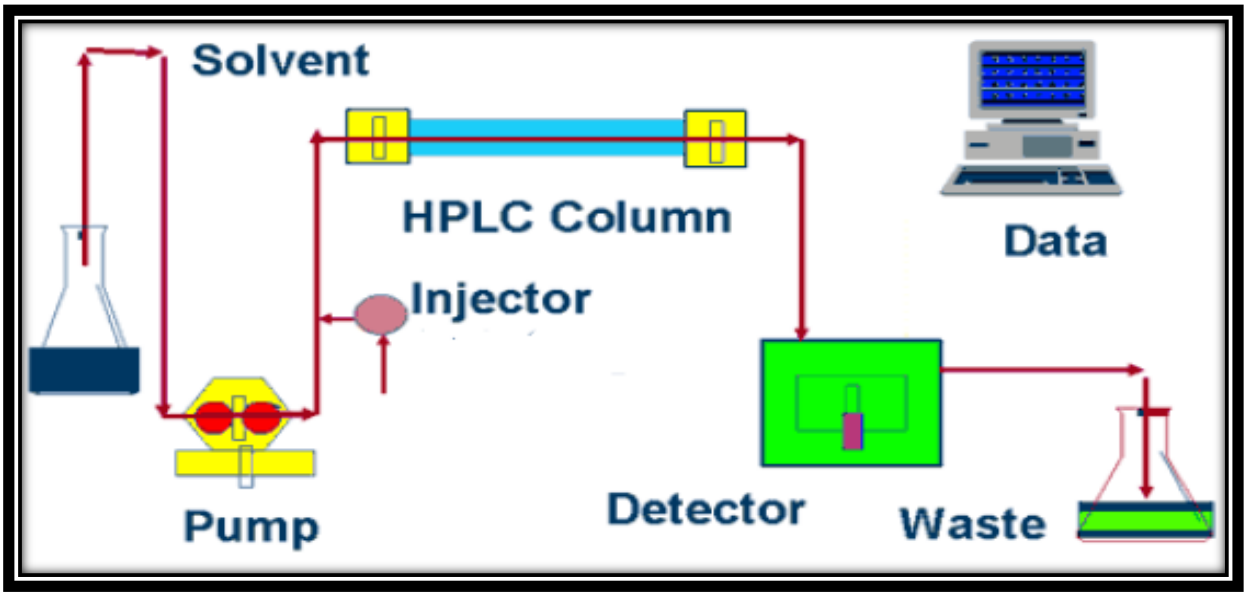

Figure (1.13) High-pressure liquid chromatography (HPLC)

(1.5) Chromatographic Resolution[47]

The main goal of chromatography is to segregate components of a sample into separate bands or peaks as they migrate through the column. A chromatographic peak is defined by several parameters including retention time peak width, and peak height . And resolution is defined as follows:

$$R_S = \frac{2\Delta t}{w_2 + w_1}$$

where:
RS = resolution
Δt = difference between retention times of peaks 1 and 2
w_2 = width of peak 2 at baseline
w_1 = width of peak 1 at baseline .(fig.14 a ,b).

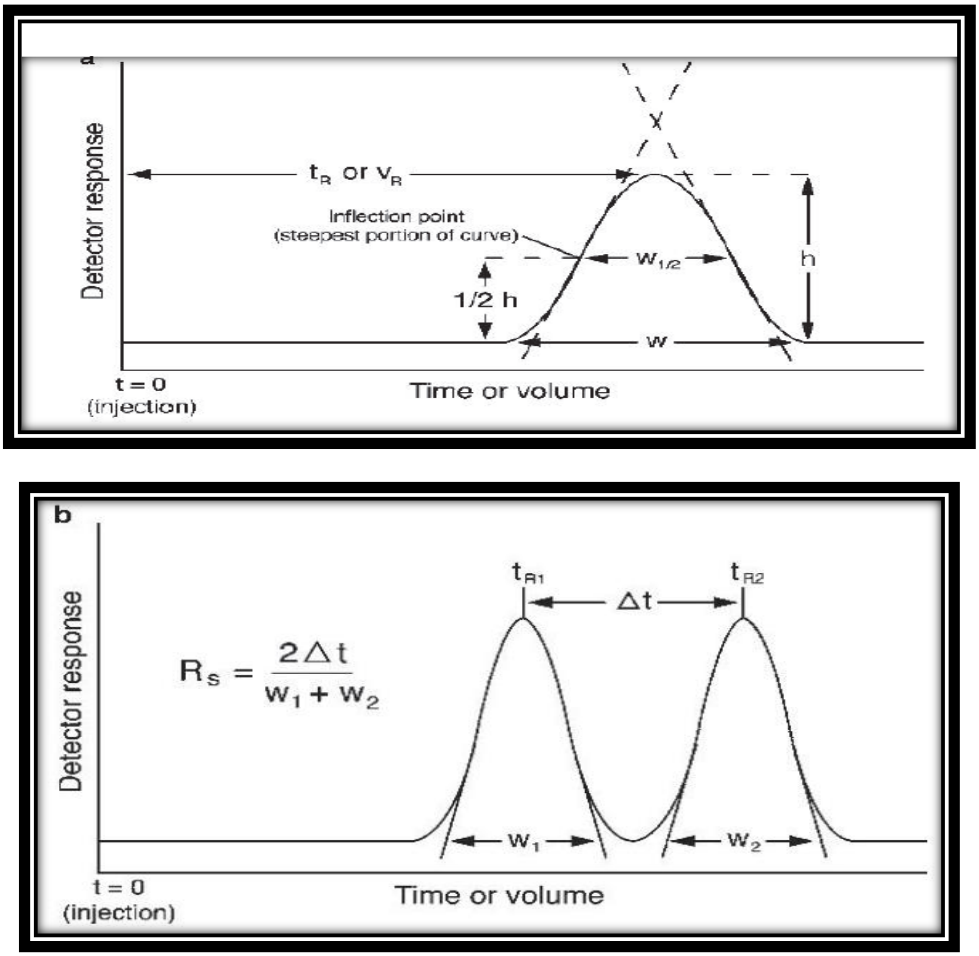

Figure (1.14) (a.one width ,b two width) for Chromatographic Resolution

(1.6) Flow Analysis

Flow analysis is the umbrella term for all analytical techniques that rely on the introduction of a sample into a flowing medium known as the carrier stream by aspiration or injection [48].

Two fundamental ideas can be used to classify flow analysis. The first is based on how samples are introduced, which can be continuous or discrete, and the second is based on the flowing medium, which can be segmented or unsegmented, as seen in[49,50] Fig. 15.

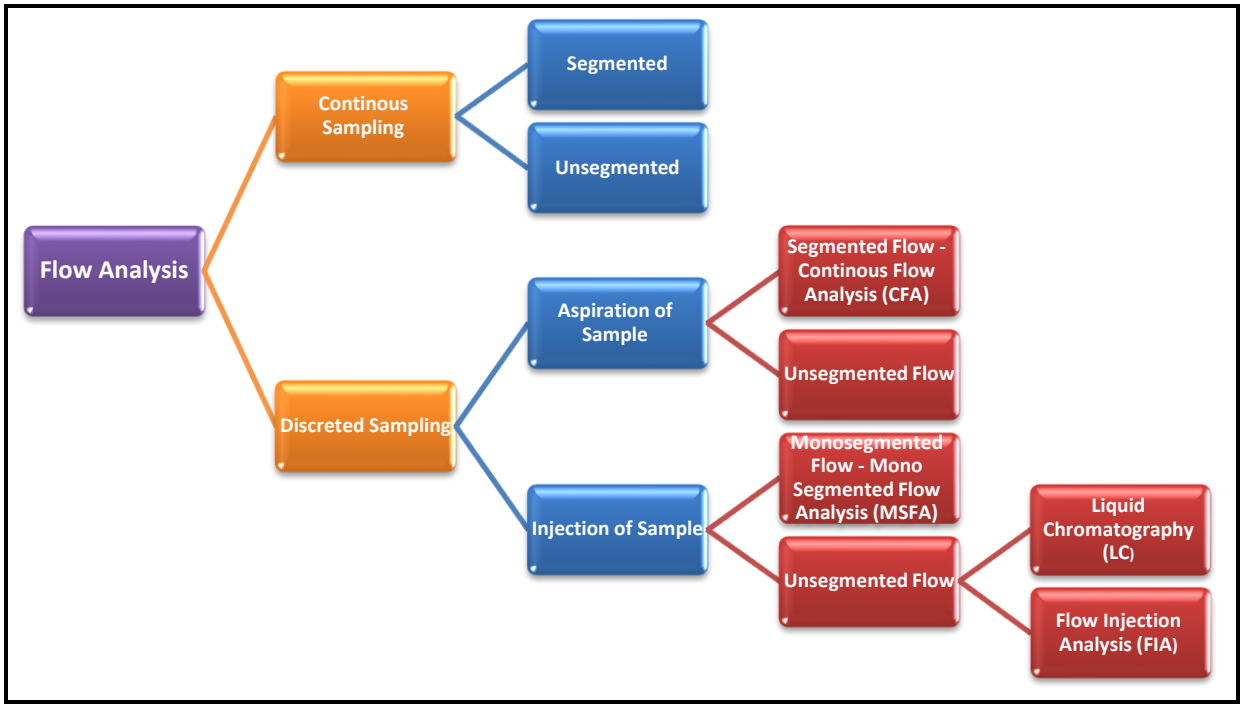

Figure (1.15) IUPAC classification of flow analysis methods

The reason for the appearance of the peak in the flow injection technique is due to the occurrence of two processes, one of which includes the formation of the dispersion phenomenon, which is a physical process, and the second includes a chemical process resulting from the interaction between the model and the detector after each of them is injected through the injection valve into an uninterrupted moving vector stream, and this causes a gradient In the

concentration and give the absorbance or the potential difference or any other physical factor that changes as a result of passing the model through it, and thus the resulting signal is recorded in a peak form for each injection process .The processes that occur within any flow injection system can be described [51,52] Fig. 16.

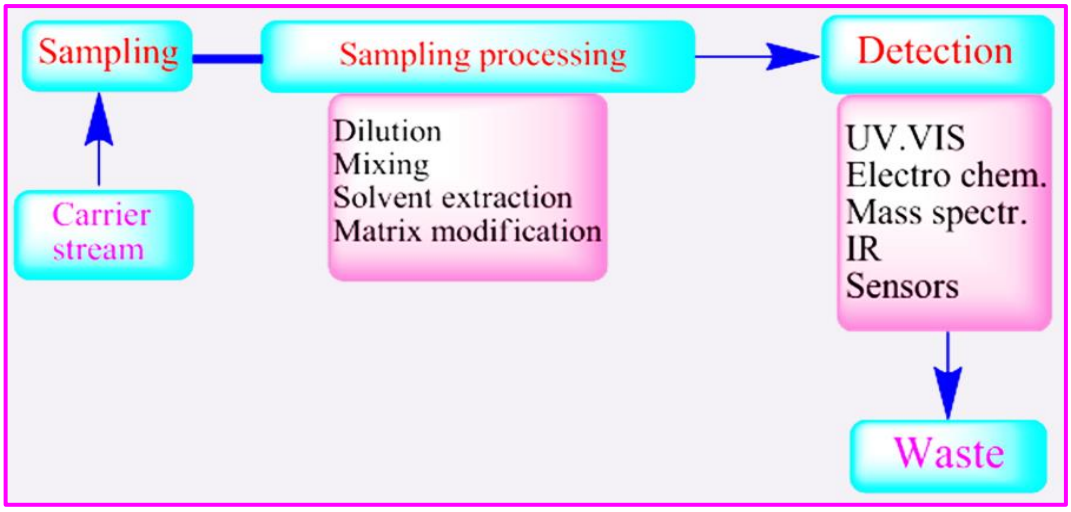

Figure (1.16) Description of the injection technique

(1.7) Flow-injection and HPLC[53,54]

Similarities between the flow injection technique and high-performance liquid chromatography, and among the similarities that were found is the ability to inject as the sample is entered by injection in both techniques, the possibility of using small volumes, the flow in the form of parts i.e. the nature of the mixture is laminar, and a comparison can be presented Simplified to show similarities between flow injection technology and high performance liquid chromatography Fig.17.

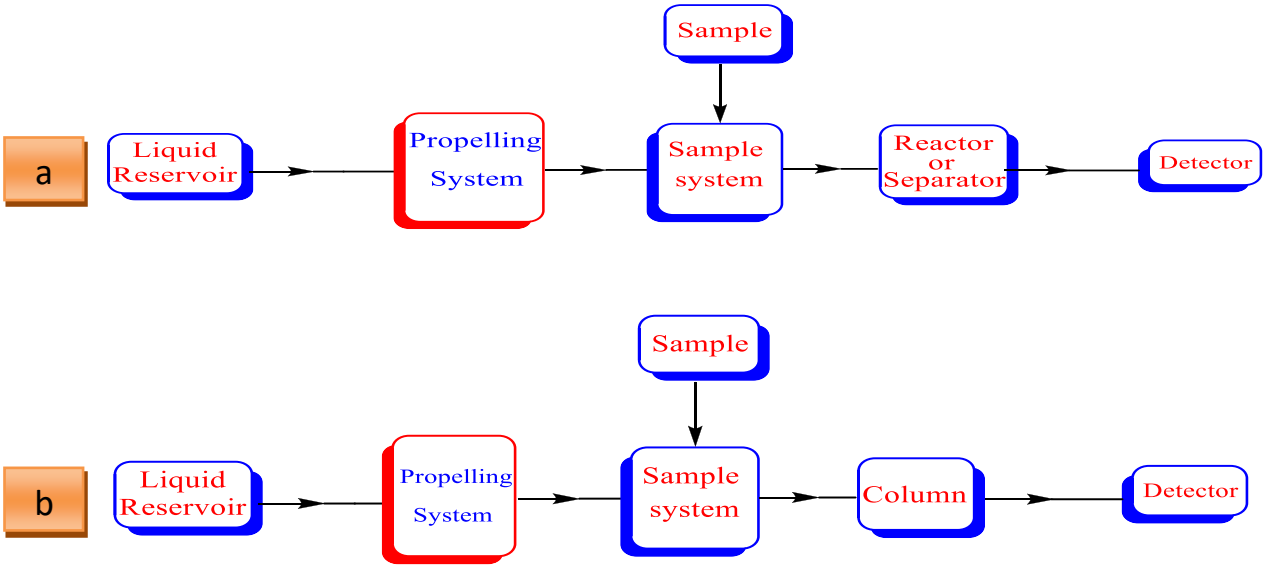

Figure (1.17) Similarities between a- FIA and b- HPLC

Despite the similarities between FIA and HPLC [55,56] , there are significant differences between the two techniques, as HPLC technology requires higher pressure than in flow injection, while FIA can work by about 1.5 atmospheres by using a simple peristaltic pump, also the liquid passes In HPLC technology, through a column tightly packed with materials, while in FIA, the liquid passes through the sample area from a narrow tube, in addition to the fact that HPLC is complex and designed to estimate several components in one sample, while FIA is characterized by its simplicity and estimation of one component in the sample, so that both (HPLC, FIA) are two different techniques due to the different principles of each[57] .

(1.8) HPLC-FIA COUPLING [58]

An HPLC-FTA coupled system consists of two injection valves, two pumps, a chromatographic column, a reactor, and a continuous detector, as well as reservoirs for the eluent(s), carrier(s), and reagent(s) (s). Depending on the position of the FIA subsystem's injection valve (as shown Fig. 18), there are two ways to implement this association: When the valve is located before the

carrier's confluence with the chromatographic effluent (A), and when the valve is located at the confluence point itself (B). To prevent the formation of air bubbles, restrictor coils are frequently used. There are only a few analytical methodologies that use these two modes.

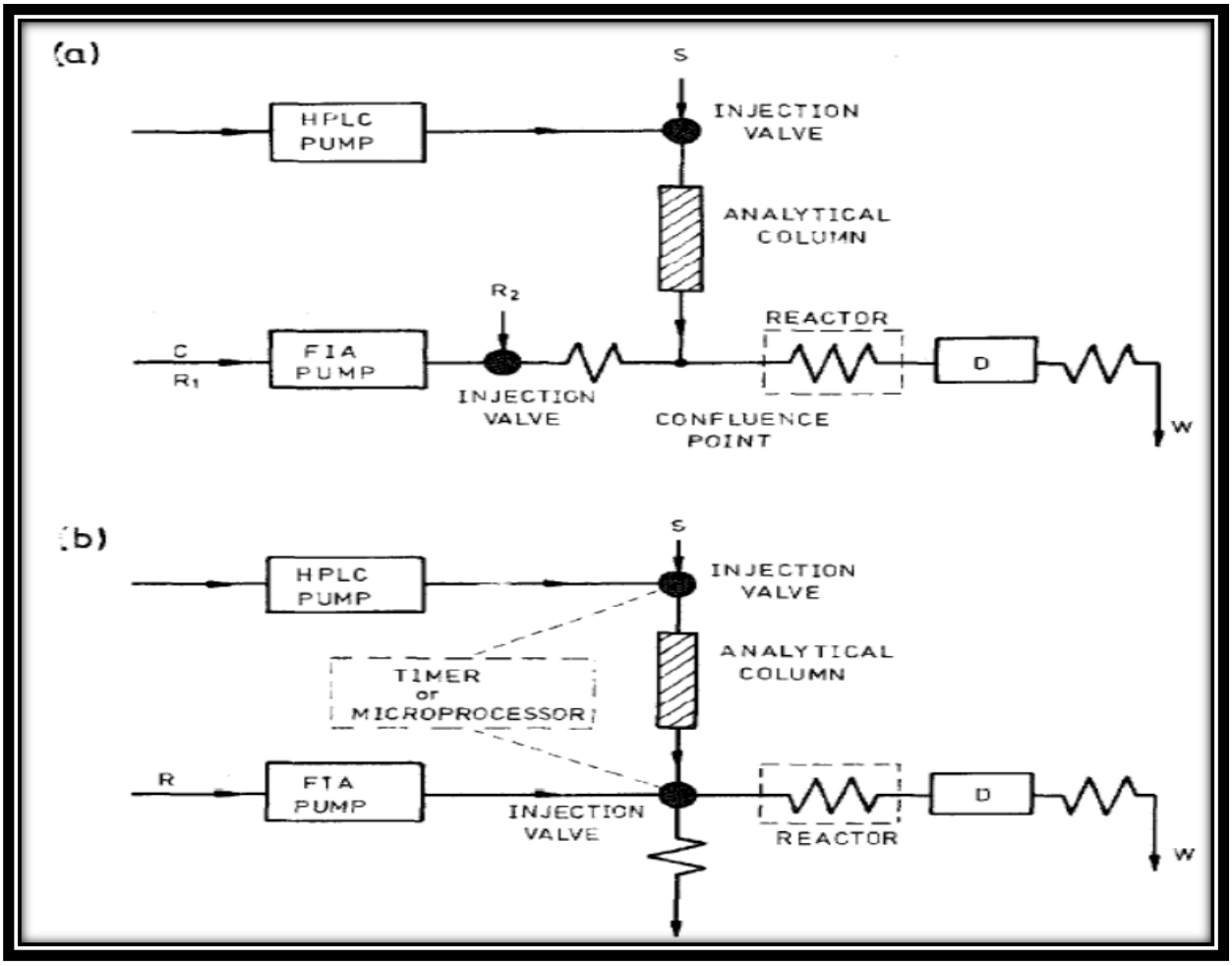

Figure (1.18) General arrangement of HPLC-FIA combination: (A) with FIA injection prior to the confluence with the chromatographic eluate; (B) with injection of the chromatographic eluate. C = carrier; R = reagent; S = sample; D = detector; W = waste.

As previously indicated, there are additional options for using two valves in an on-line HPLC-FIA coupled system[59]. The chromatographic effluent fills a sampling valve's loop, which injects samples of it into the reagent stream at regular intervals (Fig. 16B). In this case, automatic simultaneous operation of the two valves is required. This setup has been used to resolve mixtures of reducing sugars with photometric detectionllg and amino acids with amperometric detectioniz[60].

(1.9) Microfluidics

Microfluidics refers to technologies and methods for regulating and modifying fluid flows on a millimeter scale. Such fluid-related phenomena have long been studied as part of the fluid mechanical component of colloid science [61] and plant biology [62], and they depend on many fundamental features of viscous flow dynamics[63]. Ruzicka and Hansen described an unique microsystem technique for the first time in 1984. The microsystem consisted of integrated microconduits with microscopic potentiometric or optical detectors, as well as integrated gas diffusion or ion exchange units [59]. Another experiment involved using a tiny syringe instead of a peristaltic pump. Lab-on-Valve is a monolithic construction with a channel system, flow cell, and detector positioned over a multi-position valve. The channels diameters of the Lab-on-Valve system are measured in centimeters and fractions of millimeters([64],[65]) Fig.19.

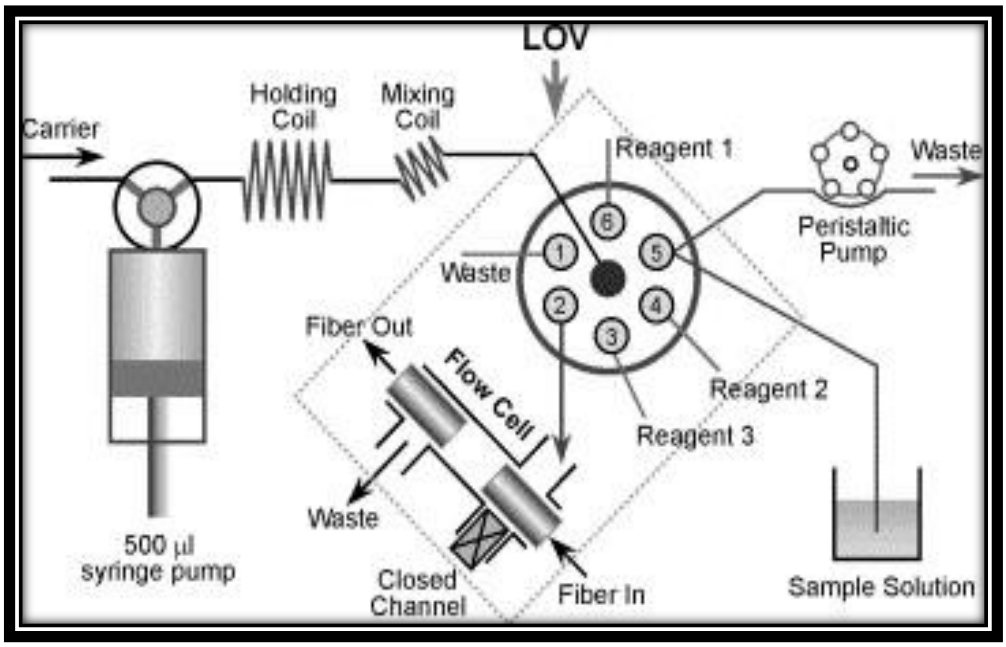

Figure (1.19) Lab-on-Valve system

Microfluidics was a word applied in the early 1990s to characterize microsystems. The sizes of channels in microfluidics were reduced to tens of micrometers, paving the door for the production of a complete Lab-on-a-chip or micro total analysis system (μTAS). As shown in Fig. (20 a,b) a microfluidic

system comprises of a thin piece of glass or polymeric plate with microchannels and diameters of a few centimeters [66-68]

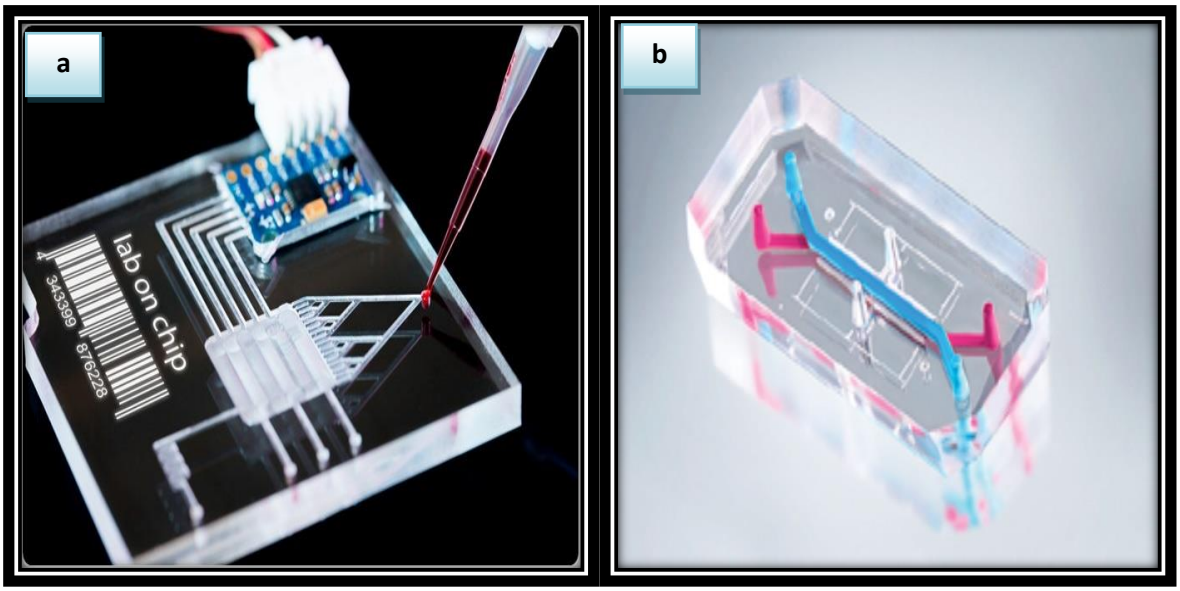

Figure (20 a, b): The micro channels of microfluidic systems

(1.10) Monolith

Separation science advances are largely driven by new developments in column technology[69]. Throughout the history of HPLC, columns packed with silica particulate materials have been the preferred packing material. In 1973, the first commercially available columns containing 10m silica C18 particles were introduced. Since then, the particle diameter has been systematically reduced in order to achieve faster separations while also increasing separation efficiency [69,70]. Because of the spherical packing, the external porosity of packed columns is fixed. As a result, column designs that allow for independent control of characteristic size (such as particle diameter) and porosity have the potential to produce intrinsically better chromatographic performance. As a result, polymer-monolith stationary phases have emerged as an appealing alternative for packed columns, with particular application in biomolecule analysis[71,72].

(1.10.1) Monolithic columns

In comparison to typical particle-packed columns, monolithic columns are comparatively easy to build, have good permeability, fast mass transfer, and high efficiency [73]. Organic-polymer-based monolithic columns and silica-based monolithic columns are the two basic forms of monolithic columns. Inorganic/organic monoliths are mixtures of these two categories. However, they are frequently referred to as hybrids, and the term hybrid is used in a variety of contexts, such as for columns made from a mixture of tetramethoxysilane and methyltrimethoxysilane[69].

Heat- or photo-initiated free radical polymerization of appropriate monomers and cross-linkers in the presence of porogens is a typical method for creating organic-polymer-based monoliths inside the column [74]. Using a range of functional monomers and cross linkers, organic monolithic columns can give exceptional pH stability and tremendous flexibility in tuning monolithic chemical characteristics [75].Changing the porogenic solvents, as well as the polymerization temperature and duration might also be done to vary their porosity and surface qualities. However, organic solvent swelling and a lack of mechanical stability in organic monoliths result in a reduction in lifetime and undesired low retention repeatability. [68].

Silica-based monoliths have a larger surface area, mechanical stability, solvent resistance, and separation efficiency than organic monoliths, but surface functionalization of silica-based monolithic columns is labor-intensive and time-consuming. Fig.21. Depicts the structures of packed columns and monolithic columns[76].

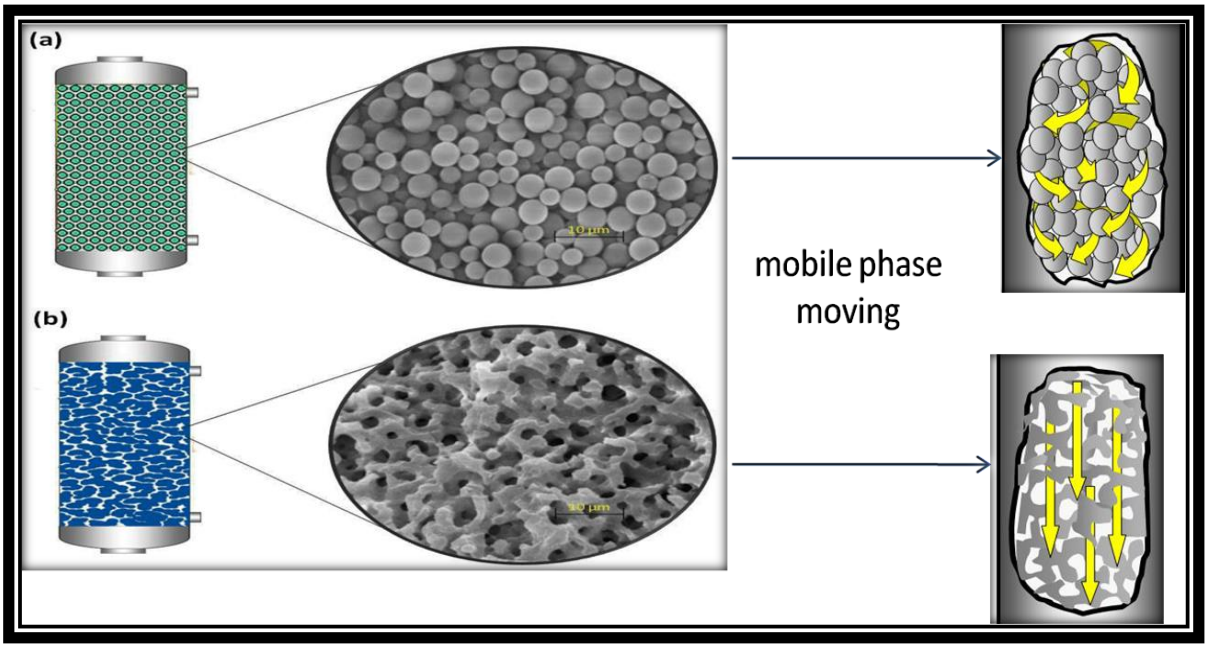

Figure (1.21)The difference in mobile phase movement in (a) packed column and (b) monolithic column

(1.10.2) Classification of monolithic columns

Monolithic chromatography columns have been made from **organic polymers** (polymethacrylate, polystyrenes, or polyacrylamides-based) and **inorganic polymers** (silica, zirconia, titania). Monolithic columns are classified as either inorganic-based (typically silica-based) or organic polymer-based monolithic columns[77].published a study of the chemistry and most recent applications of these diverse forms of monoliths as alternatives to typical packed columns in capillary electrochromatography (CEC) and micro-high performance liquid chromatography (μ-HPLC) [78] .

Carbon monoliths[72]have the potential to be suitable phases for chromatography, as well as catalyst supports [79], adsorbents [80], and porous electrodes under continuous flow circumstances, as an alternative to the three primary classes of monolithic columns [81].

(1.10.2.1) Organic monolithic phases

Kubin et al.[82] established a continuous polymer matrix for chromatographic separations in size-exclusion mode using a redox free-radical starting system in 1967, when organic monolithic phases were still in their early stages of development. Polymerisation of 100 mL of 22 % aqueous solution of 2-hydroxyethylmethacrylate with 0.2 % ethylene dimethylacrylate in a 25 mm i.d. glass tube for 24 hours at room temperature was used for the procedure.

Svec and Frechet employed macro-porous polymer monoliths, which are physically more stiff, as an effective stationary phase for HPLC in 1997, and they have been widely used for all types of chromatographic separations since then. These monolithic polymer materials were made utilizing a simple moulding technique involving the polymerisation of a mixture containing monomers, initiators, and porogenic solvents [83].

(1.10.2.2) Silica monolithic phases

In the late 1970s, Pretorious et al. [78] reported the first continuous porous silica-based foam as a chromatographic support for gas chromatography (GC), which was one of the first attempts to construct monolithic silica phases. Nakanishi and Soga [84] described a method for producing porous silica monoliths by hydrolysis and gelation of alkoxysilane solution containing poly(sodium styrenesulfonate) in 1991, and it was employed for HPLC applications.

Sol-gel processes can also be used to make inorganic silica-based monoliths [85]. This method of preparation, which takes place in a mould, does, however, result in a reduction (shrinkage) of the entire silica structure. The diameters of the products are approximately 4.6 and 7 mm, respectively, when a mould with a diameter of 6 and 9 mm is utilized. The resulting silica monoliths should be coated with polytetrafluoroethylene (PTFE) tubing or a PEEK resin to make a

column for HPLC. Because the column length is limited to 15 cm, single long and straight monoliths cannot be easily created using the sol-gel process.

Silica-based monolithic columns have also been created by loading fused silica capillaries with octadecylated 6 m particles and then thermally treating them. with dimethyloctadecylchlorosilane, the monolithic packing was reoctadecylated (C18 groups reattached to the monolith) in situ [86].

(1.10.2.3) Hybrid Organic – Inorganic Monolith

Hybrid organic–inorganic materials are referred to as materials consisting of two or more integrating components combined at the molecular or nanometer level[89]. They have several advantages, such as flexibility, long life, excellent biocompatibility, and mechanical properties organic functional groups can be distributed evenly in the structure of the inorganic matrix, which facilitates excellent performance hybrid materials can be used in many chemical areas because they are easy to process and are amenable to design on the molecular scale[40]. Owing to the individual advantages of monolith and organic–inorganic hybrids hybrid organic–inorganic monolith has attracted considerable concerns as a potential ideal material with high surface area high selectivity, excellent mechanical strength, and thermal stability. According to the chemical composition, hybrid organic– inorganic monolith can be divided into two main types: hybrid silica-based monolith (HSM) and hybrid polymer-based monolith (HPM). HSM is a monolith made of a silica precursor containing organic moieties, and it is commonly prepared by sol–gel process [89]. The sol–gel

technique is used primarily to fabricate materials starting from a colloidal solution that acts as a precursor for an integrated network polymer [90]. The mild reaction conditions and high adaptability of the sol–gel process are quite promising in the design of hybrid inorganic–organic matrices [90,91].Typical precursors include metal alkoxides and metal salts, which undergo a range of

hydrolysis and polycondensation reactions. In general, silicabased monolithic materials can have better organic solvent resistance and mechanical stability but they also have certain application restrictions, such as difficult to control the entire preparation process and a narrow pH working range (pH: 2–8) as show on Fig (22).

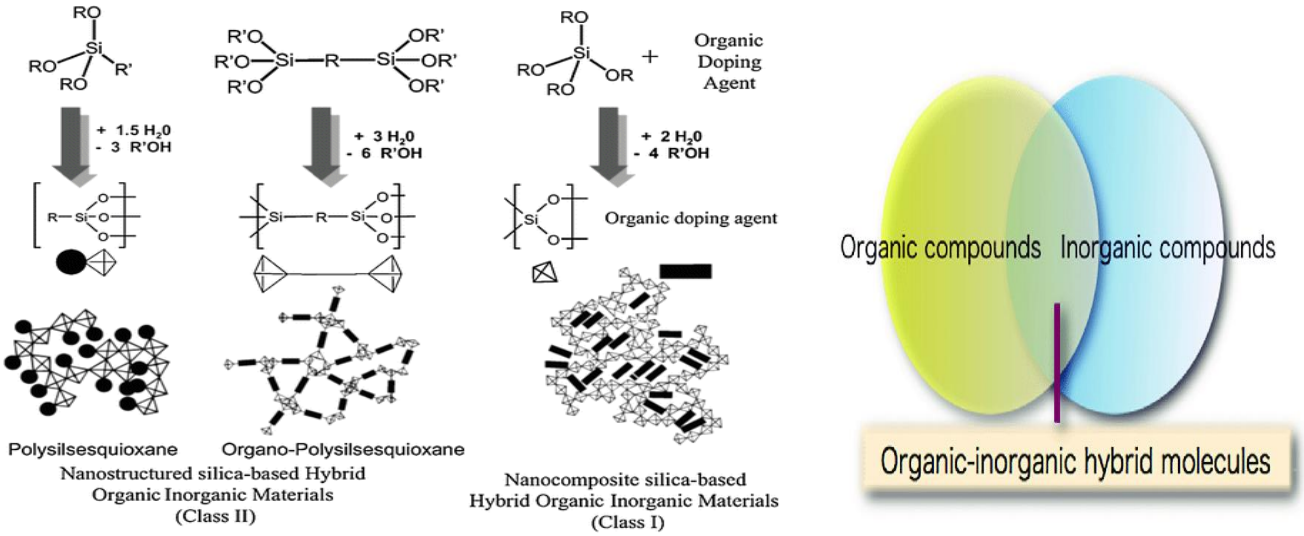

Figure (1.22)Different hybrid Organic – Inorganic Monolith

(1-11) Development of Monolithic Materials in Chromatography

Catalysis [92], filtration [93], electrochemistry [94], and separation sciences [95] are just a few of the applications for porous monolithic materials in science.

Since the 1970s, chromatographic monolithic materials have been created in a variety of shapes, including discs, stacked layers, rolled sheets, sponges, irregular pieces, tubes, and cylinders [0]. These unique monolithic structures were created using a variety of materials, including natural polymers (cellulose), synthetic polymers (porous styrene-, methacrylate-, and acrylamide-based polymers), and inorganic materials (silica).The applications and unique fluidic and surface features of this spectrum of monolithic materials have received a lot of attention. In liquid chromatography (LC), various substances are separated

using micro-particle packed columns (1 to 10 m), which have a wide surface area to interact with the solutes in the mobile phase. Despite the historical dominance of packed columns as chromatographic separation medium, a new spectrum of monolithic materials has recently been produced, enabling alternate chromatographic performance and selectivity[96,97].

(1.11.1) Monolithic stationary phases for chromatography[98,99]

Band broadening occurs in chromatography due to the following factors :

A- the presence of several flow channels of varying length and velocity.

B- Slow phase equilibration, especially in nm-sized pores.

C- Diffusion of a solute in the mobile phase.

Smaller particles (1-3 μm) in particle packed columns lower the contribution of components A and B to overall band broadening, resulting in faster equilibration and narrower bands, as well as increased efficiency (N). The main disadvantage of this method is a high pressure loss that is inversely proportional to the particle diameter squared. In compared to packed particle-based columns with a porosity of about 65 %, monolithic columns with a total porosity of about 80 %have substantially lower backpressures. Monolithic columns are thus thought to be compatible with high flow rates due to their increased porosity. The use of microparticle packed columns that generate such extreme backpressures necessitates specialized equipment (so-called ultra high performance liquid chromatography, or UHPLC) and, in some cases, extremely high temperatures[72].

(1.11.2) Monolithic columns have the following characteristics [100].

1. A continuous one-piece structure that does not require frits to maintain its structural integrity and provides great mechanical stability.

2.It has a high porosity, which means it has a high permeability .

3. The existence of large through-pores and a tiny skeleton allow for high flow rates, which can result in faster separation capabilities.

Monolithic materials have been used as high performance miniaturised columns for high performance liquid chromatography (HPLC) and phases within microfluidic chips because they possess the above characteristics [101]. They can thus be applied to high N and high speed separations, often beyond the limit of particle packed columns, and have been used as high performance miniaturised columns for high performance liquid chromatography (HPLC) and phases within microfluidic chips for example, created a new thin monolithic disk technology based on a polymer monolith as a new stationary phase in the shape of a flat "membrane" appropriate for protein separation. The innovative concept of short monolithic stiff disks has been used both conceptually [102] and practically[103].

(1.12) Chromatographic separation using glycidyl methacrylate copolymers as a mixed-mode monolith column.

Glycidyl methacrylate or (2,3-Epoxypropyl methacrylate) is an enoate ester obtained by formal condensation of the carboxy group of methacrylic acid with the hydroxy group of glycidol. It is an enoate ester and an epoxide. It derives from a methacrylic acid and a glycid [104,105] as showing in Fig (23).

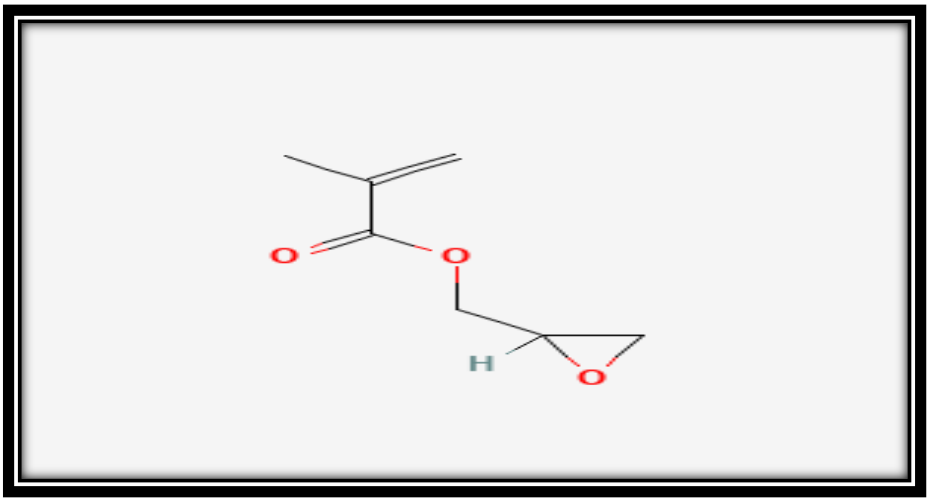

Figure (1.23) Glycidyl methacrylate(GMA)

The polymerization process of glycidyl methacrylate to form different polymer; therefor, PGMA is a one-of-a-kind structure that can be purified and stored in its homopolymer structure with a lot of control over the production procedure[(106)]. To further expand the spectrum of structures and applications of the final materials, co-polymerization with any other acrylate or methacrylate monomer is feasible. 1–16 To obtain functionalised polymers, the epoxy side chains of PGMA can be treated to a nucleophilic ring-opening process under a variety of circumstances Fig (24). Because of the large range of chemistry accessible, the nature of the functional group and the manner of the ring-opening reaction can be arbitrarily chosen. PGMA's flexibility distinguishes it as a versatile and effective reactive scaffold in polymer chemistry[(107)].

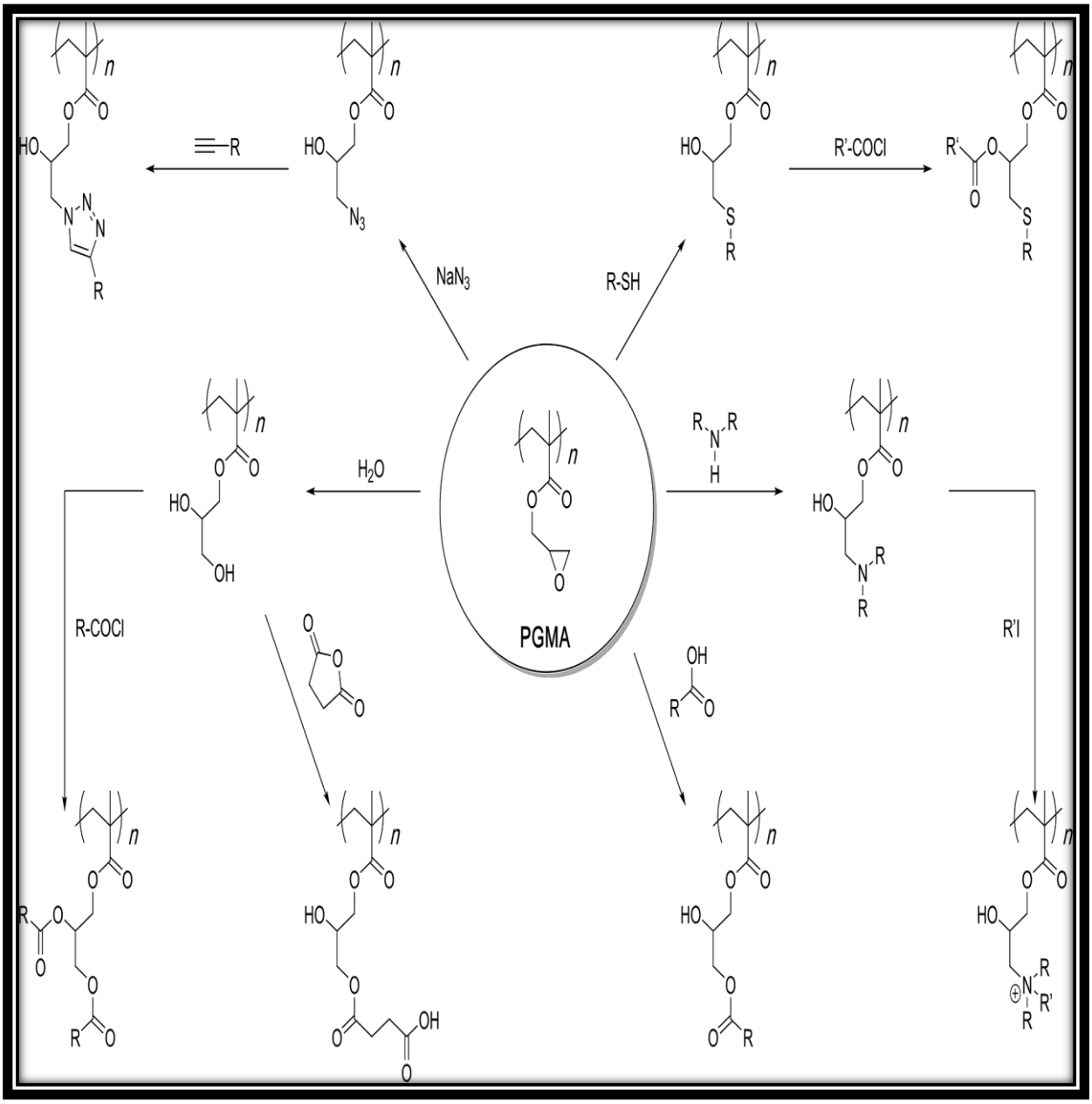

Figure (1.24) Scheme Polyglycidyl methacrylate post-polymerization modification processes.

(1.13) Different methods for various samples determination by Chromatography technique.

Many of the Chromatography analytical methods are used for the determination different samples. The tables (1.2) and (1.3) tabulate the Chromatography techniques and other methods respectively .

Table (1.2) Some of Chromatography techniques for the determination of different samples.

Seq.	Method	analytes	λ_{max} (nm)	Linear range	Detection limit	Application	Ref.
1	Online Column Switching Liquid Chromatography	clenbuterol (CLEN) and doxazosin (DOX)	250	75.0 ng/mL–200.0 µg/mL for CLEN and 37.5 ng/mL–100.0 µg/mL for DOX	8.47 and 25.66 ng/mL for CLEN and DOX	Pharmaceutical products	**108**
2	RP-HPLC and HPTLC	Ciprofloxacin Hydrochloride, Of loxacin, Tinidazole and Ornidazole	272.2, 292, 316.8, and 317.4 nm respectively.	y = 12.835x – 18.032, y = 33.788x – 47.343, y = 14.233x + 32.164, and y = 15.602x + 35.822, respectively	0.22 µg.mL-1, 0.40 µg.mL-1, 0.19 µg.mL-1, 0.37 µg.mL-1, respectively	Pharmaceutical products	**109**
3	RP-HPLC and HPTLC	Carve dilol	245	µg 200-10 mL^{-1} and 2.0-37.4 µg/spot	29 µg $mL^{-1}$and 0.05 µg/spot respectively .	Pharmaceutical products	**110**

4	(HPLC)	Amlodipine (AML)	465	2-30µg /mL	0.01µg/mL	Pharmaceutical products	**111**
5	RP-HPLC	Naproxen	254	0.5 to 80 ppm	10 ng/mL	Pharmaceutical products	**112**
6	capillary gas chromatography	Epichlorohydrin (ECH)	-------	0.6 to 3.4 µg/mL	0.15 µg/mL	Pharmaceutical products	**113**
7	RP-HPLC	Sertaconazole nitrate(SER)	260	10 to 500 µg/ml	0.1 µg/ml	Pharmaceutical products	**114**
8	Gas Chromatography	polycyclic aromatic hydrocarbons (PAHs)	----------	0.64×10^{-7} to 3.16×10^{-7}	(1×10^{-6})	Pharmaceutical products	**115**
9	RP-HPLC	Polythiazide	265	12.5–500 ng/m of prazosin and 6.25–250 ng/ml of polythiazide	0.0125 µg/ml of prazosin and 0.01875 µg/ml of polythiazide	Pharmaceutical products	**116**

Table (1.3): The other methods for determination the plant, biological and environmental samples by Chromatography technique.

Seq.	Method	Analytes	Part of Plant	Type of Elution/Mobile Phase	Conditions	Detector	Ref.
1	HPLC monolithic columns	quercetin, naringenin, ,naringin myricetin, rutin, kaempferol	tomatoes	/isocratic elution A: 50 mM phosphate buffer pH = 2.2)/ACN) ((75:25, v/v B: 2 mM formic acid/ACN (75:25, v/v)	1.0 mL/min/ 25 ◦C/one column	A: UV B: MS	117
2	TLC, HPLC, UPLC-ESI-QTOF-MS and LC-SPE-NMR	fingerprinting	aerial parts from Ipomoea aquatica	/gradient elution MeOH/H2O containing 0.05% TFA	1.0 mL/min/ 25 ◦C/two columns	UV	118
3	Ultrafast UPLC-ESI-MS and HPLC with monolithic column	vanillin, vanillic ,acid p-hydroxybenzoic ,acid p-hydroxybenzaldehyde	pods from Vanilla planifolia	isocratic elution/ACN/0.05 % TFA in H2O (12:88, v/v)	4.0 mL/min/ 35 ◦C/one column	PDA	119
4	LC columns.	glycyrrhizic and glycyrrhetinic acids	roots from Glycyrrhiza glabra	gradient elution/H2O/ACN both acidified with 0.05% TFA	2.5 mL/min/room temp./one column	PDA	120
5	(LC–MS)	proanthocyanidins	pea from Pisum sativu ,m lentil from Lens culinaris,faba bean from Vicia faba	/gradient elution H2O/ACN both with 1% acetic acid (v/v)	3.0 mL/min/ 30 ◦C/two columns	DAD	121
6	(HPLC-CE)	niaziridin and niazirin	leaves, pods, and bark from Moringa oleifera	isocratic elution MeOH/sodium dihydrogen phosphate–acetic acid buer (0.1 M, pH = 3.8) (20:80, v/v)	0.7 mL/min/ 25 C/one column	PDA	122
7	HPLC	geraniin, ellagic acid, gallic acid	rind from	isocratic elution/ACN/H2	0.5 mL/min/r	UV–Vis	123

			Nephelium lappaceum	O (30:70, v/v)	oom temp./one column		
8	(HPLC-UV)	,rutin isorhamnetine-,3-O-rutinoside isorhamnetine-,3-O-glukoside ,quercetin isorhamnetin	berries from Hippophaë rhamnoides	gradient elution/H2O/ACN (both acidified with 1% acetic acid)	3.0 mL/min/ 40 Cº/one column ppm	UV	[124]
9	(HPLC-CL)	α -solanine and -chaconine	potato tubers	isocratic elution/20 mM phosphate bu er (pH = 7.8)/ACN (65:35, v/v)	0.6 mL/mino ne column	CL	[125]
10	centrifugal partition chromatography (CPC)	lysergol and chanoclavine	seeds from Ipomea murica ta	isocratic elution ACN/0.01 M sodium dihydrogen phosphate bu er (with 0.2% (TFA (pH = 2.5) (15:85, v/v)	1.0 mL/min/ 25 Cº/one column	PDA	[126]
11	HPLC stationary phases of monolithic	vitamins K3, D3, E, and A	capsule s and pediatr ic drops	isocratic elution /ACN/MeOH both with 0.1% (v /v) formic acid (pH = 2.6, 25: 75, v /v)	4.0 mL /min /room tem /one *colu*	DAD	[127]
12	LC-ESI-MS/MS	aspirin and dipyridamole	human plasma	isocratic elution/MeOH/0. 1% formic acid in H2O (90:10, v/v)	1.0 mL/mino ne column	MS/MS	[128]
13	LC-MS/MS	codeine	human plasma	isocratic elution ACN/10 mM acetic acid (pH = (3.5 (50:50, v/v)	1.0 mL/min/ 25 Cº/one column	MS/MS	[129]
14	SPE-HPLC	Chloramphenicol	human blood	/isocratic elution mM 100 phosphate bu er (pH = 2.5)/ACN (75:25, v/v)	1.5 mL/min/ 28 Cº/one column	UV–Vis	[130]
15	(HPLC -UV)	cefadroxil, cefaclor, ,cephalexin cefotaxime, cefazolin,	milk	gradient %0.1elution /formic acid MeOH/ACN (75:25 v/v)	1.5 mL/min/-/one column	PDA	[131]

		,cefuroxime cefoperazone and ceftiofur					
16	LC-MS/MS	dapsone and N-acetyl dapsone	human plasma	isocratic elution/ACN/2 mM ammonium acetate in H2O (90:10, v/v)	0.8 mL/minone column	MS/MS	[132]
17	(Ultra-HPLC)	retinol and -tocopherol	serum and human breast milk	100% MeOH	1.5 mL/min/ 50 C°/one column	FL	[133]
18	(UV-monolithic column) off-line	Ni^{+2} and Cu^{+2}	Water waste	isocratic t Elution (pH = 8 for Ni^{+2} & pH = 4 for Cu^{+2} (30:70, v/v) (GMA-co-ACA co-AAM)	30µl/min 25 C°/one column	UV and Atomic flam	research study
19	(FIA- HPLC monolithic column) On-line	Ni^{+2} and Cu^{+2}	Water waste	isocratic Elution (pH = 8 for N^{i+2} & pH = 4 for Cu^{+2} (30:70, v/v) (GMA-co-ACA co-AAM)	50µl/min 25 C°/one column	UV and Atomic flam	research study
20	(FIA- HPLC microchip) On-line	Ni^{+2} and Cu^{+2}	Water waste	isocratic Elution (pH = 8 for Ni^{+2} & pH = 4 for Cu^{+2} (30:70, v/v) (GMA-co-ACA co-AAM)	50µl/min 25 C°/one column	UV	research study

(1.14) Aim of Study

1. Investigation & Preparation of chromatographic monolith columns .
2. Investigate different monomers and cross linker to form suitable monolith.
3. Off-line & online method for incorporation ions with the monolith column.
4. Connecting chromatography to flow-injection and micro fluidic injection techniques.
5. U.V polymerization will be used to form desire polymer.
6. Implementing the plan on Al-Ma'amira heavy water treatment plant in Hilla.

Reference

1. Vera AR. María José Rosales López · Material Characterization Techniques and Applications.; 2022. doi:10.1007/978-981-16-9569-8

2. Hole, J. A., Tathawade, P., & Pawar, S. K. review of various techniques for separating free fatty acids from vegetable oil. doi:10.34218/ijaret.11.11.2020.

3. Lesellier E, West C. The many faces of packed column supercritical fluid chromatography - A critical review. J Chromatogr A. 2015;1382(2015):2-46. doi:10.1016/j.chroma.2014.12.083

4. Hameed BS, Bhatt CS, Nagaraj B, Suresh AK. Chromatography as an Efficient Technique for the Separation of Diversified Nanoparticles. Elsevier Inc.; 2018. doi:10.1016/B978-0-12-812792-6.00019-4

5. Nielsen SS. Basic principles of gas chromatography. J Chromatogr Libr. 1977;10(C):1-31. doi:10.1016/S0301-4770(08)60223-7

6. Coskun O. Separation Tecniques: CHROMATOGRAPHY. North Clin Istanbul. 2016;3(2):156-160. doi:10.14744/nci.2016.32757

7. Bydlinski N. www.proteomics-journal.com Page 1 Proteomics. Proteomics. Published online 2013:1-25. doi:10.1002/jssc.201200569

8. Hage DS. Chromatography.; 2018. doi:10.1016/B978-0-12-816063-3.00001-3

9. Lenehan CE. Chromatography: Basic Principles.; 2013. doi:10.1016/B978-0-12-382165-2.00244-0

10. Chankvetadze B. Application of enantioselective separation techniques to bioanalysis of chiral drugs and their metabolites. TrAC - Trends Anal Chem. 2021;143:116332. doi:10.1016/j.trac.2021.116332

11. František àvec, Tatiana B. Tennikova and Zdeněk Deyl (Eds.) - Monolithic Materials_ Preparation, Properties and Applications-Elsevier Science (2003).

12. WallsLoughran, Sinéad T D. Purification of proteins fused to glutathione S-tranferase. Methods Mol Biol. 2011;681(3):151-175. doi:10.1007/978-1-60761-913-0

13. Michalski R. Ion chromatography applications in wastewater analysis. Separations. 2018;5(1). doi:10.3390/separations5010016

14. Galizia M, Manning GS, Paul DR, Freeman BD. Ion partitioning between brines and ion exchange polymers. Polymer (Guildf). 2019;165(December 2018):91-100. doi:10.1016/j.polymer.2019.01.026

15. Ebere Ec OW. Applications of Column, Paper, Thin Layer and Ion Exchange Chromatography in Purifying Samples: Mini Review open access Background: Historical Perspective. SF J Pharm Anal Chem. 2019;2(November). https://scienceforecastoa.com/

16. Aminian A, ZareNezhad B. Wettability alteration in carbonate and sandstone rocks due to low salinity surfactant flooding. J Mol Liq. 2019;275:265-280. doi:10.1016/j.molliq.2018.11.080

17. Ponton LM, Keller DW, Siperko LM, Hayes MA, Porter MD. Investigation of Adsorption Thermodynamics at Electrified Liquid-Solid Interfaces by Electrochemically Modulated Liquid Chromatography. J Phys Chem C. 2019;123(46):28148-28157. doi:10.1021/acs.jpcc.9b07717

18. Schnepper MT, Roles J, Hickman JJ, Hickman JJ. Characterization of Drug-Polymer Adsorption Isotherms in Body-on-a-Chip Systems by Inverse Liquid-Solid Chromatography. ACS Biomater Sci Eng. 2020;6(8):4462-4475. doi:10.1021/acsbiomaterials.0c00350

19. Apolinar-Valiente R, Williams P, Nigen M, Tamayo VM, Doco T, Sanchez C. Fractionation of Acacia seyal gum by ion exchange chromatography. Food Hydrocoll. 2020;98(May 2019):105283. doi:10.1016/j.foodhyd.2019.105283

20. Dasgupta PK, Maleki F. Ion exchange membranes in ion chromatography and related applications. Talanta. 2019;204:89-137. doi:10.1016/j.talanta.2019.05.077

21. Jatoi AS, Baloch HA, Mazari SA, . A review on extractive fermentation via ion exchange adsorption resins opportunities, challenges, and future prospects. Biomass Convers Biorefinery. Published online 2021. doi:10.1007/s13399-021-01417-w

22. Rigi G, Ghaedmohammadi S, Ahmadian G. A comprehensive review on staphylococcal protein A (SpA): Its production and applications.

Biotechnol Appl Biochem. 2019;66(3):454-464. doi:10.1002/bab.1742

23. Inamuddin, Rangreez TA, Asiri AM. Applications of Ion Exchange Materials in Chemical and Food Industries.; 2019. doi:10.1007/978-3-030-06085-5

24. Exchange I, Chromatography, Methods P and. Ion Exchange Chromatography. Anal Chem. 1964;36(5):51-55. doi:10.1021/ac60211a004

25. Gellerstedt G. 8.1 Gel Permeation Chromatography. Published online 1992.

26. Ma J, Sun G, Sun D, Yu F, Hu M, Lu T. Application of gel permeation chromatography technology in asphalt materials: A review. Constr Build Mater. 2021;278:122386. doi:10.1016/j.conbuildmat.2021.122386

27. Heitz W. Gel Chromatography. Vol 9.; 1970. doi:10.1002/anie.197006891

28. Striegel, A. M., Yau, W. W., Kirkland, J. J., & Bly, D. D. Modern Size-Exclusion Liquid Chromatography. John Wiley & Sons, Inc. second edition.2009 .

29. Kasai K. Frontal affinity chromatography: An excellent method of analyzing weak biomolecular interactions based on a unique principle. Biochim Biophys Acta - Gen Subj. 2021;1865(1):129761. doi:10.1016/j.bbagen.2020.129761

30. Chu Y, Tang W, Zhang Z. Deciphering Protein Corona by scFv-Based Affinity Chromatography. Nano Lett. 2021;21(5):2124-2131. doi:10.1021/acs.nanolett.0c04806

31. Kraska T. Digitalization and computational thinking in lower secondary science education using the example of paper chromatography. Chemkon. 2021;28(7):299-304. doi:10.1002/ckon.202100002

32. Dalvi SB, John A, Martin P. chromatography in dyestuff. 2021;(June).

33. Wenkert, Ernest, et al. "General methods of synthesis of indole alkaloids. VII. Syntheses of dl-dihydrogambirtannine and aspidosperma-strychnos alkaloid models." Journal of the American Chemical Society 90.19 (1968): 5251-5256.

34. Morlock GE. High-performance thin-layer chromatography combined with effect-directed assays and high-resolution mass spectrometry as an emerging hyphenated technology: A tutorial review, Anal Chim Acta. 2021, doi:10.1016/j.aca.2021.338644

35. Höpner S, Bertling M. Holes in Bones: Ichnotaxonomy of Bone Borings. Ichnosan Int J Plant Anim. 2017;24(4):259-282. doi:10.1080/10420940.2017.1289937

36. Reich, Eike, and Anne Schibli. High-performance thin-layer chromatography for the analysis of medicinal plants. Thieme, 2007.

37. Jurado-Campos N, Martín-Gómez A, Saavedra D, Arce L. Usage considerations for headspace-gas chromatography-ion mobility spectrometry as a suitable technique for qualitative analysis in a routine lab. J Chromatogr A. 2021;1640:461937. doi:10.1016/j.chroma.2021.461937

38. Micalizzi, G., Vento, F., Alibrando, F., Donnarumma, D., Dugo, P., & Mondello, L. (2021). Cannabis Sativa L.: A comprehensive review on the analytical methodologies for cannabinoids and terpenes characterization. Journal of Chromatography A, 1637, 461864.

39. Lipták BG. Instrumentation and Automation Engineers' Handbook: Volume II - Analysis and Analyzers.; 2018.

40. Poddar S, Sharmeen S, Hage DS. Affinity monolith chromatography: A review of general principles and recent developments. Electrophoresis. 2021;42(24):2577-2598. doi:10.1002/elps.202100163

41. Heftmann E.fundamentals and applicationsof chromatography and related differential migration methods . 6th edition , Journal of chromatography library — volume 69B; 2004.

42. Kårsnäs P. Chromatography, Hydrophobic Interaction. Encycl Ind Biotechnol. Published online 2010. doi:10.1002/9780470054581.eib219

43. Huang S, Ji X, Jackson KK, . Rapid separation of blood plasma exosomes from low-density lipoproteins via a hydrophobic interactionchromatography method on a polyester capillary-channeled

polymer fiber phase. Anal Chim Acta. 2021;1167:338578. doi:10.1016/j.aca.2021.338578

44. Opitz L. D Evelopment and Characterization of Affinity and Pseudo - Affinity Based Methods for Cell Culture - Derived Influenza Virus Capturing.; 2010.

45. Opitz L. Pseudo-allergic compounds screened from Shengmai injection by using high-expression Mas-related G protein-coupled receptor X2 cell membrane chromatography online coupled with liquid chromatography and mass spectrometry. J Sep Sci. 2021;44(7):1421-1429. doi:10.1002/jssc.202001163

46. Igarashi, Y., Hanafusa, T., Gohda, F., Peterson, S., & Bills, G. (2014). Species-level assessment of secondary metabolite diversity among Hamigera species and a taxonomic note on the genus. Mycology, 5(3), 102-109.

47. Cook, D. W. (2016). Chemometric Curve Resolution for Quantitative Liquid Chromatographic Analysis.

48. Van der Linden, Willem E. "Classification and definition of analytical methods based on flowing media (IUPAC Recommendations 1994)." Pure and applied chemistry 66.12 (1994): 2493-2500.

49. R Roda, A., Greco, P., Simoni, P., Marassi, V., Moroni, G., Gioiello, A., & Roda, B. (2021). Compact Miniaturized Bioluminescence Sensor Based on Continuous Air-Segmented Flow for Real-Time Monitoring: Application to Bile Salt Hydrolase (BSH) Activity and ATP Detection in Biological Fluids. Chemosensors, 9(6), 122. doi:10.3390/chemosensors9060122

50. Venkatasubramanian M, Tomsovic K. Power System Analysis.; 2005. doi:10.1016/B978-012170960-0/50056-6

51. Kikas T. Introduction to Flow Injection Analysis (FIA) Determination of Chloride Ion Concentration. J Ruzicka, E H Hansen Flow Inject Anal 2nd Ed, 1988,FIAlab Oper Manual,Skoog, Holler, Nieman Princ Instrum Anal 5th Ed Saunders Coll Publ Fort Worth, TX 1997, Ch 10. Published online 2014. ww2.chemistry.gatech.edu/class/analyt/fia.pdf

52. Taha, D. N., & Ali, K. J. Determination of Vanadium (V) by Flow injection and sequential injection analysis .Journal of Babylon University/Pure and Applied Sciences/ No.(1)/ Vol.(22): 2012 College of Science/Babylon University Scientific Conference .

53. Aljamali, N. M., Ali, K. J., Salih, N. S., & Ridha, S. H. (2014). Synthesis, Characterization and Study of Chromatography Behavior of Novel (Azo–Anil)-Heterocyclic Compounds. Asian J. Research Chem, 7(8), 702-710.

54. Fry B, Carter JF, Yamada K, Yoshida N, Juchelka D. Position-specific 13C/12C analysis of amino acid carboxyl groups – automated flow-injection analysis based on reaction with ninhydrin. Rapid Commun Mass Spectrom. 2018;32(12):992-1000. doi:10.1002/rcm.8126

55. Hang CZ, Ing XD, Ang XW, Hen LC, Jin QI. Comparative Study of Puerariae lobatae and Puerariae thomsonii by Coupled with HPLC-Electrospray Ionization-MS. Society. 2011;59(May):541-545.

56. Lu Y, Gao B, Chen P, Charles D, Yu L. Characterisation of organic and conventional sweet basil leaves using chromatographic and flow-injection mass spectrometric (FIMS) fingerprints combined with principal component analysis. Food Chem. 2014;154:262-268. doi:10.1016/j.foodchem.2014.01.009

57. Saraji M, Bidgoli AAH, Farajmand B. Hollow fiber-based liquid-liquid-liquid microextraction followed by flow injection analysis using column-less HPLC for the determination of phenazopyridine in plasma and urine. J Sep Sci. 2011;34(14):1708-1715. doi:10.1002/jssc.201000929

58. Valcarcel M, Dolores Luque De Castro M. Continuous separation techniques in flow injection analysis. A review. J Chromatogr A. 1987;393(1):3-23. doi:10.1016/S0021-9673(01)94200-1

59. Leo M.L. Nollet &Claudia Ruiz-Capillas and. Flow Injection Analysis of Food Additives. (Nollet CR-C and LML, ed.).

60. Flieger J, Flieger W, Baj J. Antioxidants : Classification , Natural Sources , Activity / Capacity. Published online 2021.

61. Herzog N, Johnstone A, Bellamy T, Russell N. Characterization of neuronal viability and network activity under microfluidic flow. J Neurosci Methods. 2021;358(November 2020):109200.

doi:10.1016/j.jneumeth.2021.109200

62. Rizkin BA, Popovich K, Hartman RL. Artificial Neural Network control of thermoelectrically-cooled microfluidics using computer vision based on IR thermography. Comput Chem Eng. 2019;121:584-593. doi:10.1016/j.compchemeng.2018.11.016

63. Zhou, L., Alcalde, R. E., Deng, J., Zuniga, B., Sanford, R. A., Fouke, B. W., & Werth, C. J. (2021). Impact of antibiotic concentration gradients on nitrate reduction and antibiotic resistance in a microfluidic gradient chamber. Science of The Total Environment, 779, 146503.doi:10.1016/j.scitotenv.2021.146503

64. Teng J, Rallabandi B, Stone HA, Ault JT. Coupling of translation and rotation in the motion of finite-length rods near solid boundaries. J Fluid Mech. 2022;938:1-28. doi:10.1017/jfm.2022.177

65. Nie FQ, Macka M, Paull B. Micro-flow injection analysis system: On-chip sample preconcentration, injection and delivery using coupled monolithic electroosmotic pumps. Lab Chip. 2007;7(11):1597-1599. doi:10.1039/b707773b

66. Cui P, Wang S. Application of microfluidic chip technology in pharmaceutical analysis: A review. J Pharm Anal. 2019;9(4):238-247. doi:10.1016/j.jpha.2018.12.001

67. Tiboni M, Tiboni M, Pierro A, et al. Microfluidics for nanomedicines manufacturing: An affordable and low-cost 3D printing approach. Int J Pharm. 2021;599(December 2020):120464. doi:10.1016/j.ijpharm.2021.120464

68. Chih-Ming Ho, Henry. Micro/Nano Technology Systems for Biomedical Applications Microfluidics, Optics, and Surface Chemistry. Published online 2010.

69. Eltmimi A. Preparation , Characterisation and Modification of Porous Carbon Monolithic Materials for Chromatographic and Electrochemical Applications. 2009;(August).

70. Maruyama J, Abe I. Influence of anodic oxidation of glassy carbon surface on voltammetric behavior of Nafion®-coated glassy carbon electrodes. Electrochim Acta. 2001;46(22):3381-3386. doi:10.1016/S0013-

4686(01)00539-4

71. S Smetop, T. Silica-based monolithic pre-columns in miniaturized liquid chromatography (Master's thesis). Published online (2016)

72. Rahmah, A., Mairizki, F., Putri, R., Zein, R., Munaf, E., Takeuchi, T., & Lim, L. W. (2014). Preparation and Characterization of Long Alkyl Chain Methacrylate-Based Monolithic Column for Capillary Chromatography in Separation of Alkylbenzene Compound. Asian Journal of Chemistry, 26(12), 3595.

73. Alkarimi AA, Welham K. Proteins pre-concentration using glycidyl methacrylate-co-stearyl methacrylate-co-ethylene glycol dimethacrylate monolith. Indones J Chem. 2020;20(5):1143-1151. doi:10.22146/ijc.49479

74. Jasinski, F., Zetterlund, P. B., Braun, A. M., & Chemtob, A. Photopolymerization in dispersed systems. Progress in Polymer Science, 84, 47-88. Id : hal-02377093. Published online 2019.

75. Ou J, Liu Z, Wang H, Lin H, Dong J, Zou H. Recent development of hybrid organic-silica monolithic columns in CEC and capillary LC. Electrophoresis. 2015;36(1):62-75. doi:10.1002/elps.201400316

76. Lin, Z., Tan, X., Yu, R., Lin, J., Yin, X., Zhang, L., & Yang, H. One-pot preparation of glutathione–silica hybrid monolith for mixed-mode capillary liquid chromatography based on “thiol-ene” click chemistry. Journal of Chromatography A, 1355, 228-237. doi:10.1016/j.chroma.2014.06.023

77. Legido-Quigley C, Marlin ND, Melin V, Manz A, Smith NW. Advances in capillary electrochromatography and micro-high performance liquid chromatography. Electrophoresis. 2003;24(6):917-944. http://www.ncbi.nlm.nih.gov/pubmed/12658680

78. Pretorius V, Davidtz JC, Desty DH. Open-pore silica foams: A new support for chromatography. J High Resolut Chromatogr. 1979;2(9):583-584. doi:10.1002/jhrc.1240020912

79. García-Bordejé E, Kapteijn F, Moulijn JA. Preparation and characterisation of carbon-coated monoliths for catalyst supports. Carbon N Y. 2002;40(7):1079-1088. doi:10.1016/S0008-6223(01)00252-4

80. Liang C, Dai S, Guiochon G. A graphitized-carbon monolithic column. Anal Chem. 2003;75(18):4904-4912. doi:10.1021/ac030146r

81. Jordá-Beneyto M, Lozano-Castelló D, Suárez-García F, Cazorla-Amorós D, Linares-Solano Á. Advanced activated carbon monoliths and activated carbons for hydrogen storage. Microporous Mesoporous Mater. 2008;112(1-3):235-242. doi:10.1016/j.micromeso.2007.09.034

82. Kubín M, Špaček P, Chromeček R. Gel permeation chromatography on porous poly(ethylene glycol methacrylate). Collect Czechoslov Chem Commun. 1967;32(11):3881-3887. doi:10.1135/cccc19673881

83. Svec F, Fréchet JMJ. Continuous Rods of Macroporous Polymer as High-Performance Liquid Chromatography Separation Media. Anal Chem. 1992;64(7):820-822. doi:10.1021/ac00031a022

84. Hou J, Sapnik AF, Bennett TD. Metal-organic framework gels and monoliths. Chem Sci. 2020;11(2):310-323. doi:10.1039/c9sc04961d

85. Almeida, R. M., & Gonçalves, M. C. Sol–gel process and products. Encyclopedia of Glass Science, Technology, History, and Culture, 2021;II:969-979.

86. Liu X, Yang C, Qian HL, Yan XP. Three-Dimensional Nanoporous Covalent Organic Framework-Incorporated Monolithic Columns for High-Performance Liquid Chromatography. ACS Appl Nano Mater. 2021;4(5):5437-5443. doi:10.1021/acsanm.1c00770

87. Rachman T. Initiator-Free Radical Reactions: Strategies Toward Development and Application in Chemical Biology, Materials Chemistry, and Synthetic Chemistry. Angew Chemie Int Ed 6(11), 951–952. Published online 2018:10-27.

88. Laaniste A, Marechal A, El-Debs R, Randon J, Dugas V, Demesmay C. “Thiol-ene” photoclick chemistry as a rapid and localizable functionalization pathway for silica capillary monolithic columns. J Chromatogr A. 2014;1355:296-300. doi:10.1016/j.chroma.2014.06.031

89. Zhu T, Row KH. Preparation and applications of hybrid organic-inorganic monoliths: A review. J Sep Sci. 2012;35(10-11):1294-1302. doi:10.1002/jssc.201200084

90. Senja MF, Akhmad S, Nur HA. Monolithic columns for the separation and analysis of proteins- A review. Res J Chem Environ. 2019;23(2):114-117.

91. Lynch KB, Ren J, Beckner MA, He C, Liu S. Monolith columns for liquid chromatographic separations of intact proteins: A review of recent advances and applications. Anal Chim Acta. 2019;1046:48-68. doi:10.1016/j.aca.2018.09.021

92. Sebai I, Boulahaouache A, Trari M, Salhi N. Preparation and characterization of 5%Ni/Γ-Al2o3 catalysts by complexation with NH3 derivatives active in methane steam reforming. Int J Hydrogen Energy. 2019;44(20):9949-9958. doi:10.1016/j.ijhydene.2018.12.050

93. Hamidipour M, Larachi F. Dynamics of filtration in monolith reactors using electrical capacitance tomography. Chem Eng Sci. 2010;65(1):504-510. doi:10.1016/j.ces.2009.06.040

94. Zhao Y, Zheng M bo, Cao J ming, et al. Easy synthesis of ordered meso/macroporous carbon monolith for use as electrode in electrochemical capacitors. Mater Lett. 2008;62(3):548-551. doi:10.1016/j.matlet.2007.06.002

95. Randon J, Huguet S, Piram A, Puy G, Demesmay C, Rocca JL. Synthesis of zirconia monoliths for chromatographic separations. J Chromatogr A. 2006;1109(1):19-25. doi:10.1016/j.chroma.2005.12.044

96. Saito Y. F. ?vec, T.B. Tennikova, Z. Deyl (eds): Monolithic materials: preparation, properties and applications. Anal Bioanal Chem. 2004;379(1):8-9. doi:10.1007/s00216-004-2566-5

97. Echevarría RN, Keunchkarian S, Villarroel-Rocha J, Sapag K, Reta M. Organic monolithic capillary columns coated with cellulose tris(3,5-dimethylphenyl carbamate) for enantioseparations by capillary HPLC. Microchem J. 2019;149:104011. doi:10.1016/j.microc.2019.104011

98. Medina G. Desarrollo de métodos de extracción empleando líquidos iónicos y polímeros monolíticos para la determinación de contaminantes ambientales en agua de río. J Soc Am. 2019;27(1):263-263.

99. Marković K, Milačič R, Vidmar J. Monolithic chromatography on conjoint liquid chromatography columns for speciation of platinum-based chemotherapeutics in serum of cancer patients. J Trace Elem Med Biol.

2020;57(April 2019):28-39. doi:10.1016/j.jtemb.2019.09.011

100. Noel Echevarria R, Carrasco-Correa EJ, Keunchkarian S, Reta M, Herrero-Martinez JM. Photografted methacrylate-based monolithic columns coated with cellulose tris(3,5-dimethylphenylcarbamate) for chiral separation inCEC.J.Sep.Sci.2018;41(6):1424-1432. doi:10.1002/jssc.201701234

101. Zajickova Z, Nováková L, Svec F. Monolithic Poly(styrene- co-divinylbenzene) Columns for Supercritical Fluid Chromatography-Mass Spectrometry Analysis of Polypeptide. Anal Chem. 2020;92(17):11525-11529. doi:10.1021/acs.analchem.0c02874

102. Dubinina NI, Kurenbin OI, Tennikova TB. Peculiarities of gradient ion-exchange high-performance liquid chromatography of proteins. J Chromatogr A. 1996;753(2):217-225. doi:10.1016/S0021-9673(96)00545-6

103. Tennikova TB, Bleha M, Švec F, Almazova T V., Belenkii BG. High-performance membrane chromatography of proteins, a novel method of protein separation. J Chromatogr A. 1991;555(1-2):97-107. doi:10.1016/S0021-9673(01)87170-3

104. Safa KD, Nasirtabrizi MH. Ring opening reactions of glycidyl methacrylate copolymers to introduce bulky organosilicon side chain substituents. 2006;304:293-304. doi:10.1007/s00289-006-0564-9

105. Reddy BSR, Balasubramanian S. Novel activated acrylates: Synthesis, characterization and the reactivity ratios of 4-acetamidophenyl acrylate copolymers with methyl methacrylate and glycidyl methacrylate. Eur Polym J. 2002;38(4):803-813. doi:10.1016/S0014-3057(01)00242-7

106. Trovato V, Vitale A, Bongiovanni R, Ferri A, Rosace G, Plutino MR. Development of a Nitrazine Yellow-glycidyl methacrylate coating onto cotton fabric through thermal-induced radical polymerization reactions: a simple approach towards wearable pH sensors applications. Cellulose. 2021;28(6):3847-3868. doi:10.1007/s10570-021-03733-w

107. Pączkowski P, Gawdzik B. Studies on preparation, characterization and application of porous functionalized glycidyl methacrylate-based microspheres. Materials (Basel). 2021;14(6). doi:10.3390/ma14061438

108. Caglar Andac S. Determination of Drugs by Online Column-Switching

Liquid Chromatography. J Chromatogr Sci. 2016;54(9):1641-1647. doi:10.1093/chromsci/bmw120

109. Kawas G, Marouf M, Mansour O, Sakur AA. Analytical methods of ciprofloxacin and its combinations review. Res J Pharm Technol. 2018;11(5):2139-2148. doi:10.5958/0974-360X.2018.00396.7

110. Abdel-gawad FM, Issa YM, Hussien EM, Ibrahim MM, Barakat S. Simple and Accurate Rp-Hplc and Tlc- Densitometric Methods for Determination of Carvedilol in Pharmaceutical Formulations. Int J Res Pharm Chem. 2012;2(3):741-748.

111. Elbashir AA, Mohammed Osman RA. A High-Performance Liquid Chromatographic (HPLC) Method for the Determination of Amlodipine Drug in Dosage form Using 1,2-Naphthoquine-4-Sulfonate (NQS). J Anal Pharm Res. 2017;6(1):2-9. doi:10.15406/japlr.2017.05.00163

112. Muneer S, Muhammad IN, Asad Abrar M, et al. High Performance Liquid Chromatographic Determination of Naproxen in Prepared Pharmaceutical Dosage Form and Human Plasma and its Application to Pharmacokinetic Study. J Chromatogr Sep Tech. 2017;08(03). doi:10.4172/2157-7064.1000369

113. Rambhade S, Chakraborty A, Patil U, Rambhade A. Journal of Chemical and Pharmaceutical Research preparations. J Chem Pharm Res. 2010;2(6):7-25.

114. Mathur M, Devi VK. Design of experiment utilization to develop and validate high performance liquid chromatography technique for estimation of pure drug and marketed formulations of atorvastatin in spiked rat plasma samples. Int J Pharm Sci Res. 2017;8(4):1708-1716. doi:10.13040/IJPSR.0975-8232.10(1).214-21

115. SA A, BE A, SO A, OM O. Quantification and Preliminary Estimation of Toxic Effects of Polycyclic Aromatic Hydrocarbon in Some Antimalarial Herbal Drugs in Southwest Nigeria. Bull Pharm Res. 2018;8(1). doi:10.21276/bpr.2018.8.1.1

116. G. Dharmamoorthy1 , K. S. Nataraj2 AKMP. New Validated Stability-Indicating Reverse-phase High-performance Liquid Chromatography Method for the Simultaneous Estimation of Prazosin and Polythiazide in their Formulations in Human Plasma. Int J Latest Res Sci Technol.

2018;14(2):252-264.

117. Biesaga M, Ochnik U, Pyrzynska K. Fast analysis of prominent flavonoids in tomato using a monolithic column and isocratic HPLC. J Sep Sci. 2009;32(15-16):2835-2840. doi:10.1002/jssc.200800730

118. Daria M, Olesia K, Dmitry B. This item is the archived peer-reviewed author-version of : Reference : 2016;14:7079-7089.

119. Sharma UK, Sharma N, Sinha AK, Kumar N, Gupta AP. Ultrafast UPLC-ESI-MS and HPLC with monolithic column for determination of principal flavor compounds in vanilla pods. J Sep Sci. 2009;32(20):3425-3431. doi:10.1002/jssc.200900353

120. Gupta S, Sharma R, Pandotra P, Jaglan S, Gupta AP. Chromolithic method development, validation and system suitability analysis of ultra-sound assisted extraction of glycyrrhizic acid and glycyrrhetinic acid from Glycyrrhiza glabra. Nat Prod Commun. 2012;7(8):991-994. doi:10.1177/1934578x1200700808

121. Jin A, Ozga JA, Lopes-Lutz D, Schieber A, Reinecke DM. Characterization of proanthocyanidins in pea (Pisum sativum L.), lentil (Lens culinaris L.), and faba bean (Vicia faba L.) seeds. Food Res Int. 2012;46(2):528-535. doi:10.1016/j.foodres.2011.11.018

122. Shanker K, Gupta MM, Srivastava SK, Bawankule DU, Pal A, Khanuja SPS. Determination of bioactive nitrile glycoside(s) in drumstick (Moringa oleifera) by reverse phase HPLC. Food Chem. 2007;105(1):376-382. doi:10.1016/j.foodchem.2006.12.034

123. Elendran S, Wang LW, Prankerd R, Palanisamy UD. The physicochemical properties of geraniin, a potential antihyperglycemic agent. Pharm Biol. 2015;53(12):1719-1726. doi:10.3109/13880209.2014.1003356

124. Michel T, Destandau E, Elfakir C. On-line hyphenation of centrifugal partition chromatography and high pressure liquid chromatography for the fractionation of flavonoids from hippophaë rhamnoides l. berries. J Chromatogr A. 2011;1218(36):6173-6178. doi:10.1016/j.chroma.2011.01.070

125. Kodamatani H, Saito K, Niina N, Yamazaki S, Tanaka Y. Simple and sensitive method for determination of glycoalkaloids in potato tubers by

high-performance liquid chromatography with chemiluminescence detection. J Chromatogr A. 2005;1100(1):26-31. doi:10.1016/j.chroma.2005.09.006

126. Maurya A, Srivastava SK. Large-scale separation of clavine alkaloids from Ipomoea muricata by pH-zone-refining centrifugal partition chromatography. J Chromatogr B Anal Technol Biomed Life Sci. 2009;877(18-19):1732-1736. doi:10.1016/j.jchromb.2009.04.036

127. Asmari, M., Wang, X., Casado, N., Piponski, M., Kovalenko, S., Logoyda, L.,& El Deeb, S. Chiral monolithic silica-based HPLC columns for enantiomeric separation and determination: functionalization of chiral selector and recognition of selector-selectand interaction. Molecules, 2021; 26(17), 5241. doi:10.3390/molecules26175241.

128. Staniak, M., Wójciak, M., Sowa, I., Tyszczuk-Rotko, K., Strzemski, M., Dresler, S., & Myśliński, W. Silica-based monolithic columns as a tool in HPLC—an overview of application in analysis of active compounds in biological samples. Molecules, 2020; 25(14), 3149.doi:10.3390/molecules25143149

129. Rp- CP. A.d.C. Cruz, E.M. Suenaga, E. Abib, J. Pedrazzoli, On-line Solid Phase Extraction Coupled With Liquid Chromatography Tandem Mass Spectrometry For The Determination Of Codeine In Human Plasma, Química Nova, 40.pdf. 2017;40(1):25-29.

130. Ali I, Gupta VK, Singh P, Singh R, Negi U. Analysis of Chloramphenicol in Biological Samples by SPE-HPLC. Anal Chem Lett. 2013;3(3):181-190. doi:10.1080/22297928.2013.806413

131. Karageorgou EG, Samanidou VF. Application of ultrasound-assisted matrix solid-phase dispersion extraction to the HPLC confirmatory determination of cephalosporin residues in milk. J Sep Sci. 2010;33(17-18):2862-2871. doi:10.1002/jssc.201000385

132. Bonde SL, Bhadane RP, Gaikwad A, Narendiran AS, Srinivas B. Simultaneous determination of dapsone and its major metabolite N-Acetyl Dapsone by LC-MS/MS method. Int J Pharm Pharm Sci. 2013;5(SUPPL 3):441-446.

133. Kučerová B, Krčmová L, Solichová D, Plíšek J, Solich P. Comparison of a new high-resolution monolithic column with core-shell and fully porous columns for the analysis of retinol and α-tocopherol in human serum and breast milk by ultra-high-performance liquid chromatography. J Sep Sci. 2013;36(14):2223-2230. doi:10.1002/jssc.201300242

134. Harris, Bryan. "Engineering composite materials. The Institute of Materials, London " (1999).

135. Axinte E. Glasses as engineering materials: A review. Materials & Design. 2011 Apr 1;32(4):1717-32.

136. Nischang, Ivo, Oliver Brueggemann, and Frantisek Svec. "Advances in the preparation of porous polymer monoliths in capillaries and microfluidic chips with focus on morphological aspects." Analytical and bioanalytical chemistry 397.3 (2010): 953-960.

137. Alkarim.A.A. An Investigation of Glycidyl Methacrylate Terpolymers for Mixed Mode LC Separations,2018. PhD Thesis (pp. 79).

138. do Nascimento, Walber Alexandre, Pankaj Agrawal, and Tomás Jeferson Alves de Mélo. "Effect of copolymers containing glycidyl methacrylate functional groups on the rheological, mechanical, and morphological properties of poly (ethylene terephthalate)." Polymer Engineering & Science 59.4 ,2019: 683-693.

139. Yu, C., Xu, M., Svec, F., & Fréchet, J. M. Preparation of monolithic polymers with controlled porous properties for microfluidic chip applications using photoinitiated free-radical polymerization. Journal of Polymer Science Part A: Polymer Chemistry, 40(6), 755-769., 2002.

140. Svec, Frantisek, and Jean MJ Frechet. "Molded rigid monolithic porous polymers: an inexpensive, efficient, and versatile alternative to beads for the design of materials for numerous applications." Industrial & engineering chemistry research 38.1 ,1999: 34-48.

141. V Viklund, C., Svec, F., Frechet, J. M., & Irgum, K. Monolithic,“molded”, porous materials with high flow characteristics for separations, catalysis, or solid-phase chemistry: control of porous properties during polymerization. Chemistry of materials. (1996), 8(3), 744-750.

142. Huo, Yuli, Peter J. Schoenmakers, and Wim Th Kok. "Efficiency of methacrylate monolithic columns in reversed-phase liquid chromatographic separations." Journal of Chromatography A 1175.1 ,2007: 81-88.

143. C. Barner-Kowollik, T. P. Davis and M. H. Stenzel, Polymer, 2004, 45, 7791-7805.

144. T. Rohr, E. F. Hilder, J. J. Donovan, F. Svec and J. M. Frechet, Macromolecules,2003, 36, 1677-1684.

145.Ouano, A. C., & Carothers, J. A,1980. Dissolution dynamics of some polymers: solvent-polymer boundaries. Polymer Engineering & Science, 20(2), 160-166.

146. Mohammed, Azad, and Avin Abdullah. "Scanning electron microscopy (SEM): A review." Proceedings of the 2018 International Conference on Hydraulics and Pneumatics—Hervex, Băile Govora, Romania. 2018.

147. Von Ardenne, Manfred. "4.4 reminiscences on the origins of the scanning electron microscope and the electron microprobe." Advances in Imaging and Electron Physics. Vol. 96. Elsevier, 1996. 635-652.

148. Egerton, R. F. Electron energy-loss spectroscopy in the electron microscope. Springer Science & Business Media, 2011.

149. Dunlap, Michael, and J. E. Adaskaveg. "Introduction to the scanning electron microscope." Theory, practice, & procedures. Facility for Advance Instrumentation. UC Davis 52 ,1997.

150. Prabu, G. T. V., Guruprasad, R., Sundaramoorthy, C., & Vigneshwaran, N. Process optimization and modelling the BET surface area of electrospun cellulose acetate nanofibres using response surface methodology. Bulletin of Materials Science, (2022) ,45(3), 1-7..

151. Maziarka, P., Wurzer, C., Arauzo, P. J., Dieguez-Alonso, A., Mašek, O., & Ronsse, F. Do you BET on routine? The reliability of N2 physisorption for the quantitative assessment of biochar's surface area. Chemical Engineering Journal, (2021),418, 129234.

152. ISO, I.Determination of the specific surface area of solids by gas adsorption–BET method. Geneva: International Organization for

Standardization, 9277, 2010.

153. Liu, Y., & Laskin, A. Hygroscopic properties of CH3SO3Na, CH3SO3NH4,(CH3SO3) 2Mg, and (CH3SO3) 2Ca particles studied by micro-FTIR spectroscopy. The Journal of Physical Chemistry A, (2009). 113(8), 1531-1538.

154. Ismail, M. A., Eltayeb, M. A. Z., & Maged, S. A. Elimination of heavy metals from aqueous solutions using zeolite LTA synthesized from Sudanese clay. Research journal of chemical sciences, (2013), 3(5), 93-98.

155. Paul, S., & Rånby, B. Methyl methacrylate (MMA)-glycidyl methacrylate (GMA) copolymers. A novel method to introduce sulfonic acid groups on the polymeric chains. Macromolecules, (1976), 9(2), 337-340.

156. Xiong, X., He, H., Shu, Y., Li, Y., Yang, Z., Chen, Y & Chen, B. The synthesis of surface-glycosylated porous monolithic column via aqueous two-phase graft copolymerization and its application in capillary-liquid chromatography. Talanta, 161, 721-729. 2016.09.034.doi:10.1016/j

157. Dwivedi SK, Razi SS, Misra A. Sensitive colorimetric detection of CN− and AcO− anions in a semi-aqueous environment through a coumarin-naphthalene conjugate azo dye. New J Chem. 2019;43(13):5126-5132. doi:10.1039/c9nj00004f.

159. Small EW, Peticolas WL. Conformational dependence of the Raman scattering intensities from polynucleotides. III. Order-disorder changes in helical structures. Biopolymers. 1971;10(8):1377-1418. doi:10.1002/bip.360100811.

160. Fan X, Zhang G, Zhu C. Synthesis of 2-[2-(5-methylbenzothiazolyl)azo]-5-dimethylaminobenzoic acid and its application to the spectrophotometric determination of nickel. Analyst. 1998;123(1):109-112. doi:10.1039/a705268e.

161. H.M. Abd El-Lateef, A.M. Abu-Dief, M.A.A. Mohamed, Corrosion inhibition of carbon steel pipelines by some novel Schiff base compounds during acidizing treatment of oil wells studied by electrochemical and quantum chemical methods, J. Mol. Struct. 1130 (2017) 522–542.

162.L.H. Abdel-Rahman, A.M. Abu-Dief, H. Moustafa, A.A.H. Abdel-Mawgoud, Design and nonlinear optical properties (NLO) using DFT approach of new Cr(III), VO(II), and Ni (II) chelates incorporating tri-dentate imine ligand for DNA interaction, antimicrobial, anticancer activities and molecular docking studies, Arab. J. Chem. 13 (1) ,2020,649–670.

163. Aşır, S., Uzun, L., Türkmen, D., Say, R., & Denizli, A. Ion-selective imprinted superporous monolith for cadmium removal from human plasma. Separation Science and Technology, (2005). 40(15), 3167-3185..

164. Abed, Ehab Fadhel, and Ahmed Ali Alkarimi. "ion exchange monolithic column for copper determination." 2022.

165. Gorshkov, A. V., Tarasova, I. A., Evreinov, V. V., Savitski, M. M., Nielsen, M. L., Zubarev, R. A., & Gorshkov, M. V.Liquid chromatography at critical conditions: comprehensive approach to sequence-dependent retention time prediction. Analytical chemistry, (2006). 78(22), 7770-7777.

166. Gilar, M., Daly, A. E., Kele, M., Neue, U. D., & Gebler, J. C. Implications of column peak capacity on the separation of complex peptide mixtures in single-and two-dimensional high-performance liquid chromatography. Journal of chromatography A, (2004). 1061(2), 183-192.

167. Gupta, V., Beirne, S., Nesterenko, P. N., & Paull, B. Investigating the effect of column geometry on separation efficiency using 3D printed liquid chromatographic columns containing polymer monolithic phases. Analytical chemistry, (2018). 90(2), 1186-1194..

168. Besada, Amir, Nabil B. Tadros, and Yousseff A. Gawargious. "Copper (II)-neocuproine as colour reagent for some biologically active thiols: Spectrophotometric determination of cysteine, penicillamine, glutathione, and 6-mercaptopurine." *Microchimica Acta* 99.1 (1989): 143-146.

169. Reuhs, B. L., & Rounds, M. A, 2010. High-Performance Liquid Chromatography. Food Analysis, 499–512. doi:10.1007/978-1-4419-1478-1_28.

170. Eren, Halit, and D. Potter. "Data Acquisition Fundamental." *Process Software and Digital Network, Journal of Instrumentation Engineer* ,2012: 330-341.

171. Krenkova J, Gargano A, Lacher NA, Schneiderheinze JM, Svec F. High binding capacity surface grafted monolithic columns for cation exchange chromatography of proteins and peptides. Journal of Chromatography A. 2009 Oct 2;1216(40):6824-30.

172. Takeuchi T. Separation of inorganic anions from biomaterial samples from Indonesian traditional fruit using monolithic column in ion chromatography capillary system. Journal of Chemical and Pharmaceutical Research. 2015;7(8):21-7.173.

173. Han H, Li J, Wang X, Liu X, Jiang S. Synthesis of ionic liquid-bonded organic-silica hybrid monolithic column for capillary electrochromatography. Journal of separation science. 2011 Aug;34(16-17):2323-8.

174. Gros N, Camões MF, Oliveira C, Silva MC. Ionic composition of seawaters and derived saline solutions determined by ion chromatography and its relation to other water quality parameters. Journal of Chromatography A. 2008 Nov 7;1210(1):92-8.

175. Luo Q, Shen Y, Hixson KK, Zhao R, Yang F, Moore RJ, Mottaz HM, Smith RD. Preparation of 20-μm-id silica-based monolithic columns and their performance for proteomics analyses. Analytical chemistry. 2005 Aug 1;77(15):5028-35.

176. Tossanaitada B, Masadome T, Imato T. Simultaneous Determination of Inorganic Anions by Sequential Injection Chromatography System Constructed from a Monolithic Column and a Microfluidic Polymer Chip with an Embedded Ion-Selective Electrode Original Paper. Journal of Flow Injection Analysis. 2012;29(2):89.

177. Wei Y, Huang X, Liu R, Shen Y, Geng X. Preparation of a monolithic column for weak cation exchange chromatography and its application in the separation of biopolymers. Journal of separation science. 2006 Jan;29(1):5-13.

178. Bruchet A, Dugas V, Mariet C, Goutelard F, Randon J. Improved chromatographic performances of glycidyl methacrylate anion-exchange monolith for fast nano-ion exchange chromatography. Journal of separation science. 2011 Aug;34(16-17):2079-87.

179. Li Y, Gu B, Tolley HD, Lee ML. Preparation of polymeric monoliths by copolymerization of acrylate monomers with amine functionalities for anion-exchange capillary liquid chromatography of proteins. Journal of Chromatography A. 2009 Jul 17;1216(29):5525-32.

180. Wang F, Dong J, Jiang X, Ye M, Zou H. Capillary trap column with strong cation-exchange monolith for automated shotgun proteome analysis. Analytical chemistry. 2007 Sep 1;79(17):6599-606.

(4.3) Published Works

1. **" Preparation and Application of (GMA-co-ACA co-AAM) as Cation-Exchange Monolithic Column for determination Nickel (II) ion** " was Published in Journal of Pharmaceutical Negative Results ¦ Volume 13 ¦ Issue 2 ¦ 2022.

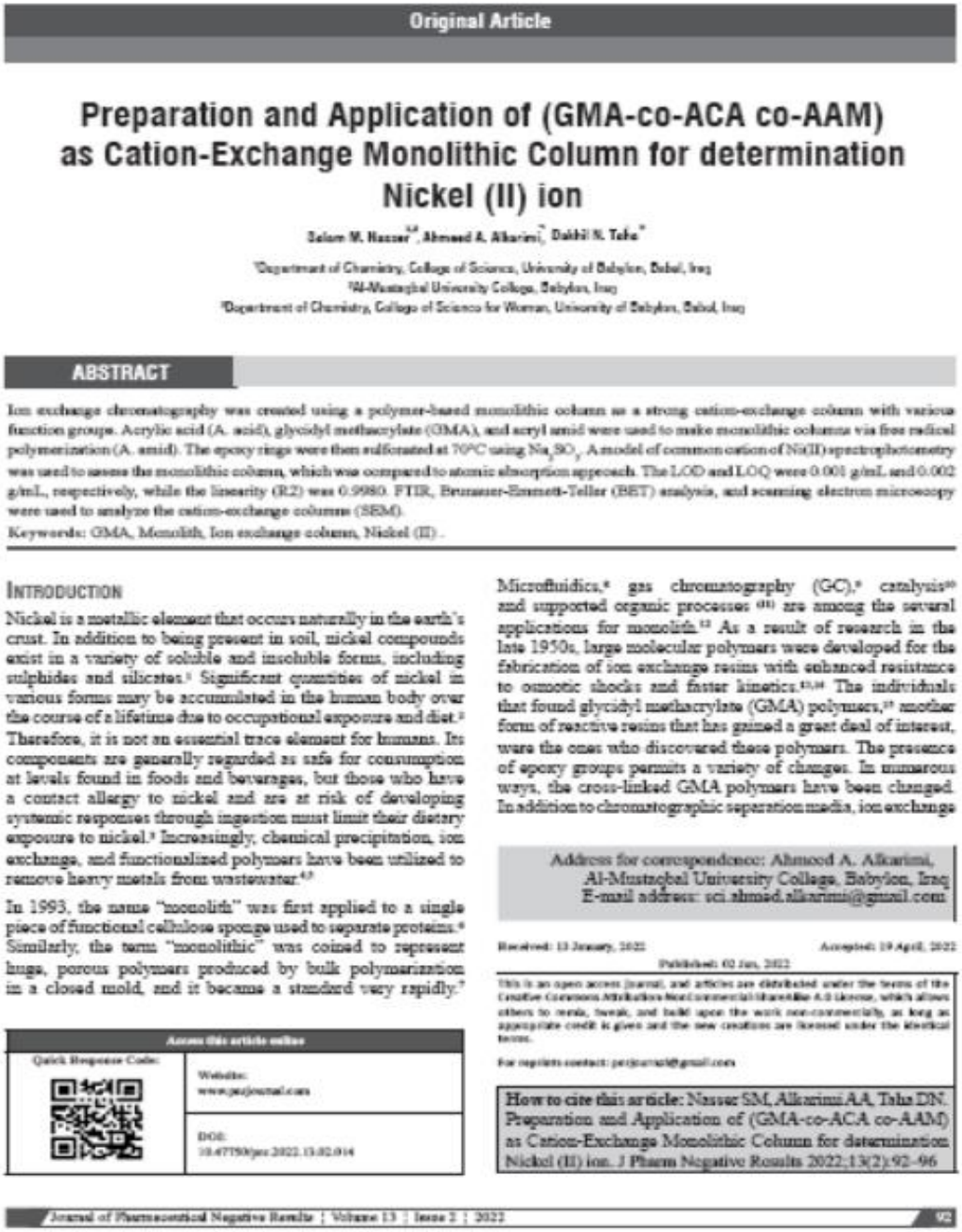

Original Article

Preparation and Application of (GMA-co-ACA co-AAM) as Cation-Exchange Monolithic Column for determination Nickel (II) ion

Salam M. Nasser[1,2], Ahmed A. Alkarimi[2], Dakhil N. Taha[3]

[1]Department of Chemistry, College of Science, University of Babylon, Babil, Iraq
[2]Al-Mustaqbal University College, Babylon, Iraq
[3]Department of Chemistry, College of Science for Women, University of Babylon, Babil, Iraq

ABSTRACT

Ion exchange chromatography was created using a polymer-based monolithic column as a strong cation-exchange column with various function groups. Acrylic acid (A. acid), glycidyl methacrylate (GMA), and acryl amid were used to make monolithic columns via free radical polymerization (A. amid). The epoxy rings were then sulfonated at 70°C using Na_2SO_3. A model of common cation of Ni(II) spectrophotometry was used to assess the monolithic column, which was compared to atomic absorption approach. The LOD and LOQ were 0.001 g/mL and 0.002 g/mL, respectively, while the linearity (R2) was 0.9980. FTIR, Brunauer-Emmett-Teller (BET) analysis, and scanning electron microscopy were used to analyze the cation-exchange columns (SEM).

Keywords: GMA, Monolith, Ion exchange column, Nickel (II).

Introduction

Nickel is a metallic element that occurs naturally in the earth's crust. In addition to being present in soil, nickel compounds exist in a variety of soluble and insoluble forms, including sulphides and silicates.[1] Significant quantities of nickel in various forms may be accumulated in the human body over the course of a lifetime due to occupational exposure and diet.[2] Therefore, it is not an essential trace element for humans. Its components are generally regarded as safe for consumption at levels found in foods and beverages, but those who have a contact allergy to nickel and are at risk of developing systemic responses through ingestion must limit their dietary exposure to nickel.[3] Increasingly, chemical precipitation, ion exchange, and functionalized polymers have been utilized to remove heavy metals from wastewater.[4,5]

In 1993, the name "monolith" was first applied to a single piece of functional cellulose sponge used to separate proteins.[6] Similarly, the term "monolithic" was coined to represent huge, porous polymers produced by bulk polymerization in a closed mold, and it became a standard very rapidly.[7] Microfluidics,[8] gas chromatography (GC),[9] catalysis[10] and supported organic processes [11] are among the several applications for monolith.[12] As a result of research in the late 1950s, large molecular polymers were developed for the fabrication of ion exchange resins with enhanced resistance to osmotic shocks and faster kinetics.[13,14] The individuals that found glycidyl methacrylate (GMA) polymers,[15] another form of reactive resins that has gained a great deal of interest, were the ones who discovered these polymers. The presence of epoxy groups permits a variety of changes. In numerous ways, the cross-linked GMA polymers have been changed. In addition to chromatographic separation media, ion exchange

Address for correspondence: Ahmed A. Alkarimi, Al-Mustaqbal University College, Babylon, Iraq
E-mail address: sci.ahmed.alkarimi@gmail.com

Received: 13 January, 2022 Accepted: 19 April, 2022
Published: 02 Jun, 2022

How to cite this article: Nasser SM, Alkarimi AA, Taha DN. Preparation and Application of (GMA-co-ACA co-AAM) as Cation-Exchange Monolithic Column for determination Nickel (II) ion. J Pharm Negative Results 2022;13(2):92-96

Access this article online
Quick Response Code:
Website: www.pnjournal.com
DOI: 10.47750/pnr.2022.13.02.014

2. "Synthesis of ((E)-2-((4 methoxyphenol)diazenyl)-4,5-diphenyl-1Himidazole (MPDADPI) for Ni (II) determination that separated off-line using monolithic column " was accepted in Journal HIV Nursing (Volume 22; issue 3; 2022).

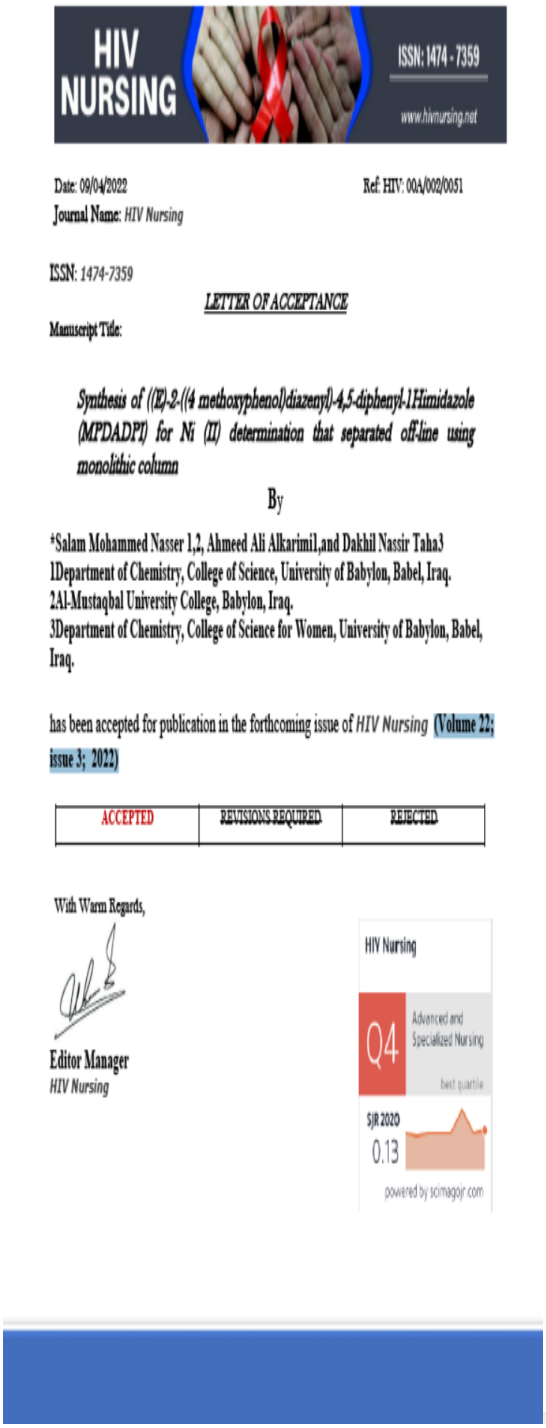

HIV NURSING

ISSN: 1474 - 7359

www.hivnursing.net

Date: 09/04/2022 Ref: HIV: 00A/002/0051

Journal Name: *HIV Nursing*

ISSN: 1474-7359

LETTER OF ACCEPTANCE

Manuscript Title:

Synthesis of ((E)-2-((4 methoxyphenol)diazenyl)-4,5-diphenyl-1Himidazole (MPDADPI) for Ni (II) determination that separated off-line using monolithic column

By

*Salam Mohammed Nasser 1,2, Ahmeed Ali Alkarimil,and Dakhil Nassir Taha3
1Department of Chemistry, College of Science, University of Babylon, Babel, Iraq.
2Al-Mustaqbal University College, Babylon, Iraq.
3Department of Chemistry, College of Science for Women, University of Babylon, Babel, Iraq.

has been accepted for publication in the forthcoming issue of *HIV Nursing* **(Volume 22; issue 3; 2022)**

ACCEPTED	REVISIONS REQUIRED	REJECTED

With Warm Regards,

Editor Manager
HIV Nursing

HIV Nursing
Q4
Advanced and Specialized Nursing
best quartile
SJR 2020
0.13
powered by scimagojr.com

HIV Nursing 2022; 22(2): 895-898 Synthess of (E)-2-(4 Methoxyphenol) Diazenyl)-4, 5-Diphenyl-1himidazole.....

Synthesis of (E)-2-(4 Methoxyphenol) Diazenyl)-4, 5-Diphenyl-1himidazole (Mpdadpi) for Ni (Ii) Determination that Separated off-Line Using Monolithic Column

*Salam Mohammed Nasser[1, 2], Ahmeed Ali Alkarimi[1], and Dakhil Nassir Taha[3]
[1]Department of Chemistry, College of Science, University of Babylon, Babel, Iraq.
[2]Al-Mustaqbal University College, Babylon, Iraq.
[3]Department of Chemistry, College of Science for Women, University of Babylon, Babel, Iraq.
*salam.mohammed@mustaqbal-college.edu.iq

Abstract

The prepared column was used to determine Ni (II) using a new Ligand (MPDADPI) imidazole that was prepared and characterized using I.R, UV-Vis, CHN, 1HNMR techniques.The absorbance of the formed complex was 518 nm. Various parameters that can be affectedon the signal response have been optimized to enhancethe sensitivity. It was found that the optimum conditions were pH 8, the concentration of the ligend 5×10 -5mol/L. The calibration cure was linear in the range of (0.03-2μg/mL). The LOD and LOQ were0.001 μg/mL 0.002 μg/mL respectively. The proposed method was used to determine microamounts of nickel directly (II). by using ter polymer monolithic column as a Cation – Exchange of glycidyl methacrylate (GMA) , Acrylic acid (A. acid) and acryl amid (A. amid) as monolith (GMA-co-ACA co-AAM) with satisfactory results.

Keywords: MPDADPI, Monolithic column, Ni (II) determination.

1. Introduction

Small traces of nickel can really be found in soil, plants, and animal tissues. Nickel is typically extracted from water. Nickel complexes that are aqueous are more corrosive than those that are insoluble [1]. Nickel causes dermatitis, pneumonia, lung cancer, and nose cancer in humans [2].Azo compound [3, 4] of any organic chemical molecule that contains the azo group (−N=N−), the functional group diazenyl R−N=N−R', where R and R' can be either aryl or alkyl [5]. Azo-imidazole compounds have a critical role in the creation of pharmacological and biological products. These chemicals are well-known for their medical uses, including antiseptics [6], antifungal [4], antibacterial and antitumor activities [7].Azo dyes are widely used in the textile [8], fiber [9], cosmetic [10], leather [11], paint and printing industries [12]. Besides their distinctive coloring function, azo compounds have been reported as antibacterial, antiviral, antifungal and cytotoxic agents [13]. Due to its convenience of preparation, high porosity, good mechanical stability, huge surface area, and high transfer efficiency, monolithic columns are of great importance. [14]. Monolithic columns are used to construct a two-dimensional separation system. The two-dimensional robotically. This method allows for easy and independent optimization of both separation stages, allows for larger sample amounts to be loaded into the first separation dimension, allows for additional sample manipulations between the dimensions, such as preconcentration or rebuffering, and allows for fraction injection to be repeated. Off-line two-dimensional systems typically employ linear gradients in the first dimension, allowing for effective peptide separation as well as on-line UV-detection monitoring of the separation [13].

2. Experimental

2.1 Apparatus

Heater (HeidolphRMHei-Standard),(Dual syringe, infusion pump (kd Scientific Holliston,MAU.S.A),Jasco pu-980 intelligent HPLC pump,(Denver Instruments Germany TP-214 Analytical Balance),(Nitrogen gas tank),(Irradiation device locally manufactured for high pressure mercury lamp have 220V 50Hz at 365 nm),(UV-Visible spectrophotometer,UV1610pc double spectrophotometer shimadzu(Japan) using lcm quartz cells ,WTW multi 740. pH-meter Germany,Water bath and shaker M00/M01Memmert, Germany Micropipette.

3. Materials and Methods

3. According to the international (Sci- Finder) program and through the foregoing and by reviewing previous studies in the course of the research that the polymer is prepared for the first time, and this in turn enhances the accuracy and modernity of the prepared polymer, as shown in the figures:

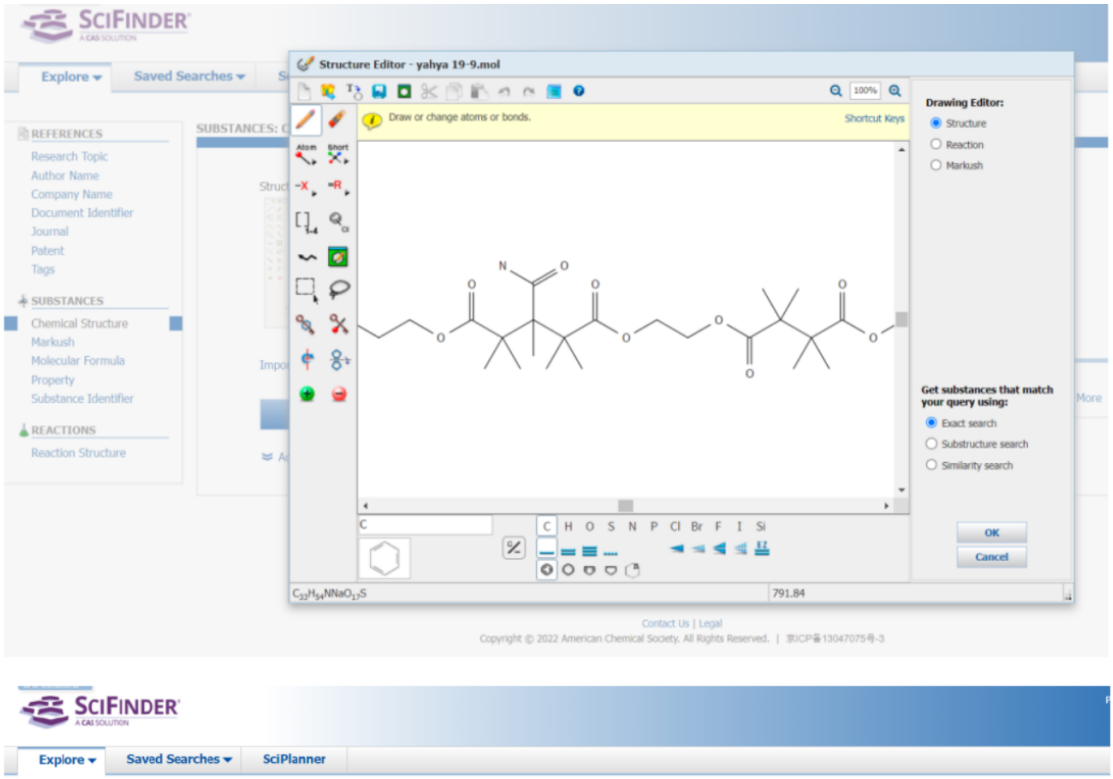

The structural formula of the structural unit of the polymer under study

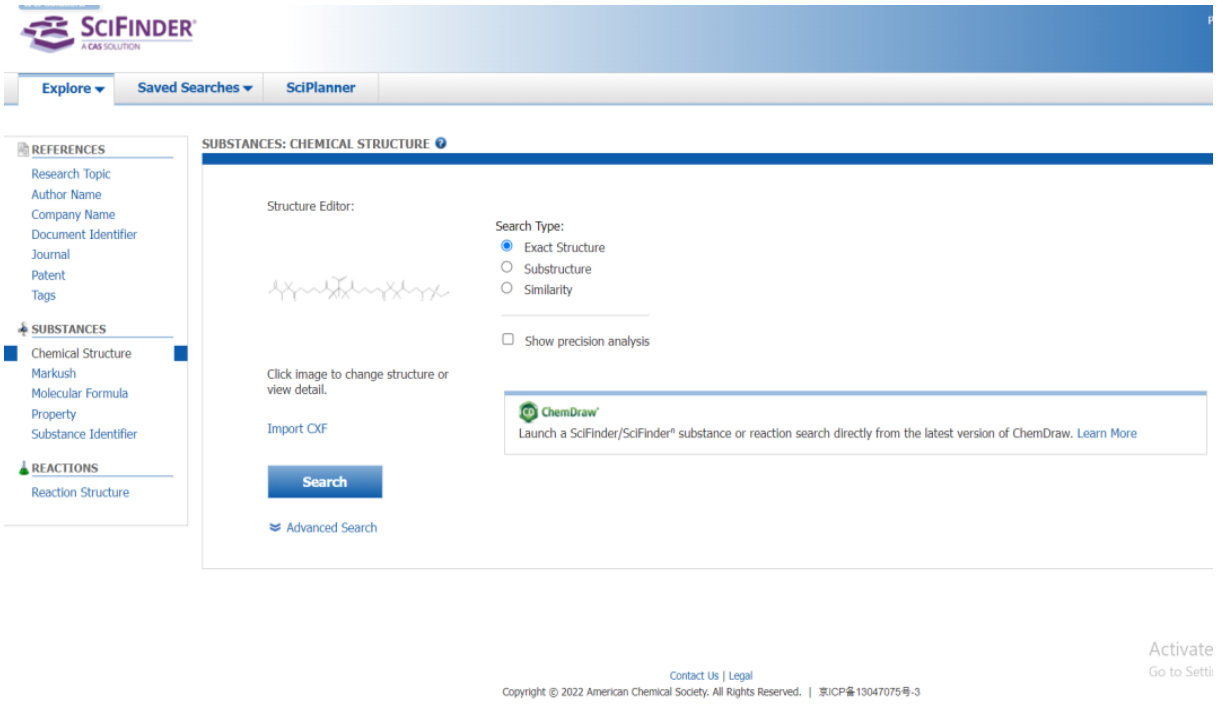

Adding the polymer composition to complete the series of the program used

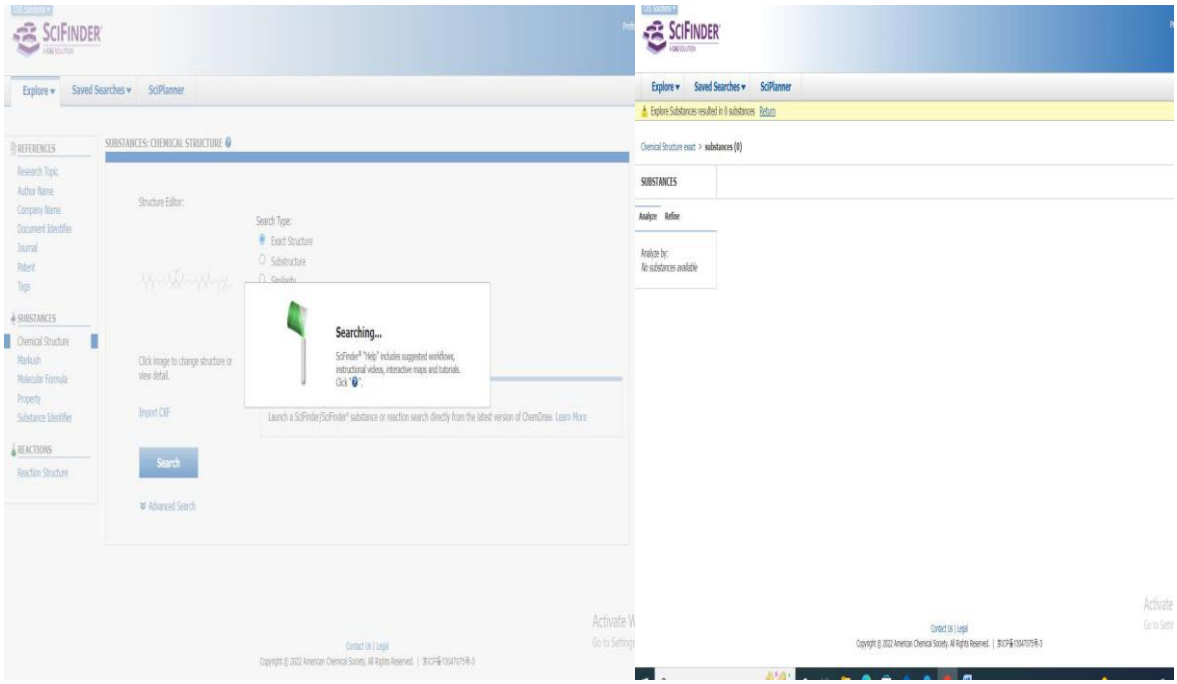

Novelty of the compound under study

4. Also, according to the international (Sci- Finder) program and through the foregoing and by reviewing previous studies in the course of the research

that the (ligand MPDADPI) is prepared for the first time,as shown in the figures.

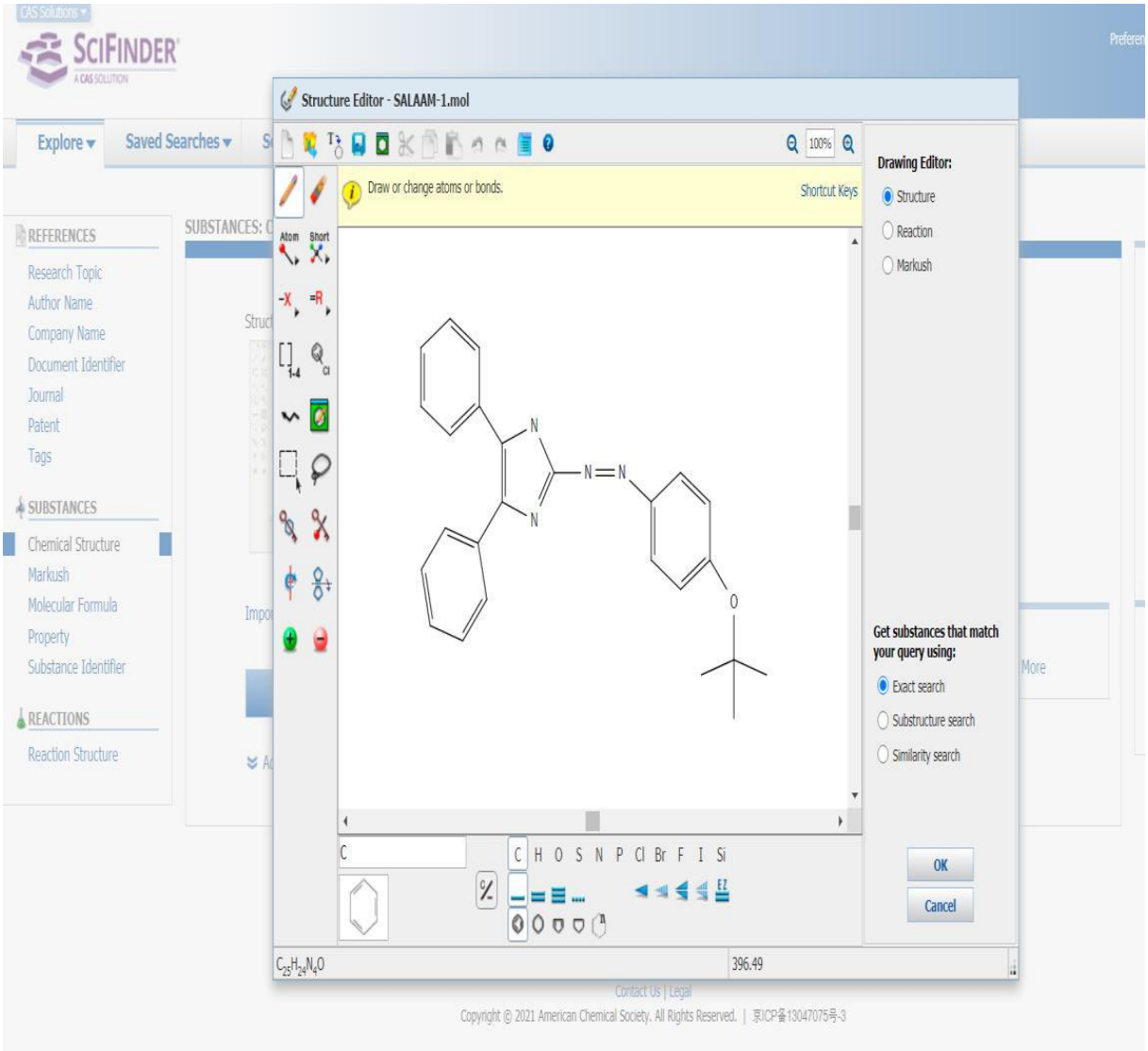

The structural formula of the structural unit of the ligand under study

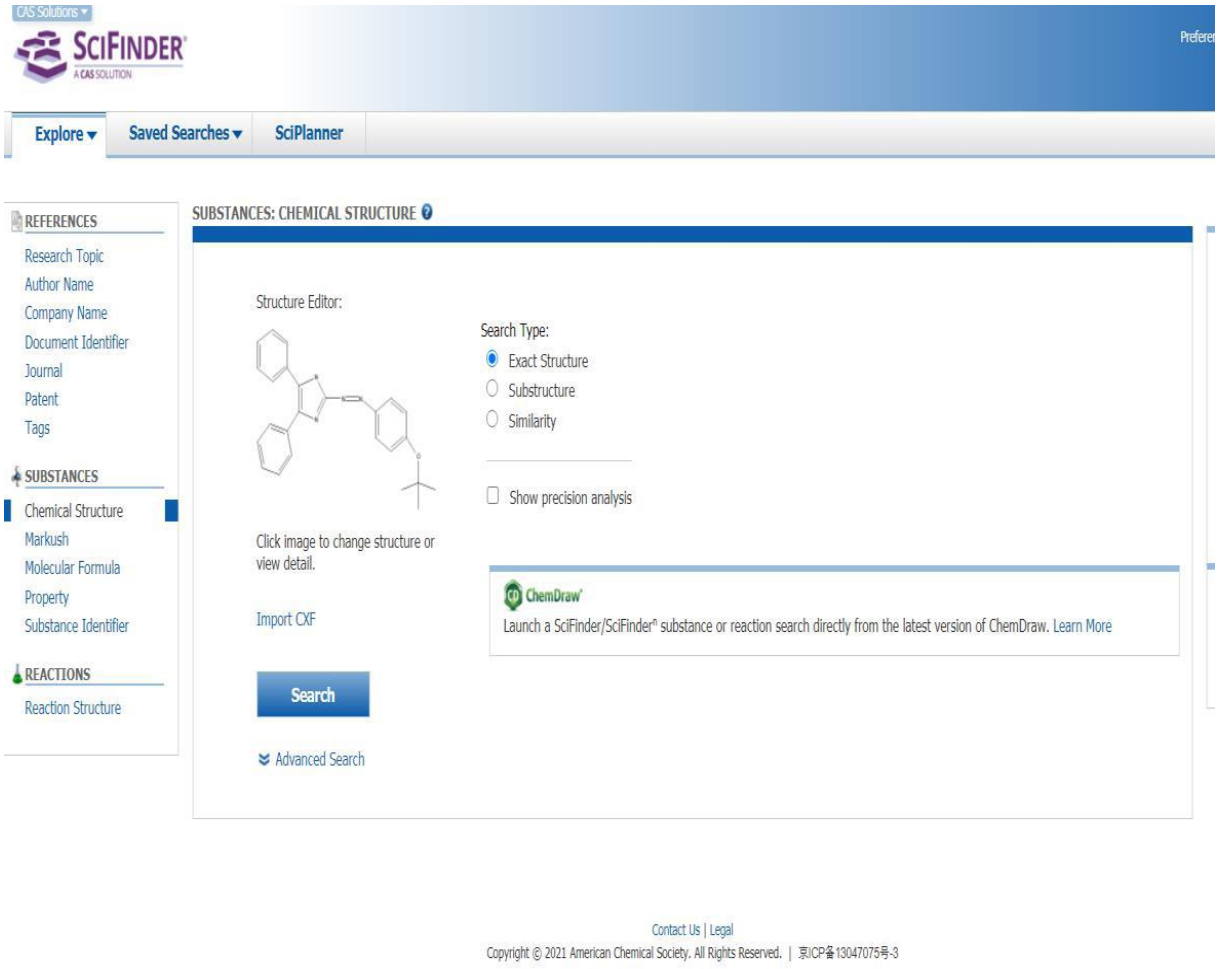

Adding the ligand composition to complete the series of the program used

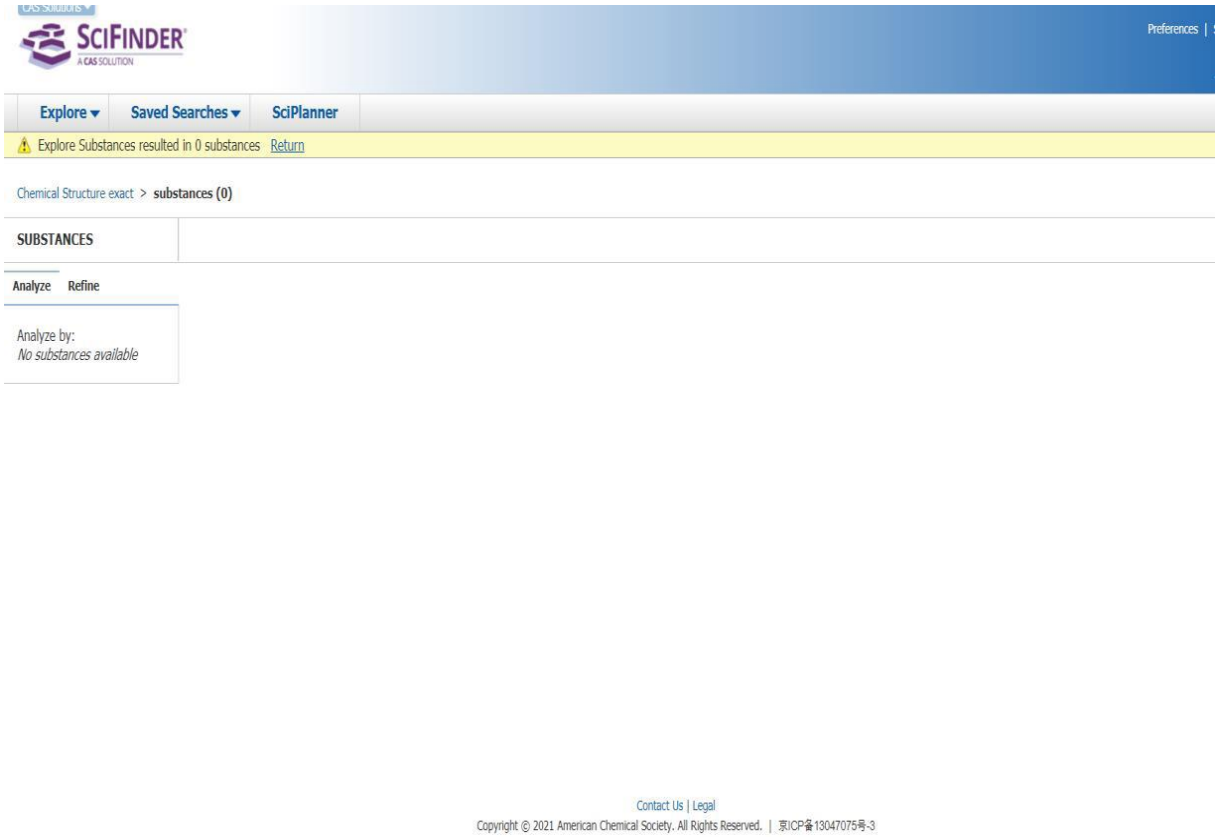

Novelty of the compound under study

(4.4) Participations

1. Eighteenth scientific symposium for post graduate studies PhD, chemistry department, college of science, Babylon University, 12 May 2022.

2. Seventeenscientific symposium for post graduate studies, chemistry department, college of science, Babylon University, 28 April 2021.Ninth scientific symposium for post graduate studies, chemistry department, college of science, Babylon University, 17 November 2014.

3. Participation in the electronic and tagged training workshop

   Terms and standards of scientific research and classification of journals 04/03/ Organized by the Scientific Supervision and Evaluation Authority on 2022.

4. International Conference and Exhibition on Pharmaceutics & Novel Drug Delivery Systems ,22 - 24 Nov 2021 ,Dubai, UAE.

5. A certificate of participation and a Medal of Creativity by the International Exhibition and Conference on Inventions, Innovations and Creativity held at the Nobel Institute in Erbil Governorate, Kurdistan Region of Iraq from March 29-31, 2022, which was held under the auspices of the French International Center for Scientists and Inventors and the participation of investment bodies for applied patents with effective economic feasibility.